Probabilistic assessment of the performance of combined sewer systems

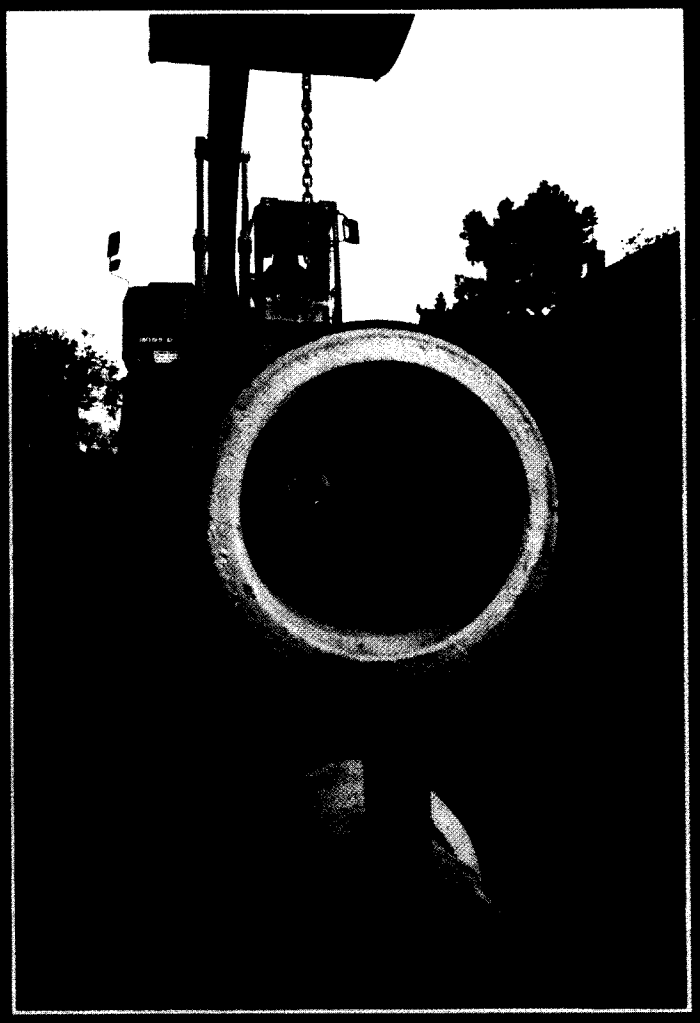

Hans Korving

Probabilistic assessment of the performance of combined sewer systems

Hans Korving

Probabilistic assessment of the performance of combined sewer systems

Proefschrift

ter verkrijging van de graad van doctor
aan de Technische Universiteit Delft,
op gezag van de Rector magnificus prof.dr.ir. J.T. Fokkema,
voorzitter van het College voor Promoties,
in het openbaar te verdedigen op dinsdag 18 mei 2004 om 13.00 uur
door Johannes Leonard KORVING
civiel ingenieur
geboren te Assen.

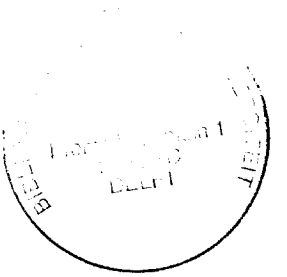

Dit proefschrift is goedgekeurd door de promotoren:
Prof.dr.ir. F.H.L.R. Clemens
Prof.dr.ir. J.M. van Noortwijk

Samenstelling promotiecommissie:

Rector Magnificus, voorzitter
Prof.dr.ir. F.H.L.R. Clemens, Technische Universiteit Delft, promotor
Prof.dr.ir. J.M. van Noortwijk, Technische Universiteit Delft, promotor
Prof.dr.ir J. Berlamont, Katholieke Universiteit Leuven
Prof.dr. R.M. Ashley, University of Bradford
Prof.dr. T. Bedford, University of Strathclyde
Prof.dr. J.L. Bertrand Krajewski, INSA de Lyon
Dr.ir. P.H.A.J.M. van Gelder, Technische Universiteit Delft

Dit proefschrift is tot stand gekomen met ondersteuning van Stichting RIONED en HKV Lijn in water.

ISBN 90-9018056-7

Keywords: sewer system, probabilistic modelling, uncertainty analysis

Cover design: Karin Boessenkool
Cover photo: Bureau voor Beeld, Hans Dijkstra

Printed in The Netherlands

The contents of this thesis can be summarised as "Shit happens".

Contents

CHAPTER 1 Introduction and scope

1.1 INTRODUCTION

Sewer systems have been designed to protect society from two important hazards: the flooding of urban areas during storms and the endangering of public health because of exposure to faecal contamination. Collection and transport of storm water prevents flooding, whereas collection and transport of wastewater contributes to a high level of public hygiene.

1.1.1 History of urban drainage

Archaeological evidence reveals that several ancient civilisations used underground collection and transport systems for wastewater and storm water (Van den Akker 1952). A well-known example is the Cloaca Maxima in Rome that was built in 200BC. The construction of modern sewers began in the 19th century, motivated by economic reasons, particularly the commercial value of faeces as fertiliser (Van Zon 1986). In addition, halfway through the 19th century, cholera and typhoid epidemics stimulated sewer construction in Western Europe. In those days, direct drainage of faeces to rivers and streams and disposal of waste into cesspools, which were only periodically emptied, resulted in insanitary conditions. Snow (1854) was the first to report that the spreading of epidemic diseases was related to the absence of both adequate drinking water and proper wastewater disposal. Since human faeces are the principal vectors for transmission of infectious diseases, urban drainage plays a direct role in removing excreta from cities and, consequently, interrupting the transmission. The situation was improved by constructing sewer systems, which collected the wastewater and drained it out of the cities.

In The Netherlands, sewer systems have existed since the Middle Ages in, for example, Deventer, Arnhem and Maastricht (Clemens 2001a). However, large-scale construction of sewer systems started only at the end of the 19th century. After the Second World War, large-scale sewer construction took place as a result of economic growth and accelerated urbanisation. This satisfied not only the need for protection of public health, but also the preparation (by means of drainage) of low-lying areas for town extension. Dijckmeester (1988) argues that living in a damp environment gives rise to a higher risk of chronic diseases, thus necessitating adequate drainage of residential areas. However, actual effects on human health are only apparent after a relatively long period (5-10 years). In addition, Dirkzwager (1997) emphasises that the economic growth and urbanisation also caused an increase in the pollution of surface waters, in particular, rivers and streams suffering from oxygen depletion. In order to improve surface water quality the Pollution of Surface Waters Act (Wvo) was passed in 1970, resulting in the large-scale construction of wastewater treatment plants (wwtp) in the

late 1960s and 1970s in The Netherlands. From then on, the focus of wastewater treatment progressed from removal of oxygen consuming substances, through nitrification of ammonium-nitrogen, to the reduction of discharges of phosphate and nitrogen for eutrophication control (Van Nieuwenhuijzen 2002).

1.1.2 Sewer systems in The Netherlands

Nowadays, 98% of Dutch houses are connected to a sewer system. Both gravity sewers (84%) and pressurised sewers (16%) are in use. There are basically two types of gravity sewers: combined systems in which wastewater and storm water are transported together in the same pipe to the treatment plant and separate systems in which wastewater and storm water are kept in separate pipes. In the separate system the wastewater is transported to the treatment plant, while the storm water is directly drained to the surface water. The combined system is the predominant type in The Netherlands, comprising 64% of gravity sewers in The Netherlands (Stichting RIONED 2002).

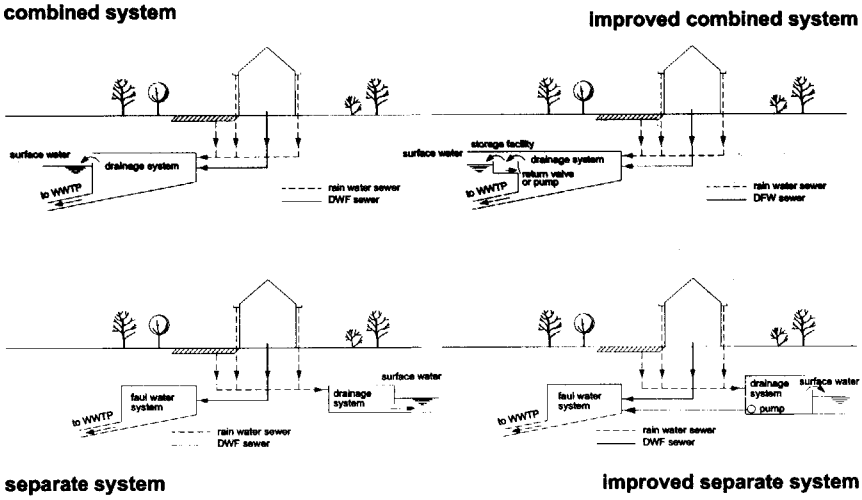

Figure 1.1 Schematic representation of sewers (adapted from Clemens 2001a).

The advantages of a combined system are its relatively low price, the ease of maintenance and its robustness (Figure 1.1, top left). A disadvantage of the system is that comparatively clean storm water is mixed with wastewater and the diluted flow transported to the wwtp, often resulting in a loss in removal efficiency caused by diluted wastewater. It is also not economically feasible to build sufficient capacity in the system to transport the flow during heavy storms. Therefore, combined sewer overflow (CSO) structures are provided. In The Netherlands, the number of CSO structures is at least 15,000 (Stichting RIONED 2002). During excessive rainfall those divert flows above a

certain level out of the sewer system to the surface water which, however, causes environmental pollution of natural watercourses.

Adding storage in series together with the overflow structure reduces the pollution problem because the additional storage reduces the spill frequency as well as the ecological impact due to the settling of suspended particles in the storage facility. This storage can be constructed as storage settling tanks, high side weir overflows, parallel storage settling sewers, hydrodynamic separators etc (see Saul 2002). Such a sewer system is called an 'improved combined' system (Figure 1.1, top right).

Sewer systems of the separate type lack the drawbacks of combined systems, but the systems are more expensive to construct (Figure 1.1, bottom left). From 1970 onwards, most sewer systems constructed in The Netherlands have been separate. Storm water and wastewater are transported separately. The system is designed to discharge the maximum wastewater flow to the treatment plant. Storm water is not mixed with the wastewater, but directly discharged to surface waters. In this way, the environmental pollution associated with combined systems is avoided. However, faulty connections, i.e. wastewater discharge into the storm water system and the other way round, can occur in the system. Clemens (2001a) estimates that 5 % of the connections in separate systems are faulty. This number increases over the years largely due to adjustments to the sewers inside buildings. In addition, the storm water flow also becomes contaminated due to atmospheric deposition and sediment wash-off from streets and roofs (Xanthopoulos and Hahn 1993).

Improvement of separate sewer systems is achieved by diverting the first amount of storm water to the wwtp through the wastewater pipes (Figure 1.1, bottom right). This reduces discharges to rivers and streams of the storm water that is expected to be most contaminated. In addition, smaller storms are completely diverted to the wwtp. Temporary efficiency reduction at the wwtp due to dilution of the wastewater flow is rather limited (Langeveld 2004).

1.2 MODELS IN URBAN DRAINAGE

In urban drainage, models are used to support technical decisions. Firstly, modelling tools are used to predict performance of urban wastewater systems in order to assess the resulting impact of discharges against appropriate environmental criteria. Secondly, they are applied to describe the structural condition of sewer assets (pipes, manholes, culverts, pumps, etc.) for rehabilitation and maintenance purposes.

The word 'model' tends to be used in different ways. It can be defined as a simplified representation of some aspect of reality with the objective of its explanation or prediction. Depending on purpose, desired accuracy, available data and other factors, models can use very different representations (e.g. mental, verbal, graphical or mathematical). This thesis examines both mathematical models to describe rainfall and sewer flow, and knowledge-based systems to describe asset condition and possible deterioration. In mathematical models the relationships between quantities (rainfall,

flows, asset condition, etc.) that can be observed in the system are described as mathematical relations. Knowledge-based systems are based on 'intuition' and experience, e.g. decision support for inspection and rehabilitation of sewer pipelines.

1.2.1 Models describing hydraulic performance of sewer systems

The purpose of hydraulic models in urban drainage is to represent a sewer system and its response to different conditions in order to support design or rehabilitation. They have three main uses: design of new systems, analysis of existing systems and operational applications such as real time control (RTC). An example of a simple model is the 'Rational Method', which converts a constant rainfall intensity into sewer runoff to study the likely effects of different intensities on sewer performance. Modern sewer models, however, are much more extended in process descriptions and require more detailed data than the 'Rational Method'. The development of these models began at the end of the 1960s (Butler and Davies 2001). The SWMM model, for example, first appeared in the USA in the early 1970s (Huber and Dickinson 1988). With increasing computer capability such complex models have become more and more standard tools in sewer system design. Recent examples of computer packages for sewer engineering are Hydroworks (Wixcey *et al.* 1992, Magne *et al.* 1996 and Wallingford Software 2000), MOUSE (DHI 1994 and Crabtree *et al.* 1994), SWMM (Huber and Dickinson 1988, Nix 1994 and Huber 1995) and Sobek (WL Delft Hydraulics 1998).

In this thesis the definitions of a sewer model describing hydraulic performance as proposed by Van Mameren and Clemens (1997) are used. It is defined by its components and comprises:

- a description of the hydraulic loads distinguished into dry weather and storm conditions,
- a description of the system's geometry, the database or geometrical model,
- a description of the hydraulic processes, the process or calculation model.

Because the hydraulic processes consist of both processes in the sewer system and processes related to conversion of rainfall into runoff, the calculation model contains two somewhat separate process descriptions: a hydraulic and a hydrologic model.

Models normally used in urban drainage comprise three main types, including empirical or black box models, conceptual or grey box models and detailed physically based or white box models. The afore-mentioned models (Hydroworks, MOUSE, SWMM and Sobek) are examples of models of the detailed physically based type. These hydrodynamic models consist of mathematical descriptions of relationships between physical parameters and are deterministic, i.e. one combination of input data always leads to the same output, so uncertainty or randomness is not taken into account. The models convert rainfall and wastewater inputs into flow-rates and water depths within the sewer system and at its outlets (e.g. CSO structures). Clemens (2001a) discusses the use of hydrodynamic models in urban drainage. Rainfall runoff models, on the other

hand, are often grey box models, as purely deterministic models appear to be unsuitable for description of hydrologic processes (Van de Ven 1989 and Clemens 2001a). Sometimes conceptual models (e.g. linear reservoirs) are also used to model in-sewer processes in order to save calculation time (see KOSIM (ITWH 1995 and Schütze *et al.* 2002), REMULI (Vaes 1999) and WEST Simulator (Meirlaen *et al.* 2001)). In addition, Rauch *et al.* (2002) describe state of the art integrated modelling of sewer systems, wwtps and receiving waters in which different kinds of models are linked to predict total system performance.

When modelling storm conditions the rainfall pattern is of particular interest (Figure 1.2). Examples of rainfall patterns used are constant rainfall, rainfall with a particular storm profile for a specified return period or a time series of rainfall. The latter, for example, is applied when modelling the operation of CSO structures. Spatial variation of rainfall becomes important when studying larger catchments (Willems 2000). The spatial extent of larger catchments is approximately 15-20 km, being the mean spatial extent of individual rain cells (see Zawadski 1973 and Willems 2000). A reliable estimation of the dry weather flow (dwf) over the day, which consists of wastewater and of leakage, is also required as model input for a combined system. Notwithstanding the significance of the geometrical data of the sewer system (Figure 1.2) for modelling purposes, its importance is often underestimated. Price and Osborne (1986) and Clemens (2001a), however, stress the importance of using a good quality database.

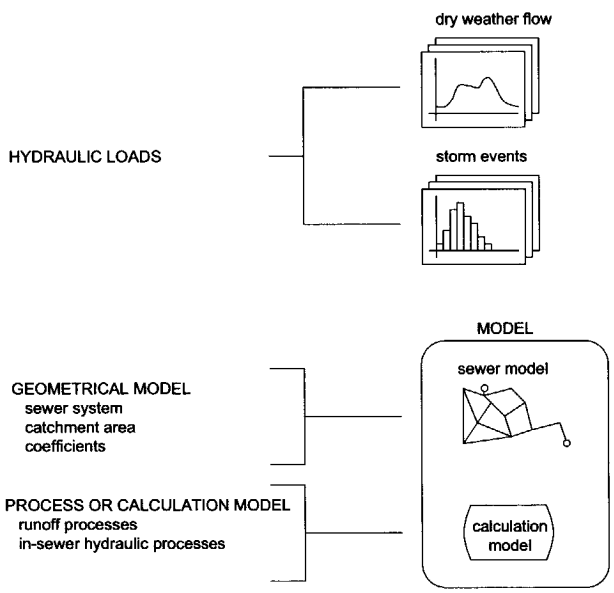

Figure 1.2 Definition of a sewer model describing hydraulic performance and its components (adapted from Clemens 2001a).

In the hydrologic part of the calculation model rainfall is converted into sewer inflow (Figure 1.2). On its way to the sewer system rainwater may soak into the ground, form puddles and later on evaporate, or be caught in leaves of trees. Moreover, it will take the rainwater some time to reach the gully pot and enter the sewer system, i.e. the overland flow. As stated before, the processes are highly complex and their description often requires conceptual models, e.g. empirical relations for infiltration modelling and a unit hydrograph for overland flow.

Hydraulic in-sewer processes are modelled in the calculation model (Figure 1.2 bottom) using the 'De Saint-Venant equations'. They form a pair of equations describing gradually varying unsteady flow in open channels, including partially filled pipes. The most common method of solution is using finite differences, involving the division of distance and time into small steps (Vreugdenhil 1989). The sewer system is described in the calculation model as a composition of links and nodes. Links represent pipes and nodes represent manholes. The links incorporate the main hydraulic properties of the sewers, including diameter, gradient and roughness. Storm water and wastewater enter the system at the nodes. Using the inflow and the hydraulic properties, in-sewer flow rates and depths are calculated.

A model of in-sewer processes that determine the composition of the flow is also provided in most software packages. These models, however, offer only limited value for sewer design and rehabilitation because the scientific knowledge, on which the process descriptions are based, is very limited (Ashley *et al.* 1999). As this thesis focuses on hydraulic processes, a discussion of in-sewer processes relating sewage composition is beyond its scope. For recent developments on in-sewer processes see e.g. Ashley *et al.* (1999), Huisman (2001), Langeveld (2004) and IWA (2004).

1.2.2 Models describing the structural condition of sewer systems

Models for maintenance of sewers are primarily used for optimisation and prioritisation of inspection and rehabilitation activities. Existing sewer systems are continuously increasing in age. As a result, the concern about their continuing performance will grow, as well as the risk of future failures.

However, age-related deterioration of sewer assets is not well understood in terms of predictability (e.g. Jones 1984 and Fenner 2000). Furthermore, detailed knowledge of the manner in which constructional and external factors determine how sewer pipes, manholes and other assets deteriorate is limited (Davies *et al.* 2001a, Fenner and Sweeting 1998 and Stein 2001). In addition, Jones (1984) suggests that the concept of a uniform rate of deterioration is inappropriate, but 'stepped' rates of deterioration are more likely. After the formation of an initial defect, such as a leaking joint or a crack due to bad bedding, actual collapse can be triggered by some random event, possibly not related to the cause of the deterioration (e.g. a heavy storm or a passing truck). Consequently, two defects which appear similar can lead to very different consequences, which makes the prediction of the collapse of a sewer difficult, not to say impossible.

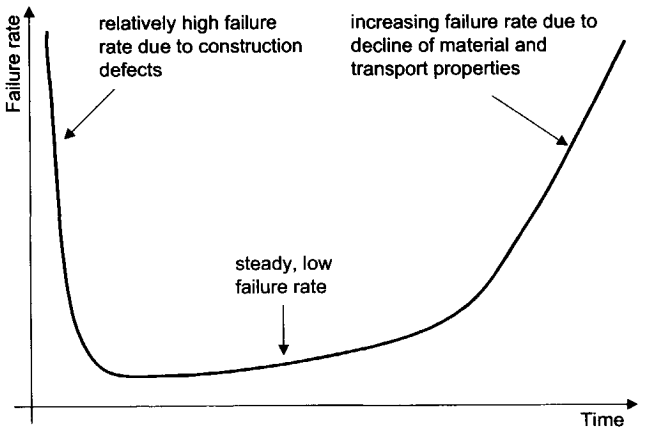

Figure 1.3 'Bathtub' shaped failure rate curve.

Some studies (Rostum *et al.* 1999 and Davies *et al.* 2001a) suggest that the well-known 'bathtub' type failure rate curve (Figure 1.3) can be applied to model the development of the condition of sewer pipes. This concept assumes a relatively high failure rate at the end of construction when backfill, traffic and soil loading is introduced to the pipe, followed by a period of relatively low failure rate. Much later, the failure rate increases due to decline of material properties and transport capacity. Failure rate is defined as the conditional probability of failure at a certain time given that the component (or system) has survived up to that time.

Notwithstanding the fact that the importance of sewer deterioration is widely recognised, only sewer corrosion is extensively described in the literature (e.g. Pomeroy 1974, Pomeroy and Parkhurst 1977, Thistlethwayte 1972, Bielecki and Schremmer 1987 and Stein 2001). The reliability of predicted sewer deterioration is discussed in Chapter 2. Factors possibly influencing deterioration and collapse of sewers include sewer material, age, type, depth, size, shape, length and gradient, traffic flow above sewer (e.g. total vehicle, goods vehicle and bus flow), construction type, bedding material and soil type (e.g. corrosivity and fracture potential) and joint type (Jones 1984, Fenner and Sweeting 1999, Davies *et al.* 2001a and Baur and Herz 2002). In particular, repeated sewer failure is considered indicative for future events, suggesting that current reactive maintenance (e.g. jetting) tackles symptoms, not causes.

Literature on failure of assets other than sewer pipes, however, is very limited. The assets studied include pumps (Ermolin *et al.* 2002, Joosten 2002 and Korving 2003a and 2003b), gates and valves (Pohl 2002), build-up of sediments and blockage of sewers (Fraser *et al.* 1998, Gérard and Chocat 1999 and Blanksby *et al.* 2002) and sewer joints (Williams *et al.* 2002).

The majority of decision support models rely on criteria defining pipes with specified characteristics as either high or low risk of failure (e.g. Kerkhof 1988, Cobbaert 1998, Fenner and Sweeting 1998, and Anderson 1999). However, these methods may not universally apply to all catchments because defined criteria can be valid just for a specific situation. In particular, the criteria in the UK Sewerage Rehabilitation Manual (Water Research Centre 2001) were largely derived from collapses in ageing inner city networks.

In order to avoid the danger of inappropriate maintenance, suitable techniques are needed to analyse past performance in a specific catchment and identify the correct subset of sewers for which maintenance will be most effective. Examples of decision support models for maintenance and rehabilitation are presented by Fenner and Sweeting (1998 and 1999), Rostum *et al.* (1999) and KEMA (2001). Methods supporting inspection of sewers can be found in Baur and Herz (2002), and Hahn *et al.* (2002).

A recent development regarding decision making on sewer maintenance is based on 'performance indicators' (OFWAT 2001, Ashley and Hopkinson 2002, Fenner and Saward 2002 and Matos *et al.* 2003). However, much work is still required in order to understand which performance indicators are most appropriate.

In addition to the afore-mentioned models, automated interpretation of CCTV data and other sensor information is applied to ensure a more reliable prediction of sewer condition. Wirahadikusumah *et al.* (1998), for example, present an automated method to interpret sensor information in order to identify defects using fuzzy set theory and fuzzy logic. Similar work is presented by Moselhi and Shebab-Eldeen (1999), and Xu *et al.* (1998) on the assessment of sewer pipe deformation and classification of surface defects using pattern recognition and image analysis. Loke *et al.* (1997) for their part emphasise the potential for neural networks as a tool for classification of sewer defects and assessing sewer condition using CCTV data.

Although in related fields much work has been carried out to determine functionality of assets, caution is required when considering the transferability of such techniques. For example, Rostum *et al.* (1999) mention that failure patterns and availability of field data are different for sewer and water mains, resulting in the need for different methods to predict asset condition. Examples from other areas of asset management comprise management of water mains reliability arising from failure of components of water distribution networks (Xu and Goulter 1998), statistical methods for estimating rehabilitation needs of water mains and software for prioritising their maintenance (Lei and Sægrov 1998, and Sægrov *et al.* 1999). In addition, Van Noortwijk (1996) defined optimal replacement strategies for structures under stochastic deterioration, such as bridges, and Pandey (1998) developed models to determine optimal inspection intervals and repair strategy of oil and gas pipelines.

1.3 STATE OF THE ART IN SEWER SYSTEM MANAGEMENT IN THE NETHERLANDS

In The Netherlands, municipalities are responsible for collection and transport of storm water and wastewater. Water boards, for their part, are responsible for the treatment of both and are concerned with protection of the quality of natural watercourses, thus imposing restrictions on wastewater discharges. Their responsibilities stem from the Dutch Pollution of Surface Waters Act (Wvo) of 1970. This Act charges the Dutch Provinces with the task to protect the quality of natural watercourses. They, for their part, delegated this task to the water boards. The Act serves as the basis for the quality requirements of wwtp effluents, as well as for the regulation of sewer overflows with respect to the effects on natural watercourses. However, quantification of these effects is problematic because the determinative processes are complex and the knowledge on them is very limited (Harremoës and Madsen 1999). Moreover, measurement data on pollution loads from sewers are lacking and existing sewer models are unable to predict those loads (Ashley *et al.* 1999).

The management of sewer systems outside buildings is specified in guidelines and standards, such as the Dutch NPR 3220 and the European NEN-EN 752-5 (sewers and drains) and NEN-EN 752-6 (pumping stations). The European standards incorporate the Dutch. Sewer management is defined as taking care of the proper performance of a sewer system. It concerns formulating goals with respect to sewer performance, translating these goals into performance requirements in order to assess the efficiency of sewer management and defining standards enabling quantitative testing of the performance requirements (NPR 3220). For example, one of the goals of a sewer system is to avert calamities during heavy storms. This leads to the performance requirement that the flow capacity in the system should be large enough to prevent flooding and safeguard public health. The standard for quantitative testing is that the flooding frequency should not exceed 1 in 2 years. The guidelines discriminate between the performance of the sewer system regarding environmental impacts, flooding and asset condition.

The purpose of sewer operation and maintenance is to ensure that the infrastructure performs in accordance with the requirements defined in NEN-EN 752-2:

- sewers operate without blocking,
- flooding frequencies shall be limited to prescribed values,
- public health shall be safeguarded,
- sewer surcharge frequencies shall be limited to prescribed values,
- health and safety of operator personnel shall be safeguarded,
- receiving waters shall be protected from pollution within prescribed limits,
- sewers shall not endanger existing adjacent structures and utilities,
- required service life and constructional integrity shall be achieved,
- sewers shall be watertight in accordance with testing requirements.

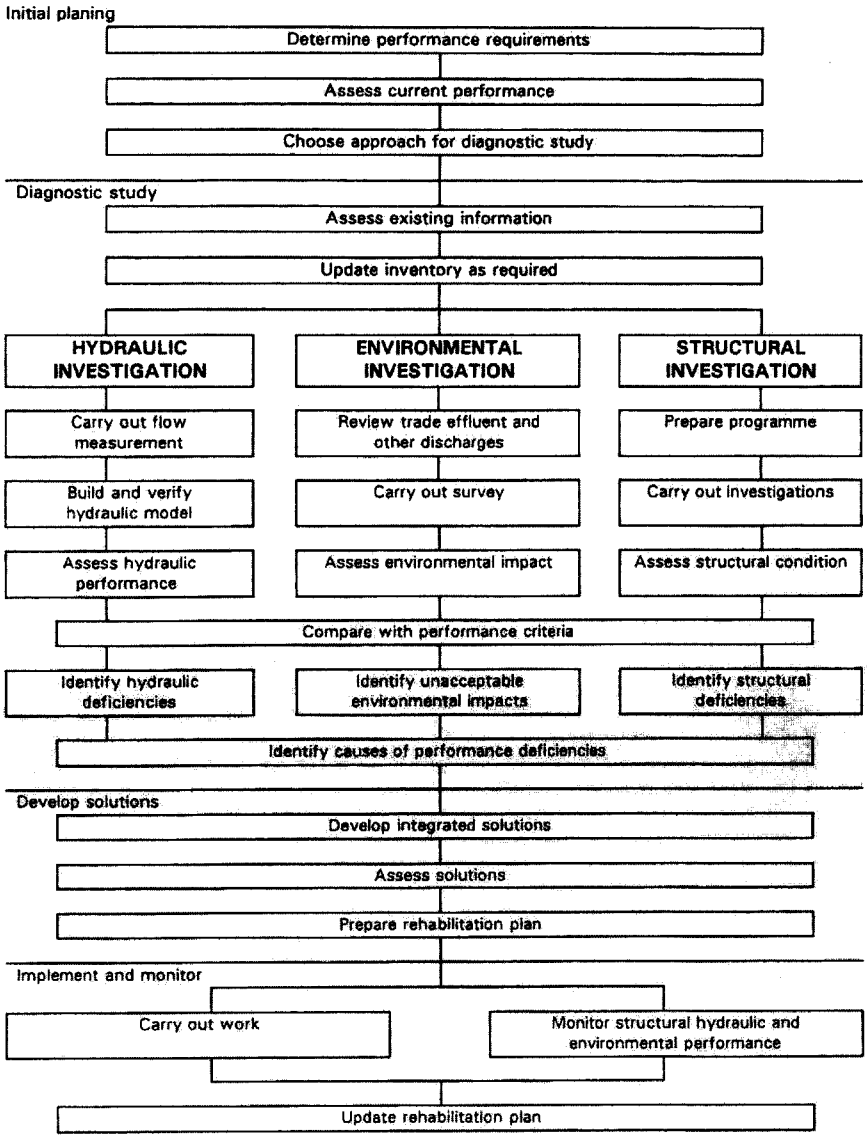

Figure 1.4 Activities related to sewer system management (NEN-EN 752-5).

Figure 1.4 presents the activities related to sewer operation and maintenance as described in NEN-EN 752-2. It consists of four main activities: investigation (inspection, calculation, etc.), assessment of performance/condition, development of solutions and preparation and implementation of interventions. In the chart three

different tracks can be distinguished, i.e. hydraulic, environmental and structural assessment.

Assessments consist of both calculations and inspections. Hydraulic performance (overflows and flooding) is assessed on the basis of calculations, whereas the results of visual inspections (possibly combined with prediction of service life) determine whether rehabilitation of the structural condition is needed. Adding pollutant concentrations to CSO volumes would enable the quantification of environmental impacts. However, the possibilities of environmental assessment remain limited due to scarcity of measurement data and limited knowledge of processes. Such an approach is, therefore, not included in standard procedure in The Netherlands. The results of the three assessments can only be combined on the basis of expert knowledge. However, the larger the sewer system, the more complicated this task becomes.

To evaluate the hydraulic performance of a sewer system two criteria are of importance: the discharge capacity of the system under extreme storm conditions and the storage capacity of the system using a continuous rainfall series. Sufficient discharge capacity prevents flooding in residential areas, while sufficient storage limits emissions of polluted wastewater to natural watercourses. A sewer flow simulation model is necessary in order to understand the hydraulics of the system. In 'Leidraad Riolering' (Stichting RIONED 1999) the Dutch guidelines for hydrodynamic calculations of sewer systems are described, providing the basis for assessments of storage and discharge capacity. An introduction to the guidelines is given in Van Mameren and Clemens (1997) and Van Luijtelaar and Rebergen (1997).

The structural condition of sewers, on the other hand, should not hamper the required system performance regarding watertightness, stability, flow (gradient), pollution and public health (NPR 3398, NEN 3399 and Stichting RIONED 1997a). Maintenance and rehabilitation, therefore, intend to maintain the operational functions, as well as to extend the service life of a sewer system. NPR 3398 covers the inspection and condition assessment of sewers, whereas NEN 3399 provides a coding system for the visual inspection of sewers. A description of selection methods for interventions and of implementation techniques can be found in the Dutch guidelines (Stichting RIONED 1998) and Stein (2001).

1.3.1 Management regarding hydraulic performance

Traditionally, the hydraulic capacity of sewer systems was designed using a constant rainfall intensity of 60 l/s/ha in flat areas and 90 l/s/ha in sloping areas. Maximum in-sewer water levels of 0.2 m below ground level were accepted (Van Luijtelaar 1999). A few years ago, however, a new approach based on the Dutch guidelines (Stichting RIONED 1999) has been introduced. This approach calculates the response of a sewer system to 10 synthetic design storms with return periods between 0.25 and 10 years (example in Figure 1.5) using a hydrodynamic model. These synthetic storms were derived from the rainfall time series from De Bilt, The Netherlands (1955-1979). The

required return period, however, is not prescribed, but for flooding a return period of 2 years is generally considered acceptable (Clemens 2001a). Moreover, based on IDF (intensity-duration-frequency) analysis Vaes *et al.* (2002) doubt if the design storms can represent actual rainfall events.

The new European standard (NEN-EN 752-4) calls for a different approach regarding flooding and is to be adopted in The Netherlands. Surcharge and flooding frequencies (see Table 1.1) are the basis for the sewer design simultaneously considering backwater effects. A sewer system based on this standard should protect against surcharging of sewers and flooding of streets and buildings resulting from storms with the frequencies recommended in Table 1.1. This means that the flooding criterion relates to a maximum water level in a manhole. The frequencies to be used depend on the specific use of the area studied.

However, Van Luijtelaar (1999) emphasises that these surcharge and flooding criteria cannot be met in flat areas like The Netherlands because the difference between ground level and surface water level is relatively small (see Figure 1.6). In flat areas, depression storage contributes considerably to the total storage volume reducing flooding problems. However, this is not accounted for in the European standard. Therefore, Van Luijtelaar (1999) argues that the storage required to cope with extreme storm events is provided by depression storage in flat areas instead of in-sewer hydraulic capacity.

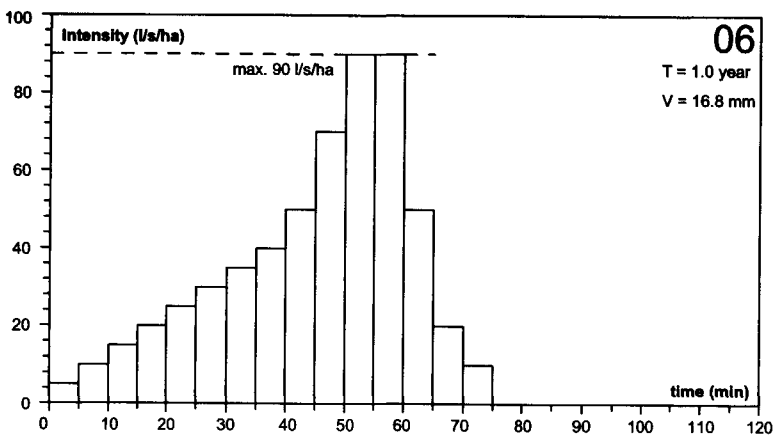

Figure 1.5 Design storm event no. 6 (Stichting RIONED 1999).

Table 1.1 Recommended design frequencies of NEN-EN 752-4.

	Design storm frequency SURCHARGING	Design storm frequency FLOODING
Rural areas	1 in 1 year	1 in 10 years
Residential areas	1 in 2 years	1 in 20 years
City centres, industrial/commercial areas		
with flooding check	1 in 2 years	1 in 30 years
without flooding check	1 in 5 years	-
Underground railway/underpasses	1 in 10 years	1 in 50 years

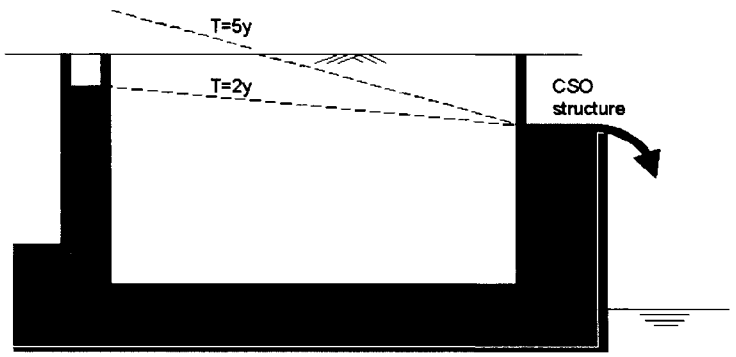

Figure 1.6 Hydraulic gradient resulting from calculations with different design storms (T=2 years and T=5 years). The once in 5 years storm event causes flooding.

The approach to deal with the environmental impacts of Dutch sewers, on the other hand, originates from two international agreements. These agreements aim at reducing pollution loads by 50% compared to the 1985 situation: the North Sea Action Plan (NAP) and the Rhine Action Programme (RAP).

In terms of overflows from sewer systems the required pollutant reduction has been translated into a 'reference system' which is defined as follows: "A combined sewer system should emit a pollution load less than or equal to that from a theoretical sewer system with 7 mm in-sewer storage, 2 mm additional storage in a settling facility and a pumping capacity equal to 0.7 mm/h plus the dry weather flow." (CUWVO Werkgroep VI 1992). However, with this 'reference system' the discharge limits remain poorly defined because the determination of pollution in overflow volumes is not outlined. In order to solve this problem the reference system has been recently redefined considering pollutant loads (CIW 2001). The new standard is expressed in terms of kilograms COD (chemical oxygen demand) discharged to the receiving waters per ha contributing area and per year. The discharge limit is fixed on 50 kg COD/ha/a.

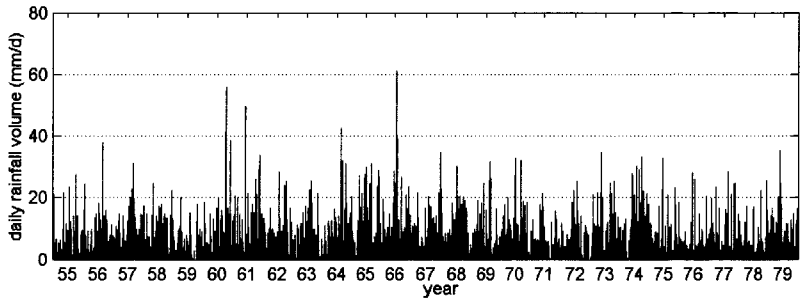

Figure 1.7 Rainfall series De Bilt 1955-1979 (daily rainfall volumes [mm/d]).

Assessment of sewer overflows requires application of a long time series of rainfall to determine return periods of overflow volumes, peak discharges, etc. The Dutch guidelines prescribe the series to be used: a continuous series of rainfall volumes as observed with an interval of 15 minutes in De Bilt, The Netherlands, during the years 1955-1979 (Figure 1.7). However, no specific software package is prescribed for building the hydrodynamic model of the sewer system. The modelling gives a time series of CSO events with a certain volume of which the return periods can be determined.

Summarising, single events with a specific return period are applied for the assessment of the hydraulic capacity. The storm event to be used is chosen on the basis of its return period. Thus, only extreme situations of rainfall are considered and it is impossible to determine the return period of a flooding event. However, it can be doubted whether these events are typical of actual rainfall patterns in The Netherlands.

In contrast, studying the performance of CSO structures requires the use of a continuous rainfall series of a certain length, taking into account the interdependency of storm events and dry periods and enabling the calculation of return periods of the effects of medium and heavy storms. However, the pollutant loads of sewer overflows remain uncertain, since the prevailing pollutant concentrations in overflow volumes are unknown and the knowledge of determinative processes is limited.

1.3.2 Management regarding structural condition

Sewer performance is influenced by the structural condition of the objects of which the systems consist. For example, blockage of an inverted siphon obstructs the sewer flow (see e.g. Stein 2001), corrosion of the wall of the sewer due to H_2S formation increases the probability of pipe collapse (see e.g. Davies *et al.* 2001a) and failures of sewage pumps affect the hydraulic performance of a sewer system with respect to CSOs (see e.g. NWRW 1989b and 1990, and Schwartz 1989). In order to assess the performance of a sewer system and to make decisions on possible solutions for deficiencies found, knowledge of the structural condition of the objects is indispensable.

Inspection is applied for pipe condition assessment. It concerns collecting data on the structural condition of objects in a sewer system and comprises observation, recognition, coding and assessment of the deterioration of sewers. Assessment can be carried out by e.g. prediction of remaining service life or knowledge based modelling of transition of sewers between specified classes of sewer condition (Rostum *et al.* 1999, KEMA 2001, and Baur and Herz 2002). Subsequently, possible interventions in order to correct observed deficiencies are developed. Interventions include cleaning, repair, renovation and replacement (NEN-EN 752-7). Their implementation is planned using decision support models, e.g. by means of a priority matrix (Kerkhof 1988) or more complex models (Fenner and Sweeting 1999, and Fenner and Saward 2002). In conclusion, inspection enables condition assessment and planning of interventions accounting for priorities of the management authority.

In The Netherlands, inspection methods and their use are described in NPR 3398. These guidelines also include the translation of inspection results into the necessity of implementing solutions. NEN-EN 752-6 describes the management required for pumping stations.

Several inspection methods are available, both visual and non-visual (see e.g. Stein 2001). Visual methods are inspection of the sewer either from the manhole or from within the sewer. It can be carried out by means of mirrors, photographic camera, remotely controlled CCTV (video), 'light line' visual methods or man entry. Each of these methods has its limitations, for example, the sight of photo inspections from a manhole is limited to 5 m and video inspections from within the sewer require prior cleaning, thus removing a possible sediment bed. 'Light line' visual inspection is based on generating a line of light around the sewer circumference, which enables the detection of changes in sewer shape. Only visual inspection methods are discussed in detail because they are most widely applied in The Netherlands and elsewhere.

Non-visual methods comprise, for example, measurement of the temperature of the sewage (high temperatures promote corrosion), the depth of the sediment bed, the acidity of condensation on the sewer wall (low pH enables biogenic sulphuric acid corrosion), the remaining thickness and acceptable loading of the sewer wall (analysis of cores bored from the wall), the internal cross sectional profile (high resolution sonar), the leaktightness of a pipe section, the groundwater level (infiltration or leakage). Acoustic methods, such as sonar, enable inspections below water level.

Examples of alternative techniques for diagnosing the condition of sewers are infrared thermography, sonic distance measurement and ground penetrating radar (see Wirahadikusumah *et al.* 1998). Other recent developments include the KARO system, a remotely controlled robot inspection system using various sensors (optical, ultrasonic and microwave), and the PIRAT system, a measuring system which combines laser technology and ultrasonic measurement to determine the inner geometry of sewers and classify their condition (see Fenner 2000 and Stein 2001).

Above water level, visual inspections can be used to determine the location, cause and extent of deterioration, i.e. blockage, pipe collapse, sediment or grease build-up, intruded tree roots, chemical corrosion or mechanical wear of the pipe, defective connections, open or displaced joints, cracking or fracturing of the pipe, deformation of the pipe, leaktightness of the pipe or connection and soil erosion outside the pipe wall. In addition, the quantity and composition of sewage, the condition and age of the pipe, the soil type, the groundwater table and the traffic volume in the street give an indication of the load and the carrying capacity of the sewer.

To enable objective recording and comparison of visual information from inspection guidelines NEN-EN 752-5 and NPR 3398 recommend the use of a uniform standard coding system. In The Netherlands, the coding system is specified in NEN 3399 and mainly applies to concrete sewers. It provides a methodology for the coding of inspection results with respect to watertightness, pipe stability and flow. Different types of observations are distinguished (Table 1.2). Each observation is classified on a scale from 0 to 5 according to its severity (0 = not visible, 1 = least severe/not present and 5 = most severe). The observation type with the highest classification is indicative for a pipe section. Whether interventions or additional investigations are necessary is assessed on the basis of this classification.

Table 1.2 Coding of observations according to Dutch guidelines (NEN 3399).

	Observation type		Classification *
LEAKTIGHTNESS	A1	infiltration of groundwater	1, 2, 3, 4 or 5
	A2	ingress of soil from surrounding ground	1, 2, 3, 4 or 5
	A3	longitudinal displacement	1, 2, 3, 4 or 5
	A4	radial displacement	1, 2 or 5
	A5	angular displacement	1 or 5
	A6	intruding sealing ring	1, 3 or 5
	A7	intruding sealing material	1, 2, 3, 4 or 5
STABILITY (pipe wall)	B1	break/collapse	1 or 5
	B2	surface damage by corrosion or mechanical action	1, 2, 3, 4 or 5
	B3	fissure (cracks and fractures)	1, 2, 3, 4 or 5
	B4	deformation of cross sectional shape	1, 2, 3, 4 or 5
FLOW (gradient)	C1	intruding connection	1, 3 or 5
	C2	root intrusion	1, 2, 3, 4 or 5
	C3	fouling	1, 2, 3, 4 or 5
	C4	encrustation of grease or other deposits (except for sand)	1, 2, 3, 4 or 5
	C5	settled deposits (sand and waste)	1, 2, 3, 4 or 5
	C6	other obstacles	1, 2, 3, 4 or 5
	C7	water level	1, 2, 3, 4 or 5

* Classification code '0' indicates 'not visible' (e.g. due to high water level or root intrusion).

At present a new European coding system is being developed (pr EN 13508-2). It is a standard for the coding of information from visual inspection of drain and sewer systems. Its objective is to harmonise sewer inspections because at present the amount of detail recorded varies between countries. Standard pr EN 13508-2 tries to ensure that there is an equivalent code for every observation recorded in an existing national system, allowing for existing data to be transferred. After completion this standard will have to be implemented in The Netherlands, calling for additional training of inspection personnel.

NPR 3398, NEN 3399 and pr EN 13508-2, however, only define performance requirements of sewers. Requirements for the other objects in the sewer system, e.g. manholes, gullies, gully pots, pumping stations, outfalls, rising mains, overflows, inverted siphons and valves, are not provided. However, they contribute considerably to the performance of a sewer system. For example, problems with respect to manholes include defective covers, problems with access due to defective ladders, chemical attack of the fabric, infiltration or leakage, sediment build-up and oxygen deficiency or odour issues. The main problems with inverted siphons are sedimentation and blockage. Problems associated with pumping stations comprise blockage of pumps, valves and screens, power failure, failure of the rising main and electrical or mechanical failure of a component of the pump or its control equipment. With respect to gullies and gully pots falling leaves in autumn and blossoms in spring give rise to problems. Therefore, municipalities need to define requirements for the other objects (manholes, pumps, valves etc.) themselves in order to assess their performance and prevent problems due to their malfunction.

The purpose of a sewer inspection determines its requirements, such as accuracy of inspections, number of manholes or sewers to be inspected and frequency of inspections. Prioritisation of sewer maintenance requires a representative sample of sewers from the network. Especially operational planning asks for detailed and relatively accurate information (NPR 3398). It is also important to inspect a sufficient number of manholes. Prior to inspection the manholes can be randomly chosen from either the whole sewer network or a specific category of sewers. These categories are defined on the basis of sewer characteristics including age, function, pipe material and soil type. Usually, a sample of 10-20% of the total number of manholes is sufficient (NPR 3398). The frequency of inspections is, on the one hand, determined by the quality of the assets and local conditions, on the other by hydraulic and structural performance criteria. This results in an average frequency of once in 5 to 10 years (NPR 3220). Inspection routines including frequencies and locations should take into consideration the importance of and possible threats to each asset, e.g. the gradient of pipelines, the risk of blockage of manholes and inverted siphons, the ageing of equipment in pumping stations, the frequency of overflows and the seasonal problems with gullies or gully pots (NEN-EN 752-7).

1.4 UNCERTAINTY AND RISK ASSOCIATED WITH SEWER SYSTEM MANAGEMENT

The long service life of sewers requires management that can cope with future situations. However, future developments with respect to the sewer infrastructure, e.g. population growth and climate change can be easily either over- or underestimated. The extent to which future developments are unknown increases with time (Figure 1.8). On the other hand, it is likely that uncertainties, which confront planners, will be resolved over the course of time by new information or new technologies. Furthermore, the precautionary principle (European Environment Agency 2001) applies very often. It is aimed at avoiding potentially damaging impacts of substances that are persistent, toxic or liable to accumulate, even when there is no scientific evidence of a causal link between emissions and effects. As a result, policy-making with respect to infrastructures can be highly uncertain (see e.g. Hall 1980 and Meijer and Ruijgh-van der Ploeg 2001). Management of infrastructures, such as sewer systems, should be future oriented, accounting for possible uncertainties in its strategies and allowing for interim adaptation (Walker *et al.* 2001).

Over the last decades the idea of coping with present and future uncertainties has been increasingly adopted in infrastructure design. For example, the Delta Committee included uncertainties in their investigations on flood prevention in The Netherlands already in the late fifties of the last century (see e.g. Van Dantzig 1956). Bedford and Cooke (2001) present illustrations from other sectors, including the aerospace, nuclear and chemical process sector. In the aerospace sector, for example, a systematic concern with risk assessment began after the fire of the Apollo test AS-204 on January 27, 1967, in which three astronauts were killed. The analysis of uncertainties has its roots in the mathematical sciences and is described in many textbooks, such as Benjamin and Cornell (1970), Ang and Tang (1984) and Pratt *et al.* (1995).

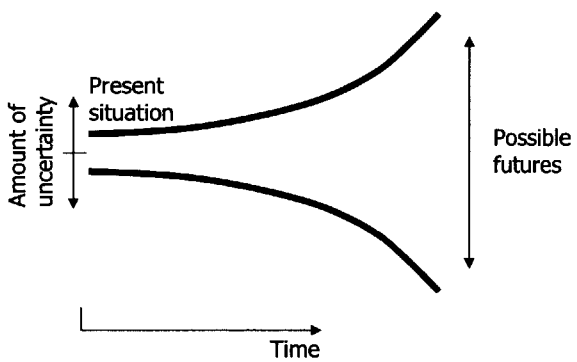

Figure 1.8 The 'trumpet of uncertainty' (after Rosenhead 1989). The extent to which the future is unknown or unknowable increases with time.

Although risk assessment is a well-established discipline in e.g. dike design and production plant design, it is not common in sewer infrastructure design, operation and rehabilitation. For example, spatial variability in rainfall and risk of technical failure of a pumping station are not included in sewer design and rehabilitation. In addition, the costs of damage due to overflows and flooding are highly uncertain.

Only recently, attention is being paid to the role of uncertainty in urban drainage (see e.g. Beck 1996, Willems 2000 and Harremoës 2002) because the transient character of the urban wastewater system is increasingly recognised. The introduction of wastewater control infrastructure has removed society's diurnal and weekly effects from surface waters, consequently diverting attention to more rare and predominantly more extreme events. As a result, there is an increase in concern for the long-term reliability of the wastewater control infrastructure (Beck 1996 and Harremoës 2002). Recent increases in computer capacity, however, provide opportunities for computationally demanding uncertainty analyses. For example, when it comes to impacts on receiving waters, risk-based approaches are used to some extent, including CSO (Grum and Aalderink 1999 and Willems 2000) and wwtp emissions (Vanrolleghem and Keesman 1996, Reda and Beck 1997, Rousseau *et al.* 2001 and Bixio *et al.* 2002), water quality criteria such as dissolved oxygen depletion (Beck 1996 and Hauger *et al.* 2002) and the assessment of ecotoxicological risks (Novotny and Witte 1997, and Verdonck *et al.* 2001).

1.4.1 Approaches to design and operation

Through the years the approach to design and operation of (infra)structures has changed from an empirical, iterative approach to a deterministic, predictive approach (Harremoës and Madsen 1999, and Harremoës 2002). The empirical approach is based on 'trial and error', the deterministic approach uses specific safety factors to meet design criteria. Using the former, remarkable engineering has been accomplished, e.g. Roman aqueducts, drainage in ancient Greece and medieval gothic cathedrals. However, the road to this success has been paved with many mistakes, such as the leaning tower of Pisa and the introduction of chemicals that mistakenly were regarded as harmless, such as asbestos and halocarbons (European Environment Agency 2001). The empirical approach attempts to develop knowledge of all elements of a structure, so that the performance of the structure is predictable. This produces structures designed to meet predetermined requirements.

In order to cope with uncertainty, for example, regarding system loading and knowledge of effects, the deterministic predictive approach uses safety factors. The magnitude of a safety factor evolves historically, from high values when a technology is just starting to gradually lower values till a lower ceiling is reached. Both common sense and successful or unsuccessful experience determine its value. Table 1.3 shows that, for example, in 70 years the allowable stress for mild steel increased with approximately 60% in the United States. This is due to improved quality control in the mills resulting in an increase of minimum strength and increased confidence in the design process due to experience resulting in a decrease of safety factors (Galambos 1992).

Table 1.3 Evolution of the allowable stress for mild steel structures in the USA (Galambos 1992).

Year	Minimum strength (N/mm^2)	Safety factor (-)	Allowable stress (N/mm^2)
1890	197	2.00	97
1918	190	1.72	110
1923	228	1.83	124
1936	228	1.65	138
1963	248	1.67	152

FC = Safety factor

Design criterion:

$$\sigma \leq \sigma_{allowable} = \frac{\sigma_{limit}}{FC}$$

1.4.2 Role of uncertainties in sewer assessment

Decision-making on sewer system management requires the use of models to predict compliance with performance criteria because measurements are usually unavailable. Butler and Davies (2001) emphasise that the accuracy and usefulness of a model is influenced by the extensiveness of the model, the reliability and completeness of the scientific knowledge on which it is based and the appropriateness of its simplifications. Therefore, each assessment contains a certain measure of uncertainty because it is based on either calculated CSO loads and flooding events, or predicted condition and remaining service life of sewer assets. The question that arises is which elements in the assessment of sewer systems should be acknowledged as uncertain and to what extent are decisions sensitive to these uncertainties.

Uncertainties can be part of the external inputs or the sources, the system itself or the pathway and the impacts of the functioning of the system or the receptors (European Environment Agency 1999). This is illustrated in Figure 1.9. Sources comprise a wide range of relevant driving forces, whereas receptors reflect the interests of parties that depend on the performance of the system. All uncertainties may give rise to wrong decisions.

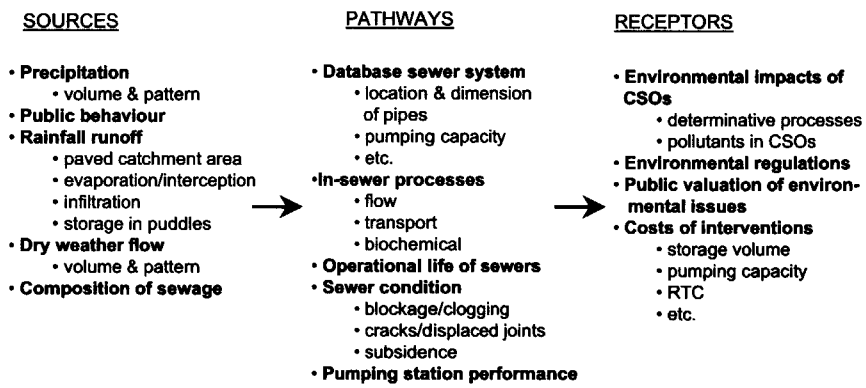

Figure 1.9 Uncertainties influencing sewer system assessment comprise uncertainty of sources, pathways and receptors.

Uncertainties in sources (Figure 1.9) may result from rainfall measurement errors (Rauch *et al.* 1998), spatial and temporal variability in rainfall (Schilling and Fuchs 1986, and Lei and Schilling 1996, Einfalt *et al.* 1998 and Willems 1999), variation in dry weather flow (dwf) due to varying inputs from households (Butler 1991 and Butler *et al.* 1995) and leaking groundwater (Murray 1987 and Clemens 2001a).

Due to the strongly simplified way in which the rainfall runoff process is described in the model, uncertainty is introduced. Variability of runoff in time and local differences in runoff parameters (initial losses, infiltration, etc) is not taken into account and knowledge of processes is insufficient (Van de Ven 1989 and Clemens 2001a).

Descriptions of a sewer system through models are imperfect because the physical phenomena are not exactly known and some variables of lesser importance are omitted for efficiency reasons. This results in model uncertainty with respect to hydraulics (Beck 1996, and Lei and Schilling 1996) and in-sewer processes determining sewage composition (Ashley *et al.* 1999 and Langeveld 2004). Model uncertainties may also stem from estimation or calibration of model parameters (Price and Catterson 1997, and Clemens 2001a) and numerical calculation errors (Clemens 2001a).

In addition, the data set applied in a sewer model is never entirely perfect. Data errors (geometric structure of the sewer system, catchment area, runoff parameters, etc.) considerably influence calculation results (Price and Osborne 1986, and Clemens 2001a).

Hydraulic performance, however, is assessed assuming perfect technical functioning of all objects in a sewer system leading to uncertainty in model assumptions. For example, risk of technical failure of pumping stations, subsidence and deterioration of sewer pipes, and clogging of culverts are not taken into consideration. Moreover, the influence of time dependent sewer deterioration is not accounted for in hydraulic sewer assessments. Except for biogenic sulphuric acid corrosion of sewer pipes (Bielecki and Schremmer 1987), there are no reliable models describing sewer deterioration because knowledge of deterioration processes, for example, clogging, root intrusion, fouling, ingress of soil and longitudinal or radial pipe displacement is limited (Davies *et al.* 2001a). In addition, factors that impact the structural condition of a sewer the most (including soil type, sewer material and joint type) are only partly known (Davies *et al.* 2001b).

Assessment of sewer deterioration is usually performed by means of visual inspection and coding of observations. The assumed relationship between observations and actual structural deficiencies, however, is debatable and the ability of a coding system to represent deficiencies can be questioned. Moreover, coding of photographs and CCTV pictures by inspection personnel entails the possibility of misinterpretation. The inspection methods themselves also impose restrictions (Stein 2001), for example, limited sight for inspections from manholes and necessary cleaning of sewers prior to CCTV inspection from within the sewer pipe. As a result, prediction of the remaining operational life of sewers depends highly on the limitations of the assessment method.

With respect to receptors (Figure 1.9, right), it is generally accepted that the quality of natural watercourses deteriorates due to CSOs (see e.g. House *et al.* 1993) and urban flooding causes damage, including damage to buildings and disruption of traffic. Deterioration comprises water quality changes (dissolved oxygen, polluted sediments, etc.), human health risks and aesthetic contamination (floating waste, algal growth, etc.). The consequences of urban flooding consist of direct damage (material damage to roads or buildings, and loss of human or animal life), indirect damage (administrative and labour cost), and social or psychological consequences (König *et al.* 2002 and Penning-Rowsell *et al.* 2003).

However, the severity of CSOs is uncertain because CSOs are intermittent loads and their composition strongly varies (Beck 1996). Measurement data of pollution loads from sewers are unavailable and current sewer models are unable to predict them (Ashley *et al.* 1999). Moreover, translation of uncertain pollutant loads to effects on natural watercourses and their ecology is problematic because the knowledge of water quality processes is rather limited and the resilience of receiving water bodies is uncertain (Shanahan *et al.* 1998 and Harremoës and Madsen 1999). Therefore, environmental regulations based on available knowledge also incorporate uncertainties.

The valuation of environmental effects may also give rise to uncertainties in sewer assessments. Some authors claim that environmental effects can be quantitatively capitalised (see e.g. Crabtree *et al.* 1999 and Novotny *et al.* 2001). Others, on the other hand, are opposed to this approach and value the effects in a more qualitative way (see e.g. Nijkamp and Van den Berg 1997, Reda and Beck 1997, and Gilbert and Janssen 1998). An example of the former is the 'Contingent Valuation Method' as applied to urban water management by Novotny *et al.* (2001) which explores the public 'willingness to pay' for environmental restoration projects. Authors supporting the more qualitative approach, however, stress that quantitative valuation is unable to take into account uncertain and imprecise information that plays an important role in environmental impact modelling.

With respect to urban flooding, for example, the cost of direct damage to buildings and their interior can be estimated based on data from insurance companies relating historical floods to corresponding damages. However, these damage cost may vary widely with standard deviations in the order of the average damages (König *et al.* 2002). As a result, the benefits of rehabilitation are difficult to quantify with respect to both CSOs and flooding.

The environmental standards for sewer systems show changes during the last 60 years in The Netherlands. They evolved from a required dilution of the wet weather flow (wwf) (Van den Akker 1952), to a calculated maximum overflow frequency per year (Ribius 1951), then to restrictions with respect to calculated overflow volumes (CUWVO Werkgroep VI 1992) and, only recently, overflow loads (CIW 2001). Parallel to these emission based criteria, an immision based approach to water quality assessment has been developed based on the impacts of CSOs on receiving waters (CUWVO

Werkgroep VI 1992). This 'Waterkwaliteitsspoor' may impose additional measures on CSOs compared with current emission-based standards.

In addition, because of the long service life of sewers (30-60 years), future developments significantly influence the system performance, not only developments in system input, but also in public perception and policy-making. There are several examples of infrastructure designs that failed to meet a change in the demand for the goods or services it supplied (Hall 1980). Future developments with respect to sewer assessment include deterioration of sewers, change of regulations, climatic change, change of public perception of the environment and development of receiving water quality.

1.5 OBJECTIVE OF THE THESIS

Management of sewer infrastructure concerns a trade-off between required serviceability and scarce financial resources. Serviceability of sewer systems, defined as "The ability of an asset to deliver a defined service to customers", concerns preventing flooding and protecting public health, provided that the environment is safeguarded. In The Netherlands, annual investments in sewer system rehabilitation comprise approximately 1 billion Euros and the total sewer infrastructure is valued at approximately 47.5 billion Euros (Stichting RIONED 2002). In the near future, a large length of sewers will require rehabilitation in The Netherlands because 22% of the sewers is older than 40 years (Stichting RIONED 2002) and their average service life is approximately 60 years. In The Netherlands, it is acknowledged that current environmental standards for sewer systems call for major adjustments in sewer infrastructure. Therefore, the amount of money invested in sewer rehabilitation will remain large in the future.

The technical functioning of all objects in the sewer system is directly responsible for affecting serviceability (OFWAT 2001, Korving 2003a and Korving *et al.* 2003). However, with respect to management of sewer systems, uncertainty of knowledge and availability of assets are not considered. For example, in model results, on which decisions are based, uncertainties can be present due to spatial and temporal variability in rainfall, errors in the geometrical database of the sewer system, errors in the model structure chosen, lack of knowledge on the relevant processes and numerical calculation errors. Moreover, the hydraulic performance and structural condition of a sewer system are usually assessed separately (NEN-EN 752-5), i.e. failures of pumping stations, subsidence of sewer pipes and clogging of culverts are ignored when modelling hydraulic performance.

Usually, serviceability is assessed assuming perfect technical functioning of all objects in the system. As a consequence, the risks of technical failure of assets and uncertainties in information are ignored, leading to a too optimistic perception of serviceability. However, unavailability of assets and uncertainty of sources, pathways and receptors should be accounted for when assessing sewer serviceability (OFWAT 2001, Ashley and

Hopkinson 2002, and Korving 2003a). In the UK 'Common Framework for Capital Maintenance Planning', failure of assets has already been accounted (UKWIR 2002).

When it comes to uncertainties with respect to sewer performance uncertain damage appears to be caused by an uncertain source. In order to deal with this situation, firstly, the uncertainty needs to be quantified. Subsequently, the extent to which performance is affected can be reduced using the knowledge of this uncertainty.

The objective of this thesis is to provide a methodology which accounts for uncertainty and risk in the assessment of sewer performance in order to support the operation and maintenance of sewer systems.

A key aspect of the thesis is serviceability of sewer systems accounting for uncertainties in knowledge and possible failure of assets. The interrelationship of the different aspects influencing sewer performance (e.g. rainfall, dwf, asset performance and sewer characteristics) is studied in order to describe the way in which they affect each other and the performance of the system as a whole. In order to account for the consequences of uncertainty and failure, criteria for sewer system performance are needed. So far, several attempts have been made to develop appropriate performance criteria, e.g. Ashley and Hopkinson (2002), Geerse and Lobbrecht (2002), Le Gauffre *et al.* (2002) and Sægrov Schilling (2002) and Matos *et al.* (2003).

1.6 OUTLINE OF THE THESIS

In this thesis two parts are distinguished. The first part deals with the theoretical basis of the assessment of uncertainty and risk and the second focuses on the application of this theory in several case studies concerning hydraulic performance and structural conditions of sewers.

Chapter 2 presents the different types of uncertainty and categorises the uncertainties playing a role in sewer system design and rehabilitation. Classification of the uncertainties is required, since reduction of each type of uncertainty requires its own approach. In addition, specific ways for how to deal with uncertainties in sewer design and rehabilitation are shown.

Methods of uncertainty and risk analysis, which can be applied in sewer system design and rehabilitation, are discussed in Chapter 3. The presented methods include decision analysis, Monte Carlo simulation, risk-based economic optimisation, Bayes weight assessment, Bayesian estimation and fault trees. They are aimed at quantifying uncertainty and failure with respect to sewer system performance and describe their interrelationship.

Chapters 4 and 5 present the case studies where specific methods are applied to assess the hydraulic performance and structural condition of sewers. These chapters focus on the serviceability of sewer systems and the way in which this concept can be applied in practice. Serviceability should account for relevant uncertainties and failures, and reflect the cost consequences of decisions on sewer management.

With respect to hydraulic performance, the way in which this is affected by uncertainties of rainfall input, model parameters and model calibration is studied in Chapter 4. Subsequently, the influence of uncertain cost and damage on optimal storage of a sewer system is explored using risk-based optimisation. Chapter 5 discusses the impact of asset condition on serviceability with respect to possible pump failure and accuracy of coding of visual inspections.

Finally, in Chapter 6, the content of this thesis is summarised, general conclusions are drawn and considerations are made about the role of probabilistic techniques in the assessment of sewer system performance.

CHAPTER 2 Uncertainties

2.1 INTRODUCTION

Annually, approximately 1 billion Euros is invested in sewer system rehabilitation in The Netherlands (Stichting RIONED 2002). In some cases, however, the appropriateness of investments in sewer rehabilitation is doubtful because decisions on investments in sewer rehabilitation often have to be made with unreliable or incorrect information on the structural condition and the hydraulic performance of a sewer system (Clemens 2001a), and with insufficient knowledge of sewer-related processes (Harremoës 2002). For example, replacing a sewer length that appears to be of sufficient structural quality after removal, building a storage tank that is too large to ever be filled during a storm, or real-time control of a sewer system that does not function properly with respect to hydraulics. As a consequence, making decisions on such investments involves considerable financial risks.

In the past, uncertainty and risk analysis in sewer system maintenance and rehabilitation received limited attention. Only recently, the importance of uncertainty and risk is recognised by an increasing number of authors. For example, Schilling (1984), Schilling and Fuchs (1986), Harremoës (1994), Fankhauser (1997), Grum (1999), Willems (2000) and Clemens (2001a) pay attention to uncertainties in modelling and prediction of CSOs (combined sewer overflows), their effects on receiving waters and flooding. In other disciplines uncertainties have usually been studied more extensively. The results of these studies are partially applicable to uncertainty analysis regarding sewer system maintenance and rehabilitation. For example, error propagation and uncertainty analysis in hydrology is treated by Dawdy and Bergmann (1969), Chow *et al.* (1988) and Høybye and Rosbjerg (1999). Beck (1987), Høybye (1998) and Portielje *et al.* (2000) discuss uncertainty regarding modelling of receiving water quality.

Risk is defined as the product of the probability of occurrence of an event and its (capitalised) consequences. It is related to the failure of systems. A sewer system fails if it can no longer perform (one of) its principal function(s), i.e. protection of human health, prevention of flooding and reduction of CSO impacts on the environment. A failure mode is defined as the manner in which a structure responds to a hazard, e.g. clogging of a sewage pump due to advection of dirt. A combination of one or several hazards and modes may lead, with a certain probability, either to failure or collapse (CUR 1990). Failure is also referred to as serviceability or deficiency of the sewer system (e.g. OFWAT 2001, Ashley and Hopkinson 2002, Le Gauffre *et al.* 2002, and Sægrov and Schilling 2002).

This chapter discusses the uncertainties which affect sewer system maintenance and rehabilitation. In particular, it is important to discern between different types of

uncertainty to get an impression of how to deal with their influence on sewer system maintenance and rehabilitation individually.

Firstly, several types of uncertainty are presented. Secondly, the reviewed theory on uncertainties is translated to sewer system management. Both hydraulic performance and structural condition are discussed. In conclusion, ways on how to cope with uncertainty (e.g. Bayes weight assessment) are described.

2.2 VIEWS ON UNCERTAINTY

In the literature many authors have addressed the classification of uncertainties. However a large variety of types exists and there is a lack of agreed terminology. Therefore, not only are uncertainties classified differently in the available methods, but different terms are also used to characterise more or less the same concept. Moreover, the methods presented to manage uncertainty also differ.

For example, Beck (1987) reviews the role of uncertainty in water quality modelling and prediction. Three types of uncertainties are identified:

- uncertainty in internal system description (e.g. errors of aggregation, numerical errors, errors of model structure and errors in parameter and state estimation),
- uncertainty in external system description (unobserved input disturbances and measurement errors) and
- uncertainty in initial state of the system.

This framework is also applied by Willems (2000).

Morgan and Henrion (1990) make a distinction between uncertainty with respect to empirical quantities and uncertainty about the functional form of models. The former arise from statistical variation or random error, subjective judgement or systematic error, linguistic imprecision, variability, inherent randomness or unpredictability, disagreement among experts, and approximation errors. Funtowicz and Ravetz (1990) argue that experts to identify impacts of uncertainty on their practice normally apply a classification by sources. In their opinion, uncertainties should be distinguished into three sorts, instead of sources, including inexactness, unreliability and 'border with ignorance'.

With reference to the afore-mentioned classifications, supplemented with a few others, Van der Sluijs (1997) proposes a two-dimensional classification using the dimensions type and source. For this, uncertainty is classified according to its source in uncertainty in input data, uncertainty in conceptual or technical model structure and uncertainty about model completeness. Uncertainties in model structure arise from lack of understanding of the system or process, simplifications and numerical errors, whereas uncertainty about model completeness covers omissions due to lack of knowledge. Regarding the type of uncertainties, the classes comprise inexactness, unreliability and ignorance.

Table 2.1 Two-dimensional classification of uncertainties after Van der Sluijs (1997)

Source \ Type	INEXACTNESS	UNRELIABILITY	IGNORANCE
INPUT DATA			
CONCEPTUAL MODEL STRUCTURE			
- parameters			
- functional relations			
- process error			
- resolution error			
- aggregation error			
- model fixes			
- numerical error			
- software error			
- hardware error			
MODEL COMPLETENESS			

According to Slijkhuis *et al.* (1999) and Van Gelder (2000), uncertainty can be divided into two categories (depending on its sources):

- Inherent uncertainty (or natural variability) that originates from variability in nature and therefore represents randomness in samples (e.g. measured rainfall volumes).
- Epistemic uncertainty that originates from lack of knowledge of fundamental phenomena (e.g. rainfall-runoff processes).

Inherent uncertainty (Figure 2.1) represents the unpredictability of physical processes, such as rainfall. For example, even in the event of larger amounts of data, one cannot predict with sufficient accuracy the maximum rain intensity that will occur in a future period. Inherent uncertainty concerns variability in time (e.g. variations of rainfall intensities in time) and in space (e.g. fluctuations in local terrain slope or spatial variation in infiltration capacity).

Epistemic uncertainty (Figure 2.1) represents the lack of knowledge of the physics, e.g. on in-sewer processes (e.g. Ashley *et al.* 1999). The two main types of epistemic uncertainty are model uncertainty due to lack of understanding of physical processes or incorrect schematisation, and statistical uncertainty due to data insufficiency. In general, epistemic uncertainty is reduced as knowledge increases and more data becomes available. Statistical uncertainty is subdivided into statistical parameter and distribution uncertainties. Willems (2000) not only subdivides model uncertainty into model parameter uncertainty and model structure uncertainty, but also estimates these two types separately. Although this subdivision is useful to prevent overestimation of parameter uncertainties, other authors, including Bedford and Cooke (2001), emphasise that separate estimation of parameter and structure uncertainty is impossible.

Inherent uncertainty is also referred to as variability, or aleatory, stochastic, irreducible or type A uncertainty. Epistemic uncertainty is sometimes called subjective, reducible, type B or state of knowledge uncertainty.

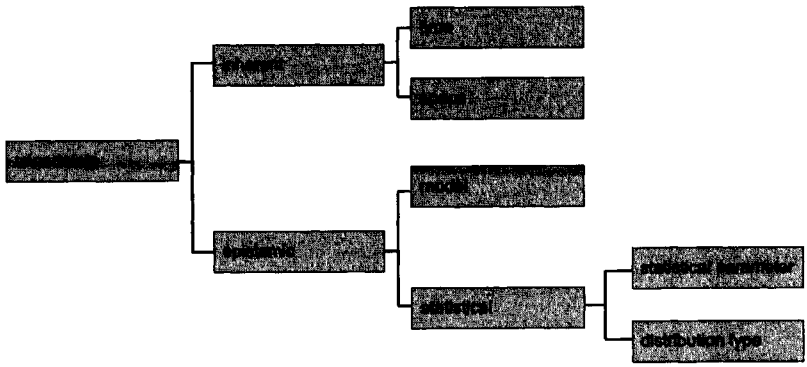

Figure 2.1 Types of uncertainty according to Slijkhuis *et al.* (1999) and Van Gelder (2000).

Both Hoffman and Hammonds (1994) and Cullen and Frey (1999) make a strict distinction between variability and uncertainty. Variability stems completely from differences in characteristics between individuals, i.e. quantities that are inherently variable over time, space or population. Uncertainty, on the other hand, is concerned with partial ignorance and includes model, parameter and scenario uncertainty. In their opinion, variability is a property of the system being studied, whereas uncertainty is a property of the observer.

Wynne (1992), however, questions the possibility of obtaining an objective definition of uncertainty and even disputes its quantifiability. In his opinion, perception of uncertainties is quite significant, but frequently overlooked. Therefore, he has introduced a categorisation based on knowledge of the outcome of system behaviour.

Uncertainties are classified on a scale ranging from certainty to ignorance (Figure 2.2) which is based on the (lack of) knowledge of probabilities and consequences (see also Rogers 2001):

- Certainty. All cause and effect relations are known and future system performance is predictable.
- Risk. System behaviour is understood and probabilities of failure can be predicted.
- Uncertainty. The important system parameters are known, however, their probability distributions are unknown.
- Indeterminacy. Probability, consequence or both are not known for a given event.
- Ignorance. Essential functional relationships are unknown, or as Wynne (1992) puts it "We don't know, what we don't know".

Equivalent classifications have been applied by several other authors, although their terminology is somewhat different (e.g. Funtowicz and Ravetz 1990, Harremoës and Madsen 1999, Meijer and Ruijgh-van der Ploeg 2001, Rogers 2001 and Harremoës 2003).

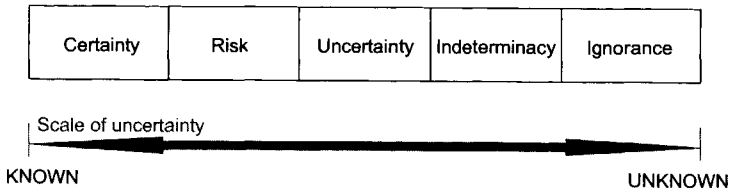

Figure 2.2 Scale of uncertainty ranging from certainty to total ignorance (adapted from Wynne 1992).

Bedford and Cooke (2001) define uncertainty as that which disappears when one becomes more certain. It differs from ambiguity, which must be removed before uncertainty can be meaningfully discussed, since uncertainty becomes contaminated when observations are described in an ambiguous language. Furthermore, they distinguish between aleatory and epistemic uncertainty. The former arises from natural variability in a system and is quantified by measurements or expert opinion. The latter, by contrast, arises from lack of knowledge of a system and cannot be measured.

Notwithstanding the practical significance of a distinction between uncertainties, Bedford and Cooke (2001) argue that its theoretical significance is limited. They claim that the same uncertainty in a different model with a different goal might be classified differently. As a consequence, the classification of an uncertainty is determined by the decision problem studied. Examples are presented in Hora (1996).

2.3 CLASSIFICATION OF UNCERTAINTY

In this thesis, the classification of Slijkhuis *et al.* (1999) and Van Gelder (2000) will be used because it enables the reduction of individual types of uncertainty. Although several authors argue that the theoretical significance of detailed classifications is limited or that classification is even impossible, it has proven to work rather well in practice (e.g. Van Gelder *et al.* 1997 and Van Noortwijk *et al.* 2001). The next paragraphs discuss the uncertainties as presented in Figure 2.1.

2.3.1 Inherent uncertainty

Inherent uncertainty represents randomness or variability in natural processes. The two main types of inherent uncertainty are inherent uncertainty in time and in space. It is sometimes also called natural variability.

2.3.1.1 Inherent uncertainty in time

Examples of inherent uncertainty in time regarding sewer rehabilitation are variations in rainfall intensities, dry weather flow (dwf), rainfall runoff, evaporation and infiltration. Inherent uncertainty, or natural variability, in time concerns future realisations of a process remaining uncertain. In other words, the fluctuations in time of the process are

not known in advance. Consequently, even unlimited data availability will not reduce this uncertainty.

The probability density function (PDF) and the auto correlation function describe a stochastic process in time (Figure 2.3). For example, the probability density function of rainfall intensity in time represents the probability of occurrence of certain rainfall intensities. When determining the probability distribution of stochastic processes in time, the problem of information scarcity arises because records are usually too short to ensure reliable estimates of events with relatively low probability of exceedance (Van Gelder 2000).

Inherent uncertainty in time is illustrated with the example of Figure 2.3. It describes the rainfall intensities measured in 1955 in De Bilt (The Netherlands) with PDF and auto correlation. If the probability of rainfall intensities is described with a lognormal PDF, the PDF of Figure 2.3 is obtained. The statistical parameters of the PDF are Maximum Likelihood estimates. In a lognormal PDF the natural logarithm of a variable is normally distributed. The PDF of a lognormal distribution is given in Appendix IV.

The correlation between rainfall intensities in time can be described with the auto correlation of the time series, which is defined as,

$$r_{x,k} = \frac{\frac{1}{n}\sum_{t=1}^{n-k}\left(x(t)-\mu_x\right)\left(x(t+k)-\mu_x\right)}{\sigma_x^{\,2}} \quad ,k = 0,1,2,... \tag{2.1}$$

where $r_{x,k}$ is correlation of rainfall intensities with time lag k, n is total number of data, $x(t)$ is rainfall intensity measured at time t, $x(t+k)$ is rainfall intensity measured at time $t+k$, μ_x is mean of rainfall intensities and σ_x is standard deviation of rainfall intensities. A large value of the auto correlation indicates a large correlation between measurements with a certain interval. The auto correlation is 1 for $k=0$. If the auto correlation drops fast with increasing k, a system has 'short memory'.

The PDF describes the number of times that rainfall intensities occur in the time series, the auto correlation gives an indication of correlation between subsequent rainfall intensities. Uncertainties in the data are transferred to the PDF and the auto correlation. Figure 2.3 shows that hardly any correlation exists between rainfall intensities with a time interval larger than 1 hour. Willems (2000) even suggests that precipitation can be considered as a purely random or white noise process.

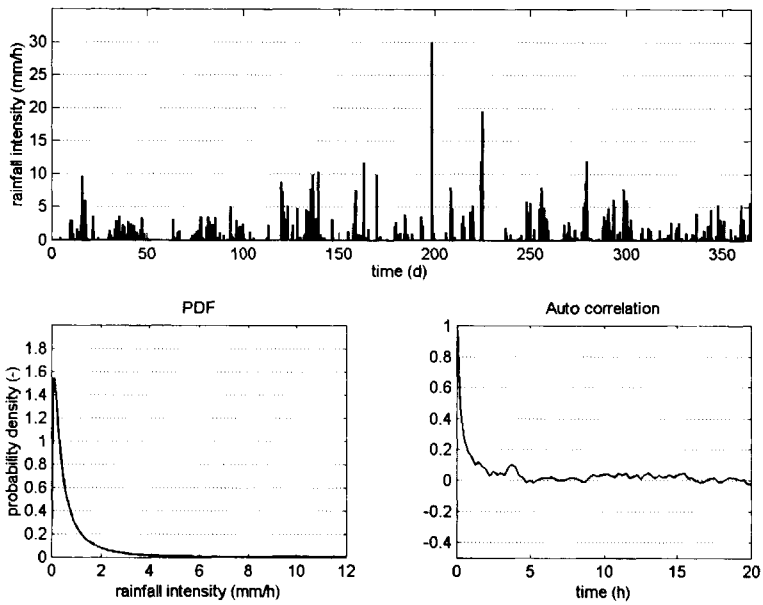

Figure 2.3 Example of inherent uncertainty in time. PDF and auto correlation completely describe a time series of rainfall intensities (measured in 1955 in De Bilt, The Netherlands). Uncertainties present in the data are translated to PDF and auto correlation.

2.3.1.2 Inherent uncertainty in space

The characteristics of inherent uncertainty in space differ from variability in time. When determining the probability distribution of stochastic processes in space (e.g. local variations in terrain slope), a problem of information scarcity is also present. It is usually too expensive to measure such quantities in great detail. However, taking more measurements as opposed to inherent uncertainty in time, reduces inherent uncertainty in space. Inherent uncertainties in space only have one realisation, whereas the ones in time have many (yearly) realisations. For example, a denser network of rain gauges reduces inherent uncertainty in space regarding precipitation. This does not simultaneously reduce its inherent uncertainty in time.

Local fluctuations in properties of (im)pervious areas can be regarded as stochastic processes in space. Other examples of inherent uncertainty in space with regard to sewer systems are sewer system geometry (sewer pipes, pumps, etc.), magnitude of contributing areas, local terrain slope, storage on street surface, not exactly horizontal position of weir crest. From field measurements the probability density function (PDF) and the spatial correlation of the afore-mentioned properties can be computed. As structures (such as sewer systems) are immobile, only one single realisation exists of, for example, local characteristics of street surfaces. Consequently, the actual properties of

the surfaces (perviousness, slope, etc) are more or less fixed after construction, although not completely known. Subsidence of sewer pipes, on the other hand, may cause considerable uncertainty regarding invert levels.

2.3.2 Epistemic uncertainty

2.3.2.1 Model uncertainty

A hydraulic, hydrological or condition model is never perfect, and neither are the required model parameters. This results from physical phenomena that are not fully understood, or some variables of lesser importance that are omitted in the model for efficiency reasons. This may cause model uncertainty. Several authors present methods to accommodate the uncertainty in sewer models (e.g. Beck 1987 and 1996, Lei and Schilling 1996, Vanrolleghem and Keesman 1996 Aalderink *et al.* 1996 and Willems 2000).

Model uncertainty is sometimes subdivided into model parameter and model structure uncertainty (e.g. Beck 1987 and Willems 2000). The latter results from imperfect descriptions of physical reality or the limitations of the modeller to describe reality. For example, when modelling sewer systems the limitations of modelling in-sewer processes regarding sewage composition are an important source of uncertainty (Ashley *et al.* 1999 and Langeveld 2004). Model parameter uncertainties exist if erroneous or limited time series of data are used for calibration or if the calibration procedure is not optimal. In addition, it also comprises measurement or estimation errors depending on the type of model input (e.g. hydraulic resistance of sewer pipes, runoff coefficients of paved areas and sizes of paved areas). As mentioned in § 2.2, it is rather complicated, if not impossible, to separately quantify parameter and structure uncertainty because of their strong interrelation.

2.3.2.2 Statistical uncertainty

The characteristics of a series of data can be described with a statistical model, a distribution function, e.g. normal, exponential and lognormal. A distribution function is defined with its parameters, which are estimated from available data.

Statistical uncertainty arises when the amount of data for estimating the probability distribution of a random variable is not sufficient. In other words, if only sparse data is available more than one distribution seems to fit the observed data and only a few can be rejected on the basis of goodness-of-fit tests (e.g. Chi-square or Kolmogrov-Smirnov). For example, a priori it is not clear whether the occurrence of rainfall intensities is exponentially or log-normally distributed or complies with another distribution type. Statistical uncertainty consists of two parts: distribution type and statistical parameter uncertainty.

Distribution type uncertainty represents uncertainty about the distribution type of a variable and arises from choosing the most appropriate distribution type for this

variable (Van Noortwijk *et al.* 2001). For goodness-of-fit tests two probability models H_1 and H_2 need to be formulated. Subsequently, a test statistic (e.g. Chi-square test) is applied to judge whether model H_1 should be rejected or not. Model H_1 is rejected if the test statistic is smaller than a predefined significance level.

However, traditional hypothesis testing has several disadvantages. It only offers evidence against a hypothesis H_1 or the alternative H_2. Acceptance of hypothesis H_1 on the basis of the traditional approach is not possible (Van Noortwijk *et al.* 2001). Moreover, Van Gelder (2000) states that the uncertainty involved in the selection of the distribution type is ignored when a single distribution type is selected and inference is made conditionally on that distribution. As an alternative, Bayesian selection methods can be used to determine how well a probability distribution fits observed data (see Carlin and Lewis 2000). Bayesian methods avoid the problems mentioned. In practice, however, the number of candidate distributions is limited due to computational limitations.

In addition to distribution type uncertainty, statistical parameter uncertainty is of importance. It also decreases with increasing data availability. Statistical parameter uncertainty is calculated either by means of Bayesian methods or bootstrapping. Bootstrapping randomly draws r replications of an original data set of sample size n with replacement. Subsequently, r values of the statistic of interest are calculated and analysed statistically. A detailed description of the bootstrap method can be found in Efron and Tibshirani (1993).

An illustration of statistical parameter uncertainty is given in Figure 2.4. A lognormal PDF has been fitted to data of calculated CSO volumes of the sewer system of 'De Hoven', The Netherlands. The statistical parameters μ_Y and σ_Y have been estimated with the Maximum Likelihood method based on these 70 calculated volumes. Subsequently, a bootstrap algorithm as described in Efron and Tibshirani (1993) has been applied to estimate variability of the statistical parameters. The figure shows that the parameters of the PDF contain a substantial amount of statistical parameter uncertainty. Expressed in terms of 'coefficient of variation' (CV) the uncertainty of the two parameters amounts to,

$$CV(\mu_Y) = \frac{\sigma(\mu_Y)}{\mu(\mu_Y)} = 0.20$$
$$CV(\sigma_Y) = \frac{\sigma(\sigma_Y)}{\mu(\sigma_Y)} = 0.08 \qquad (2.2)$$

The uncertainty may result from the fact that the number of data points is too small to estimate a reliable PDF, or that a lognormal distribution is not the correct distribution type to describe the data.

Distribution type uncertainty is illustrated in Figure 2.5. In this example the same data set is used as in the previous example. Using the CSO volumes, both the parameters of a Weibull and an exponential distribution are estimated. To graphically assess the fit between data and both distributions, the cumulative distribution function (CDF) of the data is plotted in the same figure as the estimated distribution functions. The figure shows that the Weibull distribution gives a better fit with the CSO volumes compared to the exponential type.

In practice, it is difficult to discriminate between statistical parameter uncertainty and distribution type uncertainty. For example, the distribution type itself can be uncertain due to lack of observations, which affects the uncertainty of the distribution parameters as well.

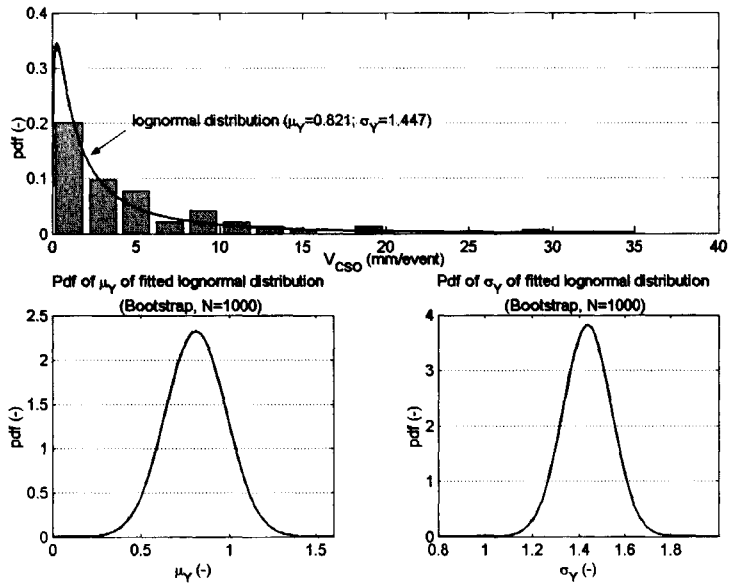

Figure 2.4 Example of statistical parameter uncertainty. The parameter uncertainties in the lognormal distribution are estimated by means of bootstrapping.

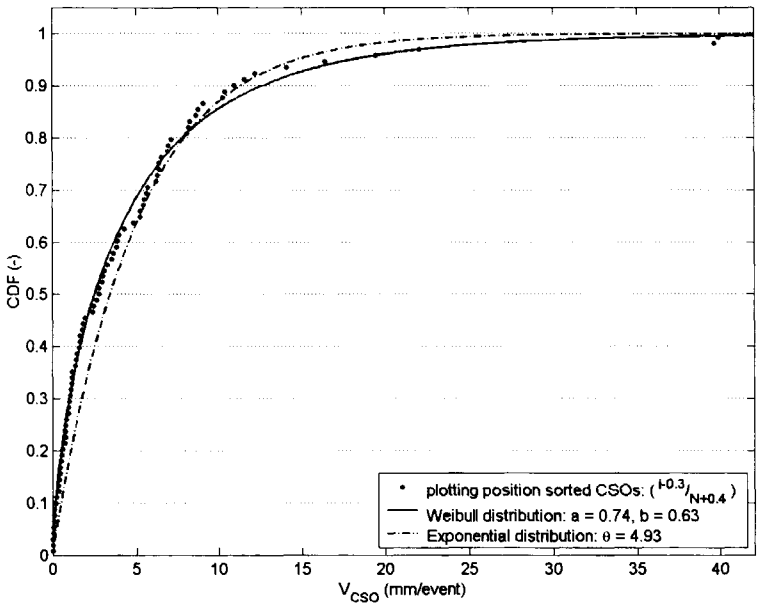

Figure 2.5 Example of statistical distribution type uncertainty, where *i* is rank of sorted CSO volumes, *N* is total number of CSO volumes, *a* is shape parameter of Weibull distribution, *b* is scale parameter of Weibull distribution and *θ* is parameter of exponential distribution. The cumulative distribution function (CDF) of the data set is graphically compared with estimated Weibull and exponential distribution functions.

2.4 UNCERTAIN FACTORS IN THE HYDRAULIC PERFORMANCE OF SEWERS

At present, assessment of sewer system performance is usually based on CSO volumes and flooding events. A diagram of the decision-making process to improve performance is presented in Figure 2.6. With regard to CSO emissions and flooding, the decisions are based on several criteria, which stem from e.g. environmental policy, construction costs, losses due to failure and environmental and town planning.

2.4.1 Hydraulic loads of sewer system

The hydraulic loads of a sewer system may be distinguished between storm events and dry weather flow (dwf). Patterns in rainfall, both in space and time, have been studied extensively during the last decades. Variability of dwf, in contrast, has achieved much less attention.

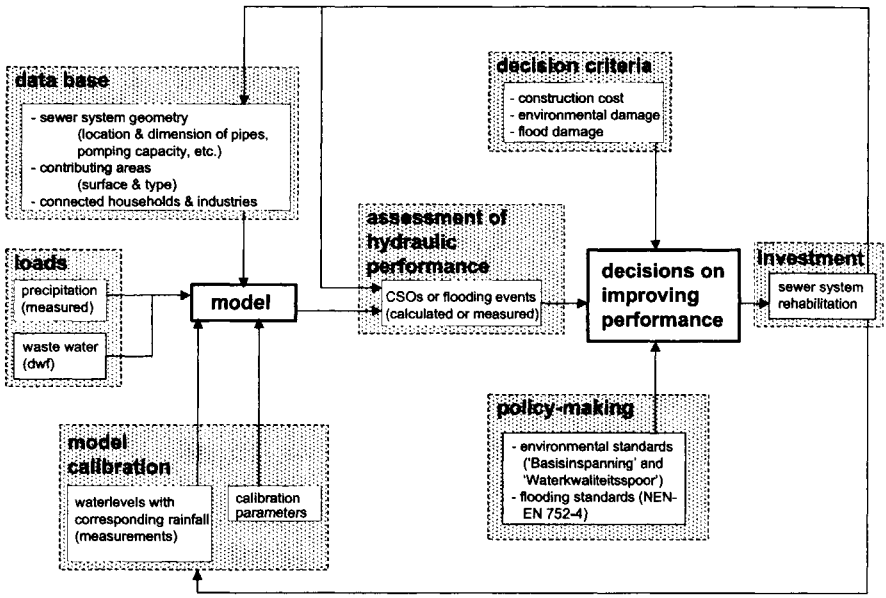

Figure 2.6 Decision-making on sewer system rehabilitation regarding hydraulic performance. Uncertainties in the various aspects influence investments in the sewer system.

2.4.1.1 Precipitation

When modelling sewer systems, rainfall input uncertainties are one of the most important sources of uncertainty (e.g. Schilling and Fuchs 1986). Rainfall input uncertainties can be separated into:

- inherent uncertainties in the rainfall process;
- uncertainties caused by measurement errors;
- uncertainties resulting from simplification of the real spatial variability of the rainfall (catchment averaged rainfall).

These uncertainties are even amplified by the rainfall runoff transformation (Schilling and Fuchs 1986).

In rainfall structure, both in space and time, certain regularities are observed. The spatial structure of rainfall shows clusters of high intensity rainfall areas embedded within rainfall areas of lower intensity (Gupta and Waymire 1979, Waymire and Gupta 1981 and Waymire *et al.* 1984). Such patterns are typically present at different spatial scales (Figure 2.7):

- At the smallest scale, individual rain cells are the building block of the spatial rainfall structure. They range from 10-30 km^2.

- The individual cells with higher intensities form clusters in small meso-scale areas, SMSA, (100-1,000 km^2). In these meso-scale areas they move with nearly identical velocities. The SMSA has an average life span of several hours.
- At a larger scale, the small meso-scale areas are clustered within larger meso-scale areas, LMSA, (1,000-10,000 km^2) with lower intensities. The lifetime of LMSA is within the order of several hours.
- The large meso-scale areas are embedded within a rainfall field with lower intensities. Their life span is one to several days.

However, other descriptions of the spatial structure of rainfall are also found in the literature. For example, Lovejoy and Mandelbrot (1985) and Lovejoy and Schertzer (1995) describe the spatial (and temporal) structure of rain using the theory of fractals. Instead of clustering rainfall at different scale levels their approach is based on the scale invariance of the structure of rainfall. The temporal structure of rainfall, on the other hand, consists of a succession of events, which is usually described by means of Poisson or Markov processes (e.g. Waymire and Gupta 1981).

Although several authors have translated the characteristic spatial rainfall structure into a model (e.g. Bras and Rodriguez-Iturbe 1976, Arnbjerg-Nielsen *et al.* 1998, Thauvin *et al.* 1998 and Thyregod *et al.* 1998), hardly any applications exist at small spatial scales, such as occur in urban areas. In these models, the rainfall structure is not described at the level of individual rain cells. However, for urban hydrology an accurate description of individual rain cells and cell clusters is important, while the description at the lager meso-scale is of minor importance. Within the rain cells spatial correlation is high.

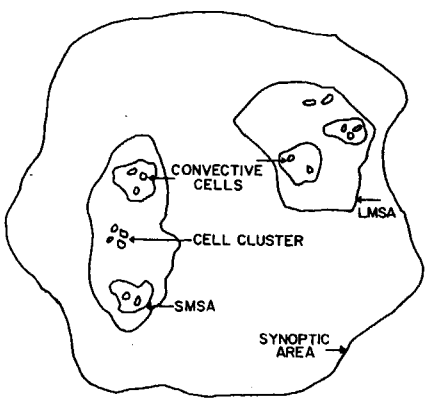

Figure 2.7 Schematic description of rainfall features (after Waymire and Gupta 1981). Areas with similar rainfall intensities are distinguished.

In urban areas spatial variation in rainfall intensities is influenced by temperature differences, the 'urban microclimate', and impacts of buildings on wind patterns (e.g. Buishand and Velds 1980). The variation can be relatively large and differs significantly from variations observed in rural areas. Accounting for these characteristics, Willems (2000) developed a spatial rainfall generator for urban catchments. He estimates that spatial variation in rainfall input accounts for approximately 30% of variability in calculated CSO volumes.

The dominant type of rain gauges applied in urban drainage is the tipping bucket rain gauge. Different authors, e.g. Sevruk (1982 and 1996), Luyckx *et al.* (1998), Rauch *et al.* (1998), describe the measurement properties of tipping bucket rain gauges. The main components of systematic error in precipitation measurements are presented in Table 2.2. Generally, these gauges appear to underestimate high intensities, while for low intensities rainfall is overestimated (Luyckx *et al.* 1998 and Einfalt *et al.* 1998).

Table 2.2 Systematic errors in precipitation measurements from tipping bucket rain gauges.

Error component	Volumetric magnitude of errors
wind speed	2 – 15 % (Sevruk 1996)
	3 – 5 % (Luyckx *et al.* 1998)
wetting of internal walls	2 – 10 % (Sevruk 1982)
evaporation	0 – 4 % (Sevruk 1982)
splashing	1 – 2 % (Sevruk 1982)
calibration of rain gauge	10 % (Rauch *et al.* 1998)
	3 – 4 % (Luyckx *et al.* 1998)
loss of winter precipitation (due to heated gauge)	30 % (Rauch *et al.* 1998)
resolution error (per bucket volume)	0.1 mm (Luyckx *et al.* 1998)

Catchment averaged rainfall is estimated on the basis of point rainfall measurements introducing additional uncertainty. According to Willems (2000), spatial averaging of point rainfall measurements includes three types of uncertainties:

- point rainfall measurement errors,
- estimation error due to averaging over catchment area,
- natural variability in the precipitation process.

Errors related to spatial averaging of rainfall are important with respect to uncertainties in modelling of urban rainfall runoff processes. This is stressed by e.g. Schilling and Fuchs (1986), who demonstrate that lack of spatial resolution of rain data causes severe loss of modelling reliability. Systematic errors result from wrong assumptions about spatial homogeneity of rainfall and dominating directions of storm movement (Schilling 1984). Another source of uncertainty is that rain gauges in the centre of a catchment overestimate areal rainfall. With respect to magnitude of uncertainties Willems (2000) concludes that if a rain gauge network is very dense, estimation errors can be neglected compared to the other uncertainties mentioned. For rainfall volumes larger than 0.5 mm the impact of measurement errors is also negligible

Whether rainfall input uncertainty can be reduced is dependent on the type of the uncertainty. The inherent uncertainty in time cannot be reduced because it results from natural variability in rainfall. The inherent uncertainty in space, however, will decrease with more dense networks. The magnitude of the measurement error of a rain gauge is a function of the measured volume and the resolution of the gauge. As a result, reduction is only possible if more accurate gauges are installed.

2.4.1.2 Dry weather flow

Dry weather flow (dwf) consists of domestic and industrial wastewater and leaking groundwater. Dwf from households is directly related to drinking water consumption and varies during the day (see e.g. Butler *et al.* 1995). However, the drinking water consumption over the day differs from dwf discharges because part of the water is not drained to the sewer system due to e.g. garden sprinkling and evaporation, or is retarded due to temporary in-house storage e.g. in washing machines and baths.

Differences in amount and pattern of domestic discharges are dependent on size and characteristics of urban areas (Clemens 2001a). For example, Butler *et al.* (1995) show that the domestic wastewater discharges differ between a city in England and in Malta. Both amount and pattern (morning and evening peaks) are different at the two locations. The amount of industrial discharges strongly depends on the type of industry.

Infiltration may contribute considerably to dwf, especially in older sewer systems with high ground water levels (Clemens 2001a and Karpf and Krebs 2003). For example, Schaum (2001) estimates that leakage contributes to 40 % of dwf in the city of Apeldoorn, The Netherlands.

Table 2.3 Variation of calibrated dwf due to fluctuations in domestic sewage and leaking groundwater for the sewer system of De Hoven, The Netherlands (Clemens 2001a).

event	Average (μ) (m^3/h)	Std (σ) (m^3/h)	CV (%)*
1	25.95	0.08	0.30
2	49.19	3.12	6.34
3	65.48	2.73	4.17
4	63.89	1.39	2.18
5	49.88	1.16	2.33

* CV = coefficient of variation = (σ/μ)*100%

Dwf patterns show substantial variation in time. Table 2.3 presents averages and standard deviations of calibrated dwf in a sewer model. The model was calibrated using an automatic algorithm (Clemens 2001a). The average domestic sewage discharges amount to 22 m^3/h. The calibrated dwf, however, can be considerably larger (for particular storm events up to 65 m^3/h). The maximum dwf equals 2.52 times the minimum value. Calibrated dwf varies from one event to another mainly due to fluctuating groundwater levels that are strongly correlated with the water levels in the

neighbouring river IJssel. Karpf and Krebs (2003) also found this correlation between dwf and river water levels for the city of Bamberg, Germany.

The results are comparable to measured daily variations of the inflow of wwtps (wastewater treatment plants) over the year in Germany (Brombach *et al.* 2002) and The Netherlands (Stok 2003). Although the inflow variations of a wwtp measured by Stok (2003), are smaller than calculated by Clemens (2001a), they vary substantially over the year (Table 2.4). The average daily inflow (only during dry days) is equal to 1.25 times the minimum value.

Table 2.4 Measured inflow of wwtp 'Katwoude', The Netherlands, during dwf (Stok 2003). Daily averages for each month based on inflow measurements during dry days (2000-2002). The average inflow is approx. 9600 m^3/d

Month	Jan.	Feb.	Mar.	Apr.	May	June
Inflow (m^3/d)	10524	10732	10348	9613	9314	9137
Month	July	Aug.	Sept.	Oct.	Nov.	Dec.
Inflow (m^3/d)	8564	9314	9585	9763	9070	9289

2.4.2 Database of sewer system

For many sewer systems the original information on their construction, geometry and details are at best available in drawings, maps or written manuscripts. The accuracy of such information sources is questionable for several reasons (Clemens 2001a):

- discrepancies between original plans and actual construction that were not corrected afterwards in revised plans,
- subsidence of sewers,
- loss of original information (e.g. due to fire) and
- poor documentation of constructional details.

In practice, reliable information on structure and geometry is only obtained by detailed field investigations.

The data set applied in a hydrodynamic model is never entirely perfect. Errors in the database of a sewer system affect calculation results of hydrodynamic models. Within a sewer database, five groups of data are distinguished, including geometry of sewer system, hydraulic parameters, runoff parameters, catchment area and structure of sewer system. Possible database errors are summarised in Table 2.5. The average values and standard deviations of the parameters are based on expert judgement (Clemens 2001a).

Table 2.5 Errors in the database of a sewer system (after Clemens 2001a). The data are used as input for hydrodynamic models.

Category	Aspect	Average	Standard deviation
Geometry of sewer system	Invert level (both up- and downstream)	-	0.05 m
	Weir crest level	-	0.01 m
	Street level	-	0.01 m
	Profile diameter	-	0.5 %
	Switch on/off level pumping station	-	0.01 m
Hydraulic parameters	Hydraulic roughness	3.0 mm	1.0 mm
	Weir coefficient	1.4 (-)	0.35 (-)
	Local loss coefficient	1.2 (-)	0.4 (-)
	Pumping capacity	-	5.0 %
Runoff parameters	Infiltration rate	2.0 mm/h	30.0 %
	Initial depression losses	0.5 mm	30.0 %
Catchment area	Catchment area	-	5.0 %
Structure of sewer system	Shape of profiles	-	-
	Non-existing structures	-	-
	Conduits left out	-	-

Structural errors substantially impact reliability of hydrodynamic calculations (Clemens 2001a). They comprise profile errors (e.g. round pipes instead of egg-shaped), pipe dimension errors, non-existing structures and conduits left out. Their influence on calculated CSO volumes and water levels is large (Price and Osborne 1986 and Clemens 2001a). However, structural errors are difficult to determine prior to calculation. More accurate measuring or model calibration substantially reduces uncertainty

Clemens (2001a) demonstrates that no single group of database errors dominates variance of calculated CSO volumes and numbers of flooded manholes. Errors in amount of catchment area have the largest impact. However, when the number of errors in the structure of the sewer system increases (>10 % of total number of conduits), it dominates other errors. These structural errors produce distinct peaks in predicted CSO volumes. In steeper sewer systems the impact of errors in the database is more distinct.

2.4.3 Models for assessment of hydraulic performance

In urban drainage, decisions on interventions related to the rehabilitation of a sewer system are usually based on simulation results (i.e. CSO volumes or flood depths). Simulation models used in urban drainage consist of two separate process descriptions:

- rainfall runoff process (hydrologic model),
- in-sewer hydraulic processes (hydraulic model).

When the simulation model is calibrated using measurement data for the hydraulic behaviour of a sewer system, the accuracy and reliability of results increases.

Consequently, model calibration reduces risks related to possible wrong interventions. Both data availability and model structure affect the accuracy of a calibrated model.

2.4.3.1 Hydrologic model

The hydrologic part of sewer models comprises processes that transform rainfall into runoff including:

- interception by vegetation and wetting of dry surface,
- depression storage,
- infiltration,
- evaporation and
- overland flow.

These processes are very simplified in the usual models introducing uncertainty. In addition, uncertainties may stem from inherent variations in time, local differences in surface characteristics and lack of data. Schilling and Fuchs (1986) show that uncertainties in rainfall input are amplified by the rainfall runoff transformation.

The output of the hydrologic part of the model serves as input for the hydraulic part. However, calculated runoff cannot be compared with field measurements because it is usually not measured as a separate quantity. Although a variety of runoff models exist, they show only little differences in process descriptions (see Van de Ven 1989).

Initial losses consist of storage in depressions and losses due to interception by vegetation and due to wetting of dry surfaces. Surface storage is the amount of rain that is caught in small local depressions in the pavement. Regarding interception, there is an initial retention period, after which excess rain falls through the vegetation cover to the soil. Losses due to interception are small in magnitude (<1 mm) and are usually neglected or combined with depression storage in sewer models. Wetting losses occur when the street surface is dry at the beginning of a storm.

The magnitude of initial losses depends on the type and state of maintenance of the street surface, the humidity and temperature of the surface and the previous history of a storm, since water stored in depressions vanishes between successive storms due to evaporation and infiltration. However, exact figures for initial losses are scarce. Table 2.6 summarises field data available in literature (Clemens 2001a).

Table 2.6 Wetting losses and surface storage (Clemens 2001a).

	roofs		roads	
	flat	sloping	impervious	semi-pervious
wetting losses (mm)	0 - 0.5	0.1	0.07 - 0.7	0 - 1.5
surface storage (mm)	2 - 2.5	0.1	0.3 - 1.7	0.8 - 6.0

Evaporation is the vaporisation of water from plants and open water bodies (e.g. puddles). It is a continuing, constant loss. Its rate depends on variables including:

- temperature,
- wind speed,
- atmospheric humidity,
- rate of heat influx,
- intensity of sunshine and
- colour of surface.

In general, none of these are known in detail when modelling a sewer system. Furthermore, Van de Ven (1989) concludes that it is impossible to quantify the evaporation for an individual storm. Therefore, calculated monthly averages of potential evaporation are applied (Penman 1948). Figure 2.8 shows the 'Penman evaporation' as applied in sewer models. During summer this evaporation is slightly higher than the long-term potential evaporation of De Bilt, The Netherlands (1971-2000).

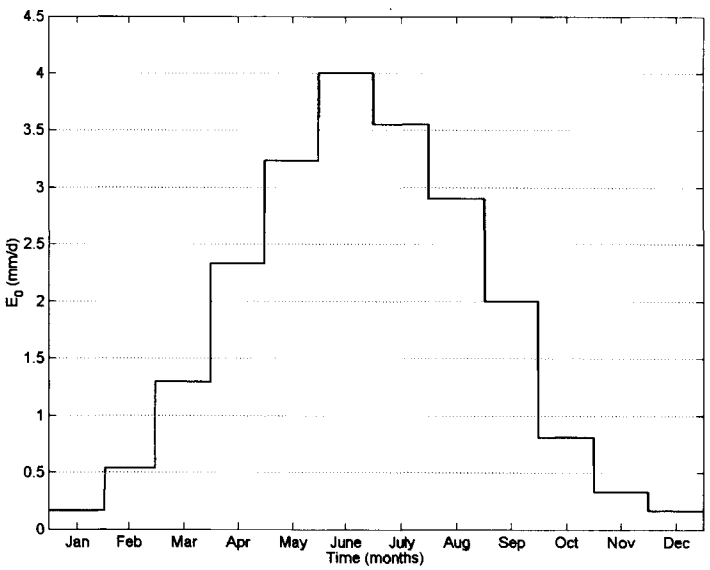

Figure 2.8 Monthly averaged evaporation (Penman 1948) as applied in sewer models in The Netherlands.

Table 2.7 Infiltration capacity of different surfaces (Clemens 2001a)

	infiltration capacity (mm/h)
brick paving	7 - 353
paving-stones	1 - 254
grass	10 - 500
soil without vegetation	10 - 100

Infiltration is a complicated process in which rain infiltrates into the soil. Depending on the initial conditions, the infiltration rate will decrease as the unsaturated zone becomes filled. As soon as this zone becomes saturated, the minimum infiltration capacity is reached. Infiltration rates reported in the literature are shown in Table 2.7. A widely accepted model is the Horton infiltration model (Horton 1940).

$$f(t) = f_c + (f_b - f_c)e^{-k_d t} \quad \text{decrease of infiltration rate} \tag{2.3}$$

$$f(t) = f_b + (f_b - f_c)e^{-k_r t} \quad \text{increase of infiltration rate} \tag{2.4}$$

where $f(t)$ is infiltration rate (mm/h), f_c is minimum infiltration capacity (unsaturated zone filled), f_b is maximum infiltration capacity (unsaturated zone fully available), k_d is recession factor (descending leg) and k_r is recession factor (rising leg). According to Van de Ven (1989), a constant rate model is less accurate than more complicated models. However, it can be used for practical purposes because it is easy to calibrate.

2.4.3.2 Hydraulic model

Runoff from street surfaces and dwf drain to the sewer system. The resulting flow in the sewers is described with the well-known 'De Saint Venant equations' (De Saint Venant 1870). These equations read,

$$\frac{\partial Q}{\partial t} + \frac{\partial}{\partial x}\left(\beta \frac{Q^2}{A}\right) + gA\frac{\partial h}{\partial x} + c\frac{Q|Q|}{RA} = 0 \tag{2.5}$$

$$\frac{\partial Q}{\partial x} + \frac{\partial A(h)}{\partial t} = \frac{\partial Q}{\partial x} + B(h)\frac{\partial h}{\partial x} = 0 \tag{2.6}$$

where Q is discharge (m^3/s), c is resistance coefficient (-), A is cross-sectional area (m^2), h is water level (m), B is width of free water surface (m), x is location along x-axis (m), g is gravitation (m/s^2), t is time (s), R is hydraulic radius (m) and β is Boussinesq's number (-). The first equation represents the momentum balance, whereas the second represents the mass balance.

For these equations no analytical solution is known, thus implying that numerical methods are necessary to solve them. In hydrodynamic models finite difference methods are used to transform the partial differential equations into finite difference equations. Clemens (2001a) extensively studied hydrodynamic models used in urban drainage, their characteristics, simplifications and limitations.

In general, uncertainties in results of hydrodynamic models result from incomplete or incorrect process descriptions and numerical or software errors. Modelling errors may result from (see Clemens 2001a):

- incorrect description of processes;
- numerical errors due to specific calculation method (e.g. choice of step size (Δx) and time step (Δt));

- simplification or omission of minor processes;
- database errors;
- impacts of programmers' solutions (e.g. difficulties in implementation of formulae and numerical difficulties in software).

The simplifications as applied in most hydrodynamic models are widely accepted, but should be taken into account for a correct interpretation of model results. Software induced errors are present, but normally stay within acceptable limits. With regard to errors in process descriptions, it is apparent that some processes cannot be modelled accurately. For example, house outlets, gully pots and conduits enabling connection to the sewer system are usually not accounted for in the calculations, although they may hold a significant storage capacity (up to 10% of in-sewer storage). In addition, most models assume that all runoff enters the sewer system at manholes. In fact, it enters the system at many more inlets affecting actual in-sewer flow.

In particular, the prediction of CSO volumes and flood depths is inaccurate due to shortcomings of the hydrodynamic models. The amount of pollution in CSOs cannot be predicted, since in-sewer processes are not completely understood and concentrations of pollutants in CSOs are highly variable (e.g. NWRW 1989a and Gromaire-Mertz *et al.* 1998). Furthermore, flood depths cannot be predicted with sufficient accuracy because conventional models cannot deal with surcharged conditions and an interaction between street flow and in-sewer flow is not included (Maksimovic and Prodanovic 2001). Nor can the models be relied on for long return period events, since only little data are available to check their results.

In conclusion, uncertainties in the results of hydrodynamic models are mainly due to incorrect description or simplification of processes and errors in the database of the sewer system. The former is reduced by more detailed process knowledge and descriptions, the latter by field measurements of sewer system data.

2.4.3.3 Model calibration

Calibration is the process in which model structure and parameters are adapted in such a manner that the model reproduces measured behaviour as well as possible. Calibrating a model reveals discrepancies between model and observed reality. It also enables the quantification of systematic errors, which may stem from incomplete process descriptions in the model, errors in the database of the sewer system and measurement errors. However, calibration of hydrodynamic models is only rarely applied in practice, because (see Clemens 2001a):

- calibration is regarded as time-consuming;
- field measurements are regarded as expensive;
- methods to calibrate a model and objectively judge calibration results are lacking.

In The Netherlands, for example, only a limited number of cases are known of calibrated models of sewer systems. As a result, unnecessary uncertainty on CSO volumes and resulting inappropriateness of investments is introduced (see e.g. Price and Catterson 1997).

In the literature different methods are presented for the optimisation of parameters in a hydrodynamic model. For example, Clemens (2001a) applies maximum likelihood estimation, while Reichert (1997) and Bates and Campbell (2001) recommend a Bayesian approach to parameter estimation.

The uncertainties in the calibration of a hydrodynamic model result from either the available measurement data or the chosen model structure. Due to calibration the uncertainties from different sources (e.g. database of sewer system, dwf, runoff parameters, model structure) are aggregated into the model parameters. Especially model structure uncertainty is transferred to parameter uncertainty. As a consequence, uncertainty in model parameters is possibly overestimated. The same applies to distribution type uncertainty, which shifts to statistical parameter uncertainty due to parameter estimation.

Due to simplifications or errors in the model structure, a strict physical interpretation of calibration parameters is not always possible. As a result, calibrated model parameters may adopt values that are physically less probable. Moreover, it is difficult, if not impossible, to estimate the improved accuracy of a 'better' model because uncertainty related to model structure and model parameters is strongly correlated. According to Bedford and Cooke (2001) among others, separate estimation of parameter and structure uncertainty is impossible, since essentially all models are 'false'.

Willems (2000), however, claims that structure uncertainty of different model structures can also be estimated and discriminated from parameter uncertainty. Model structure uncertainty is defined as overall model uncertainty minus all other known uncertainty sources. This approach, however, assumes that models are calibrated by changing the structure instead of the parameter values, that the variances of the various uncertainty sources (input uncertainty, model structure uncertainty and measurement errors) are independent and additive, and that uncertainty of model parameters can be estimated with expert knowledge. The approach relies heavily on the modeller's skills and his ability to estimate the model parameters and their variation. This means that it is still impossible to separately estimate structure and parameter uncertainty of calibrated models, since the estimation of model parameter uncertainty is based on expert knowledge. Essentially, this approach defines model uncertainty as stemming completely from model errors and simplifications (i.e. structure uncertainty) assuming that parameter uncertainty can be neglected.

Morgan and Henrion (1990) and Bedford and Cooke (2001) propose to assimilate different model structures into a single 'metamodel', containing the models as special cases and introduce a discrete parameter indicating the weight of each model. Uncertainty about model structure is converted into uncertainty about these weights. However, the highest weight does not indicate that the model is 'correct', it only distinguishes the model that is 'approximately correct'. This approach is comparable to Bayes weight assessment.

Values of calibrated parameters in a hydrodynamic model may vary from one storm event to another, or even during the storm event itself, due to an incomplete or incorrect process description in the model (see Clemens 2001a and Grum 1998). Therefore, the portability of parameters between different storm events is rather limited (Bates and Campbell 2001). Table 2.8 shows the results of the calibration of a hydrodynamic model of a sewer system (Clemens 2001a). The calibrated parameter values differ for two storm events. For example, the difference in dwf and infiltration rate between the events is due to different ground water levels in August and October.

Table 2.8 Parameter values obtained for two calibration runs with different storms (Clemens 2001a).

A storm 25/08/98	μ	σ	CV* (%)
N*(m^3/h)	26.16	0.07	0.27
B*(mm)	0.4905	0.00875	1.78
I*(mm/h)	0.229	0.0015	0.66
F*(s)	277.035	7.9375	2.87
CC*($m^{0.5}$/s)	1.035	0.0185	1.79

B storm 24/10/98	μ	σ	CV* (%)
N*(m^3/h)	51.97	0.675	1.30
B*(mm)	0.44815	0.015275	3.41
I*(mm/h)	0.1834	0.00335	1.83
F*(s)	669.635	11.8975	1.78
CC*($m^{0.5}$/s)	1.28295	0.071375	5.56

* CV = coefficient of variation = (σ/μ)*100%

N* = dwf (m^3/h)
B* = storage on street surface (mm)
I* = constant infiltration rate (mm/h)
F* = lineair reservoir constant (s)
CC* = weir coefficient ($m^{0.5}$/s)

$\mu(N^*)_A : \mu(N^*)_B = 0.50$
$\mu(B^*)_A : \mu(B^*)_B = 1.09$
$\mu(I^*)_A : \mu(I^*)_B = 1.25$
$\mu(F^*)_A : \mu(F^*)_B = 0.41$
$\mu(CC^*)_A : \mu(CC^*)_B = 0.81$

2.4.4 Environmental and flooding standards

Environmental and flooding standards (next to public health) are an important motivation for maintenance and rehabilitation of sewer systems. These standards may change through the years due to changes in knowledge and public perception of sewer impacts and policy-making on impact reduction. Evidently, social, economic, political and cultural changes in a society cannot be predicted, nor can their consequences for the operation and maintenance of sewer systems.

In The Netherlands, a sequence of different environmental standards has been applied to sewer systems over the years:

- Until 1951, a 'dilution factor approach' was applied. It required that sewer flow should be diluted 3 to 10 times before a CSO started working (Van den Akker 1952).
- From 1951 until 1992, a different approach based on allowable overflow frequency, was used (Ribius 1951). The frequency is calculated with a simple reservoir model of the sewer system. The allowable maximum varies between 3 and 10 events per year depending on the water board and the type of receiving water.

- From 1992 until 2001, the requirements of the 'Basisinspanning' had to be met (CUWVO 1992). It demanded that each sewer system should perform equivalent to a 'reference' sewer system in terms of pollution load. The reference system has an in-sewer storage capacity of 7 mm, additional storage in a settling tank of 2 mm and a pumping capacity of 0.7 mm/h plus dwf. Performance is checked for annual CSO volumes. These volumes are calculated using a (simplified) hydrodynamic or reservoir model of the system.
- In 2001, the reference system performance was more clearly defined (CIW 2001). It now equals an annual discharged COD load of 50 kg COD per hectare of impervious area. The COD concentration is assumed to be 250 mg COD/l.
- Since 1992, the 'Waterkwaliteitsspoor', a method assessing receiving water quality, has been developed in addition to afore-mentioned emission-based methods (CUWVO 1992). It considers impacts of CSOs on a watercourse depending on its function.

However, the effects of CSOs on water quality still cannot be predicted with sufficient reliability because knowledge of processes is rather limited. Moreover, the relationship of discharge limit and required water quality improvement is debatable (Clemens 2001a). As a consequence, reliable checking of system compliance is impossible.

Flooding of sewer systems used to be assessed on the basis of constant rainfall intensities (60 or 90 l/s/ha depending on ground slope) accepting maximum in-sewer water levels of 0.2 m below ground level (Van Luijtelaar 1999). Only recently, a new approach has been introduced which assesses sewer flooding on the basis of calculated hydraulic performance for predefined storm events with specific return periods (0.25-10.0 years) and shapes (peak at beginning or end of storm).

However, flooding (i.e. depression storage and overland flow) cannot be accurately represented in a sewer model (e.g. Maksimovic and Prodanovic 2001). When a sewer system becomes surcharged, the reliability of model results depends strongly on the description of the interaction between surface flow and underground sewer system. In addition, the hydraulic resistance of gully pots and their connections are often neglected and overland flow is not included in the model (De Haan 2002). As a result, calculated flood depth and duration are unreliable, resulting in inaccurate flooding assessments.

2.5 UNCERTAIN FACTORS IN THE STRUCTURAL CONDITION OF SEWERS

Good planning for sewer maintenance and rehabilitation requires valid condition assessments. In most cases, however, good information on the condition of sewer assets, such as pipes, pumps, inverted siphons, CSO structures and manholes, is scarce (Fenner 2000). The condition of sewers is identified by internal visual examination using CCTV (closed circuit television), photographs or by other methods, such as high-resolution sonar and laser measurements. Based on these examinations sewers are

classified from no visible defect to severely deteriorated (see NEN 3399 and pr EN 13508-2). Visible structural defects of sewer pipes include longitudinal cracks and fractures, circumferential cracks and fractures, broken or deformed pipes, corrosion, fouling, collapse, defective connections, debris, deposits, deviations in line and level, root intrusion, rats and infiltration. Mortar loss and displaced or missing bricks are typical defects of brick sewers.

Usually, the results of visual (or non-visual) inspections are applied for assessment of the structural condition of sewers. Sewers are classified from these inspections. Decision-making on sewer rehabilitation (see Figure 2.9) relies on a prioritisation of sewers regarding their condition class. For prioritising, models are used either to predict the remaining service life of sewers or the transition sewers between condition classes (e.g. KEMA 2001 and Baur and Herz 2002). Sewers that do not meet required performance criteria (watertightness, structural stability, flow and contamination) have to be either cleaned, repaired or replaced.

Lately, there is a tendency towards proactive or preventive maintenance instead of corrective repair, i.e. fixing problems after failure (see Fenner 2000 and Ashley and Hopkinson 2002). Therefore, more effective tools are required in order to accurately predict condition and performance of sewers.

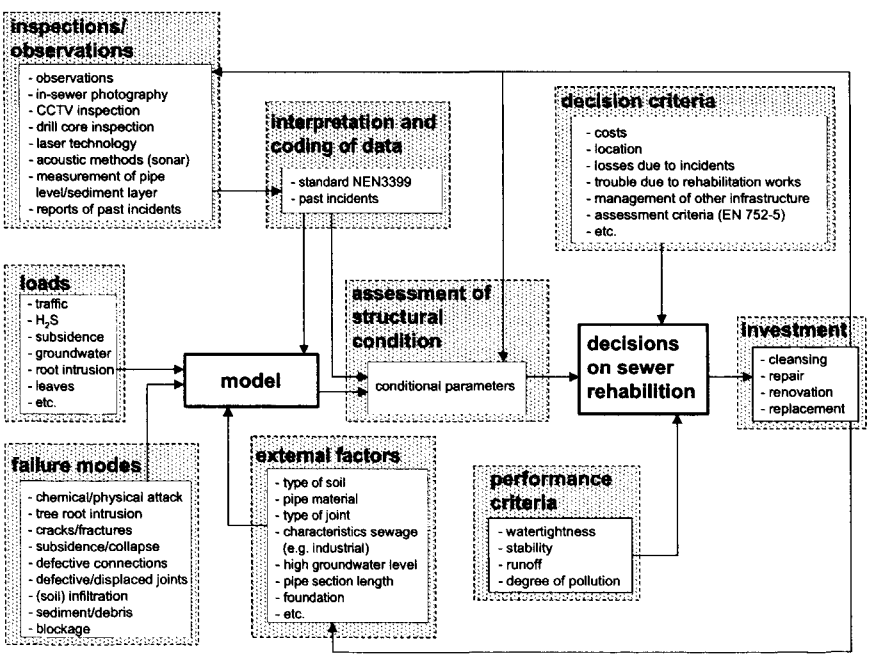

Figure 2.9 Decision-making on sewer system rehabilitation regarding structural condition of sewer system. Uncertainties in the various aspects influence investments in the sewer system.

2.5.1 Loads and external influences

Different sewer ageing rates may result from differences in soil conditions, pipe materials, nominal sizes, quality of pipe laying, type of sewer system (combined or separate), quality of sewage (Stein 2001). However, agreement has not been reached yet for several explanatory variables for sewer deterioration (see Table 2.9). Fenner and Sweeting (1999), for example, suggest that pipes most prone to failure have specific characteristics including long lengths, small diameters, shallow depths, slack to moderate gradients and foul sewers. Davies *et al.* (2001b), on the other hand, consider factors such as sewer depth, root intrusion, infiltration, burst history, traffic loads and total vehicle flow as statistically not significant in predicting the probability of failure of a sewer. The presence of debris (bricks, gravel, etc) is indicative of possibly increased risks of a sewer failure.

It is generally acknowledged that sewer deterioration is influenced by corrosion of cementitious material due to hydrogen sulphide. The hydrogen sulphide cycle comprises the following steps. Under anaerobic conditions the sulphide reducing bacteria (*Thiobacillus desulfuricans*) present in slime layers and sewage reduce sulphates in the sewage to form dissolved hydrogen sulphide. When exposed to water and under anaerobic conditions a mixture of H_2S and HS^- is formed. Subsequently, hydrogen sulphide gas is released from the sewage and oxidised by bacteria (*Thiobacillus thiooxidans*) at the pipe wall in the presence of moist. This results in the forming of sulphuric acid, which is capable of attacking cementitious materials. The strength of the corrosive action depends on sulphide concentration, acidity, biochemical oxygen demand (BOD), residence time, temperature and flow conditions (Bielecki and Schremmer 1987). Nevertheless, accurate prediction of the corrosion rates is still problematic.

There is less published on the failure of assets other than sewers, including pumps, valves, tanks and siphons. The failure rate of pumps, for example, is affected by several factors including composition of the sewage, succession of dry and wet periods, wastewater production in the catchment area, condition of the sewer system, cleaning frequency of the sewers and street surfaces, flow condition in the sewer, design of the sewage pump and wet well, air leakage into the pump and air pockets in the pressurised interceptor (see Joosten 2002). According to Pohl (2002), the failure of valves in sewer systems is affected by the following variables: power failure, blockage, rusting, corrosion or jamming of valves and leaking of seals.

Table 2.9 Summary of explanatory variables for sewer deterioration.

		Davies *et al.* (2001a)	Davies *et al.* (2001b)	Fenner and Sweeting (1999)	Hahn *et al.* (2002)	Baur and Herz (2002)
Sewer pipe	sewer condition	•				•
	sewer depth	•		•		
	sewer age			•		•
	sewer size	•	•	•		•
	sewer shape			•		•
	sewer material	•	•	•	•	•
	sewer gradient			•		•
	joint type			•		
	pipe length	•	•			
	pipe structure				•	
Wastewater	sewer use/purpose	•	•	•		•
	wastewater temperature				•	
	BOD concentration				•	
	corrosive chemicals				•	
	wastewater velocity				•	
Ground	infiltration/inflow	•				
	groundwater regime	•	•			
	soil type			•	•	
	soil fracture potential	•	•			
	soil corrosivity/acidity	•	•			
Road	surface loads				•	
	road classification	•				•
	traffic flow	•		•	•	
	goods vehicle flow	•				
	bus flow	•	•			
Other	root intrusion/trees nearby	•				
	burst history	•				
	presence of debris	•	•			
	construction type			•		
	installation history				•	
	property age	•				

2.5.2 Observations and coding of inspection data

Usually, an estimate of the actual condition of a complete sewer network is based on a limited number of inspections of sewers with similar characteristics. These inspections are often extrapolated over the whole network. Therefore, uncertainty about the structural condition of a sewer network depends on the representativeness of the sample. Müller and Dohmann (2002a and 2002b) have defined the amount of selective inspections needed for a representative sample. This is based on predefined confidence levels resulting from a required safety of the condition description for the whole sewer population. Moreover, the accuracy of a specific inspection method, the number of manholes or sewers inspected and the frequency of inspections are of importance. For example, inspections from a manhole have a limited sight (<5 m). In addition,

depending on the technology applied and the deposits, visual in-sewer inspections require prior cleaning. As a result, an existing sediment bed and possible debris are removed. In addition, the reliability of CCTV inspection data depends on the experience of the camera driver (e.g. speed and angle of the camera).

CCTV inspection is unable to directly measure any aspect of sewer condition. It relies on an intermediate visual interpretation by inspection personnel. As a consequence, sewer condition assessments based on CCTV data are subjective. However, the results can be supplemented by more objective methods, such as sonar or laser measurements. Interpretation of CCTV data is further restricted by the quality of the picture and the view obtained. For example, when cameras only provide an axial view down the sewer, they might fail to observe vital defects at connections. Currently, however, most cameras have tilting heads.

The interpretation of pictures assumes a clear relationship between observations and actual structural deficiencies. However, Jones (1984) and Davies *et al.* (2001a) stress that sewer deterioration processes are non-linear. Especially, sewer collapse is often triggered by some random event (e.g. heavy storm or water main break) that may not be related to the cause of the deterioration. Therefore, it is impossible to predict collapse, but it is possible to judge whether a sewer has deteriorated sufficiently for collapse to be likely.

Finally, coded inspection data serve as input for models describing sewer condition. In each model the accuracy of model output is dependent on the input. Therefore, the measurement uncertainty of inspection data affects decision-making on sewer rehabilitation. The reliability of these models is described in the next paragraph.

2.5.3 Models for the assessment of sewer conditions

The accuracy of any condition assessment model cannot be greater than the original information about the state of the network. Therefore, the quantity and extent of available data (including records of CCTV data, sewer collapses, soil maps and other external factors) determine the choice of an appropriate technique. Existing knowledge of determinative processes also affects the assessment performed.

2.5.3.1 Models describing deterioration processes

As pointed out in Chapter 1, knowledge of deterioration processes is rather limited. Some processes, such as corrosion and sedimentation, are qualitatively understood. However, quantitative prediction remains very inaccurate. Davies *et al.* (2001) and Stein (2001) summarise current knowledge on determinative processes for sewer deterioration (e.g. corrosion, pipe cracking, sedimentation and leakage) and external factors affecting these processes.

Even the knowledge on sewer corrosion, which has been most extensively studied, is rather limited. Therefore, predicted corrosion rates are highly uncertain. Sulphide formed in the sewage of a filled pipe may cause problems at locations where a

pressurised sewer drains into a gravity sewer. At these locations turbulence may be increased. Several models have been developed to describe sulphide formation both in pressurised and partly filled sewers which is subdivided into two types: qualitative models indicating the probability of corrosive attack and quantitative models estimating sulphide formation in sewer sections. An example of the qualitative models is the Z-index as described by Pomeroy (1974). Quantitative models for both filled (pressurised) and partly filled sewers (see Appendix I) have been developed by e.g. Pomeroy (1959 and 1974), Thistlethwayte (1972), Boon and Lister (1975), Hadjianghelou *et al.* (1984), Nielsen and Hvitved-Jacobsen (1988), and Tanaka and Nielsen (2002).

The afore-mentioned formulae are fully empirical and relate sulphide formation to a limited number of variables including BOD concentration, COD concentration, sewage temperature and pipe geometry (Bielecki and Schremmer 1987). Moreover, it is assumed that no sulphide is present at the beginning of a pipe section, newly formed sulphide is not oxidised, the amount of sulphate in the sewage is always sufficient, sulphide is only formed in the biofilm and the origin of the sewage is mainly domestic.

Using the formulae for sulphide build-up, the corrosion rate of cementitious material is calculated as described in Pomeroy (1974). The approach is also highly empirical (see Appendix I). Many factors in Pomeroy's equations have to be selected on the basis of engineering judgement, thus introducing substantial uncertainty.

The accuracy of models describing sulphide build-up and corrosion rate of cementitious material has been studied by several authors (e.g. Hadjianghelou *et al.* 1984, Haase and Polder 1988 and Beeldens and Van Gemert 2001). Hadjianghelou *et al.* (1984) oppose the assumed relationship between sulphide build-up rates and BOD or COD concentrations, respectively. Haase and Polder (1988) conclude that no correlation between sulphide flux from sewage to air and sulphide concentration in the sewage could be found. Moreover, their measurements (Rotterdam, The Netherlands) were much more in accordance with the Pomeroy formula than with the Boon and Lister formula, which is an indication for high turbulence levels. According to Beeldens and Van Gemert (2001), measured sulphide production rates and corrosion rates (Oostende and Lissewege, Belgium) are even larger than predicted with Pomeroy's formula. This occurs mostly at locations where pressurised sewers drain into gravity sewers.

Sediment build-up mainly results from structural causes including location in sewer network, shallow slope, loops, shape of pipes and special structures (inverted siphons, connections, crossings with water mains, etc.). The sedimentation rate depends on the flow field, the nature of particles and the concentration in suspension or near the bed.

Despite the recent developments in prediction methods, analytical prediction of sedimentation is still in its infancy. (Ashley *et al.* 2000). However, for determination of the risk of sediment build-up in each section of a sewer system, models have been successfully applied by e.g. Gérard and Chocat (1999) to the entire catchment of Lyon (France) and Ashley *et al.* (2000) for locating engineered sediment traps. A large drawback, however, of these models is their site specificity.

2.5.3.2 Models describing the transition between condition classes

Several authors describe changes in sewer condition not on the level of individual deterioration processes, but on the level of sewer condition classes in which all explanatory processes are aggregated.

According to Rostum *et al.* (1999) and Baur and Herz (2002), the deterioration of sewers can be described in relation to the transition of sewers between defined classes of sewer condition. A 'cohort survival model' with a corresponding 'Herz distribution' (Herz 1996 and 1998) is applied to predict transition moments from one class to the next. Cohorts are defined as sets of assets installed in the same year and with a particular probability of failure. The model input consists of CCTV data. Furthermore, the model does not predict the behaviour of individual sewers, but the deterioration (and rehabilitation need) of whole sewer districts. However, uncertainty of sewer classification is not accounted for. In addition, the method requires both long-term failure data (e.g. break type and time of break) and detailed information on individual pipe lengths including year of construction, material, dimensions, surrounding soil and CCTV inspections. In most European countries, except for Norway, this kind of data is seldom available.

A comparable model is being developed in The Netherlands (KEMA 2002). However, this model predicts the behaviour of individual pipes. By means of statistics CCTV inspections and expert opinion are combined in order to describe the probability of transition between condition classes. In contrast to the previous method, the KEMA model accounts for uncertainties in sewer classification as well as in condition development. Ongoing research on failure modelling in pipe networks concentrates on, for example, Weibull proportional hazard models (Le Gat and Eisenbeis 2000) and Markov models with a logistic failure rate (Poinard *et al.* 2003).

2.5.3.3 Decision support models for inspection, maintenance and rehabilitation

Regarding maintenance and rehabilitation, models are applied for decision support and condition prediction. In a range of countries methods have been developed to prioritise maintenance and rehabilitation using selection criteria: United Kingdom (Fenner and Sweeting 1999, Fenner 2000 and Water Research Centre 2001), Belgium (Cobbaert *et al.* 1998) and Australia (Anderson 1999). A decision support system for sewer rehabilitation is being developed by Sægrov and Schilling (2002) in order to "rehabilitate the right sewer at the right time by applying the right rehabilitation technology at minimum total cost".

The majority of methods discriminate between 'critical' and 'non-critical' sewers. 'Critical' sewers are defined as the sewers with the highest economic consequences of failure (20% of UK sewers) which are maintained proactively. Maintenance is allocated based on the structural condition of sewers using CCTV inspection and their calculated hydraulic performance using computer models to simulate flows. GIS (geographical

information system) technology can be applied to represent structural and hydraulic performance together and prioritise work on critical sewers.

Fenner and Sweeting (1998 and 1999), for example, describe a tool to predict failure of sewers analysing historical sewer event data and asset information. The likelihood of sewer failure is evaluated using 'critical grid squares', i.e. pipe data are analysed for a series of grid squares identifying 'hotspots' of sewer failure. Within the grid squares most at risk a Bayesian statistical model is applied to analyse and predict the condition of individual pipe lengths.

A different approach is applied in Rotterdam, The Netherlands. Priority of sewer rehabilitation is based on the volume of sewer pipes that is permanently filled with water (even during dwf) combined with predefined condition criteria such as pipe break, displacement and corrosion (Kerkhof 1988). Available storage of a sewer can diminish due to subsidence of ground, which is the most important threat to sewer performance in Rotterdam. This storage is considered indicative for hydraulic capacity, degree of contamination, leaking joints and corrosion of the pipe.

Recently, performance indicators are being used to support decision-making on sewer maintenance (Matos *et al.* 2003, OFWAT 2001, Ashley and Hopkinson 2002, Fenner and Saward 2002, and Sægrov and Schilling 2002). These methodologies use indicators for sewer performance including hydraulic, environmental, structural, economic and social aspects. For example, Ashley and Hopkinson (2002) apply performance indicators to measure and demonstrate 'serviceability' of a sewer system. An advantage over the other methods presented is its potential to rationalise and integrate strongly differing aspects of sewer system performance.

With respect to prioritising inspection of sewers and selecting most appropriate rehabilitation techniques decision support systems are being developed. An expert system for prioritising inspection of sewers is developed by Hahn *et al.* (2002). The method aims at targeting the critical areas in a sewer system based on predicted criticality of sewer pipes. A Bayesian belief network is applied to include uncertainties in expert beliefs in the decision process. Decision support for the selection of sewer rehabilitation technologies is based on e.g. pair wise (Plenker 2002) or multi-attribute comparison of alternatives (Shebab-Eldeen and Moselhi 2001).

The afore-mentioned decision support models, however, give no explanation for individual deterioration processes, but are only applicable for decision support. Moreover, their accuracy has been tested only to a limited degree.

2.5.4 Performance criteria

Performance requirements for the different sewer assets (pipes, pumps, manholes, etc.) are dependent on their type. For sewer condition, these requirements comprise watertightness of the pipe, stability of the pipe wall and gradient of the flow (NPR 3220). For other assets there are no prescribed performance indicators available in The Netherlands. As a consequence, management authorities need to establish their own criteria. For that purpose, Matos *et al.* (2003) present several performance indicators for sewer assets.

Table 2.10 Warning and intervention criteria for sewer inspections in The Netherlands (NPR 3398). Observations are classified on a scale from 1 (least severe/not present) to 5 (most severe).

		Observation type	Warning criterion	Intervention criterion *
LEAKTIGHTNESS	A1	infiltration of groundwater	≥3	4-5
	A2	ingress of soil from surrounding ground	≥2	-
	A3	longitudinal displacement	3-5	5
	A4	radial displacement	2-5	5
	A5	angular displacement	5	-
	A6	intruding sealing ring	3-5	5
	A7	intruding sealing material	3-5	5
STABILITY (pipe wall)	B1	break/collapse	5	-
	B2	surface damage by corrosion or mechanical action	≥3	-
	B3	fissure (cracks and fractures)	≥3	-
	B4	deformation of cross sectional shape	3-4	-
FLOW (gradient)	C1	intruding connection	3	3-5
	C2	root intrusion	2-3	3-5
	C3	fouling	2-3	3-5
	C4	encrustation of grease or other deposits (except for sand)	2-3	3-5
	C5	settled deposits (sand and waste)	2-3	3-5
	C6	other obstacles	2-3	3-5
	C7	water level	2-3	-

* In case no intervention criterion is given, inspection provides insufficient information to initiate rehabilitation, which calls for additional investigations.

Usually, visual inspections or CCTV data serve to provide information for sewer condition assessment. Due to the afore-mentioned uncertainties in inspection, coding and modelling of sewer conditions, these assessments can be rather uncertain. Therefore, assessment criteria should take possible uncertainties into account in order to avoid unnecessary rehabilitation. In The Netherlands, two types of criteria are used for condition assessment: warning and intervention criteria (Table 2.10). Exceedance of the 'warning criterion' asks for additional investigations, whereas exceedance of the 'intervention criterion' logically initiates sewer rehabilitation. These criteria have been

defined in terms of ranges instead of fixed values in order to account for possible uncertainties in the classification of inspections.

2.6 UNCERTAIN FACTORS IN COST AND DAMAGE

Decisions on maintenance and rehabilitation must be made under considerable uncertainty. In practice, such decisions are often taken intuitively. However, a more rational approach is desired. For example, maintenance and rehabilitation are optimised using economic cost criteria (see e.g. Van Dantzig, 1956). This would require the formulation of a cost function. A straightforward way to formulate a cost function is by capitalising both costs of maintenance or rehabilitation and damage due to system failure. Failure is defined as non-compliance of a sewer system with performance criteria regarding CSOs, flooding and structural integrity.

Comprehensive estimation of costs for sewer maintenance and rehabilitation is difficult. As a result of differences in the length of sewer networks, the age of sewer pipes, the type of discharges and the gradient of sewer pipes, these costs differ widely (Stein 2001). Losses due to failure (e.g. sewer collapse, CSOs and flooding) consist of, for example, the volume of sewage spilled to the surface water, the flood depth and number of flooding events and the impact of closed roads due to sewer collapse. They are also difficult to capitalise due to lack of knowledge and data, and changing perceptions of adverse effects, especially the environmental damage caused by CSOs. Consequently, determination of damage cost is subjective.

2.6.1 Cost of operation and maintenance

The costs of operation and maintenance are strongly dependent on the assets within a specific sewer network. In The Netherlands, the operational costs of sewer systems are approximately 10 Euros per metre per year (Stichting RIONED 2002). This results in costs per inhabitant per year ranging from 37 to 66 Euros. For comparison, in Germany the annual costs amount to approximately 9 Euros per metre (Pecher 1994). These are direct costs that include staff, energy and rehabilitation. The variation per inhabitant, however, is larger (90% of costs per inhabitant between 13 and 90 Euros per year).

In general, the costs of inspection of sewer systems depend on inspection equipment used (mirrors, photographs or CCTV), location and accessibility of manholes, diameter of sewer pipes, total length of sewers to be inspected, presence of obstacles in sewers or other assets, prior removal of sediments and required form and level of reporting (Table 2.11). Moreover, safety measures in order to protect inspection personnel from toxic gases such as hydrogen sulphide increase cost. Inspection costs of pumping stations are dependent on the capacity of pumps and the significance of the station within the sewer system, since more important pumping stations are usually inspected more often to reduce risk. The latter also holds for sewer pipes.

Table 2.11 Factors determining inspection costs of different assets (Stichting RIONED 1997b and Stein 2001).

Structure	Costs depend on
Sewer pipes	- location and accessibility of manholes (difficult accessibility increases cost)
	- size of sewer
	- inspection technique (mirrors, photographs or CCTV)
	- presence of hydrogen sulphide (safety measures for inspection personnel)
	- total length to be inspected
	- presence of obstacles
	- prior removal of sediments
	- required level of reporting
	- significance of sewer pipe
Manholes	- presence of hydrogen sulphide (safety measures for inspection personnel)
	- accessibility of manhole (difficult accessibility increases cost)
	- required level of reporting
CSO structures	- comparable to manholes
Pumping stations	- capacity of pumps
	- significance of pumping station in sewer network

Maintenance activities mainly consist of cleaning of manholes, gully pots and CSO structures (Table 2.12). They are carried out either manually or by a combination of water jetting, pigging and vacuuming (see Stein 2001). The cost of hand cleaning or excavation strongly depends on the situation regarding polluted sediment or dirt (RIONED 1997b and Butler and Davies 2001). In particular, removal of dirt from the inside of a pump is quite laborious.

Table 2.12 Factors determining maintenance cost of different assets (Stichting RIONED 1997b and Stein 2001).

Structure	Cost depend on
Sewer pipes	- size of sewer
	- cleaning method (jetting, rodding, boring, flushing, etc)
	- amount of sedimentation
	- necessity of dumping of (contaminated) sludge
	- presence of other assets (valves, pumps, etc)
	- reactive or planned maintenance
	- accessibility of sewers(difficult accessibility increases cost)
Manholes	- accessibility of manhole
	- reactive or planned maintenance
	- amount of sedimentation
	- necessity of dumping of (contaminated) sludge
Gully pots	- comparable to manholes
CSO structures	- comparable to manholes
Pumping stations	- maintenance frequency
	- pumping capacity
	- number of pumps
	- storage volume of wet well
	- obstructed part of pump

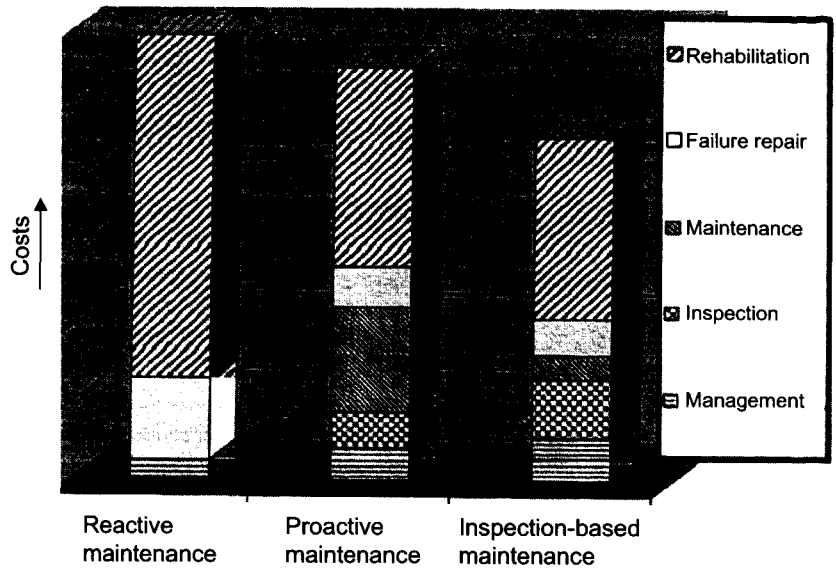

Figure 2.10 Relative distribution of costs for different operation and maintenance strategies (adapted from Haussmann 1997, as cited in Ertl 2003). Bars only provide a qualitative indication of costs.

Haussmann (1997) shows that the application of different maintenance strategies (reactive, proactive or inspection-based) leads to different cost distributions (cited in Ertl 2003). For example, the costs of rehabilitation decrease when proactive or inspection-based strategies are applied (see Figure 2.10). On the other hand, the cost of both inspection and maintenance are logically increased.

2.6.2 Cost of structural rehabilitation

As for operation and maintenance, rehabilitation costs may vary widely. Structural rehabilitation of sewer systems comprises repair, renovation and replacement. Their costs usually consist of a fixed and a variable part. Fixed costs are allocated to the project as a whole, whereas variable costs are a function of the system geometry. Therefore, variable costs of sewer rehabilitation are often assumed to be proportional to the length of the pipe section to be replaced or the volume of the storage tank to be built. Geerse and Vrisou van Eck (2001), however, conclude that the cost of replacement per metre of sewer length may vary considerably. This was based on expert opinion and cost data from rehabilitation projects in Rotterdam, The Netherlands. On average, the cost of replacement amounts to 550 Euros per metre sewer length with a variation of approximately 45 Euros. The variation results from external factors including cover depth, type of road surface, amount of traffic and soil contamination.

Table 2.13 Factors determining rehabilitation or reconstruction cost of different assets (Stichting RIONED 1997b, Geerse and Vrisou van Eck 2001 and Stein 2001).

Structure	Cost depend on
Sewer pipes	- size of sewer
	- rehabilitation method (pipe replacement, jacking, bursting, lining, etc)
	- cover depth
	- soil type (possibly contaminated)
	- bedding and backfill
	- open trench or trenchless construction
	- sewer material
	- road works
	- cover depth
	- amount of traffic (regarding diversions)
	- presence of trees or existing underground infrastructure
Manholes	- diameter of incoming sewers
	- location
	- material (small sewers (<300mm) allow PVC manholes)
	- construction method
	- presence of trees or existing underground infrastructure
Gully pots	- location
	- presence of trees or existing underground infrastructure
CSO structures	- comparable to manholes (cost approx. 10% higher due to weir)
Pumping stations	- wet or dry well
	- pumping capacity
	- number of pumps
	- storage volume of wet well
	- presence of telemetrics
	- removal of old parts
Storage sedimentation tank	- storage volume
	- emptying with or without pumps
	- removal of old parts
	- compliance with town planning (regarding new storage tanks)

Rehabilitation costs per metre sewer length are affected by several factors, including sewer diameter, total replaced sewer length, cover depth of sewers, construction method (open trench or trenchless), whether the rehabilitation project is separate or integrated with road works, tender method, project organisation, existing underground infrastructure, presence of contaminated soil, necessary traffic diversions, and sewer material (see also Table 2.13). According to Peters (1984), not only traffic disruption, but also loss of trade to business and damage to buildings, underground infrastructure and trees contribute to the cost of sewer rehabilitation. However, estimation of most of these costs is problematic. Uncertainty in rehabilitation cost decreases, when similar building projects have been carried out in the past.

Apart from sewer pipes, other assets may also require rehabilitation. The most important factors affecting costs comprise location of the asset and presence of trees or underground infrastructure (Table 2.13). With respect to both manholes and CSO structures, the size of incoming sewers and the construction method are also of importance. The costs of rehabilitating pumping stations depend on the type of pumping station (wet or dry well), the capacity of the pumps, the number of pumps

installed, the storage in the wet well and the presence of telemetrics. Variable costs of storage sedimentation tanks are related to the storage volume, the application of pumps for emptying and specific town planning requirements.

2.6.3 Damage due to CSOs

2.6.3.1 CSO impacts

It is generally acknowledged that CSO events are harmful to the quality of receiving waters (see e.g. House *et al.* 1993 and Novotny and Witte 1997). The impacts depend on both characteristics of the catchment producing the sewage and storm water runoff, and the characteristics of the receiving watercourses (e.g. size and type). However, the extent to which receiving waters are affected is not fully understood due to the transient character of CSOs, the time varying composition of overflow volumes and the complexity of processes in receiving waters (Beck 1996, and Ellis and Marsalek 1996). Moreover, Novotny and Witte (1997), and Ellis and Marsalek (1996), among others, emphasise that impacts of CSOs cannot be evaluated only considering exceedance of water quality standards. Conversely, an integrated and comprehensive assessment of storm water impacts on ecology is needed by means of e.g. biological monitoring.

According to Ellis and Hvitved-Jacobsen (1996), water quality impacts comprise:

- physical habitat changes,
- water quality changes,
- public health risks,
- aesthetic deterioration.

The physical habitat in urban streams changes due to increased sedimentation and high erosion potential due to CSOs. These processes influence stream morphology and substrate conditions. For example, Pedersen and Perkins (1986) and Davis *et al.* (2003) report that benthic communities that tolerate successive erosion and deposition and can utilise transient, low-quality food dominate urban streams. Water quality changes include dissolved oxygen (DO) depletion, eutrophication, sediment and toxic pollutant impacts and ecotoxicological impacts on biological communities. Fish kills are the most apparent acute effect of DO depletion. Materials accumulating on the bed of receiving waters generally provide a poor habitat for plant and animal species. With respect to aesthetic pollution, House (1996) stresses that the public's perception of water quality is often solely based on aesthetic appearance of watercourse and surroundings.

Table 2.14 Ranges of event mean concentrations of CSOs (in mg/l). Average values between brackets.

	Kerkrade (NWRW 1989a)	Loenen (NWRW 1989a)	'Le Marais', Paris (Gromaire-Mertz *et al.* 1998)	'Dorp-Oost', Vlist (Stichting RIONED *et al.* 1999)
BOD (mg/l)	15.0 – 232 (**74.6**)	8.9 – 141 (**39.9**)	67 – 296 (**181**)	9 – 105 (**35**)
COD (mg/l)	60.6 – 725 (**243**)	52.2 – 877 (**271**)	123 – 736 (**428**)	35-600 (**160**)
$N_{Kjeldahl}$ (mg/l)	3.8 – 31.7 (**13.4**)	3.3 – 26.3 (**10.4**)	-	5 – 22 (**11**)
P_{total} (mg/l)	0.9 – 7.5 (**3.0**)	0.9 – 7.2 (**2.9**)	-	1 –5.6 (**2**)
TSS (mg/l)	56.3 – 1081 (**320**)	20.9 – 1201 (**303**)	105 – 559 (**307**)	10 – 660 (**105**)

BOD = biochemical oxygen demand (mg O_2/l)
COD = chemical oxygen demand (mg O_2/l)
$N_{Kjeldahl}$ = total ammonium nitrogen and organic bound nitrogen (mg/l)
P_{total} = total phosphorus (mg/l)
TSS = total suspended solids (mg/l)

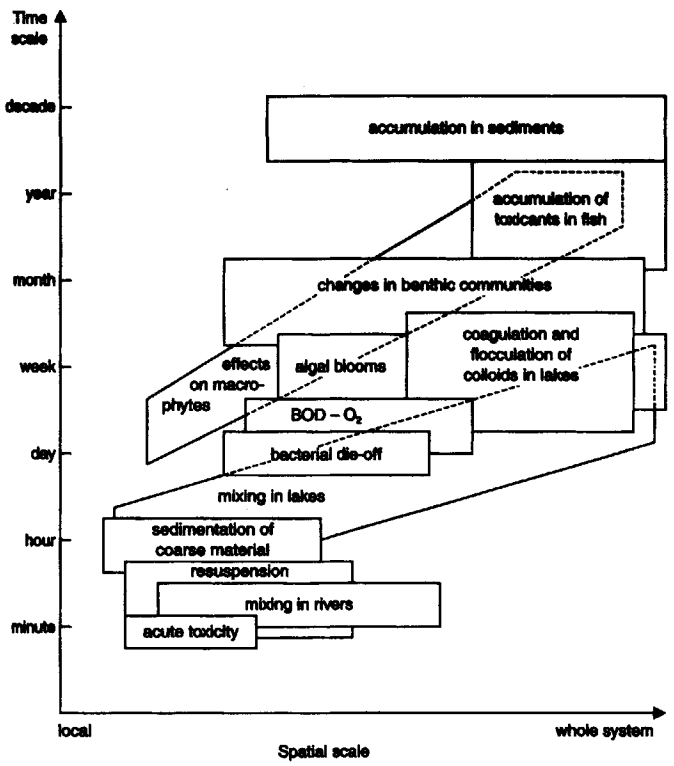

Figure 2.11 Characteristic time and spatial scales with respect to receiving water impacts (after Aalderink and Lijklema 1985).

However, the impacts of CSOs on receiving waters vary substantially and quantification is rather complicated. Firstly, water quality impacts may differ widely due to variations in volume, duration, composition and frequency of CSOs. In general, CSO volumes are highly variable between different storm events. Their composition shows an even larger variability (see Table 2.14) and is even subject to changes during a CSO event.

Secondly, the time and space scale of pollutant effects are highly variable (see Figure 2.11) due to both differences in nature of contaminants, and physical, chemical and (micro)biological processes in the receiving waters (see Aalderink and Lijklema 1985). The effect of a pollutant can be acute, accumulative or both (Figure 2.11).

Thirdly, most water quality models cannot account for the complex dynamic and event based nature of intermittent CSO discharges. Most models only consider equilibrium conditions. Therefore, they are unable to cope with transient loading due to CSOs (Shanahan *et al.* 1998). Not to mention the complexity of modelling impacts on plant and animal life within streams.

2.6.3.2 Valuation of CSO impacts

In order to choose between different options of sewer rehabilitation, the water quality impacts of CSOs must be valued in monetary, qualitative or other terms. For monetary valuation of nature several methods have been developed. These methods determine the economic value of human use of the environment. They are divided into two basic approaches: direct and indirect methods. Direct methods estimate individuals' preferences for environmental quality directly by asking them to state their 'willingness to pay' (WTP) for an increase in environmental quality. Indirect methods seek to recover estimates of WTP for environmental quality by observing individuals' behaviour in related markets. Each method has its own shortcomings and possible bias. The following evaluation methods are described in Appendix II (see Lorenz 1999, Pandey and Nathwani 2003 and Penning-Rowsell 2003):

- travel costing method,
- hedonic pricing method,
- contingent valuation method,
- conjoint analysis,
- production factor method,
- averting behaviour method,
- Life Quality Index.

Economic valuation methods have seldom been applied to sewer rehabilitation. Applications of contingent valuation are presented by Crabtree *et al.* (1999), Novotny *et al.* (2001) and Green (2003). These studies estimate the benefits of urban stream flow control and restoration by employing a survey of residents to assess their maximum 'willingness to pay'. Notvotny *et al.* (2001), for example, presented respondents with alternative scenarios and asked if they were willing to pay a certain amount of money for the realisation. As reference points, average public expenditures on other public services

(e.g. fire brigade and library) provided by their state and local government were provided. Streiner and Loomis (1995) applied the hedonic pricing technique. In their study the impact of urban stream restoration on property values in counties in California (USA) has been valued.

Economic optimisation or cost-benefit assessment, as applied to dike design by e.g. Van Dantzig (1956) and Van Gelder (2000), would enable more objective decision-making on maintenance and rehabilitation of sewer systems. It determines the optimal intervention by a minimisation of total cost comprising investment with respect to maintenance or construction and cost of environmental damage due to overflows. Expected total costs are discounted either over a bounded (e.g. 50 years) or unbounded time horizon, assuming that the value of money decreases with time. Other approaches to economic assessment of restoration projects of urban watercourses are life-cycle assessment (Bishop 2000 and Cashman *et al.* 2002), cost-benefit analysis using Life Quality Index (Pandey and Nathwani 2003), multi-criteria and scenario analysis (Nijkamp and van den Bergh 1997), and stochastic dominance assessment (Tung *et al.* 1993, Reda and Beck 1997 and Duchesne *et al.* 2001).

However, several other authors oppose the afore-mentioned economic valuation of nature. In their opinion, not all information relevant for decision making (e.g. biodiversity) can be capitalised. With respect to most goods and services provided by nature, no markets or ownership rights exist. As a result, no price is paid for their use or deletion. In addition, conflicting interests (e.g. social and environmental) cannot be expressed in conventional economic optimisation.

Instead of expressing environmental values in monetary terms, the concept of 'environmental function' has been applied by e.g. Gilbert and Janssen (1998) and Lorenz (1999). Environmental function is defined as the set of ecological and physical processes responsible for the provision of environmental goods or services. Nature, in this particular case a natural watercourse, provides a range of environmental goods and services for society. Such functions describe the relationship or interaction between ecological processes (e.g. erosion, sedimentation and waste dumping) and socio-economic activities (e.g. drinking water production, wood, fishing, recycling of wastes, transport and recreation). The pressure of society on nature is in indicators for environmental quality including productivity, structure and resilience.

Assessment of quantities or indicators expressed in different terms, e.g. monetary, nominal or qualitative, requires the use of multi-criteria decision methods or scenario analyses (e.g. Nijkamp and Van den Bergh 1997 and Bender and Simonovic 2000). Qualitative indicators, for example ranging from 'good' to 'bad', may be assessed using fuzzy set theory (see Zadeh 1965).

In conclusion, a purely economic valuation of losses due to CSOs remains highly uncertain because it is impossible to express all damage in monetary terms. However, the 'environmental function' concept and related techniques (such as multi-criteria

analysis) only transfer the problem of expressing loss in monetary terms to assigning weights to nominal or linguistic indicators in order to enable assessment. Scenario analysis or cost-benefit analysis using a Life Quality Index are expected to be most promising for the assessment of environmental damage due to CSOs because it can, though only partly, account for uncertainties.

2.6.4 Damage due to flooding

2.6.4.1 Flooding impacts

Often roads and tunnels are the first points to flood in a city, which results in a disruption of traffic. Other impacts related to urban flooding include flooded houses and basements, collapse of sewers, subsidence of streets and pavements, dirt left behind on streets and loss of trade to business. Flooding of property also brings damage to health.

Damage and losses due to flooding are either direct or indirect. Furthermore, direct and indirect damage may be subdivided into tangible or intangible damage (see König *et al.* 2002 and Penning-Rowsell *et al.* 2003).

- Direct damage includes material damage to property (e.g. buildings and basements) caused by the floodwater. In the UK, for example, much of the event damage cost is for inventories. The magnitude of direct, tangible damage either equals the cost of restoration of the property to its condition prior to the flooding event, or the market value if restoration is not worthwhile. The severity ranges from rotten floors and wall panelling to cracks in foundations. There is a significant difference between damage caused by sewage or surface runoff due to the composition.
- Indirect losses are losses caused by a disruption of society (e.g. traffic disruption) or an interruption of the economic activities (e.g. loss of industrial production) and the additional costs of emergency works.
- Intangible losses due to flooding comprise, for example, health impacts or inconvenience due to post-flood recovery. The monetary evaluation of these consequences is difficult, if not impossible to establish but their importance may be crucial. Moreover, most of these consequences cannot be removed directly after the flooding.

However, current sewer models have shortcomings with respect to modelling of flooding. Most models allow sewage to flow out of the sewer system on to the streets, but modelling overland flow to different surfaces is impossible. Generally, surcharged flow and flooding are modelled by means of the 'Preissmann slot' (see Clemens 2001a). According to Maksimovic and Prodanovic (2001) and De Haan (2002), predicted flood depths are unreliable in commercially available models because:

- sewer flow and street flow are strictly separated in the model, hindering interaction,
- overland flow is not included in the model,

- hydraulic resistance of gully pots and connections is ignored in the model,
- transitions between different surface types are ignored in the model.

Only recently, models are being developed which describe both in-sewer and overland flow also accounting for the interactions (Djordjevic *et al.* 1999 and Schmitt *et al.* 2002).

2.6.4.2 Valuation of flooding impacts

Many studies consider impacts of fluvial flooding resulting from rivers and streams (Debo 1982, Appelbaum 1985, McBean *et al.* 1988 and Penning-Rowsell *et al.* 2003). The 'Multi-coloured manual' by Penning-Rowsell *et al.* (2003), for example, presents a range of techniques and detailed data that are used to assess (fluvial) flood alleviation projects. It covers a diversity of flood losses including direct, indirect and intangible losses to residential property, losses for retail shops, losses for offices, losses for industrial premises, road traffic disruption and emergency services costs. However, urban flooding due to blockage, pump failure, or insufficient in-sewer storage differs from fluvial flooding (see Lee and Essex 1983). Nonetheless, the data and techniques are applicable for capitalising impacts of urban flooding.

Flood damage loss is a function of the nature and extent of the flooding, including its depth, duration, sediment load and contamination with sewage. For example, the cost of traffic disruption increases with increasing flood duration (Penning-Rowsell *et al.* 2003). In most studies flood damage is evaluated under the assumption that, for given social and economic conditions, damage is a function of floodwater depth (see Table 2.15 to Table 2.18). Damage is defined as the amount of property value or the percentage of the total value of the property that is lost due to flooding.

For damage valuation a number of 'depth-damage curves' have been derived regarding homes or other buildings at risk (e.g. Debo 1982, Appelbaum 1985, McBean *et al.* 1988, Oliveri and Santoro 2000, König *et al.* 2002 and Penning-Rowsell *et al.* 2003). The monetary value of losses due to flooding are based on the following cost data: insurance data from past incidents (Van der Bolt and Kok 2000, and König 2002), estimated replacement costs (Appelbaum 1985 and Oliveri and Santoro 2000), contractors' prices for repair work (Penning-Rowsell *et al.* 2003), detailed house-to-house surveys (McBean *et al.* 1988), tax records or data on recent home sales.

The land use of a flooded area also contributes to its damage potential. For example, houses are affected differently from, on the one hand, shops and offices and, on the other, industrial premises. This is included in depth-damage curves by providing different curves for houses, shops and industrial premises (e.g. Penning-Rowsell *et al.* 2003).

Depending on the severity of flooding, several authorities are involved in emergency works and clean-up operations during and after flood events. These authorities include local authorities, water boards, the police, the fire brigade, ambulance services, voluntary services and the armed forces. Appelbaum (1985) and Penning-Rowsell *et al.* (2003) provide cost estimates of emergency services.

Most depth-damage relations concern direct damage to dwellings regarding both structure and contents. According to Penning-Rowsell *et al.* (2003), every dwelling is classified using three variables: house type, age of house and occupants' social class. Oliveri and Santoro (2000) identify similar criteria including size, construction materials, age, contents, monumental significance, use and surrounding area. Examples of depth-damage relations are presented in Table 2.15 until Table 2.18. In order to value flood damage Penning-Rowsell *et al.* (2003) apply several flood durations and depths. Short duration concerns flooding of less than 12 hours, long duration of more than 12 hours. The flood depth levels have been chosen in a such way that they describe damage to basement (-0.3 m), to ground floor (0.0 m), to carpet and floor covering (0.05 m), to internal fabric and inventory items (0.1, 0.2 and 0.3 m) and progressively to building and contents (0.6, 0.9, ..., 3.0 m).

Table 2.15 Percent damage at given flood depths (in m) and with given property type for Georgia, USA (Debo 1982).

Property type	Flood depth (m)		
	0.3	0.61	0.91
1 storey, no basement, single family	8	17	31
1 storey, with basement, single family	11	23	37
Multi-storey, no basement, single family	5	10	17
Multi-storey, with basement, single family	5	10	16
Multi-storey, no basement, multifamily	2	5	12
Multi-storey, no basement, multifamily	5	11	18

Table 2.16 Percent damage at given flood depths (in m) and with given property type for Wyoming Valley, Pennsylvania USA (Appelbaum 1985).

Property type	Flood depth (m)		
	0.3	0.61	0.91
1 storey, no basement	10	14	26
1 storey, with basement	18	20	23
1½ and 2 storey, no basement	9	13	18
1½ and 2 storey, with basement	11	17	22

Table 2.17 Percent damage at given flood depths (in m) and with given property type for Palermo, Italy (Oliveri and Santoro 2000).

Property type	Flood depth (m)			
	0.25	0.50	0.75	1.00
2 storey building	4.8	7.8	12.5	15.6
4 storey building	5.3	7.5	8.8	9.0

Table 2.18 Relationship between flood depths (in m) and damage costs* (in US$) depending on interior standards for Bærum, Norway (König et al. 2002).

Property type	Flood depth (m)		
	< 0.05	0.05 – 0.25	> 0.25
High standard (furnished)	8000	28000	48000
Medium standard (partly furnished)	4000	13000	27000
Low standard (not furnished)	2000	6000	12000

* Factors possibly increasing or decreasing average damage include floor space, composition of floodwater and type of building.

Comparison of Table 2.15, Table 2.16 and Table 2.17 shows that flood damage for individual buildings is highly variable both within and across categories of buildings, and within and across occupants' social classes (see also McBean 1988). Averages represent only a rough indication for damage because the standard deviation is in the order of the average damage (König *et al.* 2002). In addition, as residential depth-damage relations reflect average losses to buildings (houses, industrial premises, etc), there may be concern about validity of information in the relations (McBean *et al.* 1988 and Oliveri and Santoro 2000):

- Curves cannot be easily transferred because they have been developed for specific areas (based on local characteristics).
- Lifestyles may have changed significantly since the curves were generated (interior standard).
- Different premises exist on what should be regarded as damage (only damage to buildings or all damage incurred including interiors and furnishings).
- Different valuation methods are applied leading to different property values (e.g. damage as percentage of total property value, damage as percentage of market value or absolute damage level based on actual repair cost).
- Damage costs based on insurance data are biased due to differences in claiming behaviour.
- Different curves are specified for different classes of residences irrespective of e.g. the quality of building and interior prior to the flooding.
- Anticipation of potential damage causes variability in actual damage (e.g. tiled instead of wooden floors).
- Damage to industrial premises is highly variable due to different activities.

2.7 COPING WITH UNCERTAINTY

In sewer maintenance and rehabilitation both underdesign and overdesign are possible due to uncertainties. This mainly results from ignorance either caused by lack of data or uncertainties about system properties or sewer-related processes. Moreover, there will always be uncertainty about the future over both the short and the long term. However, this does not imply that one should be uncertain about which options to choose. Instead, recognising that the future is uncertain influences how decisions are made and

different options adopted. Therefore, the essential question is how to deal with these uncertainties. Current practice (Stichting RIONED 1994, 1996 and 1999), however, does not account for uncertainties.

An example of decision-making under uncertainty in urban drainage is when an engineer has to decide upon a major system reconstruction in order to prevent pollution of receiving waters due to CSOs. However, due to uncertainty, CSO volumes are not exactly known. The variability of calculated annual CSO volumes for the sewer system of 'De Hoven', the Netherlands, is given in Figure 2.12. For building additional storage three options are available:

1. Design a storage facility that is sufficient for the average yearly CSO volume. At present, this is the usual approach in The Netherlands, which is in accordance with Dutch guidelines 'Leidraad Riolering' (Stichting RIONED 1994, 1996 and 1999). However, uncertainty in calculated CSO volume is not accounted for.
2. Add more safety to the design and enlarge the storage volume to 95% of the expected yearly volume. As a result, uncertainty in CSO volumes is considered.
3. Gather more accurate information on the geometry of the sewer system (e.g. profile dimensions, invert levels and weir crest levels) prior to designing. As a result, the uncertainty about actual sewer geometry decreases and a smaller storage facility can be built.

The choice for the designer depends on different aspects. The choice between alternatives 2 and 3 considers the costs of enlarging the storage volume, the implications of underdesign or overdesign of the storage facility, the costs of carrying out measurements and making necessary calculations, and a likely decrease of uncertainty about sewer geometry resulting from new information. The choice between alternatives 1 and 2, however, requires a shift from current practice to a risk-based approach to design.

The final decision is made depending on the current performance of the sewer system and the known future changes in the boundary conditions, such as environmental policy and planning. In this example, however, uncertainty about the future is not considered.

As emphasised in the previous example, uncertainties in decision-making on sewer system rehabilitation and maintenance can be reduced, except for inherent uncertainties in time. Reduction of uncertainties will cost money. The question is which uncertainty is worth reducing and at what cost. Since inherent uncertainties in time represent randomness or variations in nature, they cannot be reduced. However, taking more measurements can reduce inherent uncertainties in space. Epistemic uncertainties, on the other hand, are caused by lack of knowledge and may reduce as knowledge increases. Knowledge increases by means of:

- data gathered with measurements,
- research aiming at a better understanding of physical systems or a better use of available data,

- expert judgement and opinions enabling the estimation of probability distributions of variables that are too expensive or practically impossible to measure.

Cooke (1991) describes various methods for updating knowledge on a variable by expert judgement.

However, calculated uncertainty may also increase due to increasing knowledge, showing that an initially reliable model is shown to contain considerable uncertainty, that the variations of a measured variable (e.g. pipe size) are larger than expected or that the expected value of a variable may change due to research. Therefore, it is important to understand to what extent future reduction of uncertainties will influence the expected probability of failure.

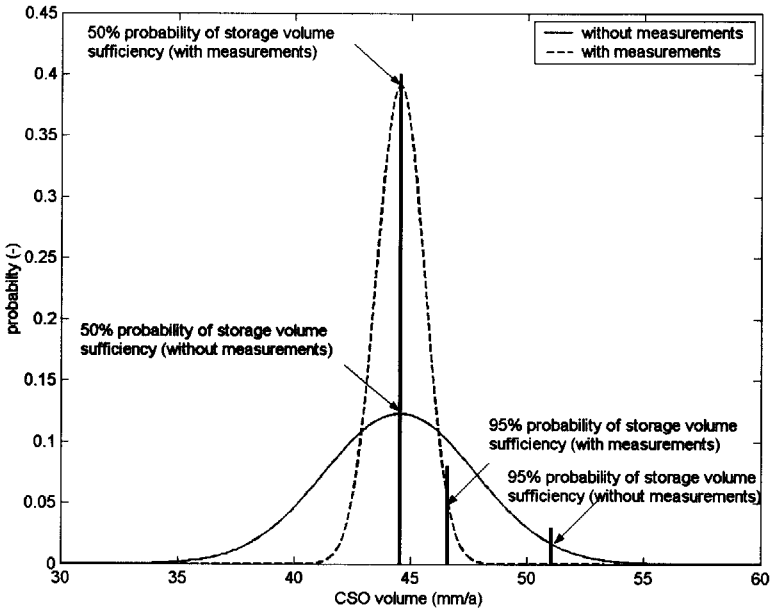

Figure 2.12 Illustrative example of design of storage volume of sewer system with and without taking measurements prior to decision-making (Korving *et al.* 2001). Measurements result in a reduction of uncertainties.

There are several techniques available to estimate uncertainty and decide whether reduction is worthwhile. These techniques are closely related to Bayesian statistics. They can be applied for the analysis of problems that arise when consequences of actions depend on an uncertain 'state of the world'. The decision-maker either has obtained or can obtain information about this uncertain state by means of sampling or experimentation. Several related techniques are discussed in Chapter 3, including

decision theory (see Pratt *et al.* 1997), Bayes weight assessment (see Bernardo and Smith 1994 and Kass and Raftery 1995), and valuation of new information (see Benjamin and Cornell 1979 and Ang and Tang 1990). Subsequently, they are applied to sewer maintenance and rehabilitation in Chapter 4 and 5 of this thesis.

2.8 CONCLUDING REMARKS

The framework applied in this thesis divides uncertainty into two main categories: inherent and epistemic uncertainty. The former represents randomness in nature, the latter represents lack of knowledge and can be distinguished in model uncertainty and statistical uncertainty. The practical significance of this classification is that the reduction of different types of uncertainty can be individually dealt with, since reduction of each type requires its own approach. However, a shortcoming of this classification is that it is not exclusive, i.e. the same uncertainty may belong to different categories. For example, due to model calibration there is a transition of model structure uncertainty to parameter uncertainty. Other authors, however, oppose this approach because the classification is too restrictive. In their opinion, the same uncertainty may be classified differently for different decision problems.

With respect to sewer systems, possible uncertainties consist of accuracy of measurements, knowledge of processes, model errors and appreciation of impacts of system failure. In particular, the uncertainty of impacts of CSOs and flooding is relatively large due the strong variation in the appreciation of effects and the uncertain likelihood of the composition of spilled sewage.

CHAPTER 3 Methods for uncertainty and risk analysis

3.1 INTRODUCTION

Often, technical design decisions have to be based on uncertain predictions and information. As a result, risk is unavoidable. By means of probabilistic modelling, uncertainties can be effectively modelled and assessed. Novotny and Witte (1997), Grum and Aalderink (1999), Willems and Berlamont (1999), Portielje (2000), Diaper *et al.* (2001), Bixio *et al.* (2002), Hauger *et al.* (2002) and Korving *et al.* (2002 and 2003) present examples of uncertainty and risk analysis in urban drainage.

There are several techniques available for modelling uncertainty and risk. The next sections introduce the techniques applied in this thesis. Firstly, using statistical decision theory the impacts of uncertainties on decisions can be systematically considered. For example, the additional value of field measurements prior to planning of sewer rehabilitation can be determined. Secondly, quantitative risk analysis can account for failure of sewer systems and uncertainty regarding system behaviour. Therefore, a risk based optimisation method is applied to determine the optimal storage volume of a sewer system accounting for the failure probability of the system. For this purpose, cost functions and failure probabilities have to be estimated. Thirdly, for the assessment of sewer system performance, knowledge of uncertainties in information, failure modes and availability of assets is needed. In particular, when failure data are available, the rate of occurrence of failures of (parts of) systems can be modelled even for ageing systems. The models applied take account of specific aspects of failure processes, such as clustered events, repair strategy, ageing and refurbishment.

The afore-mentioned techniques require an estimation of the strength and load of systems. Statistical distribution functions are used to describe strength and load in order to predict the extremes. Their parameters can be estimated using various methods, e.g. maximum likelihood or Bayesian estimation.

3.2 DECISION THEORY

Decision theory is treated in various textbooks, such as Benjamin and Cornell (1979), Ang and Tang (1990) and Pratt *et al.* (1995). It comprises the systematic analysis of decision problems utilising decision trees. In this way, decision-making with already available or new information is possible. In addition, the additional value of acquiring

new information (e.g. by means of field measurements or hydrodynamic modelling) prior to decision-making on sewer rehabilitation can be examined.

3.2.1 Decision model

According to Ang and Tang (1990), a decision model includes (1) all feasible alternatives including acquisition of additional information (if appropriate), (2) all possible outcomes associated with each alternative, (3) an estimation of the probability associated with each possible outcome, (4) an evaluation of the consequences of each combination of alternatives and outcomes, (5) the decision criterion and (6) a systematic evaluation of all alternatives.

3.2.1.1 Model components

Decision trees provide a systematic framework for decision analysis (see Figure 3.1). They consist of the complete sequence of decisions and include:

- a set of feasible alternatives: $A = \{a_1, a_2, \ldots, a_m\}$.
- a set of possible outcomes or 'states of the world' associated with each alternative: $\Theta = \{\theta_1, \theta_2, \ldots, \theta_n\}$.
- a set of possible experiments: $E = \{e_0, e_1, \ldots, e_p\}$.
- a set of potential outcomes of all experiments: $Z = \{z_0, z_1, \ldots, z_q\}$.
- monetary consequences or utility evaluations corresponding to alternative a_i, outcome θ_j, and, if appropriate, experiment e_k and the corresponding experimental outcome z_l: $u(e_k, z_l, a_i, \theta_j)$.
- probability measures for events involving combinations of θ and z: $p(z_l | e_k)$, $p(\theta_j | a_i)$ or, if appropriate, $p(\theta_j | z_l, e_k, a_i)$.

The decision-maker's preference for consequence c (relative to other consequences) is quantified by the utility $u(c)$, the decision-maker's judgement about uncertain outcome θ by the probability $p(\theta)$. A consequence c consists of a combination of an action a and an outcome θ.

The tree can be read as follows. On the left it starts with a 'decision node' indicated as a square. At this node the decision-maker chooses an experiment from a set of possible experiments (e_0 (no experiment),e_1,e_2,...). An experiment should be interpreted in a broad sense, meaning any method of gathering additional data. The symbol e_0 denotes 'no experiment'. Subsequently, there are several possible outcomes that may result from each experiment. The outcomes (z_1,z_2,...) are shown as branches originating from a circular node, called a 'chance node'. The decision-maker has no influence on these outcomes; nature controls what will occur. In general, outcomes are conditional on preceding choices, for example $p(z_1 | e_1)$ which is the probability of outcome z_1 given experiment e_1. A second decision node follows each experimental outcome. It indicates that a decision on alternative actions or interventions (a_1,a_2,...) is taken after observing

the obtained experimental data. Afterwards, several possible outcomes ($\theta_1,\theta_2,\ldots$) may occur. Again these outcomes cannot be influenced by the decision-maker. The probability of θ_j in the subsequent branches is updated depending upon the experimental outcome. Using Bayesian statistics (see § 3.2.2), it is expressed as $p(\theta_j|z_l,e_k,a_i)$, i.e. the probability of an outcome given an experiment, its result and the intervention chosen. In the case of a continuous spectrum of outcomes, a continuous pdf is used to denote the probability of the branches instead of discrete probabilities. The consequences of the sequence of choices by the decision maker and possible outcomes is expressed in a utility function $u(e,z,a,\theta)$.

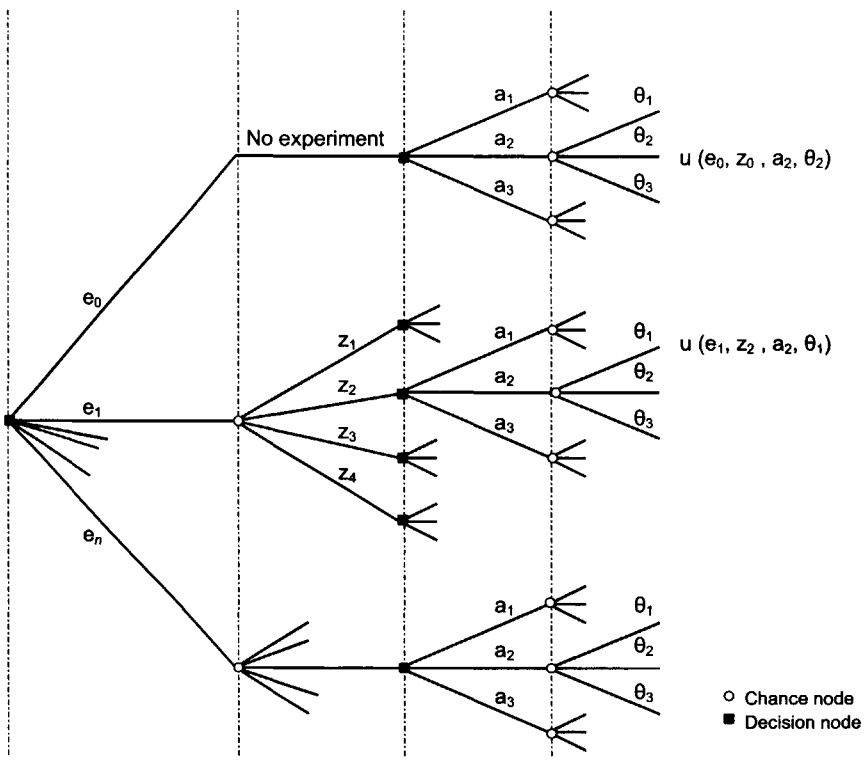

Figure 3.1 Generic decision tree.

3.2.1.2 Criteria for decision making

In general, there is no 'objectively correct' solution to a decision problem. The decision depends on the personal preference of the decision-maker, the personal judgement of the probability of possible outcomes and the observed data. The observations represent a single realisation of the process. As a result, making the 'best' decision may mean different things to different people at different times. Hence, a scale for quantifying

preferences among outcomes is required in order to rank feasible alternatives in a decision tree and make the 'best' choice.

In order to define a uniform scale for measuring the value of an alternative the concept of utility is applied (see e.g. Ang and Tang 1990, Pratt *et al.* 1995 and Van Gelder 2000). It expresses the preferences of a decision-maker in a 'utility function', i.e. the measure of the value of an alternative to the decision-maker. Finally, the alternative with the highest utility value will be preferred. When consequences (e.g. environmental damage due to CSOs) cannot be fully described by the amount of money to be paid or received, they have to be scaled. Usually, a utility of 1 is assigned to the most preferred alternative and a utility of 0 to the least preferred. The utilities of the other alternatives are determined relative to these two, usually by choosing among hypothetical lotteries searching for indifference points. However, other scales are also possible. A detailed description of utility theory including the assignment of utility functions can be found in e.g. Pratt *et al.* (1995).

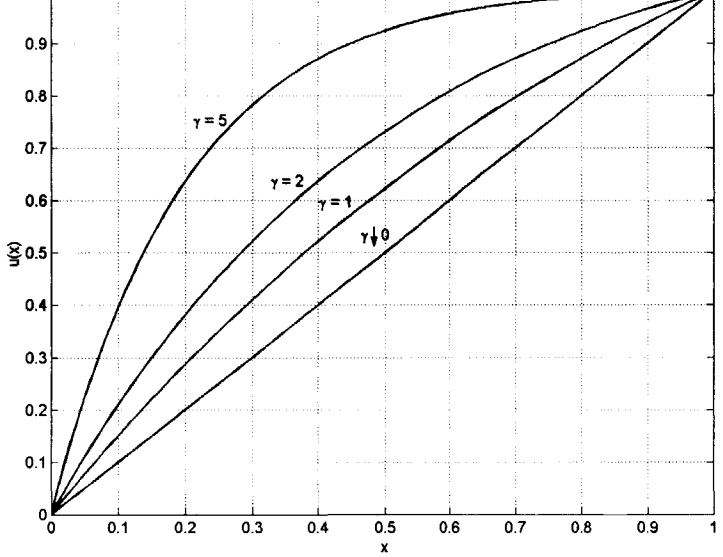

Figure 3.2 Example of utility functions ($\gamma\downarrow 0$ represents behaviour of large firms, whereas $\gamma>1$ represents behaviour of individuals). The parameter γ is the measure of the degree of risk aversion.

Most utility functions are concave (Figure 3.2 ($\gamma>1$)) indicating that marginal increases in the utility decrease with increasing value of an alternative, where γ is the measure of the degree of risk aversion. The behaviour associated with such a utility function is called 'risk-averting' (see e.g. DeGroot 1970). It indicates that the order of preference changes with the monetary value of the alternatives and the financial status of the decision-

maker relative to this monetary value. A convex utility function, on the other hand, represents 'risk-affinitive' or 'risk-seeking' behaviour. However, this preference is believed not to be realistic. Ang and Tang (1990) present several types of utility function to describe risk-averse behaviour, e.g. exponential, logarithmic and quadratic. A convex curve represents the behaviour of individuals, whereas a straight line ($y\downarrow 0$) is encountered among large firms and government organisations. It shows that individuals are more risk averting than large firms are.

In some situations, however, it can be very difficult to describe a complex consequence with a single (monetary) value. Then each consequence can be associated with a pair of numbers. This results in a decision problem with a utility function involving two or more variables. More information on multi-criteria decision analysis can be found in Keeney and Raiffa (1993).

When the consequences of each alternative can be expressed in monetary terms, the expected monetary value (EMV) is used for choosing between alternatives. The objective is either to minimise loss or maximise gain. The expected monetary value of action a_i is,

$$E\{d(a_i,\theta)\} = \sum_{j=1}^{m} p(\theta_j) d(a_i,\theta_j) \tag{3.1}$$

where $d(a_i,\theta_j)$ expresses the monetary value of consequence θ_j resulting from action a_i and $p(\theta_j)$ is the corresponding probability. It is assumed that the decision-maker can assign a monetary value to each sequence (e,z,a,θ), such that there is indifference between obtaining the full consequence arising from (e,z,a,θ) and obtaining a similar amount of money. Given the utility function the decision-maker can best choose the action with minimal expected loss (or maximum gain),

$$E\{d(a^*,\theta)\} = \max_i \left\{ \sum_{j=1}^{m} p(\theta_j) d(a_i,\theta_j) \right\} \quad \text{or} \quad E\{d(a^*,\theta)\} = \min_i \left\{ \sum_{j=1}^{m} p(\theta_j) d(a_i,\theta_j) \right\} \tag{3.2}$$

where $E\{d(a^*,\theta)\}$ is the expected cost of the optimal action.

When it is impossible to express all consequences in terms of money, the monetary value in Eq. (3.3) is replaced by a utility value,

$$E\{u(a_i,\theta)\} = \sum_{j=1}^{m} p(\theta_j) u(a_i,\theta_j) \tag{3.3}$$

where $u(\theta_j,a_i)$ is the utility of consequence θ_j resulting from action a_i. This utility is subjective and scales all non-monetary consequences. Expected utility as a decision criterion can also be applied when the utility function is non-linear and e.g. describes risk aversion (see Van Gelder 2000).

3.2.2 Decisions with available and new information

Given the probabilities of possible outcomes and the consequences of each action evaluated using existing information, the expected utility of the actions can be computed using Eq. (3.4). Such an analysis based entirely on available information is called prior analysis. If the analysis is updated with new information, it is called a 'terminal analysis'.

Both prior and terminal analysis are illustrated with an example that concerns decision-making on building in-sewer storage in order to reduce CSO emissions. In particular, the additional value of carrying out measurements for model calibration prior to decision making on storage volume is studied. The objective is to reduce the risk of disinvestment related to building either too large or too small storage. The alternative actions are weighed using the expected utility criterion.

The possible actions have been translated into a decision tree (Figure 3.3). The decision-maker has to choose between either building no storage facility, 1 mm or 2 mm of additional storage. The possible outcomes are simplified to a CSO volume of either less or more than 36.5 mm/a (based on CIW 2001). A utility $u(a_i,\theta_j)$ is assigned to each combination of an action and a consequence. Each utility has been estimated from experience and represents environmental damage to natural watercourses due to CSOs, construction costs of the storage facility and losses due to use of space by the facility. These utilities are introduced in Figure 3.3 as negative values, since they represent losses. The probabilities of possible outcomes are estimated by expert judgement and measure 0.6 and 0.4, respectively (see Figure 3.3).

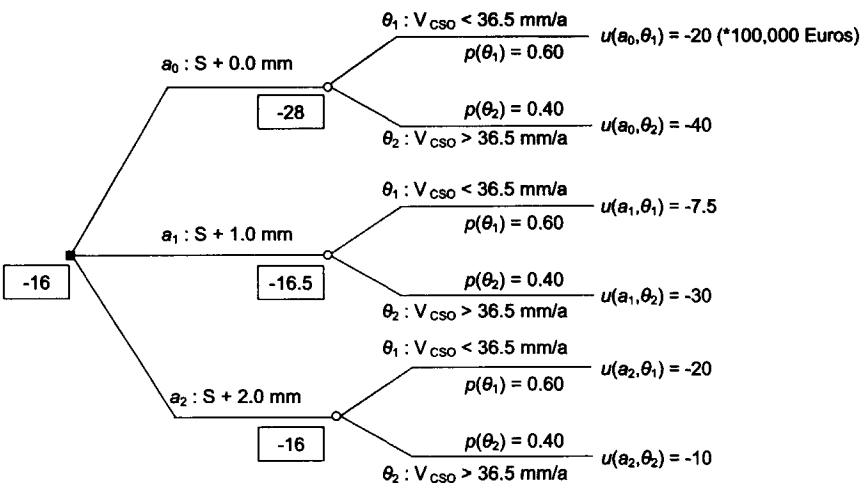

Figure 3.3 Decision tree: prior analysis of building additional in-sewer storage.

The alternatives are compared in terms of expected utilities. For example, the expected utility of the upper branches equals,

$$E\{u(a_0,\theta)\} = p(\theta_1)u(a_0,\theta_1) + p(\theta_2)u(a_0,\theta_2) = (-20 * 0.6) + (-40 * 0.4) = -28$$

The other expected utilities can be similarly calculated and amount to –16.5 and –16, respectively (see Figure 3.3). Finally, the action with maximal expected utility a_2 is chosen.

In order to improve information or reduce uncertainty, either laboratory or field tests, or research studies can be performed. Data acquisition requires time, energy and financial resources. The additional cost should be included in the decision tree. In general, additional information does not eliminate all uncertainty in a decision problem, but based on the experimental outcome the probabilities can be updated by applying Bayes' theorem (see § 3.2.2).

A decision tree with additional information resembles prior analysis, except for the updated probabilities that are used to compute expected monetary value or utility. The afore-mentioned decision problem is extended with precipitation and water level measurements for model calibration (see Figure 3.4). The cost of carrying out measurements and subsequent calibration of a sewer model is 100,000 Euros. These are added to the utilities as described in Figure 3.3. The reliability of the experimental results is shown in Table 3.1. If the actual CSO volume exceeds 36.5 mm/a, the probability that the experimental results indicate a large volume is 0.7. On the other hand, if the volume is smaller than 36.5 mm/a, the probability that the experimental results indicate a small volume is 0.8.

Using Bayes' theorem probabilities of possible outcomes are updated based on the reliability of the experimental results (Table 3.1),

$$P(\theta_i|z_k) = \frac{P(z_k|\theta_i)P(\theta_i)}{\sum_j P(z_k|\theta_j)P(\theta_j)} \tag{3.4}$$

where $p(\theta_i | z_k)$ is posterior probability of outcome θ_i after observing data z_k, $p(z_k | \theta_i)$ is probability of monitoring result z_k when outcome θ_i is known, $p(\theta_i)$ is prior probability of outcome θ_i before observing z_k, and $\Sigma\, p(z_k | \theta_i)p(\theta_i)$ is marginal probability of observations z_k irrespective of the outcome θ_i. This results in the following posterior probabilities: $p(\theta_1 | z_1) = 0.8$, $p(\theta_2 | z_1) = 0.2$, $p(\theta_1 | z_2) = 0.3$ and $p(\theta_2 | z_2) = 0.7$ respectively.

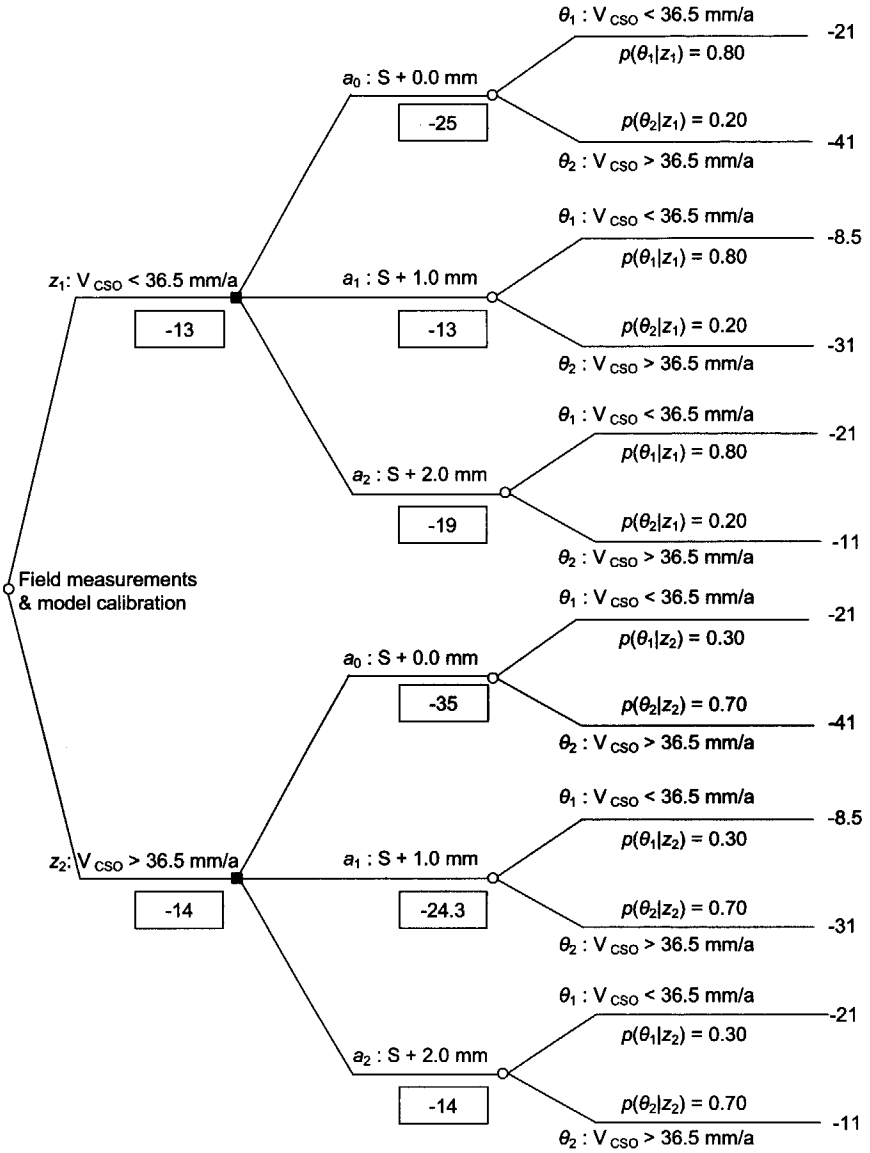

Figure 3.4 Decision tree: terminal analysis of building additional in-sewer storage.

Table 3.1 Probability of monitoring results ($p(z_k|\theta_i)$).

		Possible outcomes	
		θ_1 : $V_{CSO} \leq 36.5$mm	θ_2 : $V_{CSO} > 36.5$mm
Monitoring results	z_1 : $V_{CSO} \leq 36.5$mm	0.8	0.3
	z_2 : $V_{CSO} > 36.5$mm	0.2	0.7

If the experimental results indicate a CSO volume less than 36.5 mm/a, the expected utilities of the possible storage sizes are, respectively,

$$E\{u(a_0,\theta|z_1)\} = P(\theta_1|z_1)u(z_1,a_0,\theta_1) + P(\theta_2|z_1)u(z_1,a_0,\theta_2) = -25$$
$$E\{u(a_1,\theta|z_1)\} = -13$$
$$E\{u(a_2,\theta|z_1)\} = -19$$

As a result, design a_1 should be chosen ($E\{u(a^*,\theta)\}$=-13). Similarly, if the experimental results indicate a CSO volume more than 36.5 mm/a, design a_2 should be chosen with an expected utility $E(a^*)$ of -14.

3.2.3 Value of new information

Whether or not it is worthwhile to obtain additional information prior to decision-making depends on whether its value exceeds its cost. The value of perfect information resulting from an experiment is defined by two criteria (Benjamin and Cornell 1979):

- the difference between the prior expectation ($\Sigma\, u(a,\theta_i)p(\theta_i)$), where $u(a,\theta_i)$ is the utility associated with the best choice of action given that it is known with certainty that θ_i is the true outcome and
- the expected utility associated with decision making without an experiment.

In other words, it is the expected additional value of an experiment with 100% reliability. Hence, the expected value of perfect information ($EVPI$) is,

$$EVPI = E\{u(a^*_{PI},\theta)\} - E\{u(a^0,\theta)\} \tag{3.5}$$

where $E\{u(a^*_{PI},\theta)\}$ is the prior expected utility of an optimal action posterior to obtaining perfect information about the true outcome θ_i (excluding experimental cost) and $E\{u(a^0,\theta)\}$ is the expected utility if the experiment was not performed (e_0). The expected value of perfect information ($EVPI$) represents the maximum cost that the decision-maker can invest in order to acquire any additional information.

However, the decision-maker usually cannot obtain perfect information about the true outcome θ_i. Conversely, it is impossible to obtain perfect information by experimentation (or other research). It is obvious that the value of imperfect

information cannot exceed the value of perfect information. Therefore, the value of an experiment providing imperfect information measures,

$$EVI = E\{u(a^*,\theta)\} - E\{u(a^0,\theta)\} \tag{3.6}$$

where EVI is the expected value of information, $E\{u(a^*,\theta)\}$ is the expected utility of an optimal action including an experiment and $E\{u(a^0,\theta)\}$ is the expected utility if no experiment was performed (e_0). Hence, if EVI exceeds experimental cost, the alternative with experimentation should be selected.

Regarding the example of Figure 3.4 the expected value for a perfect test is,

$$\begin{aligned} E\{u(a^*_{PI},\theta)\} &= u(z_1,a_1,\theta_1)p(z_1,e) + u(z_2,a_2,\theta_2)p(z_2,e) \\ &= (-7.5*0.6) + (-10*0.4) = -8.5 \end{aligned}$$

The expected utilities $u(z_1,a_1,\theta_1)$ and $u(z_2,a_2,\theta_2)$ excluding experimental cost can be found in Figure 3.3. In order to calculate the expected value of information, the probabilities of possible test results need to be known,

$$p(z_k,e) = \sum_{i=1}^{n} p(z_k|\theta_i)p(\theta_i) \tag{3.7}$$

where $p(z_k,e)$ is the probability of monitoring result z_k given experiment e, $p(z_k|\theta_i)$ is the posterior probability of monitoring result z_k when outcome θ_i is known and $p(\theta_i)$ is the prior probability of outcome θ_i before observing z_k. As a result, the probability that the experiment will indicate either z_1 or z_2 is $p(z_1,e) = 0.6$ and $p(z_2,e) = 0.4$.

The expected utility if no experiment is performed $E\{u(a^0,\theta)\}$ yields -16 (see Figure 3.3). Hence, the expected value of perfect information is,

$$EVPI = E\{u(a^*_{PI},\theta)\} - E\{u(a^0,\theta)\} = -8.5 - (-16) = 7.5$$

The $EVPI$, however, only provides an upper limit to the value of information and indicates that the cost of acquiring any additional information should not exceed 750,000 Euros. As a result, the expected value of information yields,

$$EVI = E\{u(a^*,\theta)\} - E\{u(a^0,\theta)\} = ((-13*0.6) + (-14*0.4)) - (-16) = 2.6$$

indicating that the experiment is worthwhile, since its cost only amounts to 1 (*100,000 Euros).

3.3 RISK-BASED ECONOMIC OPTIMISATION

Risk based economic optimisation is illustrated with the following example. Consider a sewer system with a certain amount of in-sewer storage. In order to comply with environmental standards, this volume has to be enlarged. Economic optimisation, as applied for dike design by Van Dantzig (1956), would enable decision-making on this additional storage. It determines the optimal storage volume by a minimisation of total cost comprising initial investment for construction and cost of environmental damage due to overflows. In order to determine the optimum, damage cost and failure probability need to be estimated. The relation between storage volume and total cost is illustrated in Figure 3.5. The total costs comprise both investments and losses due to failure. Other examples of risk based economic optimisation applied in urban drainage can be found in Hauger *et al.* (2002) and Korving *et al.* (2003).

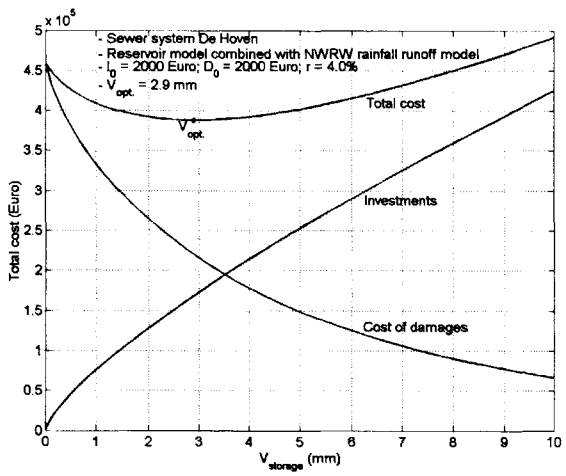

Figure 3.5 Cost as a function of sewer storage. The cost consists of both investments and losses due to CSO emissions (Korving *et al.* 2003).

3.3.1 Cost function

Economic optimisation requires a cost function. Logically, given the cost function the decision-maker will choose the decision with minimal expected costs. With respect to sewer rehabilitation, a cost function comprises construction costs and losses due to failure (e.g. reduction of biodiversity) and due to use of space (determinative for town planning). In addition, losses express the public perception of damage, i.e. willingness-to-pay. The determination of cost and damages is described in § 2.6. For some losses, however, it is difficult to express them into terms of money, e.g. the environmental

damage caused by CSOs. Moreover, determination of losses due to CSOs is subjective in terms of both appreciation of impacts and likelihood of composition. If it is difficult to describe a consequence in terms of a single (monetary) value, a multi-dimensional scale can be considered (e.g. costs, time and performance). The problem of multi-attribute utility theory is to find an expression for the utility function. Examples of environmental decision problems are presented by e.g. Gilbert and Janssen (1998) and Lorenz (1999). A comprehensive introduction to multi-criteria decision-making can be found in Keeney and Raiffa (1993).

Assume that the cost of enlarging the storage capacity of a sewer system is proportional to its volume, such that the cost of building an additional m^3 diminishes with increasing volumes,

$$I = I_0 v^{0.75} \tag{3.8}$$

where I_0 is investment (Euros) per m^3 storage volume and v is storage volume (m^3) to be built.

When available storage is too small, sewage spills into the surface water. Therefore, the cost in case of failure depends partially on the CSO volume. These amounts can be described by their probability of exceedance. Uncertainty in the statistical description of the failure probability can be integrated,

$$P_f(v) = \int_{\Theta} p(X > x_0|\theta) p(\theta|\mathbf{x}) d\theta \tag{3.9}$$

where $P_f(v)$ is the probability of failure of the sewer system and $p(\theta|\mathbf{x})$ is the posterior probability of parameter vector θ after observing data $\mathbf{x} = (x_1,\ldots,x_n)$ calculated with Bayesian analysis (see § 3.5.2).

The expected cost of damage due to CSOs is discounted over an unbounded time horizon,

$$D = D_0 \frac{P_f(v)}{T_{CSO}} \left(\frac{\alpha}{1-\alpha} \right) \tag{3.10}$$

$$\alpha = 1/(1+r/100) \tag{3.11}$$

where D_0 is the cost resulting from an overflow event (Euro), $P_f(v)$ is the probability of failure of the sewer system (i.e. an overflow event occurs), T_{CSO} is the average return period of overflow events (y), α is the discount factor (-) and r is the discount rate (%). In the Netherlands, a discount rate of 4% is applied which is based on the expected long-term interest on the capital market (Ministerie van Financiën 1995). Eq. (3.11) follows from the expected number of overflows exceeding a volume v per year given as,

$$\sum_{k=0}^{\infty} k \cdot \Pr\{\text{number of overflows in period } (0,t] = k\}$$
$$= \sum_{k=0}^{\infty} k \frac{(\lambda \cdot p \cdot t)^k}{k!} \exp\{-\lambda \cdot p \cdot t\} \tag{3.12}$$
$$= \lambda \cdot p \cdot t = \lambda \cdot p \ , \text{ for } t = 1$$

with $\lambda=1/(T_{CSO})$ being the frequency of overflows, $p=P_f(v)$ being the probability of failure of the sewer system and a Poisson process describing overflow events. The expected costs of failure per year are discounted over an unbounded time horizon as follows,

$$\frac{P_f(v)}{T_{CSO}}\left(\alpha + \alpha^2 + \alpha^3 + \ldots\right) = \frac{P_f(v)}{T_{CSO}} \frac{\alpha}{1-\alpha} \tag{3.13}$$

The costs can be discounted over an unbounded time horizon, since the expected service life of a sewer is larger than 60 years and for n >50 the contribution of losses due to failure is relatively small.

The expected total costs equal,

$$E(TC) = I + D = I_0 v^{0.75} + \frac{D_0 P_f(v)}{T_{CSO}}\left(\frac{\alpha}{1-\alpha}\right) \tag{3.14}$$

Subsequently, the economic optimum of the storage volume is found by minimising total cost (see Figure 3.5).

3.3.2 Failure probabilities

A structure fails if it can no longer perform its principal functions (CUR 1990). In the case of a sewer system, these functions imply prevention of flooding and protection of public health given that the environment is safeguarded. The probability of failure of a system due to a particular mechanism is either estimated from experience and intuition, or is calculated with a probabilistic model leading to a 'reliability function' Z,

$$Z = R - S \tag{3.15}$$

where R is resistance or strength and S load (see Figure 3.6). Therefore, the probability of failure can be represented as,

$$P_f = \Pr(Z \le 0) = \Pr(S \ge R) \tag{3.16}$$

The reliability function is a function of several stochastic variables, usually called basic variables (such as rainfall intensity, in-sewer storage, sewer pipe condition and pumping station performance).

The probability of failure can be quantified by means of several techniques including (see Ditlevsen and Madsen 1996):

- partial safety factor method,
- first order reliability method (FORM),
- numerical integration or Monte Carlo sampling.

Both numerical integration and Monte Carlo sampling are applied in this thesis.

The first is a design method based on safety factors or safety margins which does not calculate the reliability of an element (see e.g. Ang and Tang 1990 and CUR 1990). The minimum requirement for a structure is that the following condition is satisfied,

$$\frac{R}{\gamma_R} > \gamma_S S \tag{3.17}$$

where R and S are characteristic values for strength and load, respectively, and γ_R and γ_S are partial safety factors (i.e. factors determined separately for each variable).

First order reliability methods (FORM) comprise a number of approximate methods in which the failure boundary is linearised and the probability distributions are transformed to normal distributions (see Ditlevsen and Madsen 1996). An example of FORM in water quality modelling is presented by Portielje *et al.* (2000). If the failure surface is not linear, it is approximated by a tangent hyperplane (i.e. a linearisation of the reliability function in the design point). Furthermore, if the variables are not normally distributed, they have to be transformed to standard normal variables (see e.g. Rackwitz and Fiessler 1978). Finally, if the variables are stochastically dependent, a transformation to independent variables is needed using the 'Rosenblatt transformation' (see Rosenblatt 1952). A detailed description of FORM can be found in many textbooks, such as Ditlevsen and Madsen (1996).

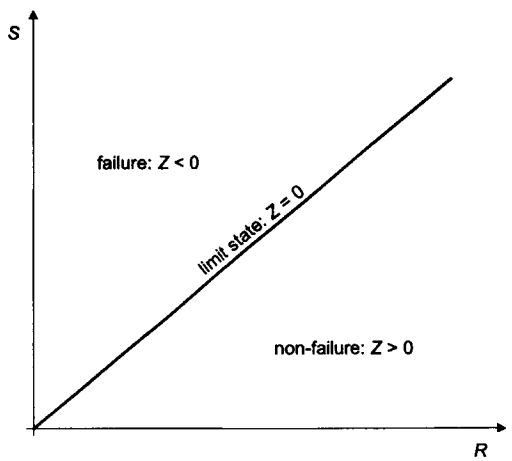

Figure 3.6 Definition of failure boundary or 'limit state' ($Z = 0$).

Numerical integration and Monte Carlo sampling are methods in which the complete probability density functions of the stochastic variables are used and the possibly non-linear character of the reliability function is accounted for (Figure 3.7). The probability of failure is given by,

$$P_f = \Pr(Z<0) = \Pr(R<S) = \iint_{Z<0} f_{R,S}(R,S)dRdS \tag{3.18}$$

where $f_{R,S}(r,s)$ is the joint probability density function of strength (R) and load (S). If the strength is given by $R=R(X_1,X_2,\ldots,X_m)$ and the load by $S=S(X_{m+1},X_{m+2},\ldots,X_n)$, the reliability function is a function of the variables X_i,

$$Z = R - S = Z(X_1, X_2, \ldots, X_n) \tag{3.19}$$

If the variables $X_1,X_2,\ldots,X_n$ are stochastically independent, the failure probability is defined as,

$$P_f = \iint_{Z<0} \ldots \int f_{X_1}(X_1) f_{X_2}(X_2) \ldots f_{X_n}(X_n) dX_1 dX_2 \ldots dX_n \tag{3.20}$$

In order to determine the probability of failure, the integral of Eq. (3.21) has to be solved using either numerical integration or Monte Carlo sampling. For example, 'Riemann integration' can be applied to solve this n-fold integral numerically (Genz and Malik 1980). The probability of failure is approximated with,

$$P_f \approx \sum_{i_1=1}^{m_1} \sum_{i_2=1}^{m_2} \ldots \sum_{i_n=1}^{m_n} \mathbf{1}(Z) f_{X_1,X_2,\ldots X_n}\left((X_{01}+i_1\Delta X_1,\ldots,X_{0n}i_n\Delta X_n)\right)\Delta X_1 \Delta X_2 \ldots \Delta X_n \tag{3.21}$$

where $\mathbf{1}(Z)$ is the indicator function ($\mathbf{1}(Z)=1$ for $Z<0$ and $\mathbf{1}(Z)=0$ for $Z\geq 0$). The integration steps m_j have to be chosen sufficiently small for reliable estimations. The number of integration steps also depends on the range in which X_j is defined. Therefore, the choice of the domain $X_j \in [X_{0j}, X_{0j} + m_j \Delta X_j]$ affects the accuracy of the approximation.

Monte Carlo simulation (see Figure 3.7) is a simple and straightforward, but computationally demanding, method that does not require the model to be linear as first-order analysis does. The method implies sampling from probability distributions of the input variables and successive simulation for all sampled inputs. An estimate of the overall reliability of the system is obtained by analysing the model outputs of all runs

A major disadvantage of the Monte Carlo technique is that a large number of simulation runs are needed to obtain a reliable estimate of overall reliability. In particular for complex systems this may result in long calculation times. To reduce the number of runs directional importance sampling or Latin Hypercube Sampling can be used (see e.g. Ditlevsen and Madsen 1996 and Portielje *et al.* 1999).

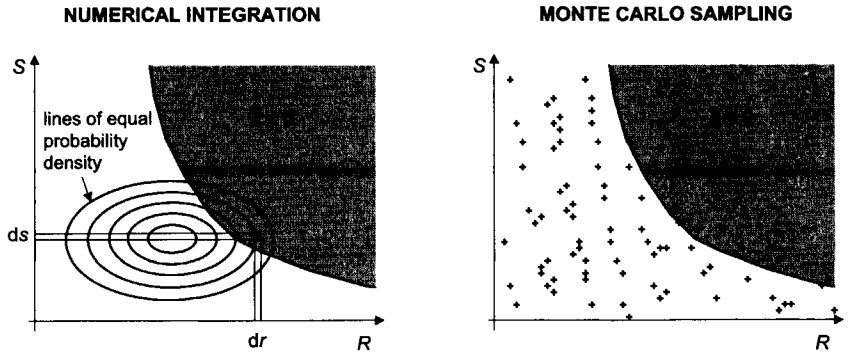

Figure 3.7 Illustration of numerical integration and Monte Carlo sampling.

When assessing the reliability of sewer systems it is important to consider the system as a whole because each component is prone to failure. Failure of one component may in turn pose a hazard to another component. For example, blockage of one sewer pipe may lead to flooding of another. Fault trees provided a useful aid in order to establish an ordered pattern in the many hazards to and failure modes of components (see e.g. Ang and Tang 1990). As defined in Chapter 2, a failure mode is the manner in which a structure responds to a hazard.

Systems that are composed of multiple components can be classified as series, parallel or combined systems (see Figure 3.8). If E_i denotes the failure of component i, the failure of a series system is defined as,

$$E_S = E_1 \cup E_2 \cup \cdots \cup E_n \tag{3.22}$$

where E_S is failure of the total system. For a parallel system the failure is defined as,

$$E_S = E_1 \cap E_2 \cap \cdots \cap E_n \tag{3.23}$$

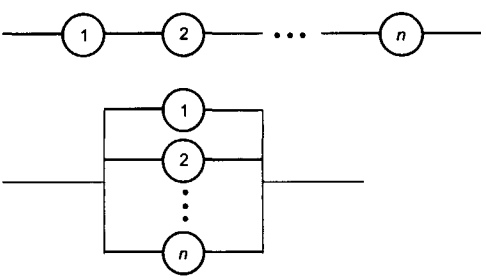

Figure 3.8 Representation of series (top) and parallel (bottom) systems.

The failure probability of a series system is always higher than the failure probability of the individual elements, but lower than the sum,

$$\max_i(\Pr(E_i)) \le P_f \le \sum_{i=1}^{n} \Pr(E_i) \tag{3.24}$$

The lower bound applies if E_i of all components is completely dependent, the upper bound if E_i is independent. Ditlevsen and Madsen (1996) present an approximation of Eq. (3.25) in which these boundaries are narrowed.

In parallel systems, on the other hand, elements can compensate for one another, i.e. failure of one element does not automatically lead to failure of the system. For ductile parallel systems (i.e. systems of which the remaining strength of the elements equals the maximal strength), the strength of a system with n elements is given by,

$$\prod_{i=1}^{n} \Pr(E_i) \le P_f \le \min_i(\Pr(E_i)) \tag{3.25}$$

These boundaries correspond to the assumption of statistical independence and perfect correlation among the failures of individual units. They are very wide and need to be narrowed for useful application (see Ang and Tang 1990).

3.4 ANALYSIS OF FAILURE DATA OF REPAIRABLE SYSTEMS

Assets in a sewer system are subject to decay and, therefore, require frequent maintenance, repair, or eventual replacement. For any maintenance strategy it is essential to be able to estimate the rate of occurrence of failure events. Also, assumptions concerning the ageing of a system and the impact of failure and repair determine the choice of the model describing system reliability.

Firstly, there is a substantial distinction between repairable and non-repairable systems. Repairable systems can, upon failure, be restored to service without replacing the system as a whole. Only parts are discarded or replaced completely upon failure. For example, a sewage pump is a repairable system because most failures, such as mechanical blockage of the impeller, can be fixed without replacing the entire pump. Non-repairable systems, however, are discarded after each failure. Secondly, repair ranges from minimal repair to renewal (or perfect) repair. Minimal repair means that after repair a system is as bad as it was prior to the failure. Renewal, on the other hand, results in systems in a like new state after the repair.

This paragraph presents models for the description of observed failure data including the renewal, homogeneous Poisson and non-homogeneous Poisson process.

3.4.1 Statistical description of failures

Failure events are characterised by their frequency or interarrival time and their duration or downtime. Let T_1, T_2,..., T_n (see Figure 3.9) denote the failure times of a system measured with respect to the initial start up of the system ($0<T_1<T_2<\ldots<T_n$). The time to failure (from T_{i-1} to T_i) is dependent on both system characteristics, such as age and loading, and quality of repairs. The time to repair Y_i is related to aspects including organisational affairs (e.g. defined priority of repairs), severity of the failure and system loading. Repair is defined as the attempt to correct or upgrade a component or system by mending, modification or adjustment. The failure interval or interarrival time X_i is defined as the time interval between the end of a repair and the occurrence of a next failure,

$$\begin{aligned} X_1 &= T_1 \\ X_2 &= T_2 - (T_1 + Y_1) \\ &\vdots \\ X_n &= T_n - (T_{n-1} + Y_{n-1}) \end{aligned} \tag{3.26}$$

If instantaneous repair is assumed (in the case of renewal and 'non-homogeneous Poisson processes), Y_i is equal to zero. The failure rate is the expected number of failures per unit of time,

$$\nu(t) = \frac{d}{dt} E\{N(0,t]\} \tag{3.27}$$

where $\nu(t)$ is the failure rate and $E\{N(0,t]\}$ is the expected number of failures in the interval $(0,t]$. Figure 3.9 illustrates the afore-mentioned definitions.

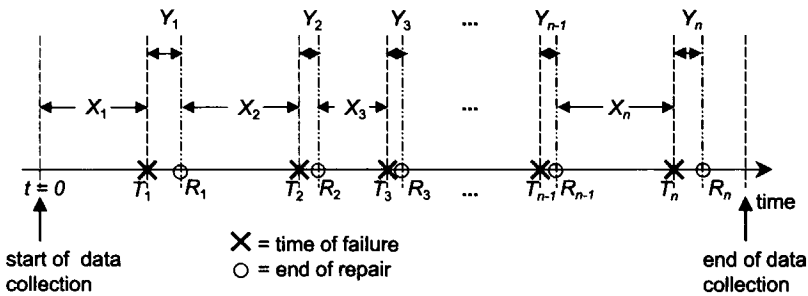

Figure 3.9 Description of failures and repairs in time, where T_i is time of failure, R_i is time of repair, $(T_i - T_{i-1})$ is time between 2 failures, X_i is time from repair $(i-1)$ until failure i and Y_i is duration of repair i (or downtime).

3.4.2 Models with constant failure rate

The simplest and best-known model describing failures in repairable systems is the 'homogeneous Poisson process' (HPP). This model has complete lack of memory, i.e. a failure is equally likely to occur at any time irrespective of the operating time of the system and its history of failures. Therefore, under the HPP model the interarrival times of failures are independent and identically distributed. In particular, the failure rate is constant and the interarrival times are exponentially distributed. However, often the assumption of completely random failures in time is not realistic.

In addition, it is possible to describe a constant failure rate with other distribution functions (e.g. Weibull, lognormal or gamma) resulting in a 'renewal process' (RP). The HPP model is a special case of this 'renewal process'. Both models assume instantaneous repair of systems upon failure, so $Y_i = 0$ in Eq. (3.27). Moreover, the system is 'as good as new' after each repair.

If the times between failures X are independent and have an exponential distribution with where $1/\lambda$, the process is called an HPP. The probability density function is defined as,

$$f(x) = \lambda \exp(-\lambda x) \quad , \qquad \text{for } x > 0 \tag{3.28}$$

where λ is the failure rate of the system. The probability density function of t_k, the time to the k^{th} failure, is given by the gamma distribution with scale parameter λ and shape parameter k (Ansell and Phillips 1994),

$$f_k(t_k) = \frac{\lambda^k t_k^{k-1} \exp(-\lambda t_k)}{(k-1)!} \tag{3.29}$$

The probability distribution of the number of failures in the period $(0,t]$ is described as (for derivation see Rigdon and Basu 2000),

$$P(N(t) = k) = \frac{1}{k!}\left(\int_0^t \lambda(x)dx\right)^k \exp\left(-\int_0^t \lambda(x)dx\right) = \frac{\lambda^k t^k \exp(-\lambda t)}{k!} \quad , \qquad k = 0,1,2,... \tag{3.30}$$

which is the Poisson distribution with parameter λt. The joint pdf of the times between the failures $T_1, T_2, \ldots, T_n$ is,

$$\begin{aligned} f(t_1,t_2,...,t_n) &= f(t_1)f(t_2|t_1)f(t_3|t_1,t_2)\times...\times f(t_n|t_1,t_2,...,t_{n-1}) \\ &= \left(\lambda \exp(-\lambda t_1)\right)\left(\lambda \exp(-\lambda(t_2 - t_1))\right)\times...\times\left(\lambda \exp(-\lambda(t_n - t_{n-1}))\right) \\ &= \lambda^n \exp(-\lambda t_n) \end{aligned} \tag{3.31}$$

An axiomatic description of the HPP can be found in Rigdon and Basu (2000).

In contrast, given the HPP model, Bayesian inference can be considered for parameter estimation (see Rigdon and Basu 2000). The number of failures N, conditioned on λ, has a Poisson distribution with mean λt. The likelihood function is,

$$p(n|\lambda) = \frac{(\lambda t)^n \exp(-\lambda t)}{n!}, \quad n = 0,1,...,n \tag{3.32}$$

The conjugate prior (see § 3.5.2.2) for the Poisson process rate λ is the gamma distribution with probability density (Bernardo and Smith 1994),

$$p(\lambda) = \frac{b^a \lambda^{a-1}}{\Gamma(a)} \exp(-b\lambda), \quad \lambda > 0 \tag{3.33}$$

Subsequently, the parameters a and b can be chosen by relating the prior mean and the prior variance,

$$E(\lambda) = \mu = \frac{a}{b} \quad \text{and} \quad \text{Var}(\lambda) = \sigma^2 = \frac{a}{b^2} \tag{3.34}$$

Then the posterior distribution of λ is,

$$p(\lambda|n) = \frac{(b+t)^{a+n}}{\Gamma(a+n)} t^{a+n-1} \exp(-(b+t)\lambda) \tag{3.35}$$

Thus, conditioned on $N = n$, the Poisson rate λ is gamma distributed with a posterior mean and variance of,

$$E(\lambda|\mathrm{x}) = \frac{a+n}{b+t} \quad \text{and} \quad \text{Var}(\lambda|\mathrm{x}) = \frac{a+n}{(b+t)^2} \tag{3.36}$$

3.4.3 Models with time dependent failure rate

Repairable systems may be either subject to ageing, affected by changes in their environment or changed due to upgrading of one of the components (downgrading is also possible). Therefore, the assumption of independent and identically distributed failures is invalid.

Since an HPP model is not suitable to model independent failures with a time-varying failure rate, alternative approaches have to be considered. An often-used extension of the HPP is the 'non-homogeneous Poisson process' (NHPP), which can describe both ageing and repair (see e.g. Ansell and Phillips 1994 and Rigdon and Basu 2000). The model is based on 'minimal repair'. As a result, the failure rate of an NHPP varies with time. As with the HPP model, instantaneous repair is assumed ($Y_i = 0$).

Models with a time-dependent failure rate were originally introduced to describe reliability of hardware and software systems. They are sometimes called growth models, since they allow for trends in the lifetimes of systems (and components). Most growth models assume a monotonic and usually positive trend. In other words, the interarrival time of failures increases and the rate of events decreases. Ansell and Phillips (1994) present models with time-dependent failure rate. This paragraph only discusses two

examples: Crow's model (Crow 1974) and Cox and Lewis' model (Cox and Lewis 1966). The former describes the changing failure rate according to a power law, whereas the latter uses a log-linear description:

- Crow's model

$$\nu(t) = \lambda\beta t^{\beta-1} \quad , \quad \lambda > 0 \text{ and } \beta > 0 \tag{3.37}$$

where $\nu(t)$ is the time-dependent failure rate, λ is the scale parameter of Weibull function, β is the growth parameter of the Weibull function determining improvement or deterioration in time and $t = 0$ is the initial start-up of the system. For $\beta > 1$ the failure rate increases and failures occur more often. For $\beta < 1$ the failure rate decreases and the system improves. For $\beta = 1$ the failure rate is unchanged. Crow's model is sometimes called Weibull model.

- Cox and Lewis' model

$$\nu(t) = \exp(\beta_0 + \beta_1 t) \tag{3.38}$$

where $\nu(t)$ is the time-dependent failure rate, β_0 is the scale parameter of log-linear function, β_1 is the growth parameter of the log-linear function determining improvement or deterioration in time and $t=0$ is the initial start-up of the system. The failure rate increases for $\beta_1 > 0$ and decreases for $\beta_1 < 0$. An advantage of the model is that the parameters β_0 and β_1 are unbounded as opposed to the parameters in Crow's model. For modelling more complex system behaviour the model has been generalised by several authors (e.g. Lewis 1972) in order to include quadratic and further polynomial terms.

Maximum likelihood (ML) estimators of the parameters λ and β in the Crow model are defined as (see Appendix III for derivations),

$$\hat{\beta} = \frac{n}{n\ln t_m - \sum_{i=1}^{n} \ln t_i} \tag{3.39}$$

$$\hat{\lambda} = \frac{n}{t_m^{\hat{\beta}}} \tag{3.40}$$

where $\hat{\beta}$ is the ML estimator of growth parameter β, n is the number of observations, t_m is the end of the observation period, t_i is the time of the i^{th} failure and $\hat{\lambda}$ is the ML estimator of scale parameter λ. Hence, the expected number of failures in time equals,

$$E\{N(t)\} = \lambda t^{\beta} \tag{3.41}$$

The ML estimator of parameters β_1 in the Cox-Lewis model can be estimated by solving (see Appendix III for derivations),

$$\sum_{i=1}^{n} t_i - \frac{n}{\hat{\beta}_1} \frac{\left(t_m \exp\left(\hat{\beta}_1 t_m\right) - \hat{\beta}_1\left(\exp\left(\hat{\beta}_1 t_m\right) - 1\right)\right)}{\left(\exp\left(\hat{\beta}_1 t_m\right) - 1\right)} = 0 \tag{3.42}$$

where $\hat{\beta}_1$ is the ML estimator of growth parameter β_1, n is the number of observations, t_n is time of last failure observed and t_i is time of i^{th} failure. Then β_0 is calculated with,

$$\hat{\beta}_0 = \log\left(\frac{n\hat{\beta}_1}{\exp\left(\hat{\beta}_1 t_m\right) - 1}\right) \tag{3.43}$$

where $\hat{\beta}_0$ is the ML estimator of scale parameter β_0. Hence, the expected number of failures in time equals,

$$E\{N(t)\} = \frac{\exp(\beta_0)}{\beta_1}\left(\exp(\beta_1 t) - 1\right) \tag{3.44}$$

The parameters of an NHPP can also be determined with Bayesian estimators (see Rigdon and Basu 2000).

Several statistical tests have been proposed for testing whether a process is an HPP against the alternative of a monotonic trend. Here the Laplace test is discussed (Ansell and Phillips 1994). The test uses a set of chronologically ordered arrival times T_1, T_2,..., T_n. If the data are time truncated (i.e. observation stops at a predetermined time t) and t_i represents the time of the i^{th} failure during the period of observation $(0,t_m]$, then the test statistic is given by,

$$U_L \equiv \frac{\left[\frac{1}{n}\sum_{i=1}^{k} t_i\right] - \frac{1}{2}t_m}{t_m\sqrt{\frac{1}{12n}}} \tag{3.45}$$

where n is the number of failures, t_i is time of i^{th} failure and t_m is the end of the observation period. For failure truncated data (i.e. observation stops after a predetermined number of failures, say n), the test statistic changes into,

$$U_L \equiv \frac{\left[\frac{1}{n-1}\sum_{i=1}^{n-1} t_i\right] - \frac{1}{2}t_n}{t_n\sqrt{\frac{1}{12(n-1)}}} \tag{3.46}$$

where t_n is both time of n^{th} failure and end of observation period.

The test statistic U_L provides an indication for the expected sum of interarrival times. For n>20 the test statistic U_L is approximately normally distributed with mean 0 and standard deviation 1 (Crowder *et al.* 1991). The null hypothesis (interarrival times independent and exponentially distributed) is rejected if,

$$U_L < -z_{\alpha/2} \quad \text{or} \quad U_L > z_{\alpha/2}$$

where z_α is the upper-tail critical value of a standard normal distribution (see Cox and Lewis 1966 for details). For $\alpha = 0.05$, the null hypothesis would be rejected if $|U_L| > z_{0.05/2} = 1.96$. Furthermore, if the value of U_L is less than $-z_{\alpha/2}$ the reliability of the system is improving, so that times between failures are on average increasing. Conversely, if U_L is greater than $z_{\alpha/2}$ the system deteriorates and times between failures decrease on average. In both cases an NHPP is required. In order to improve the performance of the test statistic when the null hypothesis is the more general renewal process, the modified Laplace test can be used (see Ascher and Hansen 1998).

3.4.4 Other models

If repair times are significantly different from zero, the HPP or NHPP model is inadequate. Then the i^{th} failure at time t_i is followed by a repair time which ends at time r_i producing a series of states with the system either failing or working (see Figure 3.9). This can be modelled with the 'alternating renewal process' (Cox 1962 and Ansell and Phillips 1994). This model assumes identical distributions for failure times x_i, as for the repair times y_i. In addition, failure times and repair times are assumed to be independent.

In the renewal process model the interarrival times consist of an 'on' and an 'off' period, i.e. a sequence of variables X with density function $f(x)$ followed by variables Y with density function $g(y)$. The time to the first failure t_1 is simply the distribution equal to the standard renewal process. However, the time to the second failure at t_2 is composed of the time x_1, to the first failure at t_1, the duration of the first repair y_1 and the time x_2 from the end of the first repair at r_1 until the second failure at time t_2. The probability density function is a convolution of $f(x)$ and $g(y)$ (see Ansell and Phillips 1994). This is repeated until the n^{th} failure.

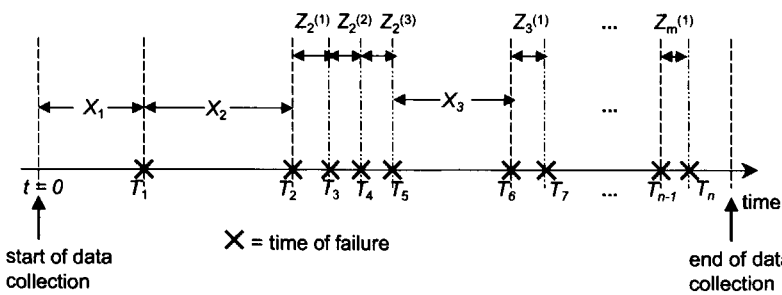

Figure 3.10 Illustration of a branching Poisson process (BPP), T_i is time of failure, (T_i-T_{i-1}) is time between 2 failures irrespective of the type (primary or subsidiary), X_i is time from last subsidiary failure k following primary failure $(i-1)$ until next primary failure i and $Z_m^{(j)}$ is time between subsequent subsidiary failures.

In some cases, a clustering of failures may occur. These bunched failures indicate that a system is not correctly repaired causing a number of subsequent failures for the same reason as the original one. The branching Poisson process (BPP) model can account for this behaviour. Bartlett (1963) proposed it as a model for traffic flow where the deceleration of one vehicle is immediately followed by a number of others.

A BPP consists of a series of primary events X (described as a Poisson process), each generating a subsidiary series of events Z (see Figure 3.10). After each failure, the system is correctly repaired with probability $(1\text{-}r)$ resulting in a next failure when the next primary failure occurs. With probability r the system is not correctly repaired and a finite, but random number of subsidiary failures will follow. The subsidiary process is assumed to be independent and to have an identical structure. This number of subsidiary failures has a discrete distribution, such as geometric, negative binomial or Poisson. The complete process is a superposition of primary and subsidiary events. In a time series the two types of failure events are indistinguishable. Rigdon and Basu (2000) derive equations for the number of failures and the failure rate. A disadvantage of the BPP model is that parameter estimation and other inferences are difficult to perform. Lewis (1967) extended the model in order to allow for an NHPP as description of the primary process instead of an HPP.

The NHPP model is restrictive due to its assumed monotonic failure rate (see e.g. Ansell *et al.* 2003). Moreover, if it is not possible to observe substantial parts of the lifetime of a system, historical observations of failure events cannot completely describe system behaviour and must be supplemented by other relevant data about the processes.

Firstly, when little is known about the behaviour of the system prior to the analysis Ansell *et al.* (2003) suggest a non-parametric, data-driven approach instead of a parametric one, such as Crow's or Cox and Lewis' model. Kernel density smoothing (see e.g. Bowman and Azzalini 1997) is applied to estimate a continuous breakdown rate, by spreading the rate at each breakdown point using a (usually normal) density function. The advantage of this approach is that fewer assumptions (e.g. non-monotonically increasing failure rates) are required compared to the Crow or Cox-Lewis model.

Secondly, there can be a number of variables that partly explain the performance of the system. For example, the performance of a sewage pump is affected by a number of aspects regarding its environment, such as composition of the sewage, type of the sewer system, groundwater infiltration due to leaking joints, ingress of soil due to settling of sewers and design of the sewage pump and the suction well. The state of the environment of the system can be described by a 'condition grade' reflecting the 'newness' of the equipment (Ansell *et al.* 2003). Such covariates can be accounted for by Cox regression (Cox 1972). Lawless and Nadeau (1995) have amended this model in order to describe repairable systems. The expectation of failures in a small epoch t_i is described as a function of a base failure rate at time t_i and the covariates (such as the

'condition grade'). Then the instantaneous failure rate is estimated at each breakdown point.

3.5 STATISTICAL ESTIMATION METHODS

Probabilistic models are applied to describe strength and load parameters with statistical distribution functions. Available data provide numerical estimates of the parameters of these models. In order to estimate these parameters several estimation methods are available, including method of moments (Johann Bernoulli, 1676-1748), maximum likelihood method (Daniel Bernoulli, 1700-1782), least squares method (Gauss, 1777-1855), Bayesian estimation method (Bayes 1763) and method of L-moments (Hosking 1990).

The classical estimation methods (method of moments, maximum likelihood method and least squares method) are treated in many textbooks such as Mood *et al.* (1974) and Benjamin and Cornell (1979). Different estimation methods, including their performance that is dependent on selected distribution type and available data, can be found in Van Gelder (2000). The next paragraphs only discuss the estimation methods that are used in this thesis: method of moments, maximum likelihood and Bayesian estimation methods.

3.5.1 Classical estimation methods

3.5.1.1 Method of moments

The method of moments assumes that the moments of a statistical distribution function are equal to the moments of an observed sample. As a result, the parameters of the distribution function can be estimated from the sample moments (see e.g. Mood *et al.* 1974). Although analytical expressions can be derived rather easily, the parameters can be biased, inefficient and sometimes even unreliable.

In general, the k^{th} moment of a probability density function $f(x)$ is defined as,

$$E(x^k) = \int_{-\infty}^{+\infty} x^k f(x) dx \tag{3.47}$$

Likewise, the k^{th} central moment (relative to $x = \mu_x$) of a probability density function $f(x)$ is defined as,

$$m_k = \int_{-\infty}^{+\infty} (x - \mu_x)^k f(x) dx = E\left((x - \mu_x)^k\right) \tag{3.48}$$

where μ_x is the expectation of the data. The first moment represents the expectation of the distribution function, the second central moment the variance. The moments of a sample (mean and variance) are defined as,

$$\bar{x} = \frac{1}{n}\sum_{i=1}^{n} x_i \tag{3.49}$$

$$s^2 = \frac{1}{n-1}\sum_{i=1}^{n}(x_i - \bar{x})^2 \tag{3.50}$$

where $\bar{x}$ is the sample mean, n is the number of samples, x_i is a random sample from the distribution function and s^2 is the sample variance. The parameters of the distribution function are estimated by equating the moments of the distribution function with the sample moments. Several estimators based on this method are presented in Appendix IV.

3.5.1.2 Maximum likelihood method

Maximum likelihood estimation is based on the joint density of the observations. The likelihood of n independent random observations X_1, X_2,..., X_n is defined as the joint density function of n random variables (see Mood *et al.* 1974),

$$\begin{aligned}\ell(x_1, x_2, \ldots, x_n|\theta) &= f(x_1, x_2, \ldots, x_n|\theta) = f(x_1|\theta) \times f(x_2|\theta) \times \ldots \times f(x_n|\theta) \\ &= \prod_{i=1}^{n} f(x_i|\theta)\end{aligned} \tag{3.51}$$

where $f(x_i|\theta)$ is the density function of x_i with parameter vector θ and $\ell(x_1,x_2,\ldots,x_n|\theta)$ represents the likelihood that the random variable adopts a particular value $x_1,x_2,\ldots,x_n$.

The maximum likelihood (ML) estimator $\hat{\theta}$ is the value of θ which maximises the likelihood function of the observations,

$$\hat{\theta} = \max_{\theta}\{\ell(\mathbf{x}|\theta)\} = \max_{\theta}\{\log(\ell(\mathbf{x}|\theta))\} \tag{3.52}$$

where $\ell(\mathbf{x}|\theta)$ and $\log(\ell(\mathbf{x}|\theta))$ have their maximum values at the same $\hat{\theta}$. Since it is often easier to maximise the logarithm of the likelihood, $\log(\ell(\mathbf{x}|\theta))$ is used instead. Thus, the ML estimator is the solution of the equation,

$$\frac{d}{d\theta}\ell(x_1, x_2, \ldots, x_n|\theta) = \frac{d}{d\theta}\log\ell(\mathbf{x}|\theta) = 0 \tag{3.53}$$

When θ is a vector, the likelihood function becomes multidimensional. If the likelihood function contains k parameters, the likelihood estimator is a solution of k equations,

$$\begin{aligned}&\frac{\partial}{\partial\theta_1}\log\ell(\mathbf{x}|\theta_1,\theta_2,\ldots,\theta_k) = 0 \\ &\frac{\partial}{\partial\theta_2}\log\ell(\mathbf{x}|\theta_1,\theta_2,\ldots,\theta_k) = 0 \\ &\qquad\vdots \\ &\frac{\partial}{\partial\theta_n}\log\ell(\mathbf{x}|\theta_1,\theta_2,\ldots,\theta_k) = 0\end{aligned} \tag{3.54}$$

Maximum likelihood estimators are efficient, consistent and sufficient, but can be biased. ML estimators for several distribution types are presented in Appendix IV.

3.5.2 Bayesian statistics

Bayesian statistics models both inherent and statistical uncertainty. It is based on the theorem of Bayes (1763). Using Bayes' theorem a prior distribution can be updated as soon as new observations are available (see Figure 3.11). The more new observations are used, the smaller the resulting parameter uncertainty. Consequently, with respect to sewer rehabilitation combining prior information with new observations will reduce the risks of interventions.

Bayes' theorem (i.e. the conditional probability theorem) can be written as,

$$\pi(\theta|\mathbf{x}) = \frac{\ell(\mathbf{x}|\theta)\pi(\theta)}{\int_{\Theta} \ell(\mathbf{x}|\theta)\pi(\theta)d\theta} = \frac{\ell(\mathbf{x}|\theta)\pi(\theta)}{\pi(\mathbf{x})} \tag{3.55}$$

where $\pi(\theta|\mathbf{x})$ is the posterior density of $\theta = (\theta_1,\ldots,\theta_d)$ after observing data $\mathbf{x} = (x_1,\ldots,x_n)$, $\ell(\mathbf{x}|\theta)$ is the likelihood function of observations $\mathbf{x} = (x_1,\ldots,x_n)$ when the parameter $\theta = (\theta_1,\ldots,\theta_d)$ is known, $\pi(\theta)$ is the prior density of $\theta = (\theta_1,\ldots,\theta_d)$ before observing data $\mathbf{x} = (x_1,\ldots,x_n)$ and $\pi(\mathbf{x})$ is the marginal density of the observations $\mathbf{x} = (x_1,\ldots,x_n)$. Fenner and Sweeting (1998), Campbell *et al.* (1999), Chbab *et al.* (2000) and Van Noortwijk *et al.* (2001) present examples of the Bayesian method applied to civil engineering problems.

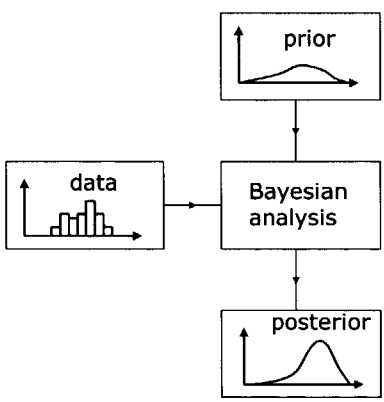

Figure 3.11 Bayesian analysis. The theorem of Bayes (1763) updates subjective beliefs on the occurrence of an event based on new data.

3.5.2.1 Numerical approximations

For evaluating complex integrals, such as the denominator of Eq. (3.56), several calculation methods can be used including:

- asymptotic approximation,
- numerical integration and
- Monte Carlo integration.

These evaluation methods are summarised in Carlin and Lewis (2000).

Asymptotic expansions for approximation of complex integrals used to be applied in the 1980s. Their accuracy depends on the parameterisation and the number of observations. The more observations are available, the more accurate the approximation. An example is the 'Laplace expansion' for determining Bayes weights (see § 3.5.2.4). More details on Laplace expansions can be found in Bernardo and Smith (1994).

Numerical integration can be used as long as the dimension of the probability model is not too large. By replacing the integral in the denominator of Bayes' theorem with a summation, the posterior density is discretised as,

$$\Pr\{\Theta = \theta_j | \mathbf{x}\} = \frac{\ell(\mathbf{x}|\theta_j)\pi(\theta_j)}{\sum_{j=1}^{k} \ell(\mathbf{x}|\theta_j)\pi(\theta_j)} \tag{3.56}$$

where,

$$\theta_j = \theta_L + \frac{2j-1}{2}\frac{\theta_U - \theta_L}{k} = \theta_L + \left(j - \frac{1}{2}\right)\Delta\theta, \qquad j = 1,...,k \tag{3.57}$$

θ_L and θ_U are the lower and upper bound for θ respectively and k is the total number of integration steps. Disadvantages of numerical integration are that the lower and upper bounds and the method of discretisation must be specified a priori.

For Monte Carlo integration, random values between 0 and 1 are drawn from a uniform cumulative distribution function $F(\theta)$. Using the inverse of F the random values θ can be calculated. Therefore, the denominator of Eq. (3.56) is evaluated by drawing m random values $(u^{(1)},\ldots,u^{(m)})$ from a uniform distribution between 0 and 1,

$$\theta^{(i)} = \Pi^{-1}\left(u^{(i)}\right), \qquad i = 1,...,m \tag{3.58}$$

where $\Pi(\theta)$ is the cumulative distribution function of $\pi(\theta)$. The integral is approximated by,

$$\int \ell(\mathbf{x}|\theta)\pi(\theta)d\theta \approx \frac{1}{m}\sum_{i=1}^{m} \ell\left(\mathbf{x}|\theta^{(i)}\right) \tag{3.59}$$

Although the Monte Carlo method can be easily applied, the inverse of the cumulative distribution function $F(\theta)$ does not always exist in explicit form and the number of necessary samples can be rather large. Monte Carlo importance sampling is a version of

the Monte Carlo method that reduces the necessary number of samples providing equivalent accuracy (for details see Bernardo and Smith 1994).

A more advanced implementation of the Monte Carlo sampling is the Markov chain Monte Carlo (MCMC) method (see e.g. Bates and Campbell 2001, and Van Noortwijk *et al.* 2004). The key idea is that instead of sampling from a prior distribution, samples are drawn from the posterior. MCMC is essentially Monte Carlo integration using cleverly constructed Markov chains. The chains are constructed so that the dependent samples are distributed according to the posterior distribution of the unknown statistical parameters (Van Noortwijk *et al.* 2004). Due to this Markovian dependence, larger sample sizes are required compared to independent sampling. The most widely used MCMC technique is the Metropolis-Hastings algorithm with the Metropolis algorithm and the Gibbs sampler as well-known special cases. Bernardo and Smith (1994) and Carlin and Louis (2000) present more details on MCMC methods.

3.5.2.2 Prior distributions

Prior distributions represent a priori information and can be either informative or non-informative. Non-informative priors allow the observations to 'speak for themselves'. Therefore, these priors describe a certain 'lack of knowledge'. The main disadvantage of non-informative priors is that they are often improper (i.e. they do not integrate to 1). An informative prior, on the other hand, reflects 'subjective beliefs' concerning unknown statistical parameters. For example, in estimating subsidence of sewers in a district the prior can represent model predictions of invert levels of sewers. Systematic measurements of these levels can be used to update this prior to a posterior. Both non-informative and informative prior distributions of several distribution types are presented in Appendix IV.

Non-informative priors represent the type of information, which makes the observations dominant when a particular likelihood model is given. There are many non-informative probability distributions available (see Berger 1985). The most important non-informative priors include:

- uniform prior,
- Jeffreys' prior,
- reference prior,
- maximal data information prior.

Bayes (1763) already used uniform priors to express a priori lack of knowledge. These priors are relatively easy to derive. A disadvantage of uniform priors, however, is their lack of invariance under one-to-one transformations (Van Noortwijk *et al.* 2004).

Jeffreys (1961) introduced an alternative to applying uniform, non-informative priors. This Jeffreys' prior is invariant under one-to-one transformations and is always

dimensionless. In order to derive this prior it is assumed that the posterior distribution of its parameters is approximately normal for $n \rightarrow \infty$. Its derivation in the one-dimensional case, as described by Box and Tiao (1973), makes use of 'Fisher's measure of information',

$$\pi(\theta) \propto \{I(\theta)\}^{\frac{1}{2}} \tag{3.60}$$

where $\pi(\theta)$ is prior distribution of parameter θ and $I(\theta)$ is Fisher's measure of information.

$$I(\theta) = -\int \ell(\mathbf{x}|\theta)\left(\frac{\partial^2}{\partial\theta^2}\log(\ell(\mathbf{x}|\theta))\right)dx \tag{3.61}$$

where $\ell(\mathbf{x} \mid \theta)$ is the likelihood function of observations $\mathbf{x}$ when parameter θ is known. The smaller the statistical uncertainty, the larger the Fisher information. In the multi-parameter case the prior distribution for a set of d parameters $\boldsymbol{\theta} = \{\theta_1, \ldots, \theta_n\}$ should be taken proportional to the square root of the determinant of Fisher's information matrix for a single observation (Van Noortwijk *et al.* 2004), which reads,

$$I_{ij}(\theta) = E\left\{-\frac{\partial^2 \log \ell(\mathbf{x}|\theta)}{\partial\theta_i \partial\theta_j}\right\}, \qquad i,j = 1,\ldots,d \tag{3.62}$$

and the corresponding non-informative Jeffreys prior is defined as,

$$J(\theta) = \sqrt{\det I_{ij}(\theta)} = \sqrt{|I(\theta)|}, \qquad i,j = 1,\ldots,d \tag{3.63}$$

For example, the Jeffreys' prior of scale parameter θ of an exponential distribution is,

$$\begin{aligned}\pi(\theta) \propto \{I(\theta)\}^{\frac{1}{2}} &= \left\{-\int_{x=0}^{\infty} \frac{1}{\theta}\exp\left(-\frac{x}{\theta}\right)\left(\frac{\partial^2}{\partial\theta^2}\left(-\log(\theta) - \frac{x}{\theta}\right)\right)dx\right\}^{\frac{1}{2}} \\ &= \left\{-\frac{1}{\theta^2} + \frac{2\theta}{\theta^3}\right\}^{\frac{1}{2}} = \frac{1}{\theta}\end{aligned} \tag{3.64}$$

According to Van Noortwijk *et al.* (2001), the Jeffreys' prior is considered to be most appropriate for purposes of 'fully objective' formal model comparison, especially for known location parameters.

The reference prior is a modified Jeffreys' prior in which the dependence among parameters (characteristic of the Jeffreys' prior) is reduced. Reference priors maximise the information of available observations using an information measure (see Bernardo and Smith 1994). Although this prior is often invariant under one-to-one transformations, it is not always dimensionless.

Maximal data information priors provide maximal average data information using an information measure as well (see Zellner 1977). However, the formulation is different from the Jeffreys' prior,

$$\pi(\theta) \propto \exp\left\{\hat{I}(\theta)\right\} \tag{3.65}$$

where,

$$\hat{I}(\theta) = \int \ell(\mathbf{x}|\theta)\log\left(\ell(\mathbf{x}|\theta)\right)dx$$

A major drawback is that these priors are not always invariant under one-to-one transformations. Furthermore, in contrast with the first three priors, it is often impossible to determine the posterior distribution of θ analytically.

On the contrary, informative priors can be used to express prior knowledge. This information results from either expert judgement or analysis of historical data. Berger (1985) presents several methods to derive informative priors. The two most important approaches are (Van Noortwijk *et al.* 2004):

- deriving conjugate distributions (i.e. assessing the parameters of an informative prior);
- using historical censored observations (e.g. observed flood depths).

There is no general approach to derive informative priors (Van Noortwijk *et al.* 2004). However, probability density functions can belong to a conjugate family of distributions for observations from a certain likelihood model, if both prior and posterior distribution belong to this family. A family of probability density functions is called conjugate if (1) for any sample size n and any observations $\mathbf{x} = (x_1,\ldots,x_n)$ the likelihood function $\ell(\mathbf{x} \mid \theta)$, regarded as a function of θ, is proportional to one of the probability density functions in the family and (2) the family is closed under sampling or under multiplication (DeGroot 1970). The main advantage of a conjugate family of distributions is that the posterior can be calculated in explicit form.

Conjugate priors can be successfully applied when they do not conflict with prior beliefs. However, only for probability models of the 'exponential family' conjugates can be easily obtained (Bernardo and Smith 1994). Furthermore, the major advantage of conjugate priors is their mathematical convenience. Expressing prior beliefs in a parametric distribution is always an approximation. In practice, however, the family of conjugate distributions appears to be rich enough to represent the available prior information.

As an example the conjugate prior of an exponential distribution function is derived. Consider independent observations $\mathbf{x} = (x_1,\ldots,x_n)$ from an exponential distribution with unknown expectation θ (θ>0). As prior distribution the inverted gamma distribution is chosen (NB if a stochastic variable has a gamma distribution, the reciprocal of this variable has an inverted gamma distribution). The likelihood function of the observations and the prior density function of θ read, respectively,

$$\ell(\mathbf{x}|\theta) = \prod_{i=1}^{n} \frac{1}{\theta}\exp\left(-\frac{x_i}{\theta}\right) \tag{3.66}$$

and

$$\pi(\theta) = \mathrm{Ig}(\theta|a,b) = \frac{b^a}{\Gamma(a)}\theta^{-(a+1)}\exp\left(-\frac{b}{\theta}\right) \tag{3.67}$$

Therefore, the posterior distribution function of θ can be written as,

$$\begin{aligned}\pi(\theta|\mathbf{x}) &= \frac{\frac{b^a}{\Gamma(a)}\theta^{-(a+n+1)}\exp\left(-\frac{b+n\bar{x}}{\theta}\right)}{\int_0^\infty \frac{b^a}{\Gamma(a)}\theta^{-(a+n+1)}\exp\left(-\frac{b+n\bar{x}}{\theta}\right)d\theta} \qquad \text{with } \bar{x} = \frac{\sum_{i=1}^{n} x_i}{n} \\ &= \frac{(b+n\bar{x})^{a+n}}{\Gamma(a+n)}\theta^{-(a+n+1)}\exp\left(-\frac{b+n\bar{x}}{\theta}\right)\end{aligned} \tag{3.68}$$

This is also an inverted gamma distribution, but the parameters changed to $(a+n)$ and $(b+n\bar{x})$, respectively.

Another useful informative prior is a distribution function based on historical data. For example, Van Noortwijk *et al.* (1997 and 2004) use records of historical river floods to estimate an informative prior on annual maximum discharges of the rivers Meuse and Rhine. The posterior density combines prior information from the historical censored data and actual observations. Unfortunately, there are no explicit expressions for prior distributions based on historical observations, and numerical methods must be used instead.

3.5.2.3 Bayesian parameter estimation

In contrast with 'classical' parameter estimation, the Bayesian approach considers the unknown parameter θ as a random variable distributed according to a probability distribution, which expresses the uncertainty about θ. Prior to data collection this density function is denoted as $\pi(\theta)$, capturing all available knowledge about the parameters. Posterior to data collection it is denoted as $\pi(\theta|\mathbf{x})$. The prior is updated to the posterior by Bayes' theorem (Eq. (3.56)).

The posterior predictive probability of exceeding x_0 is calculated from the survival function of X (i.e. the probability of exceeding x_0 given parameter vector $\boldsymbol{\theta}$), which is denoted as,

$$\overline{F}(\mathbf{x}|\theta) = 1 - F(\mathbf{x}|\theta) = 1 - \Pr(X \le x|\theta) = \int_x^\infty f(t|\theta)dt \tag{3.69}$$

This gives a posterior predictive probability of exceedance equal to,

$$\Pr(X > x_0|\mathbf{x}) = \int_\Theta \Pr(X > x_0|\theta)\pi(\theta|\mathbf{x})d\theta = \int_\Theta \overline{F}(x_0|\theta)\pi(\theta|\mathbf{x})d\theta \tag{3.70}$$

where $\Pr(X>x_0|\mathbf{x})$ is the predictive probability of exceeding x_0 when the observations $\mathbf{x}=(x_1,\ldots,x_n)$ are given.

3.5.2.4 Bayesian distribution type selection

In decision-making for sewer system management the question arises which probability distribution should be chosen to model the performance parameter, i.e. CSO volumes. Instead of choosing one probability distribution type one could also consider various possible distributions and attach weights to the distributions according to how good the fits of these distributions are. Such weight factors can be determined either with Tang weights (Tang 1980 and Van Gelder 2000) or Bayes factors (Kass and Raftery 1995 and Van Noortwijk *et al.* 2001). Van Gelder *et al.* (1999) conclude that the latter performs better (i.e. has faster convergence).

Bayes weight assessment can be used to choose one probability model from a set of possible models (e.g. Van Gelder 2000 and Van Noortwijk *et al.* 2001). For this purpose Bayes factors are used to determine weights that describe how well a probability distribution fits the data (i.e. the better the fit, the higher the weighing). Advantages of Bayesian hypothesis testing compared to traditional hypothesis testing (e.g. Chi-square test) are that the number of candidate models considered simultaneously is not limited. Moreover, models do not have to be nested (one within another). The Bayesian approach to hypothesis testing originates from Jeffreys (1961). The approach quantifies statistical uncertainty. Bernardo and Smith (1994) and Kass and Raftery (1995) present more details about Bayes factors.

Consider a data set $\mathbf{x} = (x_1,\ldots,x_n)$ and two candidate probability models H_1 and H_2. The two hypotheses H_1 and H_2 represent two marginal probability densities $\pi(\mathbf{x}|H_1)$ and $\pi(\mathbf{x}|H_2)$. Given the prior probabilities $p(H_1)$ and $p(H_2) = 1\text{-}p(H_1)$ the data produce posterior probabilities $p(H_1|\mathbf{x})$ and $p(H_2|\mathbf{x}) = 1\text{-}p(H_1|\mathbf{x})$. When the two hypotheses are considered equally probable beforehand, $p(H_1) = p(H_2) = 0.5$ are chosen.

The posterior probabilities are obtained using Bayes' theorem,

$$p(H_k|\mathbf{x}) = \frac{\pi(\mathbf{x}|H_k)p(H_k)}{\pi(\mathbf{x}|H_1)p(H_1)+\pi(\mathbf{x}|H_2)p(H_2)} \qquad k=1,2 \tag{3.71}$$

which are called Bayes weights. They represent the posterior probability of model H_k being correct given the data $\mathbf{x} = (x_1,\ldots,x_n)$. The marginal density of the data $\pi(\mathbf{x}|H_k)$ under model H_k is obtained by integrating with respect to the parametric vector θ_k,

$$\pi(\mathbf{x}|H_k) = \int \ell(\mathbf{x}|\theta_k, H_k)\pi(\theta_k|H_k)d\theta_k \tag{3.72}$$

where $\pi(\theta_k|H_k)$ is the prior density of H_k and $\ell(\mathbf{x}|\theta_k,H_k)$ is the likelihood function of the data $\mathbf{x}$ given θ_k. The results can be summarised in the 'Bayes factor',

$$B_{12} = \frac{p(H_1|\mathbf{x})/p(H_2|\mathbf{x})}{p(H_1)/p(H_2)} \tag{3.73}$$

which can be reduced using Bayes' theorem to,

$$B_{12} = \frac{\pi(\mathbf{x}|H_1)}{\pi(\mathbf{x}|H_2)} \tag{3.74}$$

An extension of Eq. (3.73) to m candidate models H_k (k = 1,...,m) can be easily obtained,

$$p(H_k|\mathbf{x}) = \frac{\pi(\mathbf{x}|H_k)p(H_k)}{\sum_{j=1}^{m} p(\mathbf{x}|H_j)p(H_j)} \qquad k = 1,...,m \tag{3.75}$$

which results in Bayes factors defined as,

$$B_{jk} = \frac{\pi(\mathbf{x}|H_j)}{\pi(\mathbf{x}|H_k)} \qquad j,k = 1,...,m \tag{3.76}$$

If the non-informative, improper, Jeffreys' prior is chosen as prior distribution, the marginal density of the data $\pi(\mathbf{x}|H_k)$ as described in Eq. (3.71) is difficult to obtain. The problem is that improper priors do not integrate to one. As a consequence, the Bayes factors of Eq. (3.75) are undefined. The problem is resolved by defining the Bayes factors differently,

$$\frac{p(H_j|\mathbf{x})}{p(H_k|\mathbf{x})} = \frac{\pi(H_j|\mathbf{x})}{\pi(H_k|\mathbf{x})} \times \frac{w(H_j)}{w(H_k)} \qquad j,k = 1,...,m \tag{3.77}$$

where $w(H_k)$ is the prior weight of probability model H_k (see Dawid 1999). Using Eq. (3.74) and (3.76) the posterior probability of model H_k being correct (i.e. the Bayes weight) can be rewritten as,

$$p(H_k|\mathbf{x}) = \frac{\pi(\mathbf{x}|H_k)w(H_k)}{\sum_{j=1}^{m} p(\mathbf{x}|H_j)w(H_j)} \qquad k = 1,...,m \tag{3.78}$$

It remains to choose prior weights $w(H_k)$. For formal model comparison Van Noortwijk *et al.* (2001) propose to use equal prior weights, $w(H_k) = 1/m$, k=1,...,m.

When using the improper Jeffreys' prior, the marginal density of the data given in (3.71) is difficult to compute. A solution is to approximate the logarithm of the marginal density with a Laplace expansion (Van Noortwijk *et al.* 2001),

$$\log(\pi(\mathbf{x}|H)) \approx \frac{d}{2}\log(2\pi) - \frac{d}{2}\log(n) + \log \ell(\mathbf{x}|\hat{\theta}, H) \tag{3.79}$$

for n→∞, where $\hat{\theta}$ is the maximum likelihood estimator under model H, d is the number of parameters in model H and n is the number of observations. The second and third term on the right-hand side of Eq. (3.80) form the 'Schwartz Criterion' for model selection. Despite the fact that the relative error in the Bayes factor using the Laplace expansion has an accuracy of $O(1)$, the approximation works rather well in practice.

Choosing the probability model with the highest Bayes weight minimises statistical distribution type uncertainty. If n is large ($n\rightarrow\infty$) and the 'real' distribution type is included in the candidate models, the posterior probability of this distribution will approach 1. In practice, however, the number of observations is limited and the 'real' distribution type is unknown.

If the probability density function of the observations is not known a priori, the posterior predictive probability of exceedance can also be calculated as a weighted average of different probability models. The weights of the candidate models are based on their Bayes factors (Van Noortwijk *et al.* 2001),

$$\Pr\{X > x_0|\mathbf{x}\} = \sum_{k=1}^{m} p(H_k|\mathbf{x}) \Pr(X > x_0|H_k, \mathbf{x}) \tag{3.80}$$

where $p(H_k|\mathbf{x})$ is the posterior Bayes weight of probability model H_k and m is the number of probability models considered.

3.6 CONCLUDING REMARKS

A risk-based approach for the economic optimisation of sewer maintenance and rehabilitation has been presented. It requires the estimation of the failure probabilities of the system and the consequences of failure of the system. A major advantage of this approach is that it enables a systematic evaluation of all alternatives. Its difficulties, however, consist of the lack of knowledge and data, and the problematic monetary valuation of losses due to failure.

The probability of failure can be determined by approximation methods or sampling techniques. A disadvantage of sampling is that it requires a large number of calculations resulting in time-consuming calculations. Since sewer systems are complex, looped networks, iterative calculations are required. Approximate methods, however, are not appropriate for reliability analysis of sewer systems because they cannot cope with time-varying loads (such as rainfall) or introduce failures in time (such as blockage or pump failure).

Several techniques for the analysis of failure data have been presented. Assets in a sewer system, such as sewage pumps, are subject to ageing. Therefore, failure events have to be analysed in chronological order. An homogeneous Poisson process is not appropriate to describe ageing assets because it assumes independent and identically distributed failures resulting in a constant failure rate. A non-homogeneous Poisson

process, on the other hand, can cope with ageing of assets and time-varying failure rates. However, it assumes instantaneous repair and independent failures, which proves to be incorrect for sewage pumps.

Bayesian statistics use subjective prior information in combination with observations to estimate the posterior probability of an event. Prior distributions can be either informative (e.g. conjugate priors or priors based on historical data) or non-informative (e.g. uniform priors or Jeffreys' priors). Each prior has its advantages and disadvantages. A uniform prior affects the approximation of the posterior probability, if the number of observations is small ($n<30$). A Jeffreys' prior can be used instead which is most appropriate for objective model comparison (e.g. Bayes weight assessment for distribution type selection). A limitation of conjugate priors is that the distribution type of the prior affects the estimated posterior probability. A large advantage is that the posterior can be calculated in explicit form. Informative priors based on historical information, however, are time-consuming, since they require extensive calculations.

CHAPTER 4 Hydraulic performance

4.1 INTRODUCTION

In current practice, assessment of sewer system performance is based on several criteria, including average return periods of CSO volumes and flooding events. However, measurements of CSO volumes and flood depths are usually not available. Therefore, models are required to assess sewer system performance for CSO and flooding criteria. These models produce time series of CSO volumes or flood depths.

Usually, assessments are based on a single model run using one time series of rainfall as system loads. Consequently, uncertainties in knowledge of sewer system dimensions and natural variability in rainfall are ignored. In addition, statistical uncertainties are normally not taken into account. Uncertainties in the assessment, however, are not restricted to calculated volumes. They also include costs and impacts of failure.

In order to assess sewer performance, knowledge of the impacts of CSOs on natural watercourses is required. These impacts, however, are uncertain as well. Their quantification is problematic because the processes determining water quality are complex and knowledge about these is limited.

In this chapter the impact of several uncertainties on the predicted hydraulic performance of a sewer system is studied. These uncertainties comprise both the inherent and the epistemic type:

- uncertain knowledge of sewer dimensions,
- natural variability of rainfall,
- remaining parameter uncertainty after calibration,
- uncertain construction cost,
- uncertain environmental damage due to CSOs.

For two case studies the impact of several uncertainties on the variation of average return periods of calculated CSO volumes has been estimated by means of Monte Carlo simulation. In addition, Bayesian estimation has been applied to take account of statistical uncertainty. Finally, a risk-based approach to sewer system optimisation is presented accounting for uncertainty in sewer dimensions, natural variability in rainfall and uncertainty in the cost function describing environmental damage.

4.2 CASE STUDIES

4.2.1 Case 'De Hoven'

The catchment 'De Hoven' (12.69 ha) is situated in The Netherlands on the banks of the river IJssel in the city of Deventer. The sewer system (storage volume 865 m^3) is of the combined type and comprises one pumping station (119 m^3/h) transporting the sewage to a treatment plant and three CSO structures (see Table 4.1). It is a small and relatively flat system. Due to high groundwater levels, infiltration comprises a considerable part of dwf. In addition, there is a direct response of groundwater levels to changes in the water level of the nearby river.

A monitoring network has been installed in the sewer system in order to obtain data on the performance of the external weirs (Clemens 2001a). As a result, water levels have only been measured at the three CSO structures. In addition, two tipping bucket rain gauges have been applied. The locations of the monitoring equipment are indicated in Figure 4.1. The design of the monitoring network, including locations and frequencies, is based on the method described in Clemens (2001a and 2002). In the course of the monitoring (August 3, 1998 - November 1, 1998) only two of the storms caused an overflow. However, a total of five storm events proved to be sufficiently reliable for model calibration.

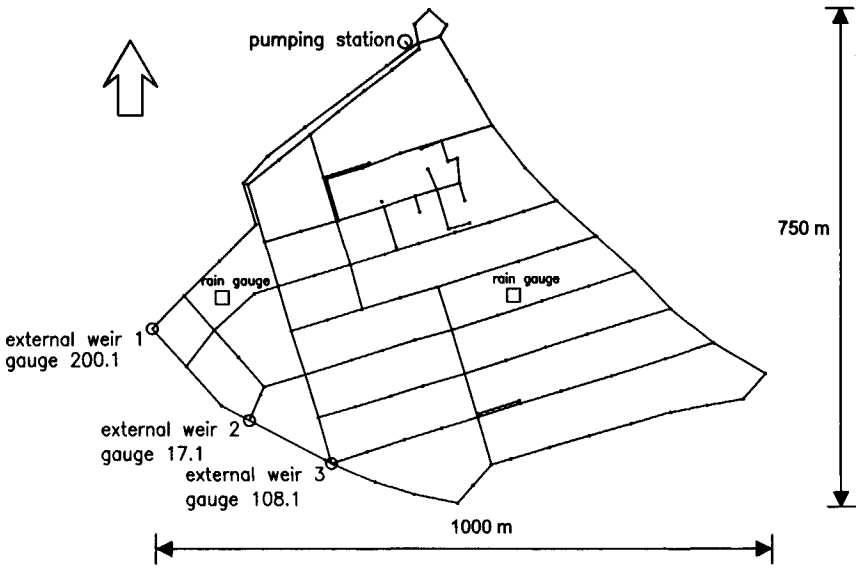

Figure 4.1 Monitoring network 'De Hoven': locations of rain gauges (□) and water level sensors (○) (reproduced with permission from Clemens 2001a).

Table 4.1 Characteristics of catchment 'De Hoven'.

Storage volume	865 m^3 (= 6.81 mm)		
Contributing area	12.69 ha		
Pumping capacity	119.0 m^3/h (= 0.94 mm/h)		
Dry weather flow	26.4 m^3/h (= 0.21 mm/h)		
Number of inhabitants	2200		
Number of CSO structures	3		
	Weir 1	**Weir 2**	**Weir 3**
Weir height	5.41 m+NAP	5.40 m+NAP	5.42 m+NAP
Weir length	0.90 m	0.35 m	0.60 m

4.2.2 Case 'Loenen'

The second catchment 'Loenen' is mildly sloping. It is a combined sewer system, which measures 900 m^3 and is equipped with one pumping station (pc = 209 m^3/h), two CSO structures located at S02 and S12 (see Figure 4.2 and Table 4.2). The former discharges to a large pond. There is a relatively large average dwf that results from several industrial discharges and inflow from an adjacent sewer system ('Veldhuizen').

Table 4.2 Characteristics of catchment 'Loenen'.

Storage volume	900 m^3 (= 3.85 mm)	
Contributing area	23.44 ha	
Pumping capacity	209 m^3/h (= 0.89 mm/h)	
Dry weather flow	78 m^3/h (= 0.33 mm/h)	
Number of inhabitants	2100	
Number of CSO structures	2	
	Weir 1	**Weir 2**
Weir height	17.75 m+NAP	18.80 m+NAP
Weir length	3.60 m	1.00 m

Table 4.3 Statistics of measuring period in Loenen (Aug. 28 – Dec. 26, 2001).

	'Loenen' (measurement period)	**Yearly averages (De Bilt, 1955-1979)**
total number of days	180	365
number of days with precipitation > 1 mm	80	129
number of days with precipitation > 5 mm	40	54
number of CSO events	16	-
total precipitation (mm)	593	800

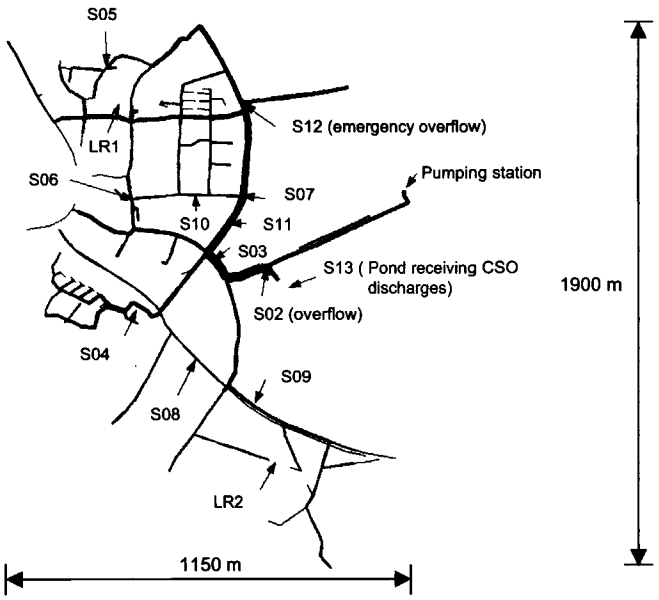

Figure 4.2 Monitoring network 'Loenen': locations of rain gauges (LR1 and LR2) and water level sensors (S02 to S12 in sewer system and S13 in pond).

The installed monitoring network (designed according to Clemens 2001a, 2001b and 2002) consisted of two automatic rain gauges, eleven water level sensors in the sewer system and one water level sensor in the pond receiving CSO discharges. Figure 4.2 shows the locations of the gauges. In addition, pumped volumes have been registered each 5 minutes. The monitoring network has been especially designed for model calibration. During the measuring period (Aug. 28, 2001 – Dec. 26, 2001), 16 overflow events occurred. The total amount of rainfall (593 mm) during these four months is relatively high compared to the average annual precipitation of approximately 800 mm in The Netherlands. This is mostly due to the relatively large number of storm events exceeding 5 mm/d. The statistics of rainfall and CSOs during the measuring period are summarised in Table 4.3.

4.3 RESERVOIR MODEL

In order to study the impact of both uncertainties in system dimensions (e.g. storage capacity and contributing areas) and natural variability in rainfall on the return period of calculated CSO volumes, the sewer systems of 'De Hoven' and 'Loenen' have been modelled as a reservoir with an external weir and a pump (Figure 4.3). A reservoir

model is chosen because large numbers of calculations with a hydrodynamic model and a rainfall series of at least 10 years are exceptionally time-consuming. In addition, rainfall runoff has been described with the 'NWRW 4.3' model (see Appendix V). This is the 'standard' rainfall runoff model in The Netherlands. It describes evaporation, infiltration, storage on street surfaces and overland flow. In the model, 12 types of contributing areas are distinguished, each characterised by a routing coefficient, an initial storage loss and, eventually, an infiltration capacity. However, the reservoir model only uses one type of contributing area. Finally, evaporation is introduced as a monthly averaged value based on potential evaporation (see Penman 1948 and Stichting RIONED 1999).

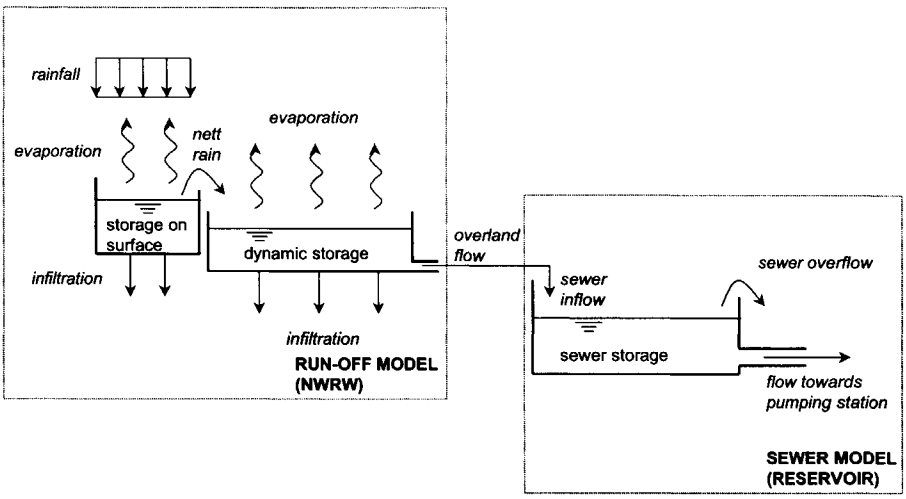

Figure 4.3 Reservoir model describing the sewer systems of 'De Hoven' and 'Loenen'. The model comprises a rainfall runoff model ('NWRW 4.3' model) and a reservoir model with an external weir and a pump.

4.3.1 Impacts of uncertainty of sewer system dimensions

The impacts of uncertainty of sewer system dimensions on the return period of calculated CSO volumes has been studied (in particular storage volume S, pumping capacity pc, contributing area A and overflow coefficient CC). Under free discharge conditions the flow across a weir is calculated with,

$$Q = L_w \, CC \, h_w^{3/2} \tag{4.1}$$

where L_w is weir length (m) and h_w is upstream water depth above the weir crest.

The uncertain system dimensions are assumed to be statistically independent and normally distributed with known mean and variance. This assumption is based on the absence of model calibration and expert opinion. Possible causes of uncertainty are

summarised in Table 4.4. Averages and standard deviations are based on expert judgement (see Clemens 2001a). The ranges for the sewer systems of 'De Hoven' and 'Loenen' are presented in Table 4.5 and Table 4.6.

As input of the computations a 10-year rainfall series (1955-1964) from De Bilt (The Netherlands) has been used. Dwf of both sewer systems is assumed constant at 26.4 m^3/h and 78.2 m^3/h, respectively. The parameters of the rainfall runoff model measure: B = 0.5 mm, I = 0.25 mm/h and F = 300 s (where B is storage on street surfaces and initial losses, I is infiltration capacity and F is flow routing coefficient).

Table 4.4 Possible causes of uncertain system dimensions (see also § 2.4).

System dimension	Possible causes of uncertainty
Storage	- unknown storage volume of household connections - errors in sewer database (e.g. invert/weir levels, pipe/ manhole sizes) - missing sewer pipes
Pumping capacity	- incorrect pumping capacity - uncertain contribution of infiltration/inflow
Contributing area	- inaccurate amount and type of catchment area - unknown drainage from pervious areas to sewer system
Weir coefficient	- broad-crested weir instead of sharp-crested - incorrect length of weir - irregularly shaped weir (e.g. angular)

Table 4.5 Ranges of varying sewer system dimensions of sewer system 'De Hoven' (Clemens 2001a).

System parameter	Mean	Std.	CV * (%)
S (m^3)	865.0	43.25	5.0
pc (m^3/h)	119.0	5.95	5.0
A (ha)	12.69	0.64	5.0
CC ($m^{0.5}/s$)	1.40	0.35	25.0

* CV = coefficient of variation = (σ/μ)*100%

Table 4.6 Ranges of varying sewer system dimensions of sewer system 'Loenen'.

System parameter	Mean	Std.	CV * (%)
S (m^3)	900.0	45.00	5.0
pc (m^3/h)	209.0	10.45	5.0
A (ha)	23.44	1.17	5.0
CC ($m^{0.5}/s$)	1.40	0.35	25.0

* CV = coefficient of variation = (σ/μ)*100%

A Monte Carlo simulation of 1000 runs has been performed for both sewer systems (for details see § 3.3.2). In each run a random value of the parameters (S, pc, A and CC) has

been drawn from the probability distributions and substituted in the model. The 4 parameter values can be drawn independently, since their covariances are equal to 0 in the reservoir model (due to absence of calibration). The CSO volumes resulting from the subsequent calculations have been summed over the storm events. A storm event is defined as an event that starts when rainfall occurs resulting in a water level rise in the sewer system above the maximum dwf level. The event lasts until the water level drops below this level. As a result, statistically independent storm events and, consequently, CSO events are created. It is important to consider that uncertainty of computed CSO volumes comprises not only model parameter uncertainty due to the uncertainty in system parameters, but also model structure uncertainty due to the strongly simplified reservoir model and inherent uncertainty in time due to the temporal variation in rainfall. Model structure uncertainty decreases when a more detailed model is applied. However, a more detailed model consists of more parameters requiring a larger amount of data for calibration. Therefore, given that sufficient data are available, a more detailed model reduces model structure uncertainty.

Exponential, Rayleigh, normal, lognormal, gamma, Weibull and Gumbel distributions are considered as candidate distribution types (see Appendix IV and Table 4.7). Using Bayes weights (see § 3.5.2) the distribution function with the best fit to the CSO data has been selected. Bayes weight assessment, however, only minimises statistical uncertainty with respect to the distribution type but does not eliminate uncertainty. Bayes weights have been calculated for 10 randomly selected runs from the complete Monte Carlo simulation (N = 1000). A limited number of runs has been selected because the analysis is computationally demanding. In the computation of the weights, Jeffreys priors have been used as prior distributions (meaning no prior knowledge) and the Laplace expansion for approximation of marginal densities.

In Table 4.7 the averages of the prior and posterior Bayes weights of 10 runs regarding the 'De Hoven' system are presented. The Weibull distribution appears to fit best with a Bayes weight of 55%. Therefore, it is chosen to describe the calculated CSO volumes per storm event. The Bayes weights of the individual runs are presented in Appendix VI. The results for one run are illustrated in Figure 4.4. Traditional goodness-of-fit tests, such as Chi-square and Kolmogorov-Smirnov, also indicate that the Weibull distribution fits best with the CSO data (Appendix VI).

Essentially, CSO volumes represent peak over threshold (pot) values. Therefore, extreme value statistics is also applicable (see e.g. Hosking and Wallis 1987, Beirlant *et al.* 1996 and Willems 2000). The approach of Beirlant *et al.* (1996) is based on a description of the properties of the tail of the observations. Bayes weight assessment can also be used above a certain threshold value focussing on the tail of the candidate distributions, e.g. left-truncated Weibull (Wingo 1989) or generalised Pareto distributions (Hosking and Wallis 1987).

Recently, distribution types describing peak over threshold values have been added to the set of candidate distributions. Figure 4.5 shows that a Pareto distribution is better capable of describing CSO volumes than the afore-mentioned Weibull distribution. A

left-truncated Weibull distribution is less appropriate because the threshold value is determined by the physics of the sewer system. As a result, the threshold is 0 by definition, which reduces the left-truncated Weibull distribution to a Weibull distribution. However, these results have not yet been applied in this thesis. Therefore, the description of CSO volumes with a generalised Pareto distribution will have to be studied in coming research.

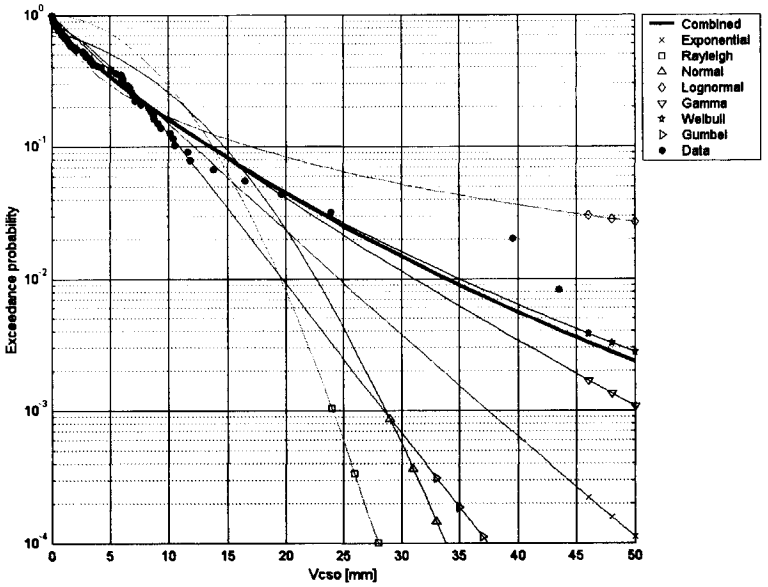

Figure 4.4 Illustration Bayes weight assessment for CSO volumes 'De Hoven' of one MC run (data refers to model results). A Weibull distribution function fits best with simulated values. As a result, the Weibull primarily determines the combined distribution of all candidate distribution types.

Table 4.7 Prior and posterior Bayes weights for calculated CSO volumes per storm event for sewer system 'De Hoven'.

Bayes weight	Exp	Ray	Nor	Lgn	Gam	Wei	Gum
Prior	0.1429	0.1429	0.1429	0.1429	0.1429	0.1429	0.1429
Posterior	0.0174	0.0000	0.0000	0.0719	0.3644	0.5463	0.0000

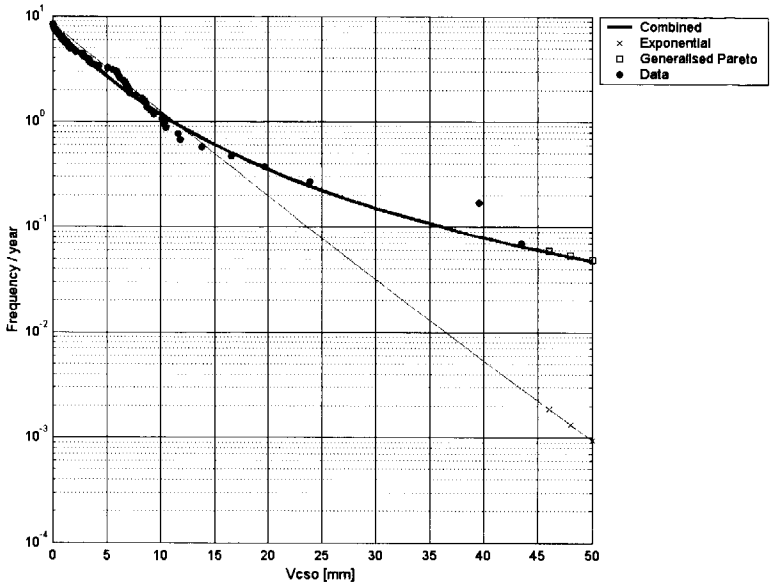

Figure 4.5 Illustration Bayes weight assessment for CSO volumes 'De Hoven' of one MC run (data refers to model results). A generalised Pareto distribution function fits better with simulated values than a Weibull distribution, especially for larger CSO volumes.

A random variable X has a Weibull distribution with shape parameter $a > 0$ and scale parameter $b > 0$ if the probability density is given by,

$$f(x) = \frac{a}{b}\left(\frac{x}{b}\right)^{a-1} \exp\left\{-\left(\frac{x}{b}\right)^{a}\right\} \tag{4.2}$$

Given the data $\mathbf{x} = (x_1,\ldots,x_n)$ the shape parameter a and the scale parameter b of a Weibull distribution can be estimated with the maximum likelihood (ML) method (see § 3.5.1). The log-likelihood of the Weibull distribution is defined as,

$$\log \ell(\mathbf{x}|a,b) = n\left(\log(a) - a\log(b)\right) + (a-1)\sum_{i=1}^{n}\log(x_i) - \sum_{i=1}^{n}\left(\frac{x_i}{b}\right)^{a} \tag{4.3}$$

With the ML method those values of a and b are chosen for which the likelihood function is maximised.

As an alternative, the parameters can be estimated using Bayes' theorem (see § 3.5.2). As the number of observations n approaches infinity, a Bayes estimate with non-informative priors tends to the ML estimate. However, the ML estimator produces a point estimate of parameters a and b, whereas a Bayesian analysis gives the probability densities of these parameters (see Figure 4.6). Under the assumption of a quadratic loss

function (DeGroot 1970), the Bayes estimates of a and b represent the expected values of the posterior distributions of a and b, respectively.

The ML and Bayes estimator of shape and scale parameter are illustrated for one Monte Carlo run. The former results in the parameter values: $a = 0.759$ and $b = 4.387$, while the latter gives the probability densities depicted in Figure 4.6. From these densities the expected values of a and b are determined by integrating (DeGroot 1970),

$$E(\theta) = \min_{\theta^*}\left\{\int_0^\infty (\theta - \theta^*)^2 \pi(\theta|\mathbf{x})\theta\, d\theta\right\} = \int_0^\infty \pi(\theta|\mathbf{x})\theta\, d\theta \tag{4.4}$$

which minimises the estimation error. It gives a shape and scale parameter of the Weibull distribution equal to 0.760 and 4.462, respectively. Especially the scale parameter is slightly different from the ML estimation. As a result, the exceedance probability based on the Bayes estimator is increased due to the spread and the shifted expectation.

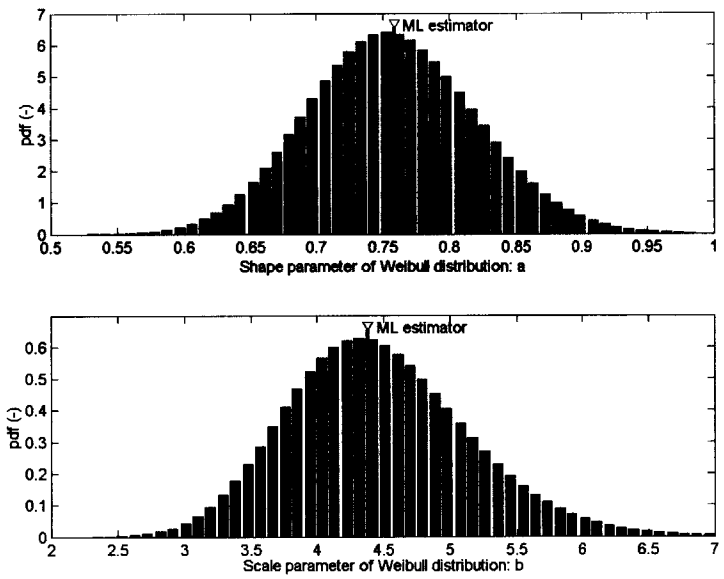

Figure 4.6 Illustration of results of Bayesian estimation of scale and shape parameters of Weibull distribution describing CSO volumes.

Computation of average return periods of calculated CSO volumes requires not only estimating the probability of exceeding of a threshold (i.e. CSO volumes per event), but also specifying the stochastic process of the occurrence times of these exceedances. The threshold exceedances are assumed to be mutually independent. This results in a definition of CSO events that is dependent on the sewer system. The occurrence of exceedances of the threshold can be regarded as a Poisson process (see e.g. Buishand 1989). Hence, the return period of a CSO volume depends on the exceedance

probability of this volume and the average return period of exceedances (irrespective of the volume),

$$\frac{1}{T_{V_{CSO}>v_0}} = \frac{1}{T_{CSO}} * \Pr\{V_{CSO} > v_0 | \mathbf{x}\} = \frac{1}{T_{CSO}}\left(1 - \Pr\{V_{CSO} \le v_0 | \mathbf{x}\}\right) = \frac{1}{T_{CSO}}\left(1 - F(v_0)\right) \quad (4.5)$$

where $T_{V_{CSO}>v_0}$ is the return period of calculated CSO volumes (V_{CSO}) larger than v_0, T_{CSO} is the average return period of CSOs irrespective of their volume, $\Pr\{V_{CSO}>v_0 | \mathbf{x}\}$ is the probability of exceeding volume v_0 given data set $\mathbf{x} = (x_1,\ldots,x_n)$ of computed CSO volumes and $F(v_{CSO})$ is the cumulative distribution function of CSO volumes. The average return period of calculated CSOs irrespective of the volume is,

$$T_{CSO} = \frac{\#\text{years (over which CSO events are measured)}}{\#\text{CSO events}} \quad (4.6)$$

With respect to the sewer system of 'De Hoven', calculated CSO volumes per storm event and their corresponding return periods are shown in Figure 4.7. Both average volume and 95% uncertainty interval are displayed. The 95% interval is based on the 0.025 and 0.975 quantile of calculated volumes. The figure demonstrates that calculated CSO volumes with a certain return period vary considerably due to uncertainties in knowledge of sewer system dimensions. The variability increases with increasing CSO volume.

The statistics of calculated average CSO volumes are summarised in Table 4.8. It shows that, for example, in the event of a return period of 0.5 years the average calculated CSO volume is 7.4 mm and the 95% uncertainty interval of this volume is 2.9 mm. However, with a larger return period of 5.0 years the average increases considerably to 24.5 mm with a larger uncertainty interval of 4.8 mm as well. When the results of Figure 4.7 are converted to average yearly values, the CSO volume is 46.3 mm/a and the overflow frequency is 9.3/a. Due to the uncertainties considered, the yearly volume and frequency vary from 35.8 to 59.1 mm/a and 6.4 to 12.8/a, respectively.

Table 4.8 Statistics of calculated CSO volumes for 'De Hoven'.

		Average	95% interval
CSO volume (mm)	T_{CSO} = 0.25 y	3.35	1.83 - 4.88
	T_{CSO} = 0.5 y	7.36	5.88 - 8.78
	T_{CSO} = 1.0 y	12.00	10.70 - 13.28
	T_{CSO} = 2.0 y	17.11	15.77 - 18.77
	T_{CSO} = 5.0 y	24.44	22.46 - 27.22
CSO volume (mm/a)	yearly average	46.26	35.77 - 59.13
Overflow frequency (1/a)	yearly average	9.31	6.40 - 12.80

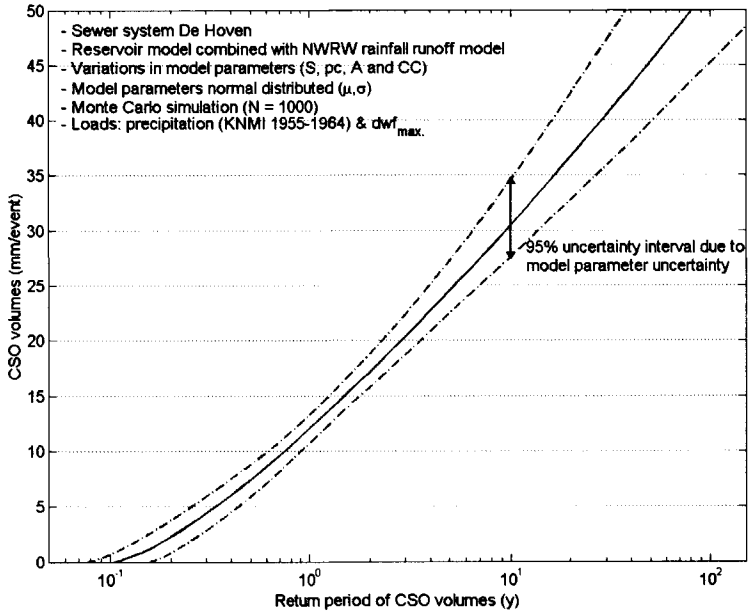

Figure 4.7 Return period of calculated CSO volumes per storm event for sewer system 'De Hoven' (CSO volumes per event Weibull distributed). Both average and 95% uncertainty interval are displayed. Variation results from uncertainty in knowledge of system dimensions.

Similar results have been obtained for the sewer system of 'Loenen' (see Figure 4.8). However, the average CSO volume as a function of the return period is considerably larger (see Table 4.9). This results from the relatively small in-sewer storage per hectare of contributing area in 'Loenen'. The variation of CSO volumes per event is in the same order of magnitude for both sewer systems when the return period is below 10 years (see Table 4.8 and Table 4.9). For T > 10 years, predicted CSO volumes become uncertain because the time series applied is only 10 years long. As a result of the small in-sewer storage, yearly CSO volumes and overflow frequency are 105.0 mm/a and 24.1/a, respectively, which is more than twice as large as 'De Hoven'. The 95% uncertainty interval of average yearly volumes and frequencies are 38.2 mm/a and 6.4/a, respectively.

Table 4.9 Statistics of calculated CSO volumes for 'Loenen'.

		Average	95% interval
CSO volume (mm)	T_{CSO} = 0.25 y	7.91	6.95 - 8.89
	T_{CSO} = 0.5 y	11.53	10.65 - 12.56
	T_{CSO} = 1.0 y	15.30	14.45 - 16.43
	T_{CSO} = 2.0 y	19.20	18.31 - 20.45
	T_{CSO} = 5.0 y	24.52	23.42 - 26.10
CSO volume (mm/a)	yearly average	104.97	86.71 - 124.91
Overflow frequency (1/a)	yearly average	23.91	19.90 - 28.40

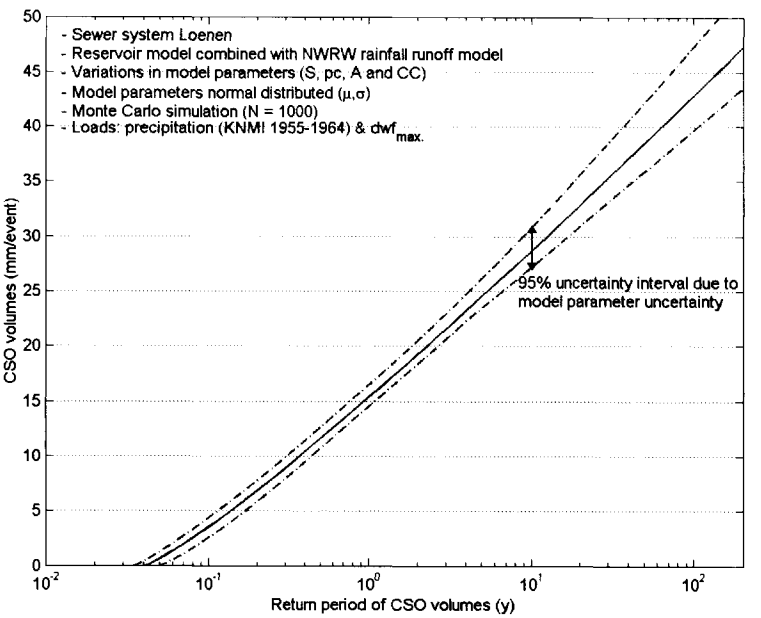

Figure 4.8 Return period of calculated CSO volumes per storm event for sewer system 'Loenen' (CSO volumes per event Weibull distributed). Both average and 95% uncertainty interval are displayed. Variation results from uncertainty in knowledge of system dimensions.

In addition to the determination of the joint impact of the uncertain dimensions, a sensitivity analysis has also been performed for the sewer system of 'De Hoven' (Korving *et al.* 2002b). For that, 12 Monte Carlo simulations of 1000 runs have been conducted applying each of the combinations of known and uncertain dimensions in Table 4.10. This gives an impression of the impact of each dimension that is uncertain. In addition, a simulation with a 25-year series has been performed, which gives an impression of the contribution of rainfall variability to overall model uncertainty.

Table 4.10 Combinations of uncertain and known dimensions applied in calculations.

Combination / Parameter	S (m^3)	pc (m^3/h)	A (ha)	CC ($m^{0.5}/s$)
A	*Unc.*	*Unc.*	*Unc.*	*Unc.*
B1	*Unc.*	Known	Known	Known
B2	Known	*Unc.*	Known	Known
B3	Known	Known	*Unc.*	Known
B4	Known	Known	Known	*Unc.*
C1	Known	*Unc.*	*Unc.*	*Unc.*
C2	*Unc.*	Known	*Unc.*	*Unc.*
C3	*Unc.*	*Unc.*	Known	*Unc.*
C4	*Unc.*	*Unc.*	*Unc.*	Known
DeBilt 55-79*	*Unc.*	*Unc.*	*Unc.*	*Unc.*

* 25-year rainfall series (De Bilt, 1955-1979) instead of 10-year series.

Again, CSO volumes have been described with Weibull distributions. On the basis of estimated parameters a and b in the Weibull distributions, their relative 95% confidence intervals have been computed for each parameter combination. These intervals are based on the 0.025 and 0.975 quantile of estimated values of the Weibull parameters and are indicative for the uncertainty in overall model results due to the uncertain dimensions considered.

The results in Table 4.11 show that the relative uncertainty interval of the Weibull parameters is reduced most when either the weir coefficient (combination B4) is varied or the contributing area (A) is fixed (combination C3). From this it can be concluded that uncertainty in CC has the smallest impact on model results. Conversely, uncertainty in A has the largest impact (combination B3). Furthermore, using 25 years of rainfall data (combination DeBilt 55-79) reduces uncertainties in model results to the same extent as using an exactly known contributing area (combination C3). This is due to the increase in total number of storm events, when a 25-year series is applied.

Table 4.11 Relative uncertainty intervals of Weibull parameters fitted to CSO data resulting from Monte Carlo simulations with 12 parameter combinations.

	A	B1	B2		C1	C2		C4	DeBilt 55-79
$\frac{a_{97.5\%}-a_{2.5\%}}{\mu(a)}$	0.28	0.20	0.17		0.26	0.26		0.28	0.24
$\frac{b_{97.5\%}-b_{2.5\%}}{\mu(b)}$	0.41	0.27	0.15		0.35	0.42		0.40	0.32

4.3.2 Impacts of natural variability of rainfall

Natural variability of rainfall has been described using a spatial rainfall generator (Willems 2001). This generator has been especially developed for the small spatial scales of urban catchments. As a result, it requires a detailed description of individual rain cells. The spatial distribution of rainfall intensity in an individual rain cell is assumed to be Gaussian shaped.

The generator is based on a model that distinguishes rainfall entities at different macroscopic scales, i.e. rain cells, cell clusters, and small and large meso-scale areas or rain storms (see Figure 4.3). The model structure is twofold: a physically-based part describing individual rain cells and cell clusters, and a stochastic part describing the randomness in the sequence of the different rain cells and storms.

Precipitation data from a dense network of rain gauges in Antwerp (Belgium) have been used for calibration of the generator. The measurements enclose 807 rain storms. The calibrated properties of the rain comprise moving velocity, moving direction, spatial extent and intensity of rain cells, and interarrival times of rain cells and rainstorms. Based on these properties the spatial rainfall generator has been constructed (see Willems 2001). Using a random generator a large number of rain cells is created accounting for interdependencies. This time series of spatial rainfall data has the same statistical properties as the data measured with the rain gauges (Willems 2000 and 2001).

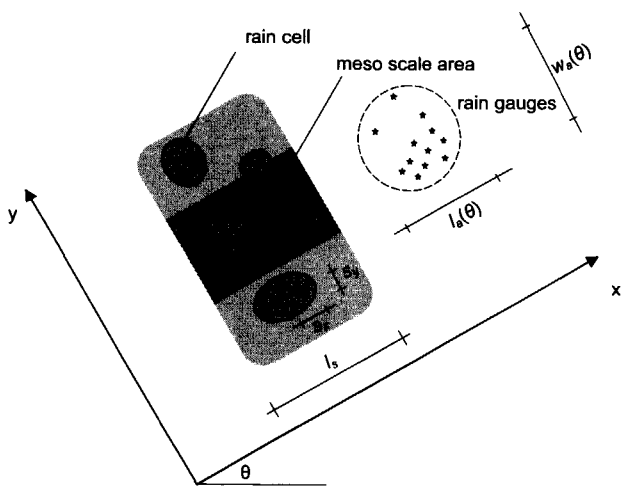

Figure 4.9 Schematic representation of spatial structure of rainfall including rain cells and meso-scale areas or rainstorms (reproduced with permission from Willems 2001), where s_x is dimension of rain cell in average moving direction (θ), s_y is dimension of rain cell perpendicular to θ, l_s is spatial extent of meso-scale area and $l_a(\theta)$ and $w_a(\theta)$ are dimension of area with rain gauges in direction θ and perpendicular to θ, respectively.

The rainfall generator calibrated for Antwerp can be used in 'De Hoven' because the generated rainfall series show considerable agreement with the 25-year rainfall series from De Bilt (The Netherlands) in terms of IDF (Intensity-Duration-Frequency) relationships. A comparison of IDF relations for De Bilt (1955-1979) and generated rainfall series is presented in Figure 4.10. The confidence limits represent the difference in IDF relations between the 500 generated rainfall series. The figure shows that the IDF curves for De Bilt are enclosed by the confidence intervals of the generated rainfall, except for events with a duration exceeding 1 hour. Therefore, the generated series are consistent with the De Bilt data. According to Willems (2000), the deviation between measurements and generated rainfall results from the assumed homogeneity of the spatial distribution in the rainfall generator and can be corrected by adding high frequency noise to the model.

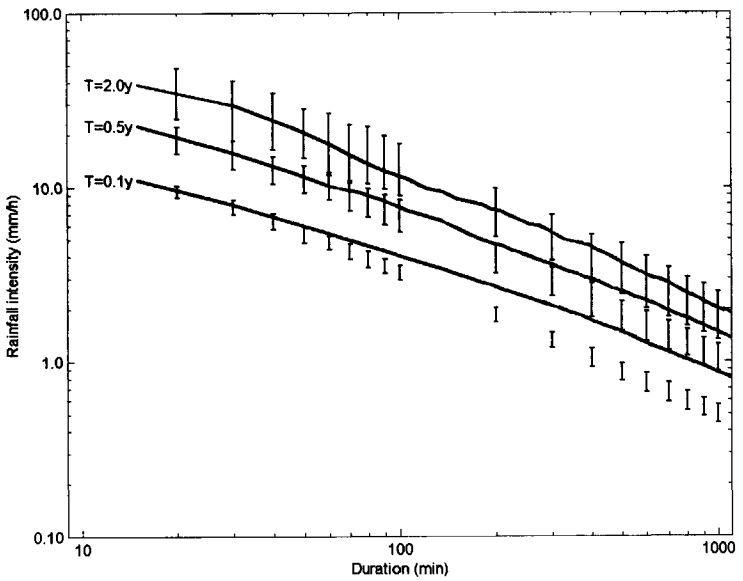

Figure 4.10 Comparison of IDF (Intensity-Duration-Frequency) curves: (1) De Bilt, The Netherlands, 1955-1979 (bold lines) and (2) confidence intervals based on 500 generated rainfall series (vertical intervals). Except for frequent events (T < 0.2 y) with longer duration (Δt > 100 min) the generated rainfall resembles the 'De Bilt' series.

In addition, Vaes *et al.* (2002) conclude that the rainfall climate in Belgium and The Netherlands is identical. Willems (2001) shows that the generated rainfall resembles the measurements from Ukkel (Belgium). The Ukkel measurements, for their part, are nearly identical to the rainfall data observed in De Bilt (The Netherlands) with respect to IDF relations (see Buishand and Velds 1980, Bouwknegt and Gelok 1988 and Vaes *et al.* 2002).

A Monte Carlo simulation of 500 runs has been performed. For each run a random series of 10 years consisting of rainfall volumes per 10 minutes has been generated at the 12 measurement locations in Antwerp. This results in a spatial rainfall field. However, only the rainfall volumes of one central location in Antwerp have been used as system loads. As a result, the error which arises from averaging rainfall over the total catchment area is not considered because the dimensions of the catchment area (1-2 km) are smaller than the average dimensions of individual rain cells (15-30 km) (Zawadski 1973 and Willems 2000). According to Willems (2000), the contribution of errors resulting from spatial variation in rainfall to variation in CSO volumes is only marginal (0-5%).

As in the previous paragraph, Bayes weights (see § 3.5.2) have been applied to determine the proper distribution type for calculated CSO volumes. The results (see Table 4.12) show that the Weibull and gamma distributions have almost equal weights, so a weighted average of the two is also possible. Weighing is based on the Bayes weights of each distribution type. However, further simulations with a mixed distribution would be much more complicated and time-consuming. Since the surplus value of a more detailed description is outweighed by the amount of work required, only a Weibull distribution has been applied. In addition, the Kolmogorov-Smirnov test also indicates that a Weibull distribution fits best with the calculated CSO volumes (see Appendix VI)

The results for the sewer systems of 'De Hoven' and 'Loenen' are shown in Figure 4.11 and Figure 4.12, respectively. With respect to the sewer system of 'De Hoven' variation in CSO volumes increases with increasing return period. The 95% uncertainty interval (based on 0.025 and 0.975 quantile) of CSO volumes is relatively large compared to the average values. This is in accordance with e.g. Schilling and Fuchs (1986) and Willems (2000), who emphasise that rainfall input errors are one of the most important sources of uncertainty (partly due to the inevitable natural variability). Furthermore, the yearly CSO volume is 38.2 mm/a and the overflow frequency is 5.8/a. Their 95% uncertainty intervals measure 35.3 mm/a and 3.1/a.

Table 4.12 Prior and posterior Bayes weights for calculated CSO volumes per storm event for sewer system 'De Hoven'.

Bayes weight	Exp	Ray	Nor	Lgn	Gam	Wei	Gum
Prior	0.1429	0.1429	0.1429	0.1429	0.1429	0.1429	0.1429
Posterior	0.1375	0.0000	0.0000	0.1073	0.3213	0.4339	0.0000

Figure 4.12 and Table 4.14 demonstrate that CSO volumes per return period are larger for 'Loenen' than for 'De Hoven'. Again, this results from the small in-sewer storage per hectare of contributing area of the former system. Regarding yearly overflow volumes and frequencies, average values amount to 69.6 mm/a and 14.2/a, respectively. The uncertainty intervals range from 21.90 to 57.24 mm/a and 4.30 to 7.40/a.

Table 4.13 Statistics of calculated CSO volumes for 'De Hoven'.

		Average	95% interval
CSO volume (mm)	T_{CSO} = 0.25 y	1.56	0.14 - 3.53
	T_{CSO} = 0.5 y	5.91	3.24 - 9.27
	T_{CSO} = 1.0 y	11.40	7.00 - 16.55
	T_{CSO} = 2.0 y	17.70	10.79 - 25.29
	T_{CSO} = 5.0 y	27.03	15.43 - 41.14
CSO volume (mm/a)	yearly average	38.17	21.90 - 57.24
Overflow frequency (1/a)	yearly average	5.84	4.30 - 7.40

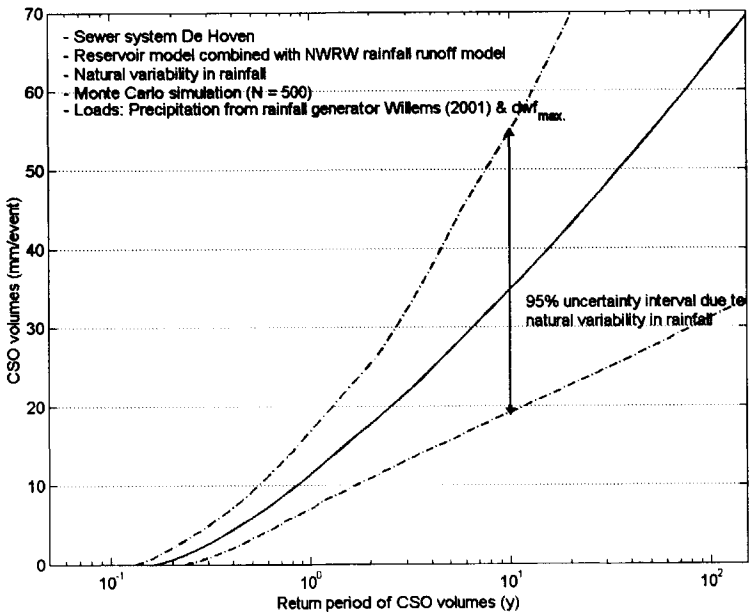

Figure 4.11 Return period of calculated CSO volumes per storm event for sewer system 'De Hoven' (CSO volumes per event Weibull distributed). Both average and 95% uncertainty interval are displayed. Variation results from natural variability in rainfall.

Table 4.14 Statistics of calculated CSO volumes for 'Loenen'.

		Average	95% interval
CSO volume (mm)	T_{CSO} = 0.25 y	5.57	4.00 - 7.38
	T_{CSO} = 0.5 y	9.87	7.15 - 12.74
	T_{CSO} = 1.0 y	14.71	10.42 - 19.78
	T_{CSO} = 2.0 y	19.97	13.80 - 26.95
	T_{CSO} = 5.0 y	27.48	18.53 - 38.03
CSO volume (mm/a)	yearly average	69.56	48.19 - 91.63
Overflow frequency (1/a)	yearly average	14.17	12.20 - 16.50

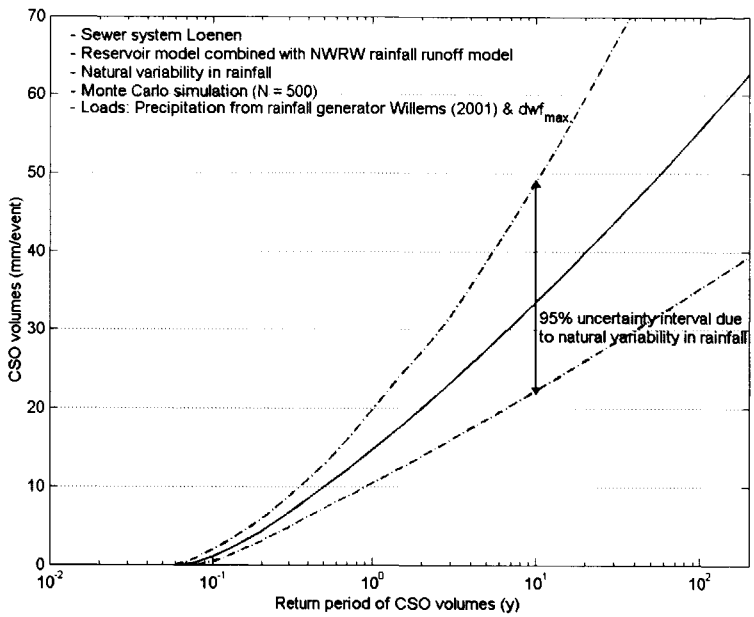

Figure 4.12 Return period of calculated CSO volumes per storm event for sewer system 'Loenen' (CSO volumes per event Weibull distributed). Both average and 95% uncertainty interval are displayed. Variation results from natural variability in rainfall.

In general, variation due to natural variability in rainfall (represented by generated rainfall series) is larger than due to uncertainty in system dimensions. On the other hand, rainfall variation results in lower average yearly CSO volumes than dimension uncertainty (Table 4.13 and Table 4.14). This also holds for average overflow frequencies.

The differences between impacts of rainfall variability and dimension uncertainty can be partly explained from the IDF relations in Figure 4.10. As a result of the large variation in rainfall volumes for T > 1 year, the generated rainfall series can hold more extremes than the De Bilt series. Conversely, the structural underestimation of events

with longer duration (Δt > 100 min) causes on average smaller yearly precipitation volumes.

4.3.3 Conclusions and discussion

Return periods of calculated CSO volumes are an important criterion in decision-making with respect to sewer system rehabilitation. In this paragraph, variability in return periods has been determined for the sewer systems of 'De Hoven' and 'Loenen'. The sewer systems have been modelled as a reservoir with an external weir and pump.

Bayes weights have been applied to estimate return periods of calculated CSO volumes taking into account the statistical uncertainty involved. Determination of the distribution type of a data set with Bayes weights takes into account statistical uncertainties, which stem from lack of data. The Bayes weights show that calculated CSO volumes per storm event can be described with a Weibull distribution.

Calculated CSO volumes vary considerably due to uncertainty in knowledge of sewer dimensions and variability in rainfall. The observed variation increases with increasing return period. In addition, uncertainty of sewer system dimensions results in larger expected yearly CSO volumes but smaller variability in CSO volumes per storm event than natural variability in rainfall. Regarding uncertain sewer system dimensions, CSO volumes are mostly affected by lack of knowledge on the dimensions of the catchment area.

A rainfall generator has been applied to describe natural variability of rainfall. It underestimates rainfall volumes of frequent events with a duration longer than approximately 2 hours. Therefore, yearly CSO volumes based on the generated series are smaller than those resulting from the De Bilt series. This also applies to yearly overflow frequencies.

4.4 HYDRODYNAMIC MODEL

This paragraph treats the impact of remaining uncertainties in the parameters of a calibrated hydrodynamic model on overall model results. Firstly, the model calibration is described in terms of procedure and results. The calibration includes a reduction of the number of parameters to be calibrated. Secondly, the impact of variance of the calibrated parameters on predicted CSO volumes is presented.

The hydrodynamic model used is Hydroworks®, version 6.0 (Wallingford Software 2000). This model describes the sewer system as a network consisting of links (representing sewers) and nodes (representing manholes, CSO structures, etc). The rainfall runoff model is based on the 'NWRW 4.3' model which is the 'standard' model in The Netherlands (see Appendix V). It comprises 12 different types of contributing areas with characteristic initial losses, routing coefficient of the Desbordes runoff routing model (Desbordes 1978, cited in Fuchs 1998) and eventually infiltration capacity of the Horton infiltration model (Horton 1940).

4.4.1 Model calibration

The hydrodynamic models of the sewer systems of 'De Hoven' and 'Loenen' have been calibrated using the calibration procedure described by Clemens (2001a). This is an event based, partly iterative approach comprising (1) a check on structural errors in sewer database, (2) a selection of storm events and model parameters for calibration, (3) a search for optimal model parameter values and (4) an analysis of residuals.

The calibration of the sewer model of 'De Hoven' is described in detail by Clemens (2001a). During calibration, structural errors have been removed from the sewer database including several geometrical errors (e.g. incorrect invert levels) and possible storage in house and gully pot manifolds. The latter are not included in the model, which results in an underestimation of available in-sewer storage. The dwf pattern of 'De Hoven' has been derived from recorded pumping data (Clemens 2001a).

During the measuring period (Aug. 3, 1998 - Nov. 1, 1998), only 2 storm events caused an overflow. Furthermore, 3 other storm events occurred which did not cause an overflow, but contained reliable information for model calibration (Clemens 2001a). In particular, 3 events have been studied with respect to impacts of parameter uncertainty on overall model results: 25/08/98, 07/10/98 and 24/10/98 (see Table 4.15).

The number of potential calibration parameters is overwhelming (i.e. hydraulic roughness of 123 conduits and 141 manholes, weir coefficient of 3 CSO structures, 9 storm runoff parameters for various surface types and dwf). Therefore, Clemens (2001a) suggests to choose between these parameters on the basis of 'singular value decomposition' (SVD), which provides information on the identifiability of each parameter. This results in an initial set of 10 parameters. This 'full' parameter set is presented in Table 4.16. Because of the high correlation between several parameters after calibration, the set has been reduced to 5 parameters by clustering the runoff parameters of all area types and the weir coefficients. However, despite this reduction, the fit between measurements and calculations (in terms of mean squared error) should be maintained. The remaining parameters include dwf, initial losses, routing coefficient, maximum infiltration capacity and weir coefficient.

Table 4.15 Overview of storm events for 'De Hoven'.

Storm event	Return period (y)	Rain depth (mm)	
25/08/98	0.10 - 0.20	16.4	CSO event and low groundwater level (small dwf)
07/10/98	0.05 - 0.10	14.4	no CSO event
24/10/98	0.05 - 0.10	21.6	CSO event and high groundwater level (large dwf)

Table 4.16 Parameter sets for calibration of hydrodynamic model of 'De Hoven'.

FULL PARAMETER SET		REDUCED PARAMETER SET	
Parameter	**Description**	**Parameter**	**Description**
N1	dwf (m^3/h)	N1	dwf (m^3/h)
B2	initial losses on flat, impervious areas (mm)	B*	initial losses for all area types (mm)
B7	initial losses on inclining roofs (mm)	F*	routing coefficient for all area types (s)
F2	routing coefficient for flat, impervious areas (s)	I*	max. infiltration capacity for all area types (mm/h)
F7	routing coefficient for inclining roofs (s)	CC*	weir coefficient for all CSO structures ($m^{0.5}/s$)
I2	max. infiltration capacity flat, impervious areas (mm/h)		
I7	max. infiltration capacity inclining roofs (mm/h)		
CC17	weir coefficient for CSO structure at node 17($m^{0.5}/s$)		
CC108	weir coefficient for CSO structure at node 108 ($m^{0.5}/s$)		
CC200	weir coefficient for CSO structure at node 200 ($m^{0.5}/s$)		

A description of the model calibration for 'Loenen' can be found in Langeveld (2004). The removal of structural errors for this system consists of several incorrect invert levels and an incorrect weir height of the CSO structure. The estimated 24-hour pattern of dwf in 'Loenen' is described in Henckens *et al.* (2003).

During the measuring period (Aug. 28, 2001 - Dec. 26, 2001), 16 storm events were recorded that caused an overflow. However, only 13 have been used for model calibration because in 3 events precipitation consisted of snow leading to delayed runoff. In addition, 2 events have been added for calibration that caused water level to rise just below the weir (Langeveld 2004). Again, the impact of parameter uncertainty on overall results has been studied for 3 events: 18/07/01, 27/08/01 and 07/11/01 (see Appendix VII).

Table 4.17 Overview of storm events for 'Loenen'.

Storm event	Return period (y)	Rain depth (mm)	
18/07/01	0.10 - 0.20	13.9	CSO event
27/08/01	0.25 - 0.50	17.6	CSO event
07/11/01	0.05 - 0.10	13.1	CSO event, storm event comprising two separated precipitation periods and water level in receiving pond slightly above weir

Table 4.18 Parameter sets for calibration of hydrodynamic model of 'Loenen'.

FULL PARAMETER SET		REDUCED PARAMETER SET	
Parameter	**Description**	**Parameter**	**Description**
N1	dwf (m^3/h)	N1	dwf (m^3/h)
B2	initial losses on flat, impervious areas (mm)	B*	initial losses for all area types (mm)
B5	initial losses on flat, semi-pervious areas (mm)	F*	routing coefficient for all area types (s)
B7	initial losses on inclining roofs (mm)	I*	max. infiltration capacity for all area types (mm/h)
B8	initial losses on flat roofs (mm)	CC	weir coefficient for CSO structure ($m^{0.5}/s$)
F2	routing coefficient for flat, impervious areas (s)		
F5	routing coefficient for flat, semi-pervious areas (s)		
F7	routing coefficient for inclining roofs (s)		
F8	routing coefficient for flat roofs (s)		
I5	max. infiltration capacity semi-pervious areas (mm/h)		
CC	weir coefficient for CSO structure ($m^{0.5}/s$)		

The number of potential calibration parameters is even larger than for 'De Hoven' (hydraulic roughness of 367 conduits and 354 manholes, weir coefficient of 1 CSO structure, 12 storm runoff parameters for various surface types and dwf). By means of SVD (see Clemens 2001a), 11 parameters have been selected for calibration. This 'full' parameter set is presented in Table 4.18. As for 'De Hoven', this parameter set has been reduced to 5 parameters by clustering runoff parameters of all area types, while maintaining the fit between measurements and calculations. Once more, the remaining parameters are dwf, initial losses, routing coefficient, maximum infiltration capacity and weir coefficient. Finally, the sewer model has also been calibrated using the event of 27/08/01 and a reduced set of parameters, but without improving the database during calibration.

The actual optimisation of model parameters is based on the automatic calibration algorithm developed by Clemens (2001a). It successively applies a genetic algorithm and a combination of a Nelder-Mead and a Levenberg-Marquart algorithm. The genetic algorithm is based on maximum likelihood (ML) estimation and produces a rough estimate of optimal parameter values. It is followed by the combination of Nelder-Mead and Levenberg-Marquart algorithms for more accurate parameter estimation. The calibration results in a set of correlated model parameters. For example, a negative correlation between two parameters indicates that one parameter should be decreased, when the other is increased in order to maintain the fit between measurements and

model results. More details on the optimisation procedure are presented in Boomgaard *et al.* (2002) and Clemens (2001c).

In order to assess the quality of calibration results several measures have been applied. The residuals have been analysed with respect to the following aspects:

- **Empirical distribution function.** Comparison of the empirical cumulative probability distribution of residuals with a normal distribution indicates whether systematic errors are present. Large discrepancies are an indication of systematic errors. Applying ML estimation assumes normally distributed prior errors, which requires posterior checking.
- **Mean squared error (MSE).** The calibration procedure aims at minimising the mean squared error of measurements and model results. Therefore, the remaining MSE is checked afterwards. It is defined as,

$$\mathrm{MSE} = \frac{1}{n}\sum_{i=1}^{n} e(i)^2 \tag{4.7}$$

  where n is the number of time steps considered and $e(i)$ is the difference between a water level measurement at time i and its corresponding model result.
- **Bias and relative bias.** Bias errors are noticed as variations in model results when it has been fitted to data collected during different conditions (e.g. operating points or input characteristics). As a result, different aspects of the properties of the system are revealed. However, the model is fitted to the dominating system properties (Ljung and Glad 1994). Bias indicates systematic errors and is defined as (Clemens 2001a),

$$\mathrm{bias}\,(k) = \left(\frac{1}{n_w}\sum_{i=1}^{n_w} e(i)^2\right) - \sigma_w(k)^2 \tag{4.8}$$

  where n_w is the number of time steps within the shifting time window w, $e(i)$ is the difference between measurement and model result at time i and $\sigma_w(k)$ is the standard deviation of differences between measurements and model results for the k^{th} time window. Similar definitions can be found in e.g. Maidment (1993).
  Relative bias is the ratio between bias and variance over a time window w,

$$\mathrm{rel.bias}\,(k) = \frac{\mathrm{bias}\,(k)}{\sigma_w(k)^2} \tag{4.9}$$

  According to Clemens (2001a), a relative bias smaller than 0.2 is acceptable and an indication of a reliable model. Large (relative) bias indicates that after calibration systematic errors remain at the specific location and time.

The calibration results of 'De Hoven and 'Loenen' are presented in Appendix VII and VIII, respectively. Regarding the sewer system of 'De Hoven', only resulting parameter values and statistical properties of residuals are summarised. Further details are given in Clemens (2001a).

The overall picture for 'De Hoven' is that both optimal parameterisation and calibrated parameter values differ between the storm events considered (see Table 4.19). In particular, the results of the genetic algorithm show that the calibration is relatively sensitive to changes in dwf and infiltration rates. Furthermore, during significant time periods the relative bias is larger than the acceptable level of 0.2, especially during dwf and when the pump is running. Variation, MSE and bias reach their highest values during the actual overflow event and the emptying of the sewer system.

Parameter reduction (from 10 to 5 parameters) results in a small increase of identifiability for the storm events of 25/08/98 and 24/10/98. Furthermore, the statistical properties of the full and the reduced parameter set of these events show no significant differences. For the event of 07/10/98, however, parameter reduction did not result in an increased identifiability. The event of 07/10/98 differs from the other events because prior to this event smaller rain events occurred causing a rise in groundwater level and different initial conditions regarding infiltration capacity and initial losses. The variance of the calibration parameters of this event is relatively large.

Table 4.19 Calibrated parameters of hydrodynamic model for 'De Hoven'.

FULL PARAMETER SET (Clemens 2001a)						
	Storm 25/08/98		**Storm 07/10/98**		**Storm 24/10/98**	
Parameter	Average	95% interval	Average	95% interval	Average	95% interval
N1 (m^3/h)	26.0	25.8 - 26.1	65.3	60.0 - 70.9	49.8	47.6 - 52.2
B2 (mm)	0.36	0.32 - 0.41	3.34	2.96 - 3.77	0.55	0.49 - 0.60
B7 (mm)	0.50	0.44 - 0.57	0.28	0.20 - 0.39	0.19	0.17 - 0.23
F2 (s)	347.9	316.2 - 382.7	742.6	604.0 - 913.0	878.5	842.8 - 915.6
F7 (s)	205.3	180.5 - 233.6	742.6	604.0 - 913.0	196.5	169.2 - 227.9
I2 (mm/h)	0.19	0.17 - 0.20	0.13	0.10 - 0.18	0.23	0.21 - 0.25
I7 (mm/h)	0.31	0.29 - 0.34	0.10	0.07 - 0.14	0.07	0.06 - 0.08
CC17 ($m^{1/2}/s$)	2.16	1.94 - 2.40	-	-	1.14	0.78 - 1.77
CC108 ($m^{1/2}/s$)	0.38	0.35 - 0.41	-	-	1.17	0.74 - 1.76
CC200 ($m^{1/2}/s$)	1.75	1.58 - 1.94	-	-	1.06	0.76 - 1.48

REDUCED PARAMETER SET (Clemens 2001a)						
	Storm 25/08/98		**Storm 07/10/98**		**Storm 24/10/98**	
Parameter	Average	95% interval	Average	95% interval	Average	95% interval
N1 (m^3/h)	26.2	26.0 - 26.3	-	-	52.0	50.6 - 53.3
B* (mm)	0.49	0.47 - 0.51	-	-	0.45	0.42 - 0.48
F* (s)	277.0	261.2 - 292.9	-	-	669.6	645.8 - 693.4
I* (mm/h)	0.23	0.22 - 0.23	-	-	0.18	0.18 - 0.19
CC* ($m^{1/2}/s$)	1.04	1.00 - 1.07	-	-	1.28	1.14 - 1.43

In general, the calibrations for 'Loenen' result in different optimal parameter values for both full and reduced parameter sets (Table 4.20). For the storm event of 18/07/01 an increase of the relative bias is observed during the actual spilling and the emptying of the system. In addition, the relative bias is larger for the reduced set during the overflow than for the full set. The identifiability of parameters, however, does not increase due to the parameter reduction, since the relative bias of the reduced set is larger in the runoff phase. The overall MSE is larger and the distribution of residuals is significantly different from normal (more relatively large errors).

The results of 27/08/01 resemble the previous event. However, the calibration of the same event without improving the database produces residuals with many systematic errors. Therefore, the results of this calibration should be distrusted.

Finally, the calibration for the event of 07/11/01 differs from the other events, since the variance, relative bias and MSE decrease as a result of parameter reduction. However, there are still systematic errors present after calibration. The increased identifiability may result from the storm event comprising two relatively separate precipitation periods. In particular, the first half of the event is described better using a limited number of parameters. The water level in the receiving pond sometimes exceeds the weir level, which results in a flow from the pond to the sewer system. The model, however, assumes that the flow across the weir is only one-way (from sewer to receiving pond) and, therefore, can be described with a single weir coefficient. This affects the calibration results and is observed as an increase of (relative) bias.

Table 4.20 Calibrated parameters of hydrodynamic model for 'Loenen'.

FULL PARAMETER SET						
	Storm 18/07/01		**Storm 27/08/01**		**Storm 07/11/01**	
Parameter	Average	95% interval	Average	95% interval	Average	95% interval
N1 (m^3/h)	98.6	-	47.30	-	82.6	-
B2 (mm)	5.10	-	1.48	-	1.77	-
B5 (mm)	0.40	-	1.48	-	3.54	-
B7 (mm)	0.72	-	0.21	-	0.29	-
B8 (mm)	1.85	-	4.85	-	3.50	-
F2 (s)	289.0	-	228.2	-	846.0	-
F5 (s)	704.6	-	228.2	-	440.0	-
F7 (s)	44.4	-	85.5	-	836.0	-
F8 (s)	946.6	-	244.7	-	447.8	-
I5 (mm/h)	3.10	-	6.57	-	0.43	-
CC ($m^{1/2}/s$)	0.67	-	0.72	-	0.76	-

REDUCED PARAMETER SET						
	Storm 18/07/01		**Storm 27/08/01**		**Storm 07/11/01**	
Parameter	Average	95% interval	Average	95% interval	Average	95% interval
N1 (m^3/h)	104.4	104.3 - 104.5	66.4	66.3 - 66.5	59.9	79.4 - 79.7
B* (mm)	2.10	2.09 - 2.10	1.91	1.90 - 1.91	0.85	0.85 - 0.86
F* (s)	88.7	88.4 - 89.0	540.4	534.7 - 546.2	303.0	300.9 - 305.2
I* (mm/h)	0.44	0.42 - 0.45	0.46	0.45 - 0.46	0.35	0.35 - 0.35
CC* ($m^{1/2}/s$)	0.82	0.80 - 0.84	0.99	0.97 - 1.01	0.79	0.78 - 0.79

As previously mentioned, the optimal parameter values of both sewer systems differ for each calibration event. As a result, a sewer model calibrated with one event describes the runoff process differently compared to the same model calibrated with another event. This is caused by processes influencing sewer flow with a longer characteristic time scale than the duration of a storm event (e.g. infiltration/inflow and soil infiltration). These processes are not included in the sewer model but largely determine the initial conditions of each calibration. As a result, the portability of calibrated model parameters based on storm events is limited (see also Campbell *et al.* 1999 and Lei *et al.* 1999).

Processes with characteristic time longer than the duration of a storm event influencing sewer flow in 'De Hoven' comprise:

- the different initial condition of contributing areas for the storm events (including available storage on streets and infiltration capacity of soil),
- the possible deposition of sediments in the system,
- the increased infiltration/inflow rate due to high groundwater levels (correlation with water level of the river IJssel).

For 'Loenen' these processes include:

- the different initial condition of contributing areas for the storm events (including available storage on streets and infiltration capacity of soil),
- the interference with the water level in receiving the pond (possibly due to obstruction of pond outlet),
- the intermittent and time-varying industrial discharges,
- the possible delayed runoff from several pervious surfaces,
- the leakage of sewage to the groundwater during summer (due to low groundwater levels).

4.4.2 Impacts of resulting parameter uncertainty

The impact of calibration parameter uncertainty on calculated CSO volumes has been estimated using Monte Carlo simulation. For calculation a random value of the parameters of the reduced set ($N1$, B^*, I^*, F^* and CC^*) has been drawn from its probability distribution. These parameters are normally distributed with known mean and standard deviation (see Table 4.19 and Table 4.20). The random samples have been substituted in the hydrodynamic calculations.

Since calibrated model parameters are correlated, a dependent sampling technique is needed. Therefore, a simulation scheme based on a multivariate normal distribution, Cholesky decomposition (see e.g. Carlin and Lewis 2000), has been applied. It enables random parameter drawing from a distribution function accounting for covariances (for further details see Appendix IX). The correlations of the calibration parameters for 'De Hoven' and 'Loenen' are presented in Appendix VII and VIII, respectively.

Reliable results require a minimum number of calculations per Monte Carlo simulation. This number has been estimated on the basis of two test statistics: expected value and

variation of calculated yearly CSO volumes as a function of the number of calculations. When the statistics become almost constant, the number of runs is sufficient. For both 'De Hoven' and 'Loenen' at least 150 runs per simulation are required. Because of the restricted amount of available calculation time, for 'De Hoven' 250 runs have been performed and for 'Loenen' 180 runs.

The input of the sewer models comprises both rainfall and dwf. The first 10 years of the well-known rainfall series of KNMI (1955-1979, De Bilt, The Netherlands) have been applied. However, repeated hydrodynamic calculations using a 10-year series (resolution = 15 min) are computationally demanding. Therefore, the time series has been filtered prior to performing the Monte Carlo simulations. The filter consists of a reservoir with storage and pumping capacity smaller than the 'real' values (Table 4.21 and Table 4.22). The filter discards storm events not causing an overflow. However, a significant decrease of total CSO volume due to the filtering is not allowed. The filters applied considerably reduce the original rainfall series to 8.5% and 15.1% of its length, respectively (Table 4.21 and Table 4.22). The 24-hour dwf pattern of 'De Hoven' is described in Clemens (2001a), the modelled dwf of 'Loenen' in Henckens *et al.* (2003).

Table 4.21 Characteristics of rainfall filter for sewer system of 'De Hoven'.

	sewer system	filter
storage volume	6.81 mm	5.50 mm
pumping capacity minus dwf	0.73 mm/h	0.50 mm/h
length of original rainfall series ('De Bilt', 1955-1964)	3653 d	100 %
length of filtered rainfall series	312 d	8.5 %

Table 4.22 Characteristics of rainfall filter for sewer system of 'Loenen'.

	sewer system	filter
storage volume	3.85 mm	3.80 mm
pumping capacity minus dwf	0.56 mm/h	0.30 mm/h
length of original rainfall series ('De Bilt', 1955-1964)	3653 d	100 %
length of filtered rainfall series	552 d	15.1 %

The analysis of CSO volumes from the hydrodynamic model is similar to § 4.3.1. The volumes have been summed over the storm events in order to ensure independence of CSOs. Subsequently, Bayes weights (§ 3.5.2) have been applied to choose between candidate distribution types for CSO volumes per event. To express a lack of prior knowledge Jeffreys priors have been used. The marginal densities have been approximated using a Laplace expansion. As for the reservoir model, Bayes weight assessment has shown that a Weibull distribution fits best with the calculated CSO volumes. This has also been concluded from classical goodness-of-fit tests (Chi-square and Kolmogorov-Smirnov). Finally, given the calculated volumes of each Monte Carlo

run, the shape and scale parameters of the Weibull distributions (see Appendix IV) have been estimated using Maximum Likelihood methods (§ 3.5.1).

The results for 'De Hoven' are summarised in Table 4.23 and Table 4.24. Both CSO volumes as a function of the return period and yearly averages are presented for the calibrations of 25/08/98, 07/10/98 and 24/10/98. Furthermore, the yearly average CSO volumes of the reduced parameter set are compared with the full parameter set.

Table 4.23 demonstrates that the return periods of calculated CSO volumes vary between models based on different events. The results of 25/08/98 and 24/10/98 are based on calibrations with a reduced parameter set, whereas those of 07/10/98 represent a calibration with a full set (see § 4.4.1). The average CSO volumes per return period for the calibrated models based on 07/10/98 and 24/10/98 show similarities. The 95% uncertainty interval, however, is considerably larger for the event of 07/10/98. This interval is based on the 0.025 and 0.975 quantiles of the 250 Monte Carlo runs. The results of 25/08/98 differ from the other calibrations. The average values per return period are smaller and, even more important, the 95% uncertainty interval is quite narrow. This demonstrates the high quality of this calibration (see Clemens 2001).

Table 4.23 Statistics of calculated CSO volumes for 'De Hoven' using hydrodynamic model calibrated with different storm events.

	Return period (y)	Average CSO volume (mm)	95% interval (mm)
Storm event 25/08/98	0.25	3.00	2.96 - 3.03
	0.5	6.79	6.75 - 6.81
	1.0	11.11	11.08 - 11.14
	2.0	15.83	15.73 - 15.90
	3.0	18.73	18.60 - 18.85
	5.0	22.54	22.35 - 22.71
Storm event 07/10/98	0.25	3.79	3.28 - 4.27
	0.5	7.78	7.39 - 8.21
	1.0	12.21	11.95 - 12.59
	2.0	16.95	16.58 - 17.51
	3.0	19.86	19.28 - 20.66
	5.0	23.63	22.75 - 24.80
Storm event 24/10/98	0.25	3.76	3.62 - 3.91
	0.5	7.74	7.70 - 7.80
	1.0	12.20	11.97 - 12.45
	2.0	17.03	16.39 - 17.66
	3.0	19.99	19.06 - 20.90
	5.0	23.86	22.52 - 25.18

From Table 4.24 it can be concluded that yearly average CSO volumes vary considerably between the calibrated models. It shows that the variation between the different models is even larger than the variation due to remaining parameter uncertainty of one calibrated model. This can be explained from the transition of model structure uncertainty to the parameters during calibration. As a result, portability of calibrated parameters is rather limited. However, the difference in yearly average volumes resulting from calibrations with the full and reduced parameter sets is relatively small. This demonstrates that identifiability is increased due to parameter reduction.

Comparison of Table 4.24 and Table 4.8 demonstrates that the overall variation of CSO volumes calculated with the calibrated models is slightly smaller than the variation due to dimension uncertainty in the reservoir model. However, the variation due to remaining parameter uncertainty of the hydrodynamic model is completely enclosed by the variation due to dimension uncertainty of the reservoir model. Therefore, a reservoir model provides a reasonable approximation of yearly CSO volumes for flat catchments such as 'De Hoven' compared to a hydrodynamic model calibrated with a single storm event.

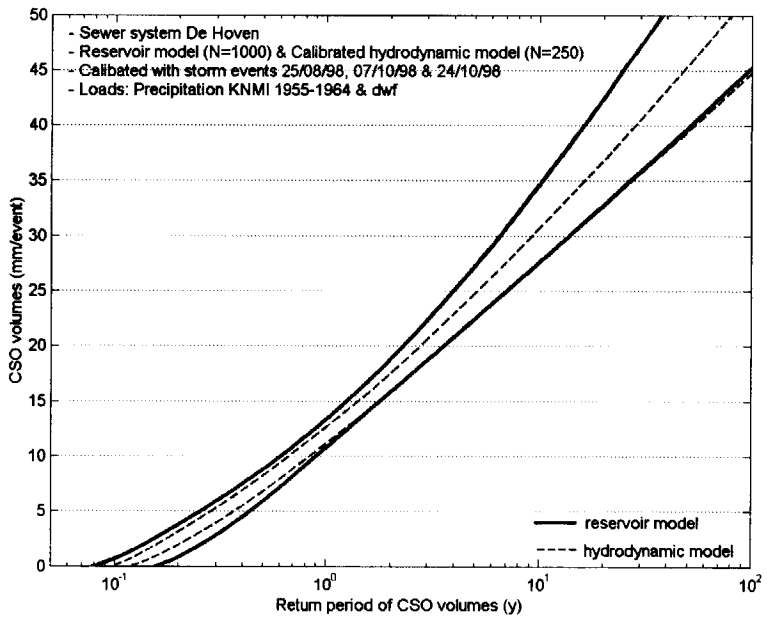

Figure 4.13 Comparison of 95% uncertainty intervals of calculated CSO volumes for reservoir model and calibrated hydrodynamic model of 'De Hoven'. The variation due to dimension uncertainty of the reservoir model encloses the variation due to parameter uncertainty of the hydrodynamic model.

Table 4.24 Comparison of yearly average CSO volumes for 'De Hoven' (full and reduced parameter sets of different storm events).

	Full parameter set		Reduced parameter set	
Storm event	Average	95% interval	Average	95% interval
25/08/98	41.2	-	41.5	41.4 - 41.6
07/10/98	48.4	45.2 - 52.7	-	-
24/10/98	49.0	-	48.1	47.9 - 48.3

With respect to 'Loenen' the results are different. Primarily, because of the mildly sloping character of the catchment, the more complicated runoff characteristics of the contributing areas and the interference of the receiving pond with the sewer system. Table 4.25 shows that the calibration based on the 18/07/01 event resembles the calibration of 27/08/01 regarding average CSO volumes per return period and variations. The calibration of 07/11/01 is different for two reasons: (1) the division of the storm event in two separate periods with increased rainfall intensities (see Appendix VIII) and (2) the water level in the receiving pond rising above weir level causing a flow from the pond to the sewer system. In particular, the average CSO volumes per return period are larger.

Table 4.25 Statistics of calculated CSO volumes for 'Loenen' using hydrodynamic model calibrated with different storm events.

	Return period (y)	Average CSO volume (mm)	95% interval (mm)
Storm event 18/07/01	0.25	5.63	5.51 - 5.71
	0.5	8.98	8.91 - 9.05
	1.0	12.46	12.44 - 12.48
	2.0	16.03	15.98 - 16.17
	3.0	18.16	18.06 - 18.37
	5.0	20.88	20.71 - 21.20
Storm event 27/08/01	0.25	5.18	5.12 - 5.22
	0.5	8.51	8.49 - 8.54
	1.0	12.02	12.00 - 12.10
	2.0	15.68	15.60 - 15.86
	3.0	17.87	17.75 - 18.12
	5.0	20.68	20.50 - 21.03
Storm event 07/11/01	0.25	6.71	6.71 - 6.71
	0.5	10.08	10.07 - 10.10
	1.0	13.61	13.59 - 13.66
	2.0	17.25	17.22 - 17.35
	3.0	19.43	19.39 - 19.56
	5.0	22.22	22.17 - 22.39

Furthermore, yearly average CSO volumes of the 'Loenen' system differ considerably:

- between the calibrations based on different storm events (Table 4.26) due to different initial conditions regarding groundwater level, availability of surface storage, etc,
- between the full and reduced parameter set of a calibration based on one storm event (Table 4.26) indicating an excessive reduction on the number of parameters,
- between the calibrated hydrodynamic models (Table 4.26) and the reservoir model describing the same sewer system (Table 4.9).

The CSO volumes predicted with the reservoir model are almost twice as large as the volumes resulting from the calibrated hydrodynamic models. Figure 4.14 illustrates this large overestimation of CSO volumes by the reservoir model, since for all return periods the 95% uncertainty interval of CSO volumes from the reservoir model is situated above the interval of the hydrodynamic model. Therefore, a reservoir model is not suitable for prediction of CSO volumes in (mildly) sloping catchments.

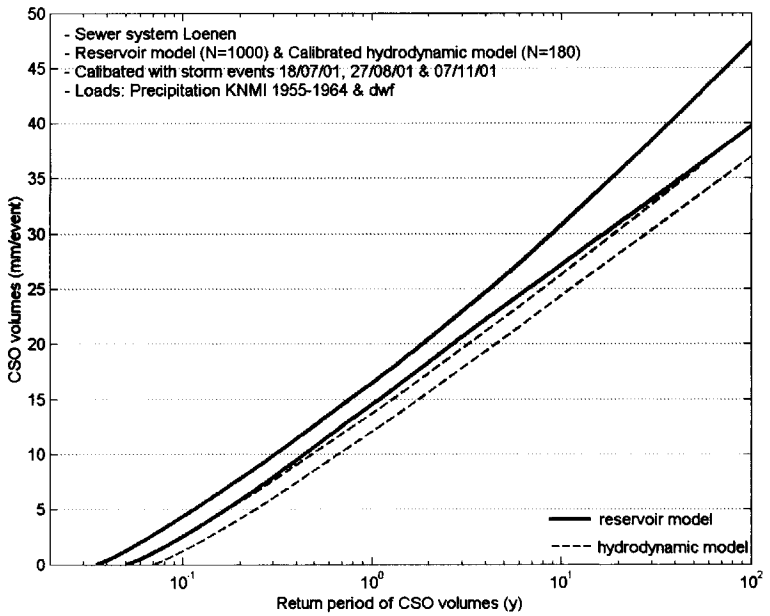

Figure 4.14 Comparison of 95% uncertainty intervals of calculated CSO volumes for reservoir model and calibrated hydrodynamic model of 'Loenen'. Within the range of return periods considered, CSO volumes predicted with the reservoir model are considerably larger than with the hydrodynamic model.

Table 4.26 Comparison of yearly average CSO volumes for 'Loenen' calculated with full and reduced parameter sets of different storm events.

	Full parameter set		Reduced parameter set	
Storm event	Average	95% interval	Average	95% interval
18/07/01	41.3	-	65.6	64.7 - 66.4
27/08/01	30.3	-	60.6	60.2 - 60.9
07/11/01	56.0	-	84.2	84.1 - 84.3

4.4.3 Conclusions and discussion

The uncertainty analysis shows that calibration does not result in more reliable model predictions. However, it does enable the detection and removal of systematic errors. The variation of return periods of calculated CSO volumes decreases due to calibration but the portability of model parameters based on single storm events is rather limited. The question remains whether the rainfall event applied for calibration is representative of a longer time series (regarding initial and boundary conditions). Furthermore, errors in calculated flows (finally resulting in CSOs) are amplified by the model because the calculation scheme of the hydrodynamic software (Hydroworks®) is not mass conservative (see Clemens 2001a).

The limited portability of parameters results from processes with a longer characteristic time scale than the duration of one storm event (infiltration/inflow, infiltration capacity of soil, time-varying industrial discharges, interference with receiving waters, etc) which determine the return period of CSO volumes. Portability can be improved by calibrating the model with multiple instead of single events. Alternatively, Bayesian calibration (see e.g. Campbell *et al.* 1999 and Kennedy and O'Hagan 2001) can be applied. This enables calibration accounting for expert knowledge of expected values of model parameters.

However, the rainfall runoff model applied can only describe the determinative processes correctly for individual storm events. It is unable to model these processes sufficiently for a series of events (see also Van de Ven 1989). A data driven approach, such as neural networks, may solve this problem, since it circumvents the difficulties of strict physical modelling. However, a disadvantage is that neural networks require a considerable amount of training data and their ability of extrapolation is rather limited.

Variation due to differences in calibrated parameter sets dominates variation due to uncertainty of individual parameters based on single storm events. The extent of this variation is comparable to the variation due to uncertainty of system dimension in reservoir model. However, for (mildly) sloping catchments such as 'Loenen' a reservoir model overestimates CSO volumes because 'dynamic' storage is not taken into account. Consequently, an approach that models a sewer system by means of a series of reservoirs consisting of separate reservoirs accounting for 'static' and 'dynamic' storage of the sewer system may be applied (Vaes 1999). 'Static' storage is defined as the in-sewer storage below the crest level of the lowest CSO structure, whereas 'dynamic' storage is the available storage volume above this level.

By reducing the number of calibration parameters their identifiability can be increased. With respect to 'De Hoven', identifiability increases due to parameter reduction. For 'Loenen', however, only the event of 07/11/01 gives evidence of improved identifiability. In addition, yearly CSO volumes of the full parameter sets are very different from the reduced sets. Therefore, the reduction from 11 to 5 parameters is considered too radical.

4.5 COST FUNCTION

Additional in-sewer storage required to comply with environmental standards (CSO reduction) can be determined by means of risk based economic optimisation (see § 3.3). This implies calculation of the optimal storage volume by a minimisation of total costs comprising initial investment for construction and losses including environmental damage due to CSOs. However, the latter can be highly uncertain because the extent to which receiving waters are affected by CSOs is not fully understood and sufficient cost data are unavailable. In addition, it is impossible to express all damages in monetary terms.

The impact of uncertainties in the cost function on optimal in-sewer storage has been studied for the sewer system of 'De Hoven'. Losses have been described with different types of cost functions containing uncertain parameters. In addition, the impact of uncertain system dimensions and natural variability in rainfall has been taken into account.

4.5.1 Risk-based economic optimisation of in-sewer storage

The storage volume to be built has been economically optimised by minimising total costs TC which consist of construction costs and losses due to (environmental) damage,

$$E(TC) = I + D \tag{4.10}$$

where I is the initial investment for construction and D is the monetary value of damage to receiving watercourse caused by CSOs. The construction costs are proportional to the storage volume to be built. The cost of building an additional m^3 diminishes with increasing storage volumes,

$$I = I_0 v^{0.75} \tag{4.11}$$

where I_0 is marginal costs of building additional storage volume and v is storage volume to be built. A failure is defined as the occurrence of a CSO irrespective of its volume.

The expected costs of failure per year have been discounted over an unbounded time horizon,

$$D = \frac{D_j(v)}{T_{CSO}}\left(\alpha + \alpha^2 + \alpha^3 + \ldots\right) = \frac{D_j(v)}{T_{CSO}}\left(\frac{\alpha}{1-\alpha}\right) \tag{4.12}$$

$$\alpha = \frac{1}{\left(1 + \frac{r}{100}\right)} \tag{4.13}$$

where $D_j(v)$ is the cost (Euro) resulting from an overflow event described with cost function j (cost functions described in next paragraph), T_{CSO} is the average return period of overflow events (y), α is the discount factor (-) and r is the discount rate. If the discount rate is increased, the present value of damage reduces and, therefore, more future damage is accepted. The time horizon is considered unbounded because the expected service life of sewers is 60-80 years in The Netherlands. With a discount rate of 4%, the additional discounted damage is reduced to 0.04 times the actual monetary value. Therefore, the expected discounted costs over an unbounded horizon of 60-80 years can be very well approximated by the expected discounted costs over an unbounded horizon.

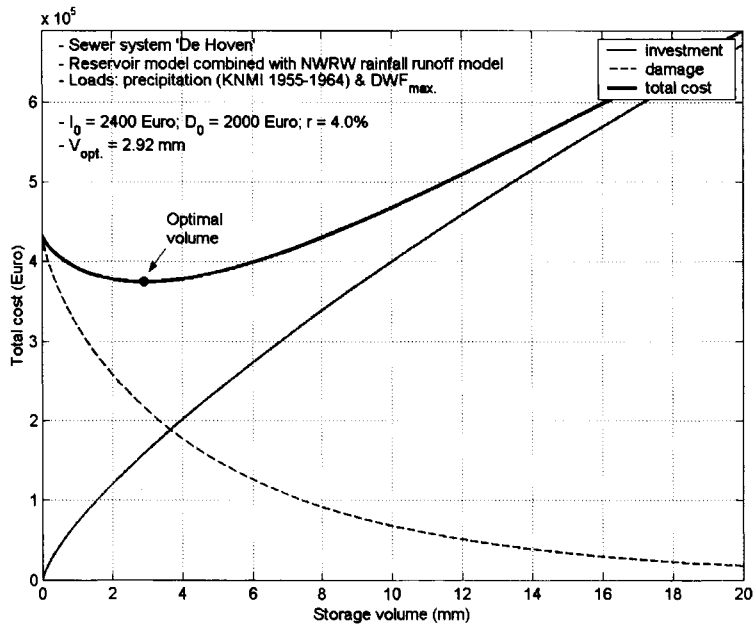

Figure 4.15 Illustration of estimation of economically optimal storage volume accounting for failure probability of sewer system. Costs of failure have been described with a step function (see § 4.5.2).

The natural variability of a CSO volume per storm event $\mathbf{v} = (v_1,\ldots,v_n)$ has been described with a Weibull survival function with parameters a and b,

$$P_f(v) = \exp\left\{-\left(\frac{v}{b}\right)^a\right\} \tag{4.14}$$

where $P_f(v)$ is the probability of failure of a sewer system above a certain CSO volume v. By minimising total costs, the expected value of optimal storage has been determined (see Figure 4.15).

4.5.2 Types of cost functions describing environmental damage

Three types of cost functions have been considered to model environmental damage due to overflows: one discrete and two continuous cost functions (see Figure 4.16). The continuous functions are proportional to the CSO volume and either Weibull-shaped or linear. Damage cost as a function of storage volume ($\tilde{v}$) is described as (see Appendix X for derivations):

1. Discrete cost function (Figure 4.16, top left),

$$E\{D_1(\tilde{v},V)\} = D_0 P_f(\tilde{v}) \tag{4.15}$$

where $\tilde{v}$ is the storage volume to be built, V is an actual overflow volume, which is a random quantity, and the probability of failure $P_f(\tilde{v})$ is defined as,

$$\Pr(V > \tilde{v}) = P_f(\tilde{v}) = \exp\left(-\left(\frac{\tilde{v}}{b}\right)^a\right)$$

2. Weibull-shaped cost function (Figure 4.16, bottom left),

$$E\{D_2(\tilde{v},V)\} = D_0 P_f(\tilde{v}) E\left\{1 - \exp\left(-\left(\frac{V-\tilde{v}}{b_1}\right)^{a_1}\right)\right\} \tag{4.16}$$

where $\tilde{v}$ is storage volume to be built, V has a Weibull distribution with scale parameter b and shape parameter a, a_1 and b_1 are parameters on which the shifted Weibull-shaped cost function is dependent. Eq. (4.16) can be numerically solved by Monte Carlo integration. Parameters a_1 and b_1 differ from a and b of the Weibull distribution describing inherent uncertainty of CSO volumes. If v_L is the CSO volume at which the damage cost becomes almost constant (i.e. almost equal to D_0), v_M is a specific part of this volume ($v_M = v_L/\gamma$, where $\gamma>1$) and $p(v_M)$ and $p(v_L)$ ($p(v_L) > p(v_M)$) are known, then a_1 and b_1 can be calculated from,

$$a_1 = \frac{1}{\log(\gamma)}\log\left(\frac{\log(1-p(v_L))}{\log(1-p(v_M))}\right)$$

$$b_1 = \frac{v_M}{\left(-\log(1-p(v_M))\right)^{1/a_1}}$$

For example, if $p(v_M) = 0.5$, $p(v_1) = 0.99$, $v_M = 5.0$ mm and $\gamma = 2.0$, then $a_1 = 2.732$ and $b_1 = 0.875$.

3. Linear cost function (Figure 4.16, bottom right),

$$E\{D_3(\tilde{v},V)\} = \frac{D_0}{v_S}\left\{P_f(\tilde{v})\left(b\exp\left(\left(\frac{\tilde{v}}{b}\right)^a\right)\Gamma\left(\frac{1}{a}+1,\left(\frac{\tilde{v}}{b}\right)^a\right)-\tilde{v}\right)\right.$$
$$\left.-P_f(\tilde{v}+v_S)\left(b\exp\left(\left(\frac{\tilde{v}+v_S}{b}\right)^a\right)\Gamma\left(\frac{1}{a}+1,\left(\frac{\tilde{v}+v_S}{b}\right)^a\right)-(\tilde{v}+v_S)\right)\right\} \quad (4.17)$$

where V is actual overflow volume, which is a random quantity, $\tilde{v}$ is storage volume to be built, v_S is CSO volume at which the environmental damage reaches its maximum (D_0) and $\Gamma(a,x)$ is incomplete gamma function for $x \geq 0$ and $a > 0$ defined as,

$$\Gamma(a,x) = \int_{t=x}^{\infty} t^{a-1}\exp(-t)dt \quad (4.18)$$

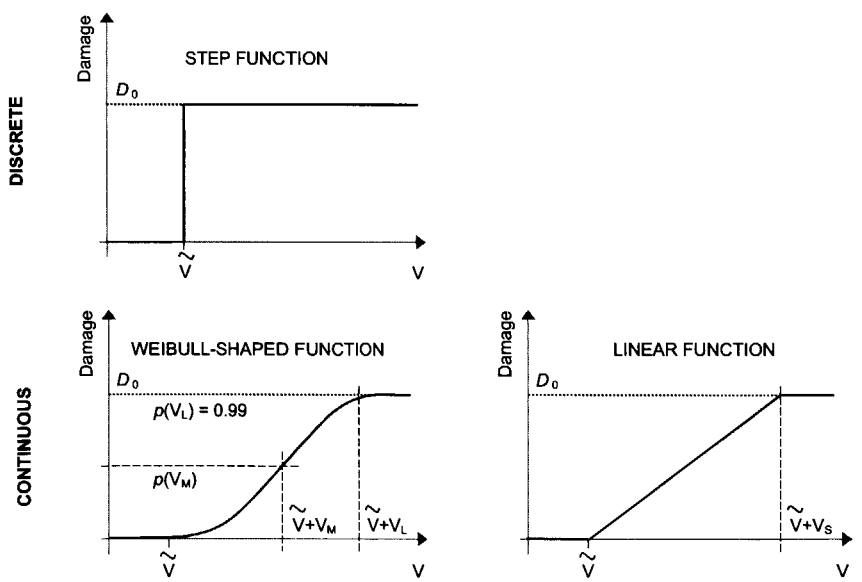

Figure 4.16 Cost functions describing environmental damage due to CSOs, where *v* is an actual overflow volume, which is a random quantity, and $\tilde{v}$ is the storage volume to be built. Both discrete and continuous types have been considered.

4.5.3 Impacts of uncertainties in parameters of cost function

The relative impact of uncertainties in the cost function on optimal in-sewer storage has been studied by means of uncertainty analysis. Storage capacity has been optimised accounting for uncertainty of investment cost, damage cost and interest rate. It is illustrated with the sewer system of 'De Hoven'.

Regarding damage cost, uncertainty of both type and parameters of the cost function has been studied. The uncertain parameters in the cost function are assumed normally distributed with known μ and σ (see Table 4.27). For a given set of calculated CSO volumes a value of all cost parameters has been randomly drawn from these distribution functions. Parameter values have been drawn from left-truncated normal distribution, which slightly shifts their expected values. The optimal storage volume has been estimated by minimising the average total cost function of 500 Monte Carlo runs. Minimisation of the average function leads to a more robust solution.

Uncertainty related to the cost function has been examined in combination with:

- the impact of uncertain sewer system dimensions,
- the impact of natural variability of rainfall.

These impacts have been estimated using Monte Carlo simulation as described in § 4.3.1. The model of the sewer system is a combination of a rainfall runoff model and a reservoir model (see Figure 4.3). The characteristics of sewer system 'De Hoven' and the uncertainty of system dimensions are summarised in Table 4.1 and Table 4.5 respectively. Modelling of natural variability in rainfall is described in § 4.3.2.

Table 4.28 and Figure 4.17 presents the results of the uncertainty analysis in terms of expected values of optimal storage volumes and 95% uncertainty intervals based on the 0.025 and 0.975 quantiles of the calculated values. For each type of cost function two situations are presented: fixed and uncertain cost parameters. In the case of fixed cost parameters, the variation of optimal volumes results completely from either uncertain sewer dimensions or rainfall variability.

Table 4.27 Uncertainty of parameters of cost functions describing damage. Parameters are assumed normally distributed with known μ and σ.

Cost function	Step		Weibull-shaped		Linear	
Parameter	Mean	Std.	Mean	Std.	Mean	Std.
I_0 (Euro)	2000	250	2000	250	2000	250
β (-)	0.75	0.05	0.75	0.05	0.75	0.05
r (%)	4.0	0.50	4.0	0.50	4.0	0.50
D_0 (Euro)	3150	1000	8350	2750	7350	2400
v_S (mm)	-	-	-	-	10.0	3.0
γ (-)	-	-	2.0	0.75	-	-
v_M (mm)	-	-	5.0	2.0	-	-

Generally, the expected value and variation of optimal in-sewer storage increases due to uncertain cost parameters. The expected value is 1 to 1.5 times larger and the variation 1.5 to 3.5 times larger. In the case of a step function, there is almost no change of expected volume due to the introduction of uncertain cost parameters.

The expected value of optimal storage accounting for natural variability in rainfall is lower than for dimension uncertainty because the total volumes of frequent storm events with longer duration are underestimated by the rainfall generator (see § 4.3.2) compared to the rain series of 'De Bilt' (1955-1979).

Table 4.28 Expected value of optimal volume (in mm) using three types of cost functions with either fixed or uncertain cost parameters.

		Fixed cost parameters		Uncertain cost parameters	
Cost function		**$E(V_{opt.})$**	**95% interval**	**$E(V_{opt.})$**	**95% interval**
Step	dimension uncertainty	5.5	3.6 - 7.2	5.6	0.1 - 9.3
	rainfall variability	2.5	0 - 4.5	2.6	0 - 7.3
Weibull-shaped	dimension uncertainty	6.2	4.3 - 7.8	6.9	0 - 12.5
	rainfall variability	2.8	0 - 6.8	4.0	0 - 12.0
Linear	dimension uncertainty	5.5	3.9 - 7.6	6.3	0 - 11.9
	rainfall variability	2.5	0 - 6.1	3.5	0 - 11.1

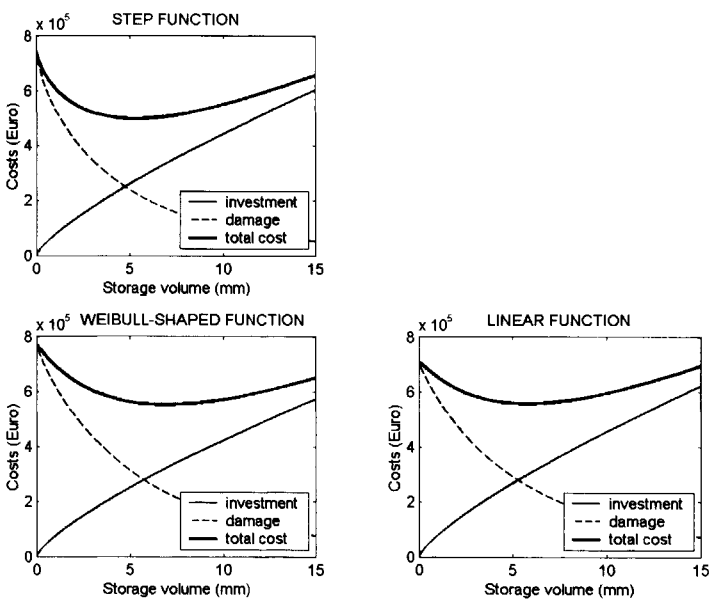

Figure 4.17 Estimation of economically optimal storage volume by minimising total costs. Both failure probability of the sewer system and uncertainty of the cost function have been taken into account. Costs of failure have been described with a step function a Weibull-shaped function and a linear function.

The results for the linear and Weibull-shaped cost function show similarities. The total cost function is flatter around the optimum compared to the step function. Moreover, total costs at the optimum volume are higher. Both aspects are an indication of a more robust solution.

An advantage of the linear function is that it can be analytically solved as opposed to the Weibull-shaped version. The linear function is also easier to assess. Therefore, a linear approximation of the Weibull-shaped function is preferred, since it reduces calculation time while maintaining accuracy.

Determining damage cost can be very subjective. It is even doubted whether it is possible to capitalise environmental damage (see § 2.6.3).

However, the willingness-to-pay per m^3 CSO volume can be estimated by assuming that current standards lead to an economically optimal solution. According to current standards, the 'Basisinspanning' (CIW 2001), a combined sewer system should emit a pollution load less than or equal to that from a theoretical sewer system with 7 mm in-sewer storage, 2 mm additional storage in a settling facility and a pumping capacity equal to 0.7 mm/h plus the dry weather flow. Current in-sewer storage 'De Hoven' yields 6.81 mm (Table 4.1). Consequently, an additional storage of $\tilde{v}$ = 2.2 mm is required to comply with current standards.

By applying a linear cost function with a maximum at v_s, the cost of environmental damage resulting from CSO volumes can be described (Figure 4.18). Subsequently, the willingness-to-pay is determined by adjusting the value of the volume v_s at which the maximum is reached such that the optimal storage ($\tilde{v}$) equals approximately 2.2 mm.

The results demonstrate that damage costs D_v per m^3 CSO volume diminish when the maximum damage D_0 increases (Table 4.29). On average the costs of 1 m^3 CSO volume equal 4.1 Euros. High values of D_v result from a steeper cost function and belong to receiving watercourses with a more sensitive habitat. For very sensitive watercourses the linear cost function approaches the step function. Low values of D_v indicate resilience of a watercourse.

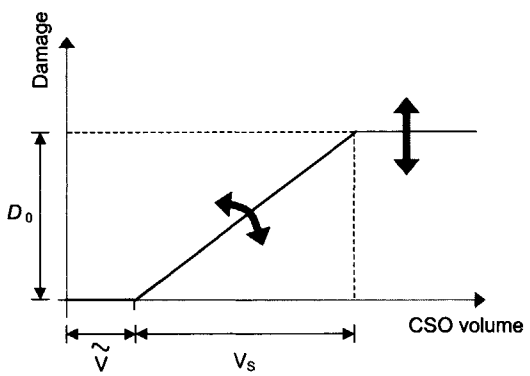

Figure 4.18 Variation of parameters in linear cost function.

Table 4.29 Expected costs per m^3 for sewer system 'De Hoven' based on linear cost function accounting for uncertain cost parameters, where D_0 is expected value of maximum damage cost, and D_v is expected value of cost per m^3 CSO volume.

D_0 (Euro)	D_v (Euro/m^3)
2500	7.58
3000	4.93
3500	4.24
4000	3.80
4500	3.55
5000	3.34
5500	3.28
6000	3.26
6500	3.26

The cost per m^3 CSO volume exceeds the treatment cost per m^3 wastewater in The Netherlands. The costs of treated effluent are approximately 33 Euro per population equivalent (p.e.) per year (Van Nieuwenhuijzen 2001). Converted to m^3 (1 p.e. ≈ 260 l/d incl. rainfall runoff and infiltration/inflow) this gives 0.35 Euros/m^3 of treated effluent, which is on average 12 times smaller than the cost per m^3 CSO volume. When considering costs per kg COD instead, the ratio between CSOs and effluent decreases to 2.5:1 (CSO ≈ 250 mg COD/l (CIW 2001) and effluent ≈ 50 mg COD/l (Van Nieuwenhuijzen 2001)).

4.5.4 Conclusions and discussion

Economic optimisation has been applied to determine the in-sewer storage required. However, the parameters of the cost function describing environmental damage can be highly uncertain. Therefore, an uncertainty analysis of the cost function has been performed. Environmental losses have been described with three types of cost functions: step, Weibull-shaped and linear. Moreover, uncertainty of the parameters of these cost functions has been considered.

In general, the introduction of uncertainty in cost parameters causes an increase of expected value and variation of the optimal storage volume. However, in case of a step function the change in expected volume is almost negligible.

In addition, economic optimisation of in-sewer storage accounting for uncertainties shows the following. In the case of uncertain system dimensions, the expected value of optimal in-sewer storage does not change very much due to uncertainty of cost parameters. In the case of rainfall variability, however, the expected value of optimal in-sewer storage increases due to uncertainty of cost parameters. The expected optimal volume is also smaller compared to the impact of dimension uncertainty due to the underestimation of the intensity of frequent storm events ($T < 0.2$ y) with relatively long duration by the rainfall generator applied.

It is impossible to completely express damage in terms of money. Intuitively, however, a proportional cost function (e.g. Weibull-shaped or linear) matches the processes determining surface water quality accounting for the proportionality of environmental damage. A linear cost function also proves to be most convenient because it can be solved analytically and is easy to assess. It also lacks the gradual changes in the Weibull cost function which erroneously suggest accuracy. For smaller or more sensitive watercourses the linear cost function becomes steeper and approaches the step function.

Based on the linear cost function the costs per m^3 CSO volume have been estimated. By assuming that current Dutch standards for CSO reduction ('Basisinspanning') lead to an economic optimum of in-sewer storage, the damage per m^3 CSO volume has been capitalised. For 'De Hoven' the costs per m^3 CSO volume are on average 4.10 Euros ranging from 3.26 to 7.58 Euros. This is 12 times larger than the cost of treatment in a wwtp.

CHAPTER 5 Operational and structural condition

5.1 INTRODUCTION

The serviceability of sewer systems is affected by the operational and structural condition of the assets comprising the system (see e.g. OFWAT 2001, Ashley and Hopkinson 2002, Geerse and Lobbrecht 2002 and Korving *et al.* 2003). For example, blockage of a sewer may result in flooding (OFWAT 2001) and failure of a pumping station may cause a CSO event (NWRW 1989b). In Chapter 1, serviceability is defined as "The ability of an asset to deliver a defined service to customers". This concerns the prevention of flooding, the protection of public health and safeguarding the environment.

Hydraulic performance of sewer systems, however, is currently assessed assuming perfect technical functioning of all assets (Stichting RIONED 1999). Therefore, the risk of blockage of a sewer or technical failure of pumping stations is usually not considered, which causes an overestimation of the level of serviceability (see e.g. Schwarz 1989, OFWAT 2001, Ermolin *et al.* 2002, UKWIR 2002, Korving 2003a and Korving *et al.* 2003). More importantly, the impact of the different aspects affecting sewer performance (such as rainfall, sewer dimensions and asset condition) and their interrelationship is only known to a limited extent.

Operation and maintenance of sewer systems aims at preserving an acceptable performance level. A key consideration is where to perform proactive maintenance in order to ensure that serviceability meets these targets. For that purpose, performance indicators need to be defined. Examples of performance indicators are presented in Ashley and Hopkinson (2002), Geerse and Lobbrecht (2002) and Le Gauffre *et al.* (2002).

Assessment of serviceability can be based on either observed deficiencies (such as number of collapses, severity of flooding, number of overflows and time between pump failures) or predicted system performance accounting for possible deterioration or failure of assets. The former can be applied to planning of proactive maintenance (see e.g. Fenner and Saward 2002) and the latter to assessing the impact of observed (or predicted) deficiencies on system level.

In order to assess the serviceability of a sewer system, its performance needs to be expressed in terms of the risk of being exposed to undesirable or even harmful consequences of failure, in particular CSOs and flooding. This is, for example, comparable to applying a dose-response relation in microbial risk assessment (see e.g. Haas *et al.* 1993) or determining the financial consequences of flooding with respect to river dikes (see e.g. Van Gelder *et al.* 1997).

This chapter discusses two examples of deficiencies possibly affecting sewer performance, namely failure of pumping stations and deterioration of sewers. Regarding sewage pumps, failure characteristics have been analysed on the basis of recorded failures of a large number of pumps in Rotterdam and Amsterdam. Subsequently, the impact of pump failures on serviceability has been estimated from model results accounting for the calculated characteristics of failures.

Deterioration of sewers (e.g. leakage, displacement, corrosion and blockage) also affects serviceability and is commonly assessed on the basis of in-sewer visual inspections. Inspection, however, is unable to measure deterioration and requires coding by inspection personnel. Poor accuracy of coding may result in a decrease of the efficiency of planned maintenance. The reliability of coding of visual inspections has been analysed on the basis of the results of entrance exams for inspection personnel. The actual impact of inaccurate coding on planning of maintenance and predictions of remaining service life, however, has not as yet been determined.

5.2 FAILURE OF SEWAGE PUMPS

Sewage pumping stations and pressure mains are critical components of sewer systems, especially in flat countries like The Netherlands. Their performance is directly responsible for affecting the serviceability of a sewer system. OFWAT (2001), Ermolin et al. (2002) and Geerse and Lobbrecht (2002) present examples of indicators measuring the performance of sewage pumps.

Quantification of the impact of failing pumps on serviceability of sewer systems requires field data. For this purpose, a 5-year series (1998-2002) of pump failure data has been provided by the Department of Public Works of Rotterdam and the Department of Water Management and Sewerage of Amsterdam. From this data both availability and reliability of sewage pumps have been modelled with various descriptions of the failure process.

The applied methodology for analysis of pump failure data accounts for the nature of the failures, the operation and maintenance procedures, the ageing of the pumps and the changes in the surroundings of the pumps. The results enable (1) quantification of the impact of failing pumps on CSOs (combined sewer overflows) and (2) optimisation of planning of failure repairs and maintenance of pumping stations.

5.2.1 Failure modes of sewage pumps

A pumping device consists of a control unit, a motor, a pump, a check valve and several other valves (see Table 5.1). In case one part fails or is put out of operation, the means of transport is unavailable leading to a failure. Pump failure is defined as the inability of a pump to perform the task it was originally designed for, which is pumping at design capacity. This definition depends on the available data on pump failure. The manner in

which a structure responds to hazards (e.g. clogging of a sewage pump due to advection of dirt) is called a failure mode. The following aspects affect the failure rate of sewage pumps (Joosten 2002):

- composition of the sewage (in particular the amount of gross solids),
- succession of dry and wet periods,
- wastewater production in the catchment area,
- type of the sewer system (combined or separate),
- condition of the sewer system (e.g. groundwater infiltration due to leaking joints, ingress of soil due to settling of sewers),
- cleaning frequency of the sewers and street surfaces,
- flow condition in the sewer,
- design of the sewage pump,
- design of the wet well,
- air in the pump or the pressurised interceptor.

The design of the wet well, the capacity of the pump, the location of individual pumps in the well and the design of the suction nozzle (see Table 5.1) affect the flow pattern in the wet well. This flow pattern determines whether deposits reach the pump or settle down in the wet well. Dirt, in particular coarse material, may cause clogging of the suction nozzle or lock the impeller. In order to reduce the probability of clogging, pumps are equipped with non-clogging impellers. Excessive deposition in the wet well should be prevented because high velocities cause erosion of sediments resulting in blockage of the pump. Therefore, frequent cleaning of the wet well is highly required.

In addition, changes of the hydraulic resistance of the discharging pressurised sewer (see Table 5.1) may cause failures. These changes probably result from scaling, sedimentation due to low velocities or air pockets.

Finally, the configuration of pumps in the pumping station largely determines the impacts of failures. When backup capacity is installed, the pumping station still manages to transport all wastewater despite the breakdown of one of the pump units (Ermolin *et al.* 2002).

Sewage pumps can be regarded as repairable systems, i.e. systems that, when a failure occurs, can be restored to an operating condition by a repair process other than replacement of the entire system. For repairable systems availability is more important than reliability. The question is whether or not a system is available and functioning.

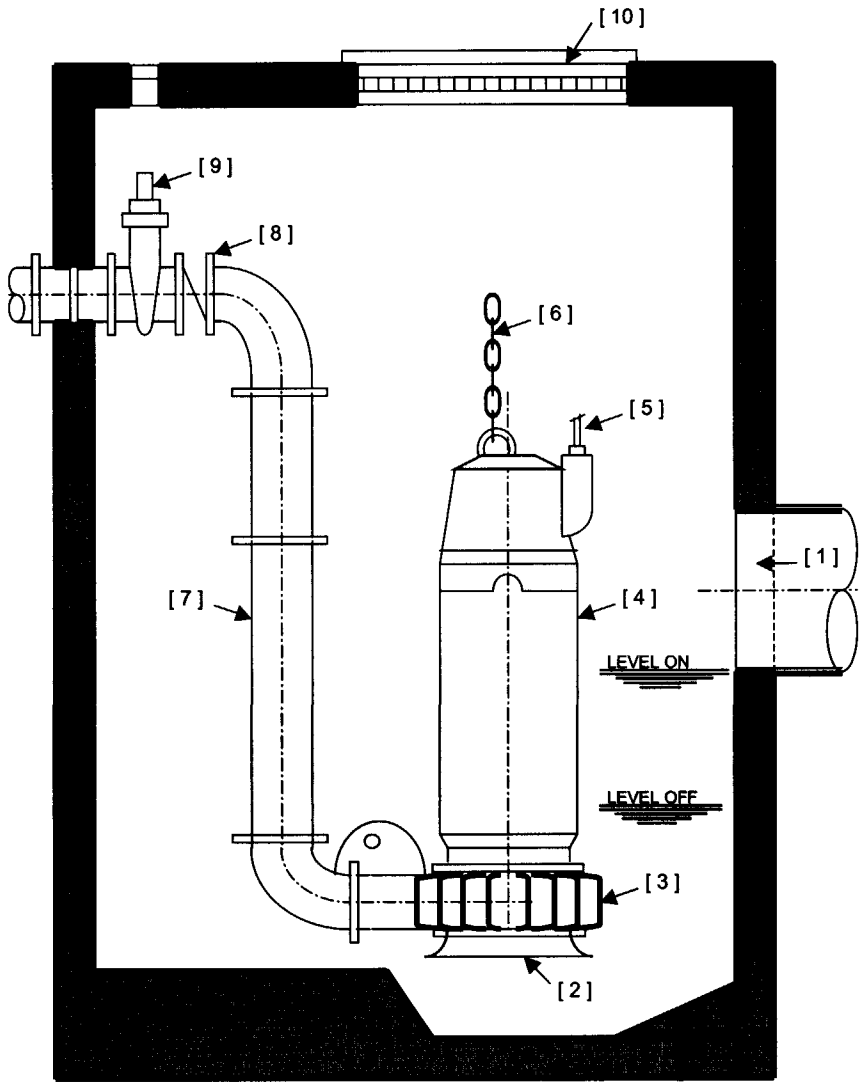

Figure 5.1 **Pumping station arrangement with submersible pump in wet well, with [1] incoming sewer, [2] suction nozzle, [3] centrifugal pump, [4] motor unit, [5] power cable, [6] fixing chain, [7] discharging pipe, [8] check valve or non-return flap valve, [9] relief valve and [10] inspection trap.**

5.2.2 Registration of pump failures

Different types of failures are reported in Rotterdam and Amsterdam. This is caused by differences in maintenance policy of a municipality, availability of backup capacity in a pumping station and type of motor starter applied. Furthermore, the availability of logs describing the nature of failures and repairs is of vital importance for successful analysis of pump failures. However, such information is often unavailable.

In Rotterdam, five types of automatically reported pump failures are distinguished:

- Thermal failures indicating either overheating of the motor of the pump or a too large current in the electrical system of the pumping device. Then the power supply is interrupted by an 'overcurrent relay'.
- Mechanical failures occurring when the check valve or non-return flap valve (see Table 5.1) behind the pump has not completely opened although the motor of the pump has been started. The check valve protects the pump against possible damage from reverse flow, for example, when the pump comes to a standstill and no head is developed. A mechanical failure is caused by a too low pressure head (or too low flow) due to, for example, obstruction of the suction, air leakage into the pump or air pockets in the pressurised sewer. Analysis shows that mechanical failures comprise up to 85% of the total number of failures.
- Electrical failures, which are indicative of incorrect switches during the start-up of the motor of sewage pumps. For electric motors different starters are applied, e.g. a pump with frequency drive, star-delta starting or even a simple knife switch (see e.g. Karassik and McGuire 1998). Each type of starter has its specific problems.
- Combined failures consist of a combination of two or more of the afore-mentioned failure types.
- Safety fuses failures mostly indicate pump maintenance. According to safety regulations the fuses need to be removed from the electrical system prior to major repairs. Removal of the fuses produces a report of a safety fuses failure. Comparison of reported failures with written logs is only partly possible, since the logs are rather incomplete.

The first three types of failures together are called TME failures. Although reported failures are distinguished in 5 categories, the majority of pump failures has a mechanical nature, mainly clogging. Another possible cause of failures is an incorrectly programmed PLC. It is emphasised that most failure reports only represent safety catches of the electric motor and the pump. They provide limited information about the actual cause of problems.

The available pump failure data give rise to possible misinterpretations. This mainly results from the necessity of independent observations. Firstly, sometimes an operator simply resets a pump after it has failed. This may result in several failures during a relatively short period. This wrongly separates a single failure event into several subevents. Therefore, it has been decided that failures with an interarrival time of less than 1 hour have a similar cause and are considered as a joint event.

Secondly, pumps can be out of operation due to long-term maintenance, which is represented by safety fuses failures in the data. Planning of maintenance aims at preserving availability and efficiency of individual pumps and the pumping station as a whole. Therefore, it is largely planned outside the wet season. On average, pumps are out of operation for maintenance purposes 3 weeks per year (Joosten 2002). Both TME (thermal, mechanical and electrical) and safety fuses failures have been analysed separately.

In Amsterdam, only three types of automatically reported pump failures are distinguished:

- thermal failures comprising a combination of failures related to the motor unit of the pump (e.g. overloading of the 'overcurrent relay' or disfunctioning of the frequency drive).
- 'level high' warnings which result from either heavy rainfall or pumps delivering less flow than required due to blockage of the suction, air leakage into the pump or air pockets in the discharge sewer. As a result, a pump can, for example, be reported 'in operation' when the motor is started but the pump is not working due to a broken shaft. In Rotterdam these failures are reported as a mechanical failure, since the check valve at the discharge side of the pump does not open completely due to too low flows. Figure 5.2 shows the impact of an obstructed suction in the sewer system of Amsterdam.
- installation failures consisting of several 'less urgent' failures, such as exceedance of switch-on level without switching-on of the preferential pump or differences in measured water levels of two gauges in the same wet well. Therefore, an installation failure only sometimes indicates a pump failure.

The interpretation of this data presents several difficulties as well. Firstly, recurrent thermal failures with interarrival times of less than 1 hour are most likely caused by the same problem and, therefore, have to be combined into one event.

Secondly, part of the installation failures represents failure of a pump. However, which part is not clear because it is a combined report. Moreover, some installation failures may even coincide with thermal failures and, therefore, can be discarded.

Thirdly, a reported 'high level' in the wet well may indicate pump failure. However, due to heavy rainfall the water level in the wet well rises as well. Therefore, during storm events the impact of pump failures cannot be discriminated from rainfall. Because of the possible misinterpretations, installation failures and 'high level' reports have not been included. As a result, the number of failures is probably underestimated, since failure is defined as the inability of a pump to pump all sewage (below a certain amount) entering the sewer system to the treatment plant. This can also be observed from the failure data. Several times the same pump is switched on two times in succession. However, at each switch-off the priority order of the pumps in a pumping station should change, which excludes two consecutive switch-ons of the same pump.

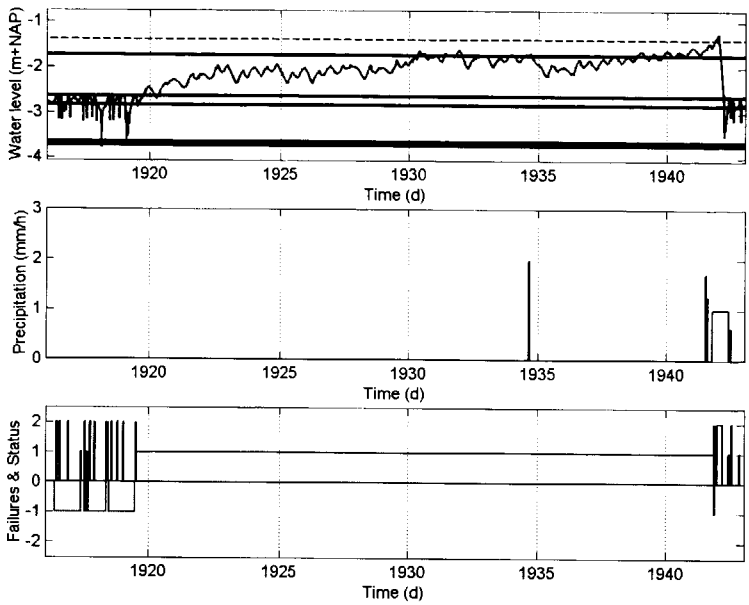

Figure 5.2 **Illustration of the impact of clogging of sewage pump on the water level in the sewer district (pumping station 'Am7', Amsterdam). From t = 1919 days to t = 1942 days, pump 1 has been switched on but the transported sewage is far below the design capacity of the pump. As a result, the water level rises until it exceeds the warning level in the wet well reported as 'level high'. After more than 3 weeks, repair personnel have visited the pumping station and cleaned the pump.**

5.2.3 Methodology for analysis of pump failure data

For the analysis of failures of repairable systems the following methodology, based on Ascher and Hansen (1998), has been applied (see Figure 5.3). The procedure especially allows for the chronological order of failure events.

The methodology consists of the following steps:

1. Validation of failure data
   Are there any outliers, errors or inconsistencies in the data?
2. Analysis of nature of failures
   Which modes of failure are important? Which types of failures can be distinguished? Does the repair policy affect failure characteristics (e.g. impact of differentiation according to repair priority on downtime)?
3. Analysis of number of failures versus operating time
   Does the pattern of failures change in time? Has there been any major system changes or changes of the maintenance policy during the operating time?
4. Test for trends in failure rate

Is the plot of number of failures versus operating time linear? Is there evidence for a trend in the failure data?

5. Description of failures with either constant or time-varying failure rate
   Should the data be modelled as a homogeneous Poisson process, a renewal process, a non-homogeneous Poisson process or any other process? What are the values of the model parameters and how can they be estimated?

By applying this procedure to failure data of sewage pumps both availability and reliability can be described. Reliability is defined as the probability that a component or system can perform a specific task under certain circumstances and during a certain time period. However, the demand for sewage pumps is intermittent, resulting in the need for a criterion in which this intermittence can be expressed. Therefore, availability (i.e. the proportion of time in which a component or system is actually functioning, or is able to function) has been applied instead of reliability as well.

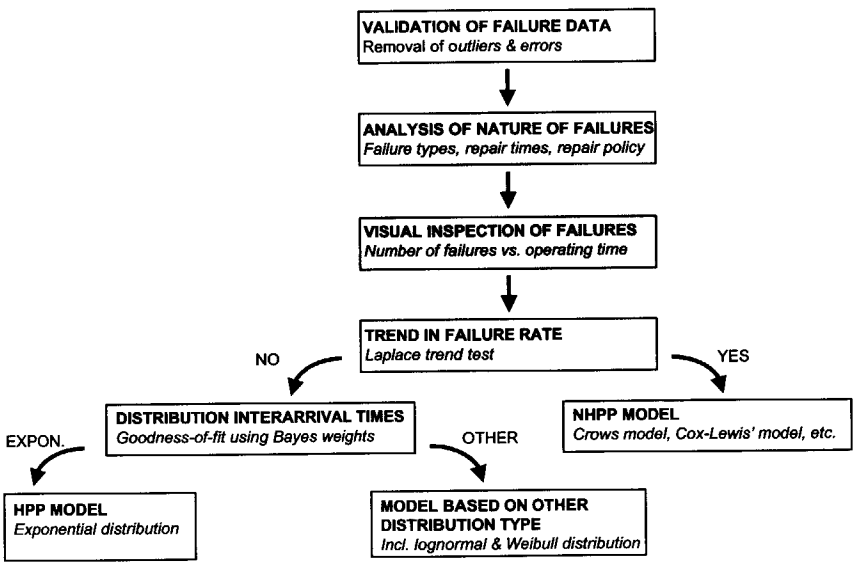

Figure 5.3 Procedure for analysis of failures of repairable systems (after: Ascher and Hansen 1998).

5.2.4 Failures of pumping stations in Rotterdam

The system of Rotterdam (Figure 5.4) covers about 200 km^2 and comprises 30 catchment areas from which the great majority is of the combined type. It is managed by the Department of Public Works of the municipality. Pumping stations transport the wastewater to five wwtps (Dokhaven, Groenedijk, Kralingseveer, Hoogvliet, Ridderkerk

and Nieuwe Waterweg) discharging to the rivers 'Nieuwe Maas' and 'Oude Maas'. They are equipped with PLCs (programmable logic controllers) controlling the flow of pumps on the basis of water level measurements in the wet well. All pumps are of the centrifugal type and the majority has non-clogging impellers. The pumping stations consist of separate pumps for dry weather flow (dwf) and wet weather flow (wwf). Sometimes additional pumps are installed in order to bypass the treatment plant and discharge directly to the river. Such a bypass is called a 'pumped overflow' (PO).

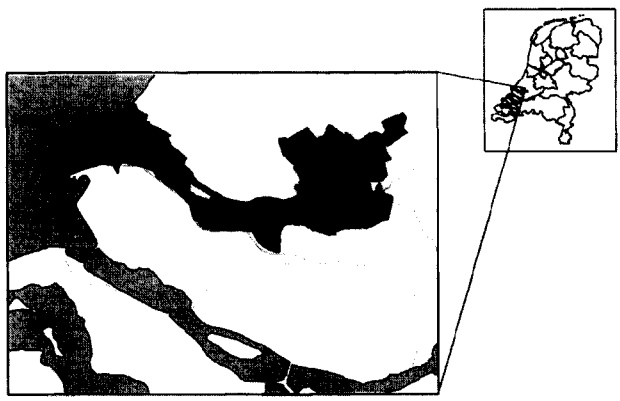

Figure 5.4 Map of catchment areas in Rotterdam, The Netherlands.

5.2.4.1 Available failure data

In Rotterdam, for approximately 120 pumping stations, the water level, sewer flow, pump status (on/off), pump failure, pressure and power consumption have been monitored continuously for at least 10 years (see Figure 5.5). Additionally, at two locations automatic rain gauges have been installed. All monitored data has been centrally recorded with an interval of 5 minutes, producing approximately 2.5 MB of data per day.

From the pumping stations equipped with automatic failure reporting, 18 have been selected for analysis (Table 5.1 and Appendix XI). This selection encloses the complete range of pumping capacities and both wet and dry well pump configurations. Each of the stations consists of 2 to 4 pumps. Reported failures of 46 pumps in total have been analysed in combination with the status of the pump.

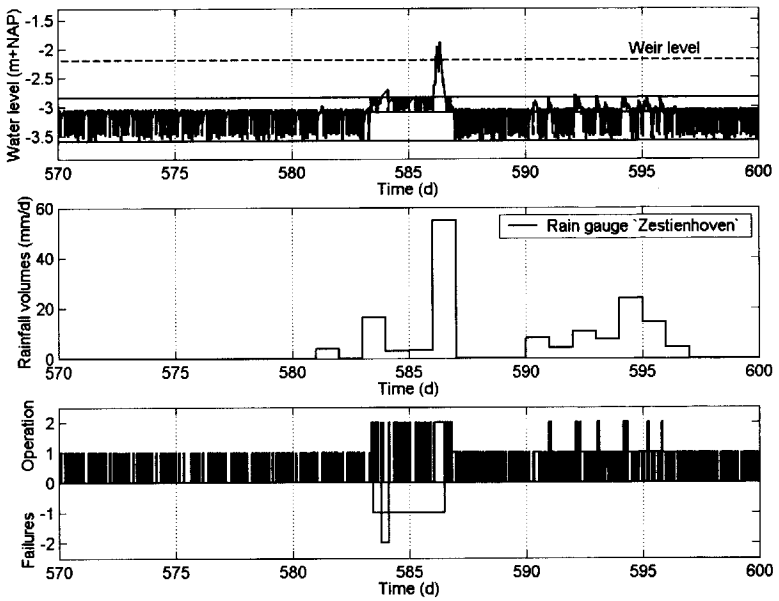

Figure 5.5 **Illustration of recorded data for pumping station 'Rm5' of Rotterdam. Either 1 (pump 1 on) or 2 (pump 2 on) indicates pump operation. Between t=580 and 590d pump 1 fails (failures=-1), after which pump 2 fails as well (failures=-2). At t=586d an overflow occurs due to heavy rainfall (almost 60mm).**

Table 5.1 **Characteristics of selected pumping stations (Rotterdam).**

Pumping station	Number of pumps	Pumping capacities (m^3/h) dwf	wwf	PO
Rm1	3	240	1261	
Rm2	4	720	2112	
Rm3	2	200	300	
Rm4	3	684	2135	
Rm5	2	150	302	
Rm6	3	360	2000	
Rm7	3	312	900	2600
Rm8	4	3718	9045	
Rm9	2	40	100	210
Rm10	3	600	1319	1574
Rm11	3	200	600	
Rm12	2	39	125	
Rm13	2	25	40	
Rm14	2	30	90	
Rm15	2	23	75	
Rm16	2	85	240	
Rm17	2	72	267	
Rm18	2	44	44	

5.2.4.2 Operation and maintenance

The Department of Public Works of Rotterdam prioritises the repairs on the basis of criteria including actual and expected precipitation, specific function of the failed pump (dwf, wwf or PO) and configuration of pumps in the pumping station. This results in three levels of repair priority:

- level 1: immediately correct the failure,
- level 2: correct the failure on next working day.
- level 3: planning of repair of the failure is unrestricted.

For example, a failed wwf pump without backup has to be repaired with the highest priority.

5.2.4.3 Statistical description of pump failures

The statistical description of failure events includes detection of trends in the failure rate, selection of a distribution type or a time-dependent model describing the failure rate and estimation of the parameters of this model (see procedure of Figure 5.3).

The different steps in the procedure are illustrated with an example, pumping station 'Rm5' in Rotterdam. This station represents a 'standard' situation for Rotterdam with respect to configuration of pumps (wet well), pumping capacity (dwf and wwf) and failure characteristics. The station consists of one pump for dwf and one pump for wwf with pumping capacities of 150 m^3/h and 302 m^3/h, respectively. Subsequently, the results for the other pumping stations are summarised.

Given the succession of failure and repair (or replacement), the time to failure, i.e. the time between two successive failures, and the time to repair, the events can be characterised by their interarrival and repair times. The interarrival time of failures is affected by the characteristics of the sewer system, the age of the pumps and the control of the pumps. The duration of failures mainly depends on the repair policy, other organisational aspects (e.g. availability of personnel) and, eventually, the backup capacity installed.

Often the statistics of interarrival times of pump failures are described as a homogeneous Poisson process (HPP) (e.g. OFWAT 2001 and Ermolin *et al.* 2002). Consequently, interarrival times are considered independent and exponentially distributed. The duration of failures is sometimes also described with an exponential distribution (e.g. Mays 1989).

However, such a simple model is only applicable if the failure rate of the system remains constant, the interarrival times are independent, the duration of failures is negligible and the system is 'as good as new' after each repair. Figure 5.6 shows that the failure rate ($\nu(t)$)of pump 1 of Rm5 is not constant and consists of possibly dependent clusters. It illustrates that for this pump an HPP model is not applicable.

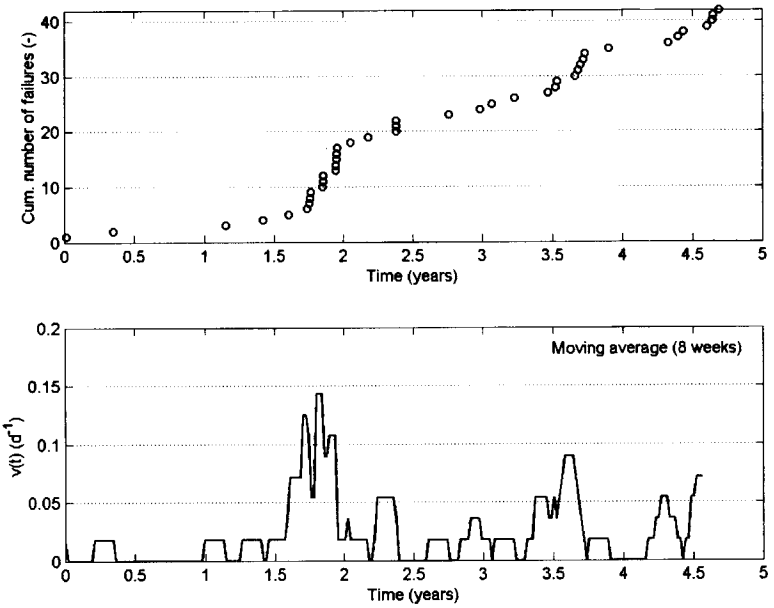

Figure 5.6 Cumulative numbers of observed TME (thermal, mechanical and electrical) failures (top) and empirical failure rate ($v(t)$) per day (bottom) of pump 1 of station Rm5.

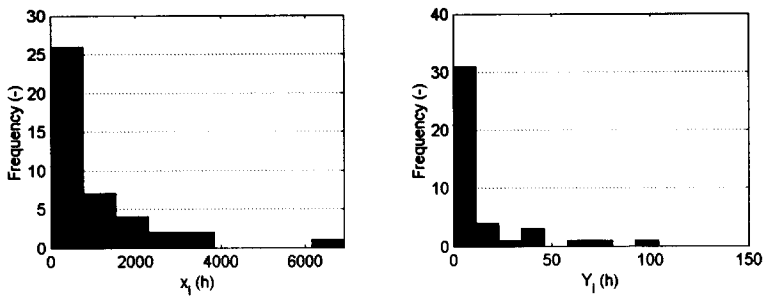

Figure 5.7 Frequencies of interarrival time (X_i) and duration (Y_i) of TME failures of pump 1 of station Rm5.

When the average number of failures increases with time, a system is called ageing. This is revealed as gradual or sudden changes of the failure rate (such as in Figure 5.8). By means of the Laplace test statistic (see § 3.4.3) trends in the failure rate can be identified. This test statistic U_L compares the sum of observed interarrival times of failures with the corresponding expected value following from an HPP. The failures of pump 1 of station Rm5 show no trend because U_L is smaller than 1.96 (upper-tail critical value in standard normal distribution).

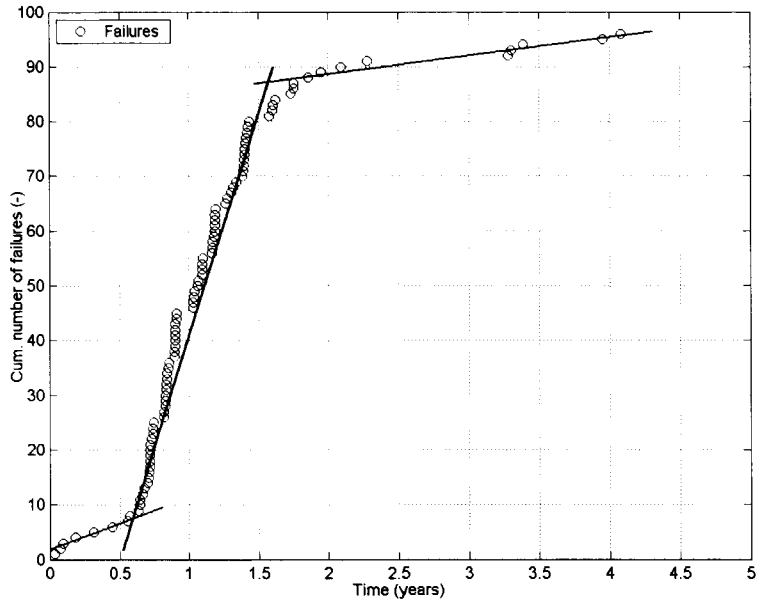

Figure 5.8 Changes in failure rate of sewage pump of station 'Rm6'. After a one-year period, in which a recurring problem causes failures, it has finally been adequately repaired.

The interarrival times of ageing systems cannot be described with an exponential model (see Ascher and Hansen 1998, and Rigdon and Basu 2002) due to its inability to describe deterioration and required repairs. Moreover, failure events of ageing systems should be analysed in chronological order (Ansell and Phillips 1994 and Ascher and Hansen 1998). A simple analysis of frequencies (Figure 5.7) neglecting the order of the time series is insufficient because it leads to incorrect estimations of the failure rate due to neglect of the impact of repairs.

In the absence of trends, interarrival times can be described with a distribution function. The key question is to find a distribution type (e.g. exponential, Weibull or gamma) to describe the data. Bayes weight assessment (see § 3.5.2) supports the selection of an appropriate distribution type. The distribution type with the largest Bayes weight fits best with the data. This also holds for describing the duration of pump failures.

Bayes weight assessment has been applied to the failure data of pump 1 of station Rm5. Jeffreys priors have been used as prior distributions (indicating lack of prior knowledge) and a Laplace approximation of the Bayes weights. Table 5.2 demonstrates that a gamma distribution fits best with observed failures. A Weibull distribution is less appropriate. The Maximum Likelihood estimators (see § 3.5.1) of parameters a and b of the gamma distribution are 0.4775 and $0.4961*10^{-3}$, respectively. Figure 5.9 compares the observed interarrival times with the estimated gamma distribution.

Table 5.2 Bayes weights for interarrival times of TME failures (station Rm5, pump 1). A gamma distribution fits best with the observed times between failures (Bayes weights based on Laplace approximation).

	Bayes weights						(Total number of failures = 42)
Rm5, pump 1	**Exp**	**Ray**	**Nor**	**Lgn**	**Gam**	**Wei**	**Gum**
Prior probability	0.1429	0.1429	0.1429	0.1429	0.1429	0.1429	0.1429
Posterior probability	0	0	0	0.0285	0.5658	0.4056	0

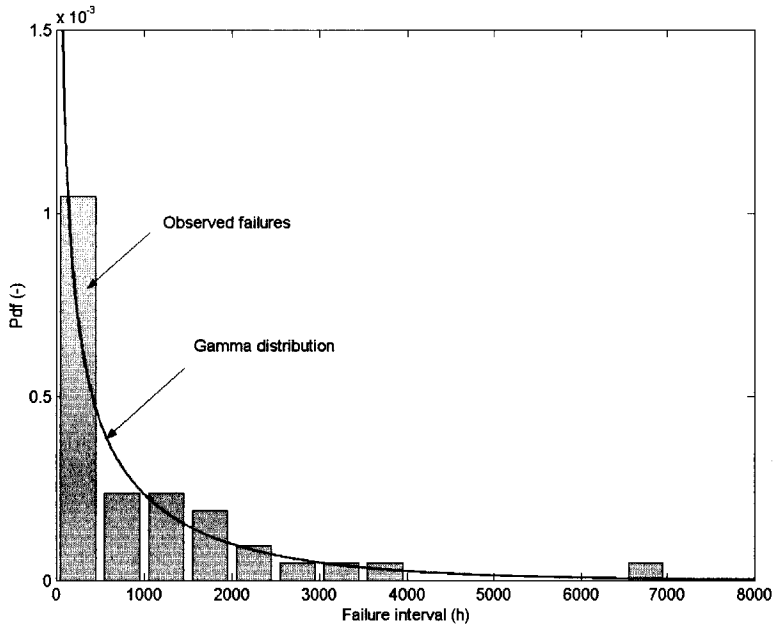

Figure 5.9 Interarrival time of TME failures of pump 1 of station Rm5 described with a gamma distribution. The average failure interval is 40.1 days (≈ 962 h).

When describing failure data with a probability distribution function, an approximately constant (or just slowly changing) failure rate is required. Sewage pumps, however, are often ageing and affected by changes in their environment (e.g. sewer system, wet well, control software). In addition, inadequate repairs and renewal of components may lead to sudden changes of the rate of failures. Therefore, models are required that can describe systems with time-varying failure rates. Non-homogeneous Poisson processes (NHPP) describe the failure rate as a function of the operating time (see § 3.4.3).

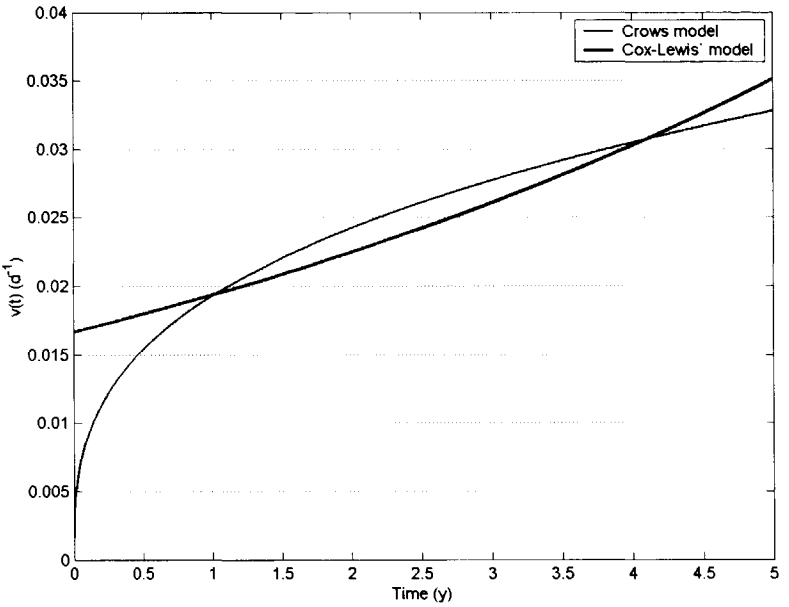

Figure 5.10 Estimated failure rate of pump 1 of station Rm5 based on Crow's and Cox-Lewis' model.

Two types of NHPP models have been used: Crow's model (Crow 1974) and Cox-Lewis' model (Cox and Lewis 1966). The former applies a power function to describe the failure rate, whereas the latter is based on a log-linear description. They are described in § 3.4.3.

Both models have been applied to the failure data of pump 1 of station Rm5, although the criteria for application are not completely met. Note, for example, that the pump is not 'as good as new' at $t = 0$, the condition of the pump at $t = 0$ is unknown and the observation period of 4.5 years is shorter than the age of the pumps. For Crow's model, the following parameter values have been estimated: $\lambda = 3.01*10^{-5}$ and $\beta = 1.3302$, where λ is the scale parameter and β is growth parameter of the Weibull function determining improvement or deterioration in time. The Cox-Lewis' model results in estimated parameters values equal to $\beta_0 = -7.2731$ and $\beta_1 = 1.70*10^{-5}$ (where β_0 is the scale parameter and β_1 is the growth parameter of the log-linear function determining improvement or deterioration in time). Both models indicate a deterioration of the pump leading to an increase of failures per time interval ($\delta > 1$ and $\beta_1 > 0$). The estimated failure rate as a function of time is presented in Figure 5.10. The observed failure rate (Figure 5.6), however, is rather different showing strong fluctuations, which possibly indicate clustered failure events. In order to deal with these fluctuations, the models need to be adjusted (see Bartlett 1963, Lewis 1967 and Rigdon and Basu 2002).

According to Ansell and Phillips (1994), the quality of Crow's model can be graphically checked with its confidence interval. This interval is approximated with,

$$\hat{\gamma} t_i^{\hat{\delta}} \pm z_{\alpha/2} \sqrt{\hat{\gamma} t_i^{\hat{\delta}}} \tag{5.1}$$

where $\hat{\gamma}$ is the ML estimator of scale parameter γ of Crow' model, t_i is the time of failure event i, $\hat{\delta}$ is the ML estimator of growth parameter δ of Crow's model and $z_{\alpha/2}$ is the 100*(1-α/2) percentile of the standard normal distribution. A sudden increase of the failure rate produces observations outside the confidence interval indicating possible dependence of events.

Figure 5.11 presents the observations and the approximation of the reliability interval. Between t_i=1 and t_i=3 years the model considerably deviates from the observations. However, except for the first failure all observations are enclosed by the 95% confidence interval. The relatively wide interval, on the other hand, could also indicate that clustering is present. Therefore, the hypothesis of dependent failures cannot be directly rejected. However, the Laplace test statistic provides no indication of a trend (U_L = 1.1622 < 1.96).

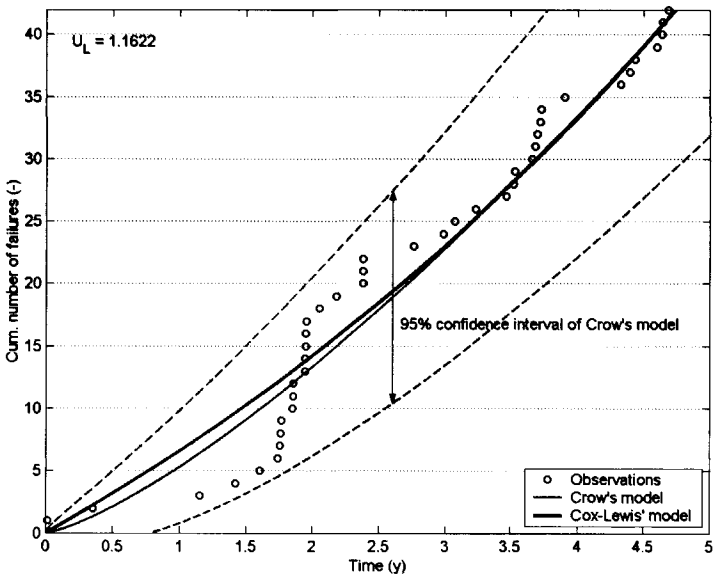

Figure 5.11 Comparison estimated rate models (Crow and Cox-Lewis) and observed failures of pump 1 of station Rm5 (including 95% confidence interval of Crow's model).

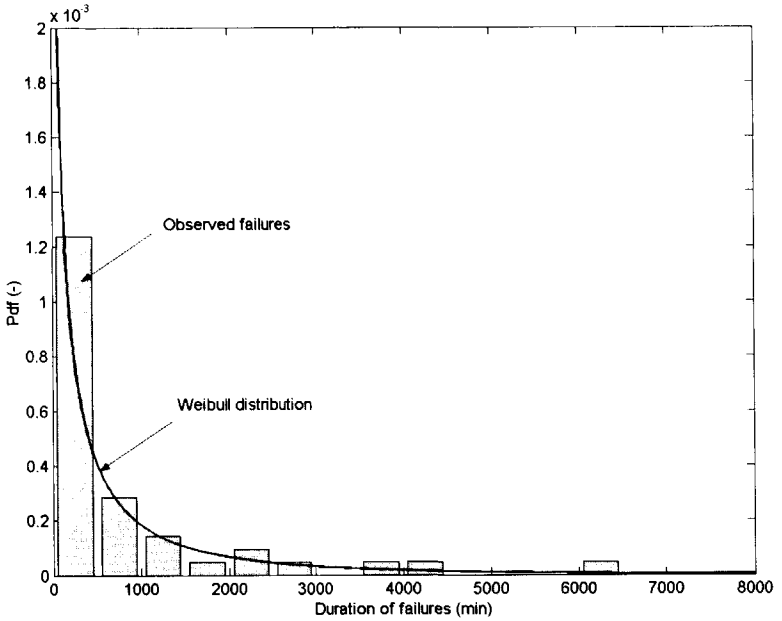

Figure 5.12 Duration of failures of pump 1 of pumping station Rm5 described with a Weibull distribution. The average duration of the failures is 13.3 hours (≈ 798 min).

The time to repair pumps consists of a reaction time and an actual repair time. The reaction time depends on the priority level of repairs for the specific pump. The nature of the failure and the complexity of disassembling the pump affect the required repair time.

The distribution type of the duration of TME failures of pump 1 of station Rm5 has been determined using Bayes weights and the parameters of the preferred distribution with Maximum Likelihood estimation. Table 5.3 demonstrates that a Weibull distribution fits best with observed times to repair. The parameters a and b of the Weibull distribution have been estimated from the data and amount to 0.5519 and 472.86, respectively. The observed duration of failures and the estimated Weibull distribution are presented in Figure 5.12.

Table 5.3 Bayes weights for duration of failures (station Rm5, pump 1). A Weibull distribution fits best with the observed repair times (Bayes weights based on Laplace approximation).

	Bayes weights				(Total number of failures = 42)		
	Exp	Ray	Nor	Lgn	Gam	Wei	Gum
Prior probability	0.1429	0.1429	0.1429	0.1429	0.1429	0.1429	0.1429
Posterior probability	0.0000	0.0000	0.0000	0.2312	0.2166	0.5522	0.0000

In the case of a time-varying demand for a pump (e.g. wwf pumps), availability is of importance. Availability is defined as the proportion of time that a component is actually working or able to work. The interest is in whether or not a system is available and functioning.

With respect to sewage pumps, there is a demand for a pump if the water level in the wet well rises above the switch-on level. Therefore, it is assumed that there is a demand for a pump either if it switches on or if it could not switch on due to a failure. Availability of a pump is calculated as,

$$1 - P(\text{failure} \mid \text{demand for pump}) = 1 - \frac{\text{number of failures}}{\text{number of pump switch ons} + \text{number of failures}} \quad (5.2)$$

It determines the proportion of cases in which a pump fails, given that it is in demand. Table 5.4 summarises the unavailability (= 1 - availability) of pump 1 of station Rm5. The average unavailability of this pump is once in 352 demands with a minimum of 210 and a maximum of 1520 times.

Table 5.4 Availability of pump 1 of station Rm5. On average, once in 352 times this pump is unable to meet the demand.

	1998	1999	2000	2001	2002	Total	Average
Number of TME failures	2	15	7	11	7	42	9
Number of switch-ons	3039	3149	3121	3197	2236	14742	2948
1/*P*(failure|demand)	1520	210	446	291	320	352	352

The duration of safety fuses failures approximately represents the long-term planned maintenance of pumps because safety regulations require removal of the fuses prior to repair activities. The duration of planned maintenance of pump 1 of station Rm5 is considerably longer than the total duration of TME failures (see Table 5.5). The duration of maintenance of this particular pump, however, is smaller than the average of all pumps, which equals 3 weeks/year (Joosten 2002). This results from the absence of backup capacity in the station, which only allows for breakdowns of short duration.

Table 5.5 Comparison of duration of TME failures and safety fuses failures of pump 1 of station Rm5.

TME failures	1998	1999	2000	2001	2002	Total
Duration per failure (min)	19.2	14.6	18.5	7.0	13.6	13.3
Number of failures (-)	2	15	7	11	7	42
Total duration (min/year)	38.4	218.7	129.8	77.3	95.1	559.4
Safety fuses failures	**1998**	**1999**	**2000**	**2001**	**2002**	**Total**
Duration per failure (h)	423	0	0	0	490	-
Number of failures (-)	3	0	0	0	1	-
Total duration (hours/year)	1270	0	0	0	490	-

5.2.4.4 Results of failure data analysis

The methodology described in the previous sections has also been applied to failure data of the remainder of the selected pumping stations in Rotterdam (Table 5.1). Again, TME failures and safety fuses failures have been separately analysed.

Distribution types describing interarrival time with a constant failure rate and those describing duration of failures have been selected with Bayes weights. Jeffreys priors have been used as prior distributions and Laplace expansions for approximation of the marginal densities. In addition, the parameters of these distributions have been determined by Maximum Likelihood estimation. Detailed results can be found in Appendix XI.

The majority of pumps has a time-varying failure rate. For pumps with more than 15 failures, trends in the failure rate have been studied using the Laplace trend test. The failure rate of half of the pumps does not exhibit a trend. Regarding the pumps with a trend, 30% improves and 70% deteriorates with time (see Appendix XI). There is no correlation between the trends and either capacity or specific function of the pump. However, correlation between pump age, pump type and (condition of) upstream sewers is possible. Unfortunately, information on age and type is not available.

The number of TME failures is presented in Table 5.6. The average number of failures equals 62 leading to an interarrival time of 29.5 days. However, this number varies considerably (min. = 0 and max. = 364) depending on the pumping station studied. However, there is no correlation found between the number of failures and either power or specific function (dwf, wwf and PO) of a pump.

In addition, the failure rate of pumps often shows an erratic course possibly indicating clusters of dependent failures. Successive failures can be dependent since they may arise from the same, inadequately fixed problem. However, information about repairs is only registered in logbooks, far from complete and difficult to access.

Table 5.7 shows the results of the Bayes weight assessment of interarrival times of TME failures. Interarrival times can only be described with a distribution function if the failure rate shows no sudden changes. The distribution type that fits best with the data differs between the pumps studied. This may result from pumps with considerable trends in their failure rate. For the majority of pumps both gamma and Weibull distribution give satisfactory results. However, no correlation is found between these distribution types and either power or specific function of a pump.

Table 5.6 Statistics of TME failures of several classes of pumps.

		Number of failures (-)	Total duration of failures (h)	1 / Unavailability
All pumps	Average	62	642	945
	Std.	79	1089	1718
	Min.	0	0	10
	Max.	364	6465	7559
Dwf pumps	Average	74	880	1659
	Std.	83	1374	2293
	Min.	0	0	19
	Max.	364	6465	7559
Wwf pumps	Average	57	530	829
	Std.	73	723	1634
	Min.	0	0	10
	Max.	292	2648	7559
POs	Average	25	79	15
	Std.	6	32	2
	Min.	18	60	13
	Max.	29	116	17
Power ≤ 5kW	Average	9	509	1470
	Std.	8	482	1067
	Min.	0	0	338
	Max.	21	1396	3435
5 < Power ≤ 25kW	Average	14	588	1182
	Std.	17	763	2243
	Min.	0	0	15
	Max.	58	2648	7559
Power > 25kW	Average	14	627	133
	Std.	13	690	142
	Min.	0	4	10
	Max.	37	2196	537

Table 5.7 Bayes weights of interarrival times of TME failures (average values of all pumping stations).

		Bayes weights						
All pumps	(n=15)	**Exp**	**Ray**	**Nor**	**Lgn**	**Gam**	**Wei**	**Gum**
Prior probabilities		0.1429	0.1429	0.1429	0.1429	0.1429	0.1429	0.1429
Posterior probabilities		0.0498	0.0000	0.0000	0.2437	0.3402	0.3659	0.0004
Dwf pumps	(n=6)	**Exp**	**Ray**	**Nor**	**Lgn**	**Gam**	**Wei**	**Gum**
Prior probabilities		0.1429	0.1429	0.1429	0.1429	0.1429	0.1429	0.1429
Posterior probabilities		0.0072	0.0000	0.0000	0.1693	0.4180	0.4055	0.0000
Wwf pumps	(n=12)	**Exp**	**Ray**	**Nor**	**Lgn**	**Gam**	**Wei**	**Gum**
Prior probabilities		0.1429	0.1429	0.1429	0.1429	0.1429	0.1429	0.1429
Posterior probabilities		0.0615	0.0000	0.0000	0.3021	0.2642	0.3717	0.0004

Failures of pumps with a time-varying failure rate have been described with two growth models: Crow's and Cox-Lewis' model (see § 3.4.3). Their parameters have been determined with Maximum Likelihood estimation. The results are presented in Appendix XI. In general, Crow's model performs better than Cox-Lewis' model because the latter was originally developed to describe the improval of a system.

The majority of pumps deteriorate in the course of time. On average, the value of parameter δ in Crow's model is larger than 1, which indicates deterioration. Moreover, there is evidence of clustered and dependent failures. More than half of the pumps studied show either a relatively wide confidence interval of Crow's model or even observations outside this interval. As a result, further analysis requires the integration of this clustering into the model (see e.g. Bartlett 1963 and Rigdon and Basu 2002).

Availability of pumps varies considerably (see Table 5.6). It is defined as the proportion of time in which a pump actually functions or is able to function. The average unavailability (= 1 - availability) of a pump varies between once in 10 and once in 7559 demands for a specific pump. It diminishes when the power of the pump is larger than 25 kW. POs differ from the other pumps, since they are unavailable each 15th demand.

The time to repair a specific pump varies from almost zero to several days per year. The average duration of failures amounts to 10 hours (see Table 5.6). Apart from POs ('pumped overflows'), the averages of pumps with different repair priorities are comparable (Table 5.8). The duration of repairs of POs is significantly shorter. Since the specific function of these pumps is to prevent overflows to sensitive watercourses, they are repaired with the highest priority. Table 5.9 shows that failure duration is preferably described with either lognormal or Weibull distributions. Lognormal is the best, Weibull second best.

Although most models describing the characteristics of pump failures assume instantaneous repair, Table 5.6 and Table 5.8 show that the repair or replacement times of sewage pumps takes several hours, or even days. As a result, a series of states with the pump either failing or working is produced. Therefore, assuming instantaneous repair of pumps is incorrect and the model should be adapted in order to describe longer repair times (see e.g. Cox 1962 and Ansell and Phillips 1994).

Table 5.8 Average and maximum values of duration of TME failures of pumps with different priority of repairs.

Priority level of repairs	Average duration of one failure (h)	Maximum duration of one failure (h)
1	8.79	17.28
1/2	2.98	4.01
2	9.74	20.47
3	12.23	14.84

Table 5.9 Bayes weights of duration of TME failures (average values of all pumping stations).

		Bayes weights						
All pumps	(n=15)	**Exp**	**Ray**	**Nor**	**Lgn**	**Gam**	**Wei**	**Gum**
Prior probabilities		0.1429	0.1429	0.1429	0.1429	0.1429	0.1429	0.1429
Posterior probabilities		0.0706	0.0067	0.0103	[illegible]	0.1306	[illegible]	0.0105
Dwf pumps	(n=6)	**Exp**	**Ray**	**Nor**	**Lgn**	**Gam**	**Wei**	**Gum**
Prior probabilities		0.1429	0.1429	0.1429	0.1429	0.1429	0.1429	0.1429
Posterior probabilities		0.1354	0.0167	0.0257	[illegible]	0.1827	[illegible]	0.0261
Wwf pumps	(n=12)	**Exp**	**Ray**	**Nor**	**Lgn**	**Gam**	**Wei**	**Gum**
Prior probabilities		0.1429	0.1429	0.1429	0.1429	0.1429	0.1429	0.1429
Posterior probabilities		0.0831	0.0000	0.0000	[illegible]	0.1302	[illegible]	0.0001
Repair priority 1	(n=7)	**Exp**	**Ray**	**Nor**	**Lgn**	**Gam**	**Wei**	**Gum**
Prior probabilities		0.1429	0.1429	0.1429	0.1429	0.1429	0.1429	0.1429
Posterior probabilities		0.0324	0.0000	0.0000	[illegible]	0.0979	[illegible]	0.0000
Repair priority 2	(n=4)	**Exp**	**Ray**	**Nor**	**Lgn**	**Gam**	**Wei**	**Gum**
Prior probabilities		0.1429	0.1429	0.1429	0.1429	0.1429	0.1429	0.1429
Posterior probabilities		0.0566	0.0000	0.0000	[illegible]	0.1754	[illegible]	0.0001
Repair priority 3	(n=8)	**Exp**	**Ray**	**Nor**	**Lgn**	**Gam**	**Wei**	**Gum**
Prior probabilities		0.1429	0.1429	0.1429	0.1429	0.1429	0.1429	0.1429
Posterior probabilities		0.1386	0.0125	0.0193	[illegible]	0.1966	[illegible]	0.0197

Table 5.10 Duration of safety fuses failures (averages of all pumping stations).

	Average	**Std.**	**Min.**	**Max.**
Duration per failure (d)	4.1	4.4	0.1	21.8
Number of failures (-)	1.3	1.4	0.0	6.7
Total duration (days/year)	6.0	6.2	0.0	22.1

Regarding safety fuses failures, the time of maintenance approaches approx. 4 days (see Table 5.10). The maximum even exceeds 3 weeks. The total number of safety fuses failures on average amounts to 1.3 with a maximum of almost 7. However, there is no correlation between the number of failures and their average duration.

5.2.4.5 Conclusions and discussion

The analysis of 46 sewage pumps in Rotterdam shows that the number of failures per year and per sewage pump varies strongly and is independent of the specific function of the pump (dwf, wwf or PO). Failures have been classified as either TME (thermal, mechanical and electrical) failures or safety fuses failures. The former results from the sewage transport process, while the latter relates to the maintenance programme. The average number of TME failures per pump is 62.3 (≈ 13 failures/year) during the observed period resulting in an average failure interval of 650 hours (≈ 27 days). The average duration of failures is approximately 10 hours, but may vary from 1 hour to several days depending on the repair priority of the pump. This is independent of the

specific function of a pump. Maintenance is performed approximately once a year and on average requires 4 days per service.

The Laplace trend test indicates that most sequences of failure events hold a trend leading to a time-varying failure rate. In some cases a pump deteriorates due to ageing, in other cases it improves due to renewal or refurbishment. Therefore, failure analysis should account for the chronological order of failures. Furthermore, failures are bunched resulting in dependency between successive events. However, required additional information on items such as nature of repair, presence of preceding dry period, changes in control software and sensitivity of frequency drives to heat is not available.

On the basis of reported failures it has not been possible to find a distribution type that unequivocally describes interarrival times of failures. Possible candidates are lognormal, gamma and Weibull distributions. Such a description, however, assumes a failure rate without trends and independence of successive failures. Analysis of the data indicates that both criteria are violated. In addition, the time of planned (annual) maintenance affects trends in failure rate. Duration of repairs is preferably described with a lognormal or a Weibull distribution.

5.2.5 Failures of pumping stations in Amsterdam

The Department of Water Management and Sewerage manages the system of Amsterdam. A large number of pumping stations transports the sewage to three wwtps (Oost (Zeeburg), Zuid (Spaklerweg) and Westpoort). In general, gravity systems are applied. Pumping stations transport the sewage through pressurised interceptor sewers from the different districts to the wwtps. The flow of the pumps is controlled by PLCs from water level measurements in the wet well. The priority order of the pumps changes at each switch-off. All pumps are of the centrifugal type with non-clogging impellers. The majority of the pumping stations are equipped with redundant pumping capacity for wwf conditions in order to minimise the impact of failures. In the case of a station with two pumps, both pumps are able to transport dwf and wwf. A small number of pumps, called 'pumped overflows' or POs, directly discharge to a watercourse and essentially function as an emergency outlet.

5.2.5.1 Available failure data

From the sewer system of Amsterdam the failures of pumps in 7 pumping stations have been analysed (see Table 5.11 and Appendix XII). The stations have different dwf and wwf capacities and consist of 2 to 5 pumps. In total 20 pumps with various pumping capacity and power have been studied.

The available data consist of recorded water level measurements (max. recording interval = 10 minutes), pump status reports (on/off switches), thermal failures, installation failures and data on the light in pumping station (on/off switches possibly

indicating visits for maintenance). For most stations only 3.5 years of continuous data has been provided. Written logs with descriptions of a small proportion of all failures have also been supplied.

5.2.5.2 Operation and maintenance

Regular inspection of the pumps and other devices in the pumping stations and preventive replacements of components is the cornerstone of the repair strategy in Amsterdam. For example, pumping station Am1 is visited for inspections at least 4 times a year. The pumps of this station have to be thoroughly checked every 2 years and the electrical installation and PLCs every year. Replacements are scheduled as follows, gaskets twice a year and bearings of the motor every 10 years. This (partly) proactive approach influences the characteristics of failures to a large extent.

5.2.5.3 Results of failure data analysis

The methodology described in § 5.2.3.3 has also been applied to the failures in Amsterdam. Thermal and installation failures have been separately analysed with respect to the following aspects:

- trends in failure rate,
- characteristics of interarrival time of failures assuming constant failure rate,
- characteristics of interarrival times of failures assuming time-dependent failure rate,
- availability in particular of pumps designed for wwf,
- moment of failures during wwf conditions,
- characteristics of duration of failures.

Distribution types of the interarrival time and duration of failures have been selected using Bayes weights. Jeffreys priors have been used as prior distributions and Laplace expansions for approximation of marginal densities. The parameters of selected distributions have been calculated with Maximum Likelihood estimation. An overview of the results is presented in Appendix XII.

Table 5.11 Characteristics of selected pumping stations (Amsterdam).

Pumping station	Number of pumps	Pumping capacities (m^3/h) dwf	wwf
Am1	3	270	630
Am2	2	108	108
Am3	3	1008	1458
Am4	2	29	29
Am5	3	165	360
Am6	5	7100	4726 (+dwf)
Am7	2	162	162

Table 5.12 Statistics of thermal failures of several classes of pumps.

		Number of failures (-)	Total duration of failures (h)	1 / Unavailability
All pumps	Average	15	365	2631
	Std.	13	705	5642
	Min.	3	0	10
	Max.	43	2493	16497
Dwf/wwf pumps	Average	16	440	3250
	Std.	14	774	6198
	Min.	3	4	10
	Max.	43	2493	16497
Wwf pumps	Average	11	95	198
	Std.	6	132	209
	Min.	7	1	50
	Max.	15	188	345
Power ≤ 5kW	Average	3	37	16459
	Std.	0	15	54
	Min.	3	26	16420
	Max.	3	48	16497
5 < Power ≤ 25kW	Average	16	136	243
	Std.	5	82	137
	Min.	9	60	10
	Max.	22	249	345
Power > 25kW	Average	17	590	667
	Std.	16	929	734
	Min.	4	0	50
	Max.	43	2493	1774

The Laplace test statistic indicates that no pump is subject to sudden changes in the failure rate (see Appendix XII). However, the reliability of the majority of pumps does decrease due to ageing. The partly proactive repair strategy probably results in a steady development of pump reliability.

Table 5.12 shows the number of thermal failures for different classes of pumps. The average number is 15 for the total observation period. Consequently, the interarrival time of failures is approximately 85 days. The maximum number of observed failures is 43, which occurred at one of the larger pumps (power > 25kW). The class of wwf pumps shows a very small variation which results from the small number (n = 2) of pumps especially designed for wwf. However, generally there is no correlation between number of failures and capacity of the pumps.

Bayes weight assessment indicates that the interarrival times of pump failures are preferably described with a gamma distribution (Table 5.13). This only applies to pumps with a constant failure rate. However, none of the pumps suffers from sudden, large changes in the failure rate. Again, Bayes weights have been calculated using Jeffreys priors and Laplace approximation of Bayes weights.

Table 5.13 Bayes weights of interarrival times of thermal failures (averages of all pumping stations).

		Bayes weights						
All pumps	(n=8)	**Exp**	**Ray**	**Nor**	**Lgn**	**Gam**	**Wei**	**Gum**
Prior probabilities		0.1429	0.1429	0.1429	0.1429	0.1429	0.1429	0.1429
Posterior probabilities		0.0794	0.0000	0.0004	0.0949	[redacted]	0.3061	0.0013

Table 5.14 Moment of thermal failures during storm events.

	Number of failures
Start of event	18 (= 58%)
End of event	13 (= 42%)
Total	31 (= 100%)

The interarrival times of failures have also been described with growth models of Crow and Cox-Lewis. Maximum Likelihood estimation has been used for parameter calculation. The results in Appendix XII demonstrate that all pumps studied are subject to ageing. Parameter β of Crow's model is larger than 1 and parameter β_1 of Cox-Lewis' model is larger than 0. Both criteria are an indication of deteriorating assets.

The impact of pump failure during wwf conditions depends on the moment of failure. The closer a failure is located to the start of a storm event, the larger its potential impact on system performance. Failures at the start of storm events mostly result from failing switch or air leakage into the pump, whereas failures at the end may arise from blockage of the suction due to increased advection of deposits.

There is no indication that wwf pumps generally fail either at the start or at the end of a storm event (see Table 5.14). The proportions are equally distributed (58% and 42%, respectively). The start of a storm is defined as the first 30% of the duration of the event. Approximately 14% of recorded pump failures occur during storm events, which is relatively low compared to expert opinion based on the situation in Rotterdam. Unfortunately, in Rotterdam reliable rainfall data are unavailable.

Table 5.12 shows that unavailability of pumps due to thermal failures is different for different power bands. Unavailability is defined as the proportion of demands for a pump in which the pump is unable to perform its required task. The smallest pumps (power $\leq$ 5kW) appear to be the most reliable ones. The average unavailability of the pumps equals 1/2631 meaning that a pump is unavailable once in 2631 demands. Minimum and maximum values are 10 and 16497, respectively. The minimum belongs to a pump that is used in case of heavy rainfall and directly discharges to surface waters only. Failure of this pump most likely results from resuspension of deposits in the wet well due to the change in flow conditions caused by the pump.

Table 5.15 Bayes weights of duration of thermal failures (averages of all pumping stations).

	Bayes weights						
All pumps (n=8)	**Exp**	**Ray**	**Nor**	**Lgn**	**Gam**	**Wei**	**Gum**
Prior probabilities	0.1429	0.1429	0.1429	0.1429	0.1429	0.1429	0.1429
Posterior probabilities	0.0225	0.0000	0.0000	[illegible]	0.2313	0.2426	0.0003

The duration of pump repairs is highly variable and runs from 0 to more than 100 days for the total observation period (Table 5.12). The average equals 365 hours (≈ 100 hours per year). This results for the most part from the failures of the dwf pumps of pumping station Am6. Because of the large amount of backup capacity (3+2 pumps) in the station, there is no need for quick repairs. When the failures of station Am6 are excluded, the average duration diminishes to approximately 20% of the original value.

Using Bayes weights (with Jeffreys priors and Laplace approximation of Bayes weights) the distribution type has been determined that fits best with the observed failures. The results in Table 5.15 and Appendix XII show that for the majority of pumps a lognormal distribution is preferred.

5.2.5.4 Conclusions and discussion

In Amsterdam the 20 pumps studied show considerable variation with respect to number and duration of failures. The average number of failures is approximately 4.3 per year and their average duration is 13.5 hours. In general, there is no correlation between failure characteristics and specific function (dwf or wwf) of the pump. However, some similarities in availability and failure duration are apparent for pumps within specific power bands. Further, the analysis shows that the interarrival time of failures is preferably described with a gamma distribution, whereas a lognormal distribution fits best with observed duration.

According to the results of the Laplace trend test, the failure rate of the pumps is not subject to sudden changes. However, the reliability of the pumps decreases due to ageing. In addition, the failure rate is not constant but failures occur in clusters. This results from inadequate repairs or external conditions. However, further analysis of the dependency proved impossible due to a lack of additional information on repairs, condition of sewers regarding sedimentation and length of dry periods prior to failures.

5.2.6 Impact of pump failures on serviceability of sewer systems

The statistical analysis of failure data of sewage pumps is illustrated with pumping station Rm5 in Rotterdam. The catchment area of Rm5 covers 10.29 ha. The station consists of one pump for dwf (pump 1) and one for wwf (pump 2) with capacities of 150 and 300 m^3/h, respectively. The priority of repairs is class 2 for pump 1 and class 1 for pump 2.

The observations show that pump 1 suffers from 42 TME failures in 5 years (see Figure 5.6). This results in an average of 8.4 failures each year. Its failure intervals can be described with a gamma distribution (see Figure 5.9), while its repair times follow a Weibull distribution (see Figure 5.12). The average failure interval of pump 1 is 40.1 days. The average duration of the failures is 13.3 hours. In addition, the failure data indicate that the average unavailability is once per 352 demands (P(failure | demand pump) = $2.8*10^{-3}$). With respect to maintenance, the pump is put out of operation 4 times in the 5-year period (= 0.8/year) and the duration of each maintenance activity is 7.3 days on average. However, the planned maintenance has not been considered in the calculations.

The characteristics of failure data (both distributions of interval and duration of failures and availability) can be used as input of a sewer model in order to estimate the impact of pump failure on CSOs and flooding. For this purpose, Monte Carlo simulation has been applied, which implies sampling from uncertainty distributions of pump failure characteristics and successive simulation for all sampled time series consisting of alternating working and failing pump states. An estimate of the overall impact of pump failures on serviceability of the sewer system is obtained by statistical analysis of the model output of all runs.

Gamma and Weibull distributions (see Figure 5.9 and Figure 5.12) describing the time interval between and duration of pump failures have been applied to describe the performance of individual pumps in time. Arrival times of the wwf pump, however, have been modelled in terms of availability, since this pump is only in demand during storm events.

A Monte Carlo simulation of 250 runs has been performed in which the sewer system is modelled as a reservoir with an external weir and a pump. The rainfall runoff model consists of the 'standard' rainfall runoff model in The Netherlands ('NWRW 4.3' model) describing evaporation, infiltration, storage on street surfaces and overland. The input of the sewer system consists of a 10-year rainfall series (De Bilt, The Netherlands, 1955-1964) and a constant wastewater production have been used. The switch-on and switch-off levels of the pumps are based on the observed relationship between storage volume and water level for the sewer system of Rm5.

Prior to each Monte Carlo, run a random time series of pump failures has been generated for both pumps. This time series has been substituted in the model of the sewer system. The interarrival time and duration of failures of the dwf pump have been drawn from the estimated gamma and Weibull distribution. The duration of the failures of the wwf pump has been drawn from the estimated Weibull distribution as well. The failures of the wwf pump, however, are assumed to be dependent on the demand for this pump. Its availability has been determined by randomly drawing a value from a standard uniform distribution on the interval [0,1]. When this value is less than or equal to the average availability, the pump fails, otherwise it functions.

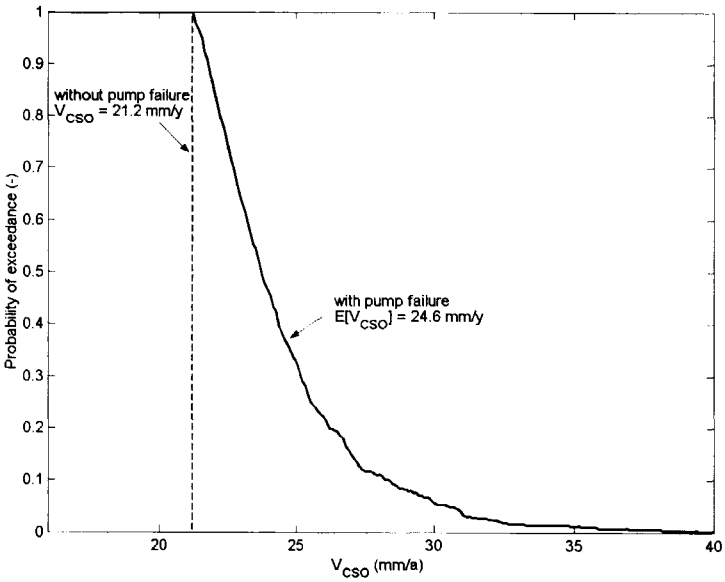

Figure 5.13 Impact of pump failure on serviceability (expressed as yearly CSO volumes) based on failure characteristics of pumping station Rm5. 'Time to failure' is gamma distributed, 'time to repair' Weibull distributed.

Figure 5.13 shows that sewer serviceability is considerably affected by failing pumps. If serviceability is expressed in terms of CSO volumes, the yearly volume without pump failures equals 21.2 mm/a. When pump failures are introduced, the expected value of yearly volumes increases to 24.6 mm/a with pump failure. Thus, the average increase due to pump failures amounts to 16%.

5.2.7 Concluding remarks

The failure characteristics of sewage pumps are different for the pumps studied in Rotterdam and Amsterdam. This mostly results from differences in nature of reported failures and maintenance strategy. In Rotterdam, the average number of failures is 13 per year and time to repair is approximately 10 hours per event. In Amsterdam, however, the number of failures is smaller (4 per year) but the duration of individual failures is longer (13.5 hours).

Compared to pumps in drinking water distribution systems and pumping stations used in polders, sewage pumps fail relatively often. This arises from the composition of the sewage and the intermittent character of the pumping. According to Mays (1989), the average interarrival time of failures of drinking water pumps is approximately 3.7 years (Table 5.16). In drinking water systems, failures of valves are even more important. Pumps used in polders suffer from failures longer than 6 hours less than

once a year (HKV 1999). Sewage pumps in wwtps require longer repair times (Table 5.16) because wwtps are predominantly equipped with redundant capacity. As a result, pump repairs are less urgent.

The large difference in the number of reported failures in Rotterdam and Amsterdam (see Table 5.6 and Table 5.12) mainly results from mechanical failures. This type of failure is only reported in Rotterdam and comprises up to 85% of all failures in Rotterdam. Mechanical failures indicate that the check valve in the discharging sewer is only partly opened due to blockage or air leakage. As a result, the pump transports less sewage than required but uses considerably more energy and the wear of the impeller is accelerated. In Amsterdam, however, hampered pumping performance is not detected until the water level in the wet well exceeds the warning sign 'level high'. This may take several days or even weeks in which the pump fails because it does not perform its required task.

Observed failures often exhibit a trend indicating a time-dependent failure rate. On the one hand, reliability decreases due to inadequate repairs or ageing, on the other, it increases due to replacement or refurbishment. Consequently, an analysis of failures of sewage pumps should take account of their sequence. Given the trend, it is incorrect to assume that a pump is 'as good as new' after repair. Therefore, the repair of sewage pumps should be modelled as 'minimal repair', i.e. the repair done on the system leaves it in exactly the same state as it was just before the failure (no change of failure rate).

Table 5.16 Comparison of interarrival time and duration of failures of sewage and drinking water pumps.

Sewage pumps in Rotterdam and Amsterdam				
	MTBF (h)	**95% interval**	**MTTR (h)**	
Sewage pumps (Rotterdam)	707	120 - 43824	7.6	
Sewage pumps (Amsterdam)	2146	748 - 10728	13.5	
Sewage pumps in wwtps (after: Assezat 1989)				
	MTBF (h)	**95% interval**	**$MTTR_S$ (h)**	**$MTTR_A$ (h)**
Screw pumps	11600	9000 - 16600	231	94
Submerged pumps (raw sewage)	4300	3500 - 5500	125	39
Submerged pumps (sludge)	15100	11600 - 21200	125	39
Pumps in drinking water systems (after: Mays 1989)				
	MTBF (h)	**95% interval**	**MTTR (h)**	
Pumps	32070	21660 - 74190	9.6	
Valves	14440	8930 - 32590	11.6	
Motors	66700	10880 - 114820	6.9	

MTBF = mean time between failures,
MTTR = mean time to repair,
$MTTR_S$ = mean time to repair without spare parts on site,
$MTTR_A$ = mean time to repair with spare parts on site.

The failures also tend to be bunched. As a result, subsequent failures are dependent and should be analysed as such. Clusters are an indication of inadequate repairs resulting in a succession of failure events due to the same, unsolved cause.

The impact of pump failure during wet weather conditions depends on the moment at which the failure occurs. The closer to the start of a storm event, the larger the possible impact of a failure. However, the analysis shows no indication that wwf pumps generally fail either at the start or at the end of a storm event. For further analysis it is assumed that failures during wet weather conditions occur at the start of a storm event in order to study the worst possible case.

The description of the duration of failures should consider that the time needed to repair a pump directly results from the repair policy of a municipality. For example, in Rotterdam a pump with a low repair priority that fails on Friday after office hours will be repaired only on the next workday during office hours. Consequently, the duration of such a failure exceeds 48 hours.

The representativeness of the situations in Rotterdam and Amsterdam, however, can be questioned because of the specific way in which pump failures are dealt with. In Rotterdam, for example, the repair of sewage pumps is prioritised on the basis of specific criteria. Furthermore, the configuration of pumps in a pumping station and the available backup capacity affects the need for repair. This may be significantly different from other management authorities.

The decisive factor for successful analysis of pump failures is the completeness of available information. The analysis shows that the recording of failure events in Rotterdam provides more useful information compared to Amsterdam. More extensive application of analysis of pump failure data requires uniformity of failure registration.

In addition, the availability of logs describing the nature of failures and repairs is of vital importance. However, both in Rotterdam and Amsterdam the additional information in logs is far from complete and needs to be improved in order to study correlation between system characteristics, case history and pump failure.

Statistical analysis of failure data provides useful information for optimisation of operation and maintenance of sewage pumps:

- decisions on either improvement of pump repairs or installation of backup capacity can be based on the statistics of the duration of failures,
- decisions on replacement of pump units can be based on the statistics of the interarrival time of failures (decreasing average interarrival time indicates ageing),
- the impacts of pump failures on serviceability of sewer systems can be estimated with simulation model accounting for the unavailability of individual pump units.

Finally, Monte Carlo simulation with added pump failures demonstrates that the serviceability of a sewer system is significantly affected by pump failures. In particular, the expected yearly CSO volume of the simplified sewer system studied increases from 21.2 mm/a without pump failure to 24.6 mm/a with pump failure, an increase of 16%.

5.3 DEGRADATION OF SEWERS

Sewer maintenance and rehabilitation are based on in-sewer inspection and monitoring. Inspection of the internal structural condition of sewers is commonly carried out by CCTV (or photographs) either from a manhole or from within the sewer. However, CCTV inspection in itself is unsuitable for directly measuring the internal structural condition. Therefore, coding of pictures by inspection personnel is required. Consequently, the assessment of sewer conditions can be subjective.

Effective investments, however, require a certain reliability of the coding of visual sewer inspections. In order to assess this reliability, the accuracy of visual inspections has been estimated using 325 examinations from the course 'Visual inspection of sewers' held by the RIONED Foundation.

Reliability of coding of visual inspections has been described with 4 criteria, including entropy of classifications, probability of incorrect coding, probability of incorrect decisions based on the classification regarding further research and replacement or cleaning of pipeline lengths. The analysis has been performed for both available pictures and observation codes as described in the Dutch guidelines (NEN 3399).

5.3.1 Available sewer inspection data

The RIONED Foundation has provided the examination results of the course 'Visual inspection of sewers' which is the entrance exam for inspection personnel in The Netherlands. It consists of three categories of questions: theoretical, visual inspection coding with both multiple-choice and open answers. Slides of (deteriorated) conduits are presented to the examinees for coding. Observation types and codes correspond to the Dutch guideline NEN 3399 and consist of three categories (A) watertightness, (B) stability and (C) gradient of flow (see Table 5.17). The codes (or classes) of each observation type vary from 1 (least severe/not present) to 5 (most severe case). Each slide is provided with a norm (correct answer) formulated by the examiners.

Only the last category of questions of the successful candidates from 1993 until 2002 has been selected. This gives a population of 325 candidates with 10 slides each. The number of times a slide has been found in the exams of successful candidates is summarised in Appendix XIII. It demonstrates that the total number of candidates having coded the same 10 pictures is 314. Several aspects (A2, A3, A4, A6, B4, C1, C2 and C3), however, have hardly been included in the exams producing less reliable estimates of coding accuracy for these aspects.

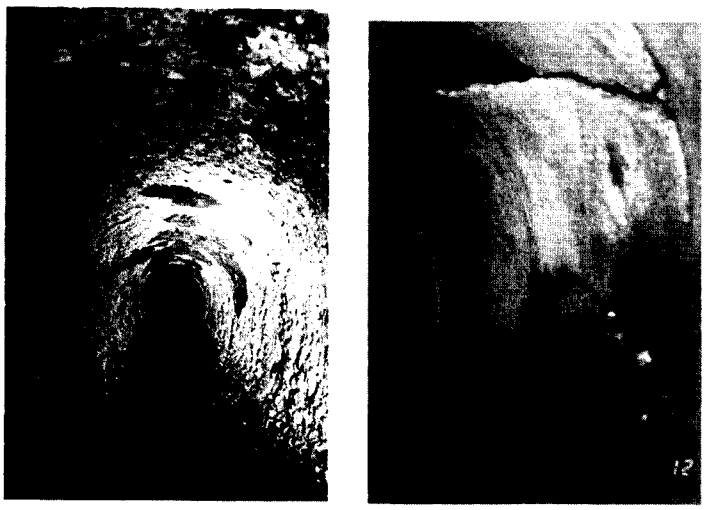

Figure 5.14 Examples of observation types (left: corrosion (B2) and right: cracks (B3)).

Table 5.17 Recommended warning and intervention criteria of sewer inspections in The Netherlands (NPR 3398).

	Observation type		Warning criterion	Intervention criterion *
LEAKTIGHTNESS	A1	infiltration of groundwater	≥3	4-5
	A2	ingress of soil from surrounding ground	≥2	-
	A3	longitudinal displacement	3-5	5
	A4	radial displacement	2-5	5
	A5	angular displacement	5	-
	A6	intruding sealing ring	3-5	5
	A7	intruding sealing material	3-5	5
STABILITY (pipe wall)	B1	break/collapse	5	-
	B2	surface damage by corrosion or mechanical action	≥3	-
	B3	fissure (cracks and fractures)	≥3	-
	B4	deformation of cross sectional shape	3-4	-
FLOW (gradient)	C1	intruding connection	3	3-5
	C2	root intrusion	2-3	3-5
	C3	fouling	2-3	3-5
	C4	encrustation of grease or other deposits (except for sand)	2-3	3-5
	C5	settled deposits (sand and waste)	2-3	3-5
	C6	other obstacles	2-3	3-5
	C7	water level	2-3	-

* In case no intervention criterion is given, inspection provides insufficient information to initiate rehabilitation, which calls for additional investigations.

In The Netherlands, a warning and an intervention criterion (NPR 3398) are applied to determine the need for maintenance and rehabilitation of sewer systems (see Table 5.17). Exceedance of the warning criterion requires further research in order to determine whether interventions are needed. In addition, exceedance of the intervention criterion initiates maintenance activities, such as cleaning, repair and replacement. The criteria concern individual observation codes and are defined in terms of ranges instead of fixed values in order to account for possible uncertainty. The accuracy of coding of visual inspections has been assessed with respect to both criteria.

5.3.2 Assessment of reliability of coding of visual inspections

Variation of coding of visual inspections has been assessed with respect to the following aspects:

- the entropy of coding results (as a measure of the variation of examination results),
- the probability of incorrect coding (compared to the norm formulated by the examiners),
- the probability of incorrect decisions regarding further research (compared to the norm formulated by the examiners and the warning criterion),
- the probability of incorrect decisions regarding interventions, such as cleaning and replacement (compared to the norm formulated by the examiners and the intervention criterion).

In particular, the last two aspects provide an estimate of the impacts of misinterpretation of visual inspections on actual maintenance and rehabilitation of sewers.

Appendix XIII summarises the coding of the slides by the examinees. The probability of an observation code and the statistical uncertainty of each observation type are shown. Observation codes are also called condition classes. Statistical uncertainty has been estimated using Bayesian analysis. However, Bayesian analysis requires conditionally independent data and the examination results may be conditionally dependent, since they represent expert opinions (see Cooke 1991). Dependence may result from identical study material, background, etc. Therefore, either the independence of coding results needs to be proven or the data need to be made conditionally independent. The latter can be achieved by analysing the probability of either correct or incorrect coding in comparison with the norm.

Table 5.18 Number of errors in examination results for different categories (type of candidate and year of examination) of candidates.

Category	Average	Std.	Min.	Max.
Inspection personnel	24.1	4.0	12.0	39.0
Others	24.9	3.7	17.0	36.0
1993 - 1997	24.6	3.9	12.0	36.0
1998 - 2002	24.3	3.9	13.0	39.0

The population of candidates is rather homogeneous because it consists of both beginners and trainees with some practical experience. Therefore, the results of their examinations can be considered independent, which enables the application of Bayesian analysis. Conditional dependence of examination candidates has been studied by comparing the average and standard deviation of the number of errors for different groups of candidates. The results show that there is no indication of significant differences in number of errors between the groups studied (Table 5.18). Therefore, it is concluded that the candidates are possibly dependent. However, the examination results should be compared with more experienced inspection personnel in order to decide whether the hypothesis of conditional dependence can be rejected or not.

The results of each observation type have been described with a multinomial distribution with 6 classes [0,1,2,3,4,5]. The sum of probabilities of the classes equals 1. The number of classes follows from the observation codes ranging from 1 to 5. In addition, class '0' describes two situations: (1) a specific defect is not visible (due to impediments) or (2) a candidate has not filled in an observation code for a specific aspect.

A stochastic variable $\mathbf{x} = (x_1,\ldots,x_k)$ has a multinomial distribution with parameters $\mathbf{p} = (p_1,\ldots,p_k)>0$ and n ($0 < p_i <1$, $\Sigma p_i < 1$, $\Sigma x_i \leq n$ and $n = 1,2,\ldots$) if the probability density function can be written as (Bernardo and Smith 1994),

$$\mathrm{Mu}_n(\mathbf{x}|p,n) = \frac{n!}{\left(\prod_{i=1}^{k} x_i!\right)\left(n-\sum_{j=1}^{k} x_j\right)!}\left(\prod_{i=1}^{k} p_i^{x_i}\right)\left(1-\sum_{j=1}^{k} p_j\right)^{n-\sum_{j=1}^{k} x_j} \tag{5.3}$$

with $x_i \geq 0$ and $\Sigma x_i \leq n$. This is the joint probability density function or likelihood of the observations x_i. The expectation and variance of the multinomial distribution are defined as,

$$E[x_i] = np_i \quad \text{and} \quad \mathrm{Var}[x_i] = np_i(1-p_i) \tag{5.4}$$

The prior distribution of the parametric vector $\mathbf{p} = (p_1,\ldots,p_k)$ can be updated with the examination results using Bayesian analysis. The conjugate prior distribution of parametric vector $\mathbf{p}$ in the multinomial distribution is a Dirichlet distribution (see Bernardo and Smith 1994) with dimension k and parameters $\boldsymbol{\alpha} = (\alpha_1,\ldots,\alpha_{k+1})$ ($\alpha_i > 0$ and $i = 1,\ldots,k+1$),

$$\pi(\mathbf{p}) = \mathrm{Di}(\mathbf{p}|\boldsymbol{\alpha}) = \frac{\Gamma\left(\sum_{i=1}^{k+1}\alpha_i\right)}{\prod_{i=1}^{k+1}\Gamma(\alpha_i)}\prod_{i=1}^{k} p_i^{\alpha_i-1}\left(1-\sum_{j=1}^{k} p_j\right)^{\alpha_{k+1}-1} \tag{5.5}$$

With a non-informative prior, the parameters α_i ($i = 1,2,\ldots,n$) in Eq. (5.5) equal,

$$\alpha_i = \begin{cases} 1 & \text{, for uniform priors} \\ 1/2 & \text{, for Jeffreys' priors} \end{cases} \tag{5.6}$$

Substituting Eq. (5.3) and Eq. (5.5) in the Bayes' theorem Eq. (3.56) gives the posterior of **p**, which is also a Dirichlet distribution. However, its parameters are updated with the observations x_i,

$$\begin{aligned} \pi(p|\mathbf{x}) &= \mathrm{Di}\left(p|\alpha_1 + x_1, \alpha_2 + x_2, \ldots, \alpha_{k+1} + n - \sum_{j=1}^{k} x_j\right) \\ &= \frac{\Gamma\left(\sum_{i=1}^{k}(\alpha_i + x_i) + \alpha_{k+1} + \left(n - \sum_{i=1}^{k} x_i\right)\right)}{\left(\prod_{i=1}^{k}\Gamma(\alpha_i + x_i)\right)\Gamma\left(\alpha_{k+1} + n - \sum_{i=1}^{k} x_i\right)}\left(\prod_{i=1}^{k} p_i^{\alpha_i + x_i - 1}\right)\left(1 - \sum_{j=1}^{k} p_j\right)^{\alpha_{k+1} + n - \sum_{j=1}^{k} x_j - 1} \\ &= \frac{\Gamma\left(\sum_{i=1}^{k+1}\alpha_i + n\right)}{\left(\prod_{i=1}^{k}\Gamma(\alpha_i + x_i)\right)\Gamma\left(\alpha_{k+1} + n - \sum_{i=1}^{k} x_i\right)}\left(\prod_{i=1}^{k} p_i^{\alpha_i + x_i - 1}\right)\left(1 - \sum_{j=1}^{k} p_j\right)^{\alpha_{k+1} + n - \sum_{j=1}^{k} x_j - 1} \end{aligned} \tag{5.7}$$

where $\Gamma(a)$ is the gamma function which is defined as,

$$\Gamma(a) = \int_{t=0}^{\infty} t^{a-1}\exp(-t)dt \tag{5.8}$$

The expected value and variance of the posterior are equal to (Bernardo and Smith 1994),

$$E[p_i] = \frac{\alpha_i + x_i}{\sum_{j=1}^{k+1}(\alpha_j + x_j)} \quad \text{and} \quad \mathrm{Var}[x_i] = \frac{(\alpha_i + x_i)\left(\sum_{j=1}^{k+1}(\alpha_j + x_j) - (\alpha_i + x_i)\right)}{\left(\sum_{j=1}^{k+1}(\alpha_j + x_j)\right)^2\left(\left(\sum_{j=1}^{k+1}(\alpha_j + x_j)\right) + 1\right)} \tag{5.9}$$

where $i = 1,\ldots,k+1$. For notational convenience x_{k+1} is defined as,

$$x_{k+1} = n - \sum_{i=1}^{k} x_i \tag{5.10}$$

The statistical uncertainty in the probability of an individual condition class i is estimated from the posterior density of p_i. The posterior density of the parameters p_i can be described with a Beta distribution with parameters α_i and α_r, since for $k = 1$ the Dirichlet distribution reduces to a Beta distribution (Bernardo and Smith 1994),

$$\mathrm{Be}(p_i|\alpha_i, \alpha_r) = \frac{\Gamma(\alpha_i + \alpha_r)}{\Gamma(\alpha_i)\Gamma(\alpha_r)} p_i^{\alpha_i - 1}(1 - p_i)^{\alpha_r - 1} \tag{5.11}$$

with,

$$\alpha_r = \left(\sum_{j=1}^{k+1} \alpha_j\right) - \alpha_i \tag{5.12}$$

The estimated statistical uncertainty is then based on the 5th and 95th percentile.

By applying Bayesian analysis, the probability of individual classes (incl. statistical uncertainty) has been updated with the examination results. The figures in Appendix XIII show that the statistical uncertainty of the calculated probability of a specific condition class decreases with increasing number of candidates.

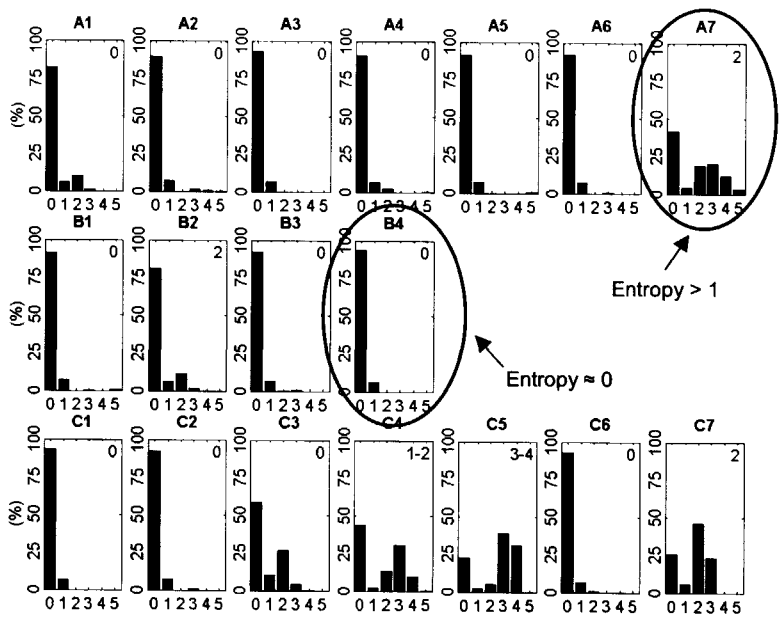

Figure 5.15 Illustration of entropy of coding of visual inspections. The larger the variation, the larger the entropy.

Entropy provides a measure of the variation of the classifications. As a result, the more different observations codes have been assigned to a specific aspect of sewer condition, the larger the entropy. It is defined as (Cooke 1991),

$$H(\mathbf{p}) = -\sum_{i=1}^{m} p_i \log(p_i) \tag{5.13}$$

where $H(\mathbf{p})$ is the entropy of a distribution function of the integers $i = 1,\ldots,M$ and p_i is the probability of an integer value i. Statistical uncertainty is not considered, since the number of observations is large.

The entropy is equal to 0 if all examination candidates give the same classification for one aspect, i.e. $p_j = 1$ for a certain j and $p_i = 0$ for $i \neq j$. Furthermore, in this specific case an entropy smaller than about 0.1 indicates a classification distributed over only 2 categories (e.g. condition type B4 in Figure 5.15) and an entropy larger than about 1 indicates a classification over 5 or more categories (e.g. condition type A7 in Figure 5.15). This figure presents the distribution of classifications for all observation types regarding one slide.

The probability of incorrect coding of visual inspections is illustrated in Figure 5.16. The probability of misinterpretation has been calculated by comparing the examination results with the norm formulated by the examiners. The norm is depicted in the upper right corner of the individual graphs. The probability of misinterpretation increases when more classifications differ from the correct answer, i.e. the 'real' condition of the sewer.

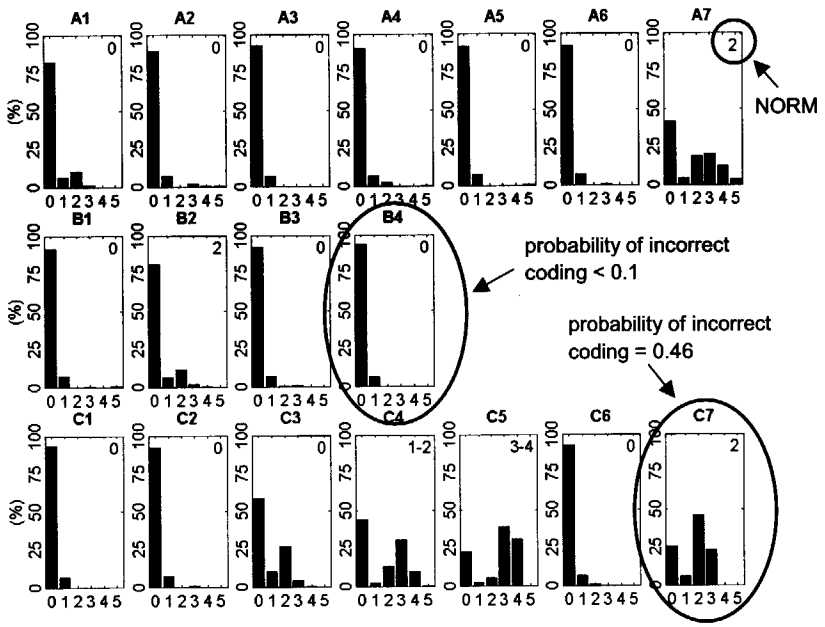

Figure 5.16 Illustration of probability of incorrect coding of visual inspections. The more classifications differ from the norm, the larger the probability.

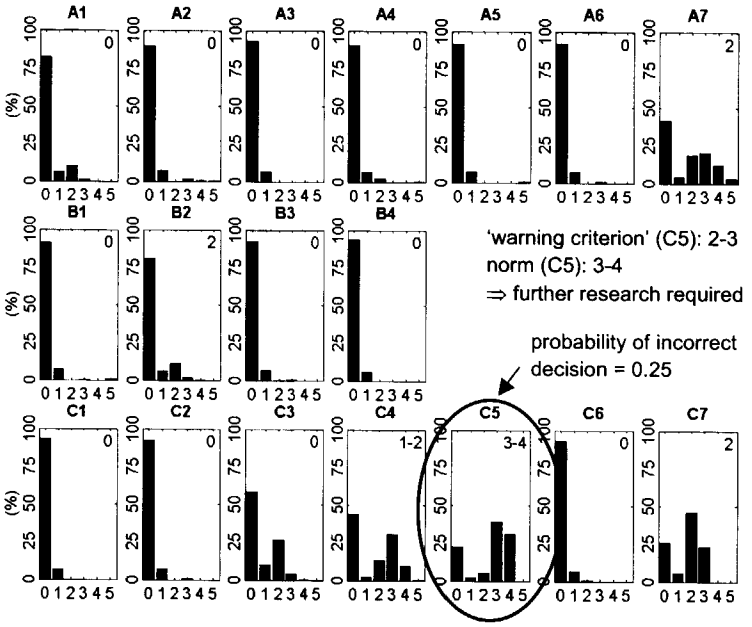

Figure 5.17 Illustration of incorrect decision-making with respect to further research. The probability of an incorrect decision depends on the warning criterion defined in NPR 3398.

The probability of wrongly performed (or omitted) further research is illustrated in Figure 5.17. Further research is needed when the classification of one or more aspects exceeds the warning criterion (NPR 3398). Its purpose is to investigate whether on further consideration the condition of the sewer reach requires rehabilitation. Incorrect impressions of the necessity of further research occur when the norm is smaller than the warning criterion but the coding suggests a higher value. Conversely, a too optimistic classification may lead to wrongly omitting further research. The probability of incorrect decisions with respect to further research has been calculated by summing the probabilities of both situations.

Correspondingly, the probability of incorrect interventions (e.g. replacement or cleaning) has been estimated. In that case, however, the intervention criterion (NPR 3398) determines the choices to be made (see Appendix XIII for results).

5.3.3 Results and discussion

The analysis demonstrates that several condition types vary considerably (see Table 5.19 and Appendix XIII). The joint entropy of a condition type has been calculated as a weighted average of all slides. The weights depend on the number of candidates which classified a specific slide.

- The entropy of the following condition types is relatively large ($H(\mathbf{p}) > 0.50$): A1, A4, A7, B2, B3, C4, C5 and C7.
- There is an increased probability of misinterpretation (Pr(misinterpretation | type) > 0.15) with respect to the following condition types: A1, A4, A7, B2, B3, C5 and C7. A larger probability of incorrect coding results in a decrease of the accuracy of prediction models for sewer condition.
- There is an increased probability of incorrect decision-making (Pr(incorrect decision | type) > 0.10) with respect to the following condition types: A4, A5, A7, B2, C4, C5 and C7. In particular, the efficiency of maintenance and rehabilitation is affected by incorrect decisions.

However, several condition types are hardly included in the examinations (less than 10% of total number). It concerns the following condition types: A2, A3, A4, A6, B4, C1, C2 and C3. As a result, conclusions on incorrect coding or decision-making are less reliable for these types.

Table 5.19 Average values of uncertainty measures for all observation types of NPR 3398.

Observation type		Entropy	Prob. incorrect coding	Prob. incorrect decisions	
				Further research	Intervention
LEAKTIGHTNESS					
ingress of soil	A2	0.39	0.10	0.10	0
longitudinal displacement	A3	0.25	0	0	0
angular displacement	A5	0.40	0.14	0.14	0
intruding sealing ring	A6	0.27	0	0	0
STABILITY					
break/collapse	B1	0.37	0.06	0.06	0
deformation of cross section	B4	0.24	0	0	0
FLOW					
intruding connection	C1	0.28	0.01	0.01	0.01
root intrusion	C2	0.40	0.04	0.03	0.01
fouling	C3	0.43	0.07	0.07	0.01
other obstacles	C6	0.39	0.01	0.02	0.02

Although the population of successful candidates consists of beginners, the analysis provides a reasonable impression of the accuracy of coding of visual inspections of sewers. On the other hand, the population is heterogeneous because both beginners and trainees with 1 or 2 years of practical experience are part of it. In order to investigate whether the observed inaccuracy changes due to increasing practical experience, the results have to be compared with coding by more experienced inspection personnel. However, such information is unavailable at the moment.

5.3.4 Concluding remarks

Apparently, there is noise in the coding of visual inspections of sewers. The accuracy of classifications is rather poor for the condition types A1, A4, A7, B2, B3, C4, C5 and C7. The majority of these types are related to blockage or leakage, which largely affect serviceability of sewer systems. Unfortunately, for some condition types (in particular A2, A3, A4, A6, B4, C1, C2 and C3) the conclusions on accuracy are less reliable because these types have only been inserted in the examinations of a relatively small number of candidates.

The contribution of inaccurate coding of sewer condition to decision-making on sewer rehabilitation has not yet been determined. Inaccurate coding may result in less reliable model predictions of future serviceability. As a result, decision-making on sewer rehabilitation becomes less reliable as well. Moreover, the probability of incorrect decision-making on additional research or interventions may reduce the efficiency of planned maintenance and rehabilitation.

The examination candidates consist of the beginners among the inspection personnel. As a result, the identified inaccuracy does not necessarily mirror the professional skills of the complete population. In order to examine whether the variation in coding of visual inspections either diverges or converges with increasing practical experience, the results should be compared with classifications by more experienced inspectors. The introduction of a re-examination (after several years in practice) can provide the necessary data.

The performance of a sewer system is significantly affected by structural deficiencies. For example, blockage of a conduit or culvert obstructs the flow and may cause flooding in upstream sections. In addition, radial displacement is indicative for irregular subsidence of sewers possibly resulting in 'lost storage'. Therefore, knowledge of sewer deterioration needs to be included in the assessment of sewer system performance. This requires a description of the deterioration of the sewer. Since the knowledge of determinative processes is limited, a stochastic description is proposed. Possible misinterpretation can be accounted for by applying a distribution function to describe the accuracy of the coding. Thus the ageing of assets and inaccuracy of inspection results can be introduced in the assessment of sewer performance.

Finally, the impacts of incorrect decision-making and inaccurate predictions of remaining service life on maintenance and rehabilitation of sewers require further research. Furthermore, the knowledge of the impact of a specific classification on the actual performance of a sewer system is rather limited and, therefore, deserves particular attention. For example, the influence of cracks on leakage and of ingress of soil on flow conditions is still unknown.

CHAPTER 6 Epilogue

6.1 SUMMARY

The research in this thesis has the objective to provide a methodology for the assessment of serviceability of sewer systems accounting for uncertainty and risk. It determines the serviceability of a sewer system with respect to environmental impacts and is based on its predicted performance. In order to account for uncertainty, several techniques for uncertainty and risk analysis have been have been applied to the assessment of the hydraulic performance and structural condition of sewers.

Chapter 1. Introduction and scope

Chapter 1 defines the scope of the research and discusses the state of the art in models describing hydraulic performance and structural condition. It also describes sewer system management in The Netherlands. Finally, the impact of uncertainties on operation and maintenance of sewer systems is introduced.

The purpose of sewer systems is to protect society from endangering of public health due to faecal contamination and flooding during storms. The majority of Dutch sewer systems (64%) are combined systems, i.e. wastewater and storm water are transported in the same pipe to the treatment plant. The remainder consists of separate sewer systems. These systems transport wastewater and storm water in separate pipes to the treatment plant or directly to surface waters respectively.

In The Netherlands, management of sewer systems is specified in several guidelines. It concerns a trade off between required serviceability and scarce financial resources. Serviceability is defined as "The ability of an asset to deliver a specific service to customers". The services offered by a sewer system consist of protection of public health and prevention of flooding provided that the quality of the environment is safeguarded. In The Netherlands, 1 billion Euros is annually invested in sewer management.

Usually, serviceability of a sewer system is assessed on the basis of model results because of insufficiency of measurements. The accuracy of the model applied depends on its extensiveness, reliability and completeness. As a consequence, each assessment of sewer serviceability can be uncertain. Hydraulic performance is assessed on the basis of calculations that support interventions reducing environmental and economic damage. Visual inspections in combination with predictions of remaining service life determine whether rehabilitation is necessary.

Chapter 2. Uncertainties

In Chapter 2, several types of uncertainties associated with sewer system management are classified. In literature, however, there is no agreement on classification of uncertainties. As a result, the methods presented to account for uncertainties are very

different. This thesis distinguishes two main types of uncertainty: inherent and epistemic. Inherent uncertainty represents randomness or variability in natural processes and is also referred to as natural variability. It comprises both uncertainties in time and space. Epistemic uncertainty represents lack of knowledge of the physical system studied and comprises model uncertainty and statistical uncertainty. The former results from lack of understanding of the physics and the latter from data insufficiency. The advantage of this classification is that it enables the reduction of individual types of uncertainty. For example, epistemic uncertainty diminishes due to increased data availability.

Assessment of sewer performance is commonly based on predicted performance levels (e.g. hydraulic modelling) or observed deficiencies (e.g. closed circuit television (CCTV) data). However, this approach has several shortcomings. Uncertainties in knowledge of system structure, system dimensions and determinative processes are ignored. In addition, natural variability of rainfall is not considered. System performance is often described with imperfect models assuming that assets are not liable to failure, such as blockage of conduits due to ingress of soil or root intrusion, subsidence of conduits and technical failure of pumps. Moreover, it assumed that deficiencies can be (visually) detected and quantified. All this leads to a too optimistic impression of sewer performance.

Estimating the costs of impacts of failure is difficult because economic valuation of environmental damage due to CSOs and indirect losses caused by flooding is subjective. In addition, performance criteria for sewer systems change through the years due to frequently changing public perception and policy-making on impact reduction.

Chapter 3. Methods for uncertainty and risk analysis

Chapter 3 discusses several techniques for estimation of uncertainties and decision-making on their reduction, including risk based economic optimisation, statistical analysis of failure data of repairable systems and Bayesian estimation methods.

By means of risk-based optimisation the optimal rehabilitation strategy of a sewer system can be determined. This not only requires the estimation of the probability of failure, but also the monetary valuation of investments and losses due to failure. The probability of failure of a system is either estimated on the basis of experience, or calculated with a probabilistic model. In this thesis, Monte Carlo sampling is predominantly applied. The optimal intervention is determined by minimising total costs consisting of both investments and losses. Expected losses are discounted over an unbounded time horizon. There are several methods available for economic valuation. However, valuation of losses is still problematic because they represent public perception of damage.

For the optimisation of repair of assets of a sewer system, an estimation of the rate of occurrence of failure events is essential. Assumptions with respect to ageing of a system and impact of failure and repair determine the choice of the failure model. Possible models are the homogeneous Poisson process (HPP) and the non-homogeneous Poisson process (HHPP). The former assumes that the interarrival times

of failures are independent and identically distributed. In addition, repair is assumed to be instantaneous and renewal. The latter can deal with ageing and 'minimal repair' of systems. In this model, failures are independent and have a time-varying rate. Model parameters are determined by means of maximum likelihood or Bayesian estimation.

Bayesian statistics combines statistical modelling of inherent and statistical uncertainty. It is based on the Bayes' theorem and updates a prior distribution with new observations. The more new observations are used, the smaller the uncertainty. Prior distributions represent 'subjective' prior knowledge and are either informative or non-informative. In this thesis, the Jeffreys' prior is primarily applied. It is a non-informative prior which is invariant under one-to-one transformations and always dimensionless. Bayes weight assessment can be applied to select a proper distribution function to describe an observed sample. Advantages of the Bayesian method are twofold: the number of candidate models considered simultaneously is not limited and there is no need of nested models.

Chapter 4. Hydraulic performance of sewer systems

Chapter 4 presents two case studies in which the impact of uncertain knowledge of sewer dimensions, natural variability of rainfall and parameter uncertainty after calibration on the predicted hydraulic performance has been examined. The catchment of 'De Hoven' is a small and relatively flat sewer system. The catchment of 'Loenen' is mildly sloping and has a relatively small in-sewer storage capacity and large average dry weather flow.

The impact of uncertain dimensions (such as storage capacity, pumping capacity, contributing area and overflow coefficient) and rainfall variability has been estimated using Monte Carlo simulation. Both sewer systems have been described with a simplified model. The uncertain system dimensions are assumed to be independent and normally distributed. Their variance is based on practical experience. Natural variability in rainfall has been described with a spatial rainfall generator.

The results show that uncertain system dimensions and rainfall variability considerably affect calculated CSO volumes per storm event. The observed variation increases with increasing return periods. Uncertainty in knowledge of sewer system dimensions results in larger expected yearly CSO volumes than natural variability in rainfall. The latter, however, causes a larger variability of CSO volume. This may result from the limitations of the rainfall generator, which underestimates the volume of frequent storm events with a duration longer than 2 hours.

In addition, Bayes weight assessment indicates that calculated CSO volumes are preferably described with a Weibull distribution. It should be noted that Bayes weights only minimise distribution type uncertainty but does not eliminate it. However, recent results show that a generalised Pareto distribution describes CSO volumes even better.

Hydrodynamic models of the sewer systems of 'De Hoven' and 'Loenen' have been calibrated with three storm events. The calibration is event-based, automatic and partly

iterative. The quality of calibration results is assessed depending upon the distribution and mean squared error of residuals, and the (relative) bias of model results.

In general, optimal parameterisation and calibrated parameter values differ between storm events. During significant time periods the relative bias is larger than acceptable, especially during dry weather flow conditions and the emptying of the system after the storm event. As a consequence, these calibration results are less reliable. The portability of calibrated parameters between storm events is limited because of time-varying inflow, infiltration capacity of soil and (industrial) discharges. Therefore, the initial conditions of each calibration are different. Portability improves when the model is calibrated with multiple events or Bayesian calibration is applied.

The impact of calibration parameter uncertainty on calculated CSO volumes has been estimated using Monte Carlo simulation. Because of the correlation between calibrated model parameters, a dependent sampling technique has been applied. Variation of calculated CSO volumes is dominated by differences between calibration events. This is in the order of the variation resulting from the uncertain dimensions of a simplified model. The variation due to uncertainty of parameters within one calibration is considerably smaller. It is also clear that, for sloping catchments, a simplified model overestimates CSO volumes. As a result, using a series of separate reservoirs may improve predictions.

The impact of uncertainties in the cost function describing environmental impacts on optimal in-sewer storage has been studied. Losses due to CSOs have been described using three types of cost functions with uncertain parameters: step, Weibull-shaped and linear. These functions have been applied to optimise in-sewer storage.

In general, the expected values and variation of optimal in-sewer storage increase because of uncertain cost parameters. However, in the case of a discrete or step function the impact of uncertain parameters is negligible. For the Weibull and linear function, the total cost function is flatter around the optimum than for the step function. This indicates a more robust solution. A linear function is preferred because it can be solved analytically and is easy to assess.

Willingness-to-pay for CSO reduction has been estimated by assuming that current Dutch standards lead to an economic optimum of in-sewer storage. For one case study, damage costs per CSO volume are on average 4.10 Euros. Compared to wastewater treatment, damage caused by CSO is approximately 12 times more expensive.

Chapter 5. Operational and structural condition of sewer systems

In Chapter 5 the impact of the operational and structural condition of a sewer system on serviceability is examined. Notwithstanding the direct impact of the condition of assets on serviceability, sewer performance is assessed assuming perfect technical functioning. Two examples of performance deficiencies affecting sewer performance have been studied: failure of sewage pumps and deterioration of conduits.

Pump failure has been studied accounting for the nature of failures, the operation and maintenance procedures, the ageing of pumps and the changes in the environment of pumps. It is defined as the inability of a pump to perform the task it was originally designed for, which is pumping at design capacity. Chronological series of failure events from Rotterdam and Amsterdam have been analysed with respect to trends in the failure rate, the interarrival time of failures, the duration of failures, the availability of pumps for wet weather flow and the time of failure during storm events.

The results show that failure characteristics of pumps in Rotterdam and Amsterdam are different. This is caused by differences in the definition of pump failure and the maintenance strategy applied. The average number of failures per year equals 13 in Rotterdam and 4 in Amsterdam, which is more often than pumps in drinking water systems, polders and wastewater treatment plants. This results from the composition of sewage and the discontinuous operation of pumps. The average duration is 10 and 13.5 hours per failure, respectively.

Often pump failures are bunched due to inadequate repairs. However, information on the nature of repairs is unavailable, since logbooks are incomplete. In addition, the failure rate shows a trend as a result of inadequate repairs, ageing, replacement or refurbishment. As a consequence, repair of sewage pumps needs to be modelled as 'minimal repair'. There is no indication for the failure of wwf pumps just at the start or the end of a storm event.

The impact of pump failure on calculated CSO volumes has been estimated using Monte Carlo simulation. For that purpose, time series of pump failures have been generated and substituted into the simplified sewer model. The interarrival time and duration of failures are derived from the observed failures in Rotterdam. The calculations show that serviceability is considerably affected by pump failures. For one case study, average CSO volumes per year are 16% larger than without pump failure. As a consequence, sewer performance can be improved by improving maintenance of pumping stations.

Assessment of sewer conditions can be subjective, since it requires interpretation by inspection personnel. In order to determine the reliability, the accuracy of visual inspections has been estimated from entrance exams for inspection personnel in The Netherlands. The reliability has been described in terms of entropy of classifications, probability of incorrect classifications and probability of incorrect decision-making with respect to maintenance and rehabilitation. The analysis has been performed for the observation codes from the Dutch guidelines (NEN 3399). The statistical uncertainty of calculated probabilities has been determined with Bayesian estimation methods.

The analysis demonstrates that the accuracy of classifications is poor for eight condition types. The majority of these aspects is related to blockage, leakage and subsidence. Since inaccurate coding of visual inspection results in less accurate predictions of remaining service life and future serviceability, decision-making on rehabilitation becomes also less reliable. As a consequence, the efficiency of interventions is reduced.

6.2 GENERAL CONCLUSION

The objective of this thesis is to provide a methodology which accounts for uncertainty and risk in the assessment of sewer performance in order to support the operation and maintenance of sewer systems. Currently, uncertainty is ignored when assessing sewer performance and an acceptable level of risk is only defined to a very limited extent. This may result in incorrect decisions. Sewer performance can be expressed in terms of serviceability, which is defined as "The ability of an asset to deliver a defined service to customers". In fact, the management of sewer infrastructure concerns a trade-off between required serviceability and scarce financial resources.

Uncertainties affecting sewer performance

In this thesis risk-based optimisation of sewer management has been successfully applied to account for uncertainties affecting the assessment of sewer performance. It is based on decision theory and requires the formulation of a cost function (describing both costs and losses) and the estimation of the probability of failure of a system. Cost functions, though subjective and debatable, have been estimated using expert knowledge, whereas failure probabilities have been calculated using Monte Carlo simulation. By applying Bayes weight assessment, distribution type uncertainty has also been accounted for.

Impact of errors in sewer database and rainfall variability on sewer performance

Errors in the sewer database and natural variability of rainfall considerably influence calculated sewer performance. The former results in larger average CSO volumes, whereas the latter has the largest impact on the variation of CSO volumes. However, rainfall variability has been described with a rainfall generator which underestimates the volume of very frequent storm events with a duration longer than 2 hours. Bayes weight assessment demonstrates that the most appropriate distribution type for CSO volumes is Weibull.

Impact of model calibration on sewer performance

The event-based calibration of a sewer model does not result in more reliable model predictions because the calibrated parameters have low portability. However, database errors can be removed during calibration, which harmonises model predictions and 'reality'. Variation of calculated CSO volumes due to differences in calibrated parameter sets based on different storm events is dominant. This variation increases with increasing return periods. Total variation is comparable to the variation due to errors in the sewer database.

Impact of uncertainty of cost parameters on optimal in-sewer storage

For a Weibull-shaped and linear cost function, uncertain cost parameters cause an increase of the expected value and variation of the optimal in-sewer storage. A step function, however, suffers from an almost negligible change. Although it is impossible

to fully capitalise environmental losses, intuitively a proportional cost function resembles the characteristics of this kind of damage. Due to its easy assessment and analytical solution, a linear cost function is preferred. If it is assumed that current Dutch standards for CSO reduction lead to an economically optimal storage volume, the damage per m^3 CSO volume is approximately 4.10 Euros per m^3 CSO volume. This is 12 times larger than the costs of treatment in a wastewater treatment plant.

Impact of failures of pumping stations on sewer performance

The failure rate of a pump can increase due to ageing or decrease due to renewal or refurbishment. Furthermore, failures of sewage pumps tend to be clustered. The analysis of failures of sewage pumps should account for the chronological order of events. The number of failures is relatively large compared to pumps in drinking water, polders and wastewater treatment plants. It varies strongly and is independent of the specific function of a pump. The average duration of failures is also highly variable and depends on the repair policy. The impact of pump failures on CSOs has been estimated with reference to the characteristics of failures in Rotterdam. Serviceability is significantly affected by the failures, since average yearly CSO volumes are more than 15% larger. Therefore, improved maintenance of sewage pumps will improve sewer performance.

Reliability of assessment of the structural condition of sewers

The assessment of the condition of the sewer is subjective, since it is partly based on the coding of pictures by inspection personnel. The accuracy of classifications is rather poor for eight condition types which are related to subsidence, blockage or infiltration/inflow. As a consequence, decision-making on sewer rehabilitation becomes less reliable. In addition, efficiency of planned maintenance and rehabilitation is reduced due to incorrect decisions. Although the population of successful candidates mainly consists of beginners, the analysis is believe to provide a reasonable impression of the accuracy of coding of visual inspections.

6.3 REMARKS ON FURTHER RESEARCH AND FUTURE APPLICATIONS

Risk-based maintenance and rehabilitation of sewer systems

In this thesis a risk-based approach to sewer maintenance and rehabilitation is proposed. It determines serviceability of a sewer system with respect to environmental impacts from predicted system performance. Flooding and public health impacts have not yet been added. However, future applications require a proper inclusion of both aspects. It is important that the approach accounts for possible uncertainties in estimated loss functions and failure probabilities, for example by means of whole life costing or scenario analysis. If a monetary valuation of impacts is difficult, multi-criteria decision analysis should be considered. In addition, there is a possibility of counting the same

impact twice, since individual aspects are partially overlapping (e.g. flooding also affects public health due to pathogens in sewage).

Since sewer systems are subject to time varying loads (rainfall and dry weather flow) and deterioration (corrosion, subsidence, blockage, etc), the approach should also consider this stochastic character of impacts. For that purpose, it should include a stochastic description of system loads (such as rainfall, infiltration and dry weather flow) and deterioration of assets (e.g. ageing of pumps and corrosion of sewers). Calculations, however, may become very time-consuming, since time series of loads and failures need to be combined randomly in a Monte Carlo analysis. Calculation time may be reduced by identifying the time-varying impacts (e.g. rainfall, soil wetness and availability of assets) causing extreme events. When random samples drawn from these stochastic variables are combined in the calculations, a set of events is generated, which includes all possible extremes.

Another important aspect is that in flat countries like The Netherlands most sewer systems are looped networks. For this type of network, the impacts of asset deterioration on system performance are more complex compared to branched networks. For example, in a branched network blockage directly causes upstream flooding, whereas in a looped network the sewage can be re-routed to the outlet (i.e. pumping station or wwtp) without causing flooding. Therefore, identified 'hot spots' of deterioration should be implemented in the analysis in order to determine their impact on the network scale. This can be computationally demanding.

Summarising, future application of risk-based maintenance and rehabilitation for sewer systems requires closer investigation of flooding and public health impacts, time-dependent failure analysis, stochastic descriptions of loads and deterioration, and network analysis. Moreover, the calculation methods applied in this thesis can be further improved. For example, the number of candidate distributions considered with the Bayes weights can be enlarged and improvement of the calibration of the hydrodynamic model can be achieved by either considering multiple instead of single events or by applying a data driven approach (e.g. neural networks) for modelling rainfall runoff. A disadvantage of data driven techniques is that their ability of extrapolation is limited.

Improving the assessment of the structural condition of sewers

Knowledge of actual impacts of observed deficiencies on serviceability and failure probability is limited. Therefore, it is to be investigated to what extent observed deficiencies affect system performance. It is recommended that the results of the examination candidates be compared with coding by more experienced inspection personnel in order to examine whether the observed inaccuracy of coding converges or diverges with increasing experience. In addition, a continuous quality assessment of inspection personnel should be introduced.

Optimisation of the maintenance of pumping stations

Analysis of pump failures provides key information for optimising maintenance of pumping stations. Successful analysis of pump failures, however, requires that recorded data describe the failure process as completely as possible. Therefore, it is recommended that the registration of failures be made uniform and pump failure is clearly defined. This will ensure that a sufficient amount of data is efficiently gathered. The registration of data on the performance of sewage pumps should include water levels in the wet well, on/off switches of the pumps, power and flow in the discharging pipe. An important indicator of the proper functioning of a pump is its efficiency, i.e. the ratio of power and flow. Below a certain efficiency level a pump should be considered 'out of operation'. In addition, logbooks should be kept in order to provide explanatory information for the pattern of the failures.

References

Aalderink H., Zoeteman A. and Jovin R. (1996). Effect of input uncertainties upon scenario predictions for the river Vecht. *Water Science and Technology*. **33** (2): 107-118.

Aalderink R.H. and Lijklema L. (1985). Water quality effects in surface waters receiving storm water discharges. In: *Water in Urban Areas. Proceedings of Technical Meeting No. 42*. April 1985. TNO Committee on Hydrological Research, The Hague.

Anderson M.J. (1999). The integration of hydraulic modelling, financial reporting, asset management and GIS in to a stormwater drainage management system. In: *Proceedings of 8th International Conference on Urban Drainage*. Sept. 1999, Sydney, Australia: 1988-1996.

Ang A.H.S. and Tang W.H. (1990). *Probability Concepts in Engineering Planning and Design. Volume II: Decision, risk and reliability*. np.

Ansell J., Archibald T., Dagpunar J., Thomas L., Abell P. and Duncalf D. (2003). Analysing maintenance data to gain insight into system performance. *Journal of the Operational Research Society*. **54**: 343-349.

Ansell J.I. and Phillips M.J. (1994). *Practical Methods for Reliability Data Analysis*. Oxford University Press, Oxford.

Appelbaum S.J. (1985). Determination of urban flood damage. *Journal of Water Resources Planning and Management*. **111** (3): 269-283.

Arnbjerg-Nielsen K., Madsen H. and Harremoës P. (1998). Formulating and testing a rain series generator based on tipping bucket gauges. *Water Science and Technology*. **37** (11). 47-55.

Ascher H. and Hansen, C.K. (1998). Spurious exponentiality observed when incorrectly fitting a distribution to nonstationary data. *IEEE Transactions on Reliability*. **47** (4): 451-459.

Ashley R. and Hopkinson P. (2002). Sewer systems and performance indicators - into the 21st century. *Urban Water*. **4** (2): 123-135.

Ashley R.M., Fraser A., Burrows R. and Blanksby J. (2000). The management of sediment in combined sewers. *Urban Water*. **2** (4): 263-275

Ashley R.M., Hvitved-Jacobsen T. and Bertrand-Krajewski J.-L. (1999). Quo Vadis Sewer Process Modelling?. *Water Science and Technology*. **39** (9): 9-22.

Assezat C. (1989). Probabilistic reliability analysis for biological waste water treatment plants. *Water Science and Technology*. **21**: 1813-1816.

Bartlett, M.S. (1963). The spectral analysis of point processes. *Journal of the Royal Statistical Society. Series B*. **25:** 264-296.

Bates B.C. and Campbell E.P. (2001). A Markov chain Monte Carlo scheme for parameter estimation and inference in conceptual rainfall-runoff modeling. *Water Resources Research*. **37** (4): 937-947.

Baur R. and Herz R. (2002). Selective inspection planning with ageing forecast for sewer pipes. *Water Science and Technology*. **46** (6-7): 389-396.

Bayes T. (1763). An essay towards solving a problem in the doctrine of chances. *Philosophical Transactions of the Royal Society of London*. **53**: 370-418.

Beck M.B. (1987). Water quality modeling: a review of the analysis of uncertainty. *Water Resources Research*. **23** (8): 1393-1442.

Beck M.B. (1996). Transient pollution events: acute risks to the aquatic environment. *Water Science and Technology*. **33** (2): 1-15.

Bedford T. and Cooke R.M. (2001) *Probabilistis Risk Analysis. Foundations and methods*. Cambridge University Press, Cambridge.

Beeldens A. and Van Gemert D. (2001). Biogene zwavelzuuraantasting: modellering versus realiteit. (in Dutch). *Rioleringswetenschap*. **1** (4): 11-34.

Beirlant J., Vynckier P. and Teugels J.L. (1996). Tail index estimation, Pareto quantile plots and regression diagnostics. *Journal of the American Statistical Association*. **91** (436): 1659-1667.

Bender M.B. and Simonovic S.P. (2000). A fuzzy compromise approach to water resource systems planning under uncertainty. *Fuzzy Sets and Systems*. **115** (1): 35-44.

Benjamin J.R. and Cornell C.A. (1979). *Probability, Statistics and Decision for Civil Engineers*. McGraw-Hill, New York.

Berger J.O. (1985) *Statistical Decision Theory and Bayesian Analysis*. Second edition. Springer, New York

Bernardo J.M. and Smith A.F.M. (1994). *Bayesian Theory*. John Wiley & Sons, Chichester.

Bielecki R. and Schremmer H. (1987). *Biogene Schwefelsäure-Korrosion in teilgefüllten Abwasserkanälen.* (in German). Sonderdruck aus Heft 94/1987 der Mitteilungen des Leichtweiss-Instituts für Wasserbau der Technische Universität Braunschweig. Technische Universität Braunschweig, Braunschweig.

Bishop P.L. (2000). *Pollution Prevention: Fundamentals and practice.* McGraw-Hill, Boston.

Bixio D., Parmentier G., Rousseau D., Verdonck F., Meirlean J., Vanrolleghem P.A. and Thoeye C. (2002). A quantitative risk analysis tool for design/simulation of wastewater treatment plants. *Water Science and Technology.* **46** (4-5): 301-307.

Blanksby J., Khan A. and Jack A. (2002). Assessment of cause of blockage of small diameter sewers. In: *Proceedings of International Conference on Sewer Operation and Maintenance. SOM 2002.* Nov. 2002, Bradford, UK. CD-ROM edition.

Blanksby J., Khan A. and Jack A. (2002). Assessment of cause of blockage of small diameter sewers. In: *Proceedings of International Conference on Sewer Operation and Maintenance. SOM 2002.* Nov. 2002, Bradford, UK. CD-ROM edition. CD-ROM edition.

Boomgaard M.E., Clemens F.H.L.R. and Langeveld J.G. (2002) Global optimisation methods in urban drainage. Application of a genetic algorithm and simulated annealing to three optimisation problems: cost optimisation, automated model calibration and monitoring network design. In: *Proceedings of 1st Annual Environment & Water Resources Systems Analysis (EWRSA) Symposium.* May 2002, Roanoke, Virginia, USA. CD-ROM edition.

Boon A.G. and Lister A.R. (1975). Formation of sulphide in rising main sewers and its prevention by injection of oxygen. *Progress in Water Technology.* **7** (2): 289-300.

Borchardt D. and Sperling F. (1997). Urban stormwater discharges: Ecological effects on receiving waters and consequences for technical measures. *Water Science and Technology.* **36** (8-9): 173-178.

Bouwknegt J. and Gelok A.J. (1988). *Regenduurlijnen voor het ontwerp en beheer van waterbeheersings- en rioleringsprojecten.* (in Dutch). Heidemij Adviesbureau, Arnhem & Landinrichtingsdienst, Utrecht.

Bowman A.W and Azzalini A. (1997). *Applied Smoothing Techniques for Data Analysis.* Clarendon Press, Oxford.

Box G.E.P. and Tiao G.C. (1973). *Bayesian Inference in Statistical Analysis.* John Wiley & Sons, Chichester.

Bras R.L. and I. Rodriguez-Iturbe (1976). Rainfall generation: A nonstationary time-varying multidimensional model. *Water Resources Research.* **12** (3): 450-456.

Brombach H., Weiss G. and Lucas S. (2002). Temporal variation of infiltration inflow in combined sewers. In: *Proceedings of 9th International Conference on Urban Drainage.* Sept. 2002, Portland, Oregon, USA. CD-ROM edition.

Buishand T.A. (1989). Statistics of extremes in climatology. *Statistica Neerlandica.* **43** (1): 1-30.

Buishand T.A. and C.A. Velds (1980). *Neerslag en verdamping. Klimaat van Nederland I.* (in Dutch). Koninklijk Nederlands Meteorologisch Instituut, De Bilt.

Butler D. (1991). The influence of dwelling occupancy and day of the week on domestic appliance wastewater discharges. *Building and Environment.* **28** (1): 73-79.

Butler D. and Davies J.W. (2001). *Urban Drainage.* E & FN Spon, London.

Butler D., Friedler E. and Gatt K. (1995). Characterising the quantity and quality of domestic wastewater inflows. *Water Science and Technology.* **31** (7): 13-24.

Campbell E.P., Fox D.R. and Bates B.C. (1999). A Bayesian approach to parameter estimation and pooling in nonlinear flood event models. *Water Resources Research.* **35** (1): 211-220.

Cardoso M.A., Coelho S.T., Matos J.S. and Matos R.S. (1999). A new approach to the diagnosis and rehabilitation of sewerage systems through the development of performance indicators. In: *Proceedings of 8th International Conference on Urban Storm Drainage.* Sept. 1999, Sydney, Australia: 610-617.

Carlin B.P. and Lewis T.A. (2000). *Bayes and Empirical Bayes Methods for Data Analysis.* Second edition. Chapman & Hall/CRC, Boca Raton.

Cashman A., Saul A.J., Savic D. and Ashley R. (2002). Whole life costing approach to sewer asset management. In: *Proceedings of International Conference on Sewer Operation and Maintenance. SOM 2002.* Nov. 2002, Bradford, UK. CD-ROM edition.

Chbab E.H., Van Noortwijk J.M. and Duits M.T. (2000). Bayesian frequency analysis of extreme river discharges. In: Tönsmann F. and Koch M. (eds.). *River Flood Defence, Proceedings of the International Symposium on Flood Defence.* Sept. 2000, Kassel, Germany. F51-F60. Kassel, Herkules Verlag.

Chow V.T., Maidment D.R. and Mays L.W. (1988). *Applied Hydrology.* McGraw-Hill, New York.

CIW (2001). *Riooloverstorten. Deel 2: Eenduidige basisinspanning.* Nadere uitwerking van de definitie van de basisinspanning. (in Dutch). June 2002. CIW, Den Haag.

Clemens F.H.L.R. (2001a). *Hydrodynamic Models in Urban Drainage: Application and calibration.* PhD thesis. Technische Universiteit Delft, Delft.

Clemens F. (2001b). A design method for monitoring networks in urban drainage. In: *Urban Drainage Modeling. Proceedings of Specialty Symposium held in conjunction with World Water and Environmental Resources Congress.* May 2001, Orlando, Florida, USA: 757-766.

Clemens F. (2001c). Calibration and verification of hydrodynamic models in urban drainage. In: *Urban Drainage Modeling. Proceedings of Specialty Symposium held in conjunction with World Water and Environmental Resources Congress.* May 2001, Orlando, Florida, USA: 61-70.

Clemens F. (2002). Evaluation of a method for the design of monitoring networks in urban drainage. In: *Proceedings of 9th International Conference on Urban Drainage.* Sept. 2002, Portland, Oregon, USA. CD-ROM edition.

Cobbaert J., Huberlant B., Provost F. and Swartenbroekx P. (1998). Hydroplan: A new approach for sewr asset management, case study Knokke-Heist. In: *Proceedings of 4th International Conference on Urban Drainage Modelling.* Sept. 1998, London, UK: 649-656.

Cooke R.M. (1991). *Experts in Uncertainty; Opinion and subjective probability in science.* Oxford University Press, Oxford.

Cox D.R. (1962). *Renewal Theory.* Methuen, London.

Cox D.R. (1972). Regression models and life tables. *Journal of the Royal Statistical Society. Series B.* **34** (2): 187-220.

Cox D.R. and Lewis P.A.W. (1966). *The Statistical Analysis of Series of Events.* Methuen, London.

Crabtree B., Hickman M. and Martin D. (1999). Integrated water quality and environmental cost-benefit modelling for the management of the River Tame. *Water Science and Technology.* **39** (4): 213-220.

Crabtree R., Garsdal H., Gent, R., Mark O. and Dørge J. (1994). MOUSETRAP - A deterministic sewer flow quality model. *Water Science and Technology.* **30** (1): 107-115.

Crow L.H. (1974). Reliability analysis for complex, repairable systems. In: *Reliability and Biometry.* Proschan F. and Serfling R.J. (eds.). SIAM, Philadelphia. 379-410.

Crowder M.J., Kimber A.C., Smith R.L. and Sweeting T.J. (1991). *Statistical Analysis of Reliability Data.* Chapman & Hall, London.

Cullen A.C. and Frey H.C. (1999). *Probabilistic Techniques in Exposure Assessment. A handbook for dealing with variability and uncertainty in models and inputs.* Plenum Press, New York.

CUR (1990). *Probabilistic Design of Flood Defences.* Report 141. Centre for Civil Engineering Research and Codes, Technical Advisory Committee on Water Defences. CUR, Gouda, the Netherlands.

CUR (1997). *Kansen in de civiele techniek. Deel 1: Probabilistisch ontwerpen in theorie.* (in Dutch). CUR-publication 190. CUR, Gouda, the Netherlands.

CUWVO Werkgroep VI (1992). *Overstortingen uit rioolstelsels en regenwaterlozingen: aanbevelingen voor het beleid en de vergunningverlening.* (in Dutch). CUWVO, Den Haag.

Davies J.P., Clarke B.A., Whiter J.T. and Cunningham R.J. (2001a). Factors influencing the structural deterioration and collapse of rigid sewer pipes. *Urban Water.* **3**: 73-89.

Davies J.P., Clarke B.A., Whiter J.T., Cunningham R.J. and Leidi A. (2001b). The structural condition of rigid sewer pipes: a statistical investigation. *Urban Water.* **3**: 277-286.

Davis N.M., Weaver V., Parks K. and Lydy M.J. (2003). An assessment of water quality, physical habitat, and biological integrety of an urban stream in Wichita, Kansas, prior to restoration improvements (Phase I). *Archives of Environmental Contamination and Toxicology.* **44** (3): 351-359.

Dawdy D.R. and J.M. Bergmann (1969). Effect of rainfall variability on streamflow simulation. *Water Resources Research.* **5** (5): 958-966.

Dawid A.P. *The Trouble with Bayes Factors.* Research Report No. 202. Department of Statistical Sciences. University College London, London.

De Haan C. (2002). Modellering van rioolstelsels tijdens water opstraat. Metingen in een schaalmodel. (in Dutch). MSc thesis. Technische Universiteit Delft, Delft.

De Saint Venant A.J.C.B. (1870). Demonstration elementaire de la formule de propogation d'une onde ou d'une intumescence dans un canal prismatique. Et remarque sur les propogations du son et de la lumière, sur les ressauts, ainsi que sur la distinction des rivières et des torrents. (in French). *Compte Rendus des Séances de l'Academie de Sciences.* **71**: 186-195.

Debo T.N. (1982). Urban flood damage estimating curves. *Journal of the Hydraulics Division.* **108** (HY10): 1059-1069.

DeGroot M.H. (1970). *Optimal Statistical Decisions.* McGraw-Hill, New York.

Desbordes M. (1978). Urban runoff and design modelling. In: *Proceedings of International Conference on Urban Storm Drainage.* Southampton, UK: 353-361.

DHI (1994). *MOUSE Reference Manual.* Edition 3.2. Danish Hydraulic Institute, Hørsholm.

Diaper C., Dixon A., Butler D., Fewkes A., Parsons S.A., Strathern M., Stephenson T. and Strutt J. (2001). Small scale recycling systems - risk assessment and modelling. *Water Science and Technology.* **43** (10): 83-90.

Dijckmeester P.N.M. (1988). *Omvang van de grondwateroverlast in het stedelijk gebied. Een inschatting.* (in Dutch). Rijkswaterstaat: Dienst Binnenwateren/RIZA, Lelystad.

Dirkzwager A.H. (1991). Sustainable development: new ways of thinking about 'water in urban areas'. *European Water Pollution Control.* **7** (1): 28-40.

Ditlevsen O. and Madsen H.O. (1996). *Structural Reliability Methods.* John Wiley & Sons, Chichester.

Djordjevic S., Prodanovic D. and Maksimovic C. (1999). An approach to simulation of dual drainage. *Water Science and Technology.* **39** (9): 95-104.

Duchesne S., Beck M.B. and Reda A.L.L. (2001). Ranking stormwater control strategies under uncertainty: the River Cam case study. *Water Science and Technology.* **43** (7): 311-320.

Efron B. and Tibshirani R.J. (1993). *An Introduction to the Bootstrap.* Monographs on Statistics and Applied Probability No. 57. Chapman & Hall, New York.

Einfalt Th., Johann G. and Pfister A. (1998). On the spatial validity of heavy point rainfall measurements. *Water Science and Technology.* **37** (11): 21-28.

Ellis J.B. and Hvitved-Jacobsen T. (1996). Urban drainage impacts on receiving waters. *Journal of Hydraulic Research.* **34** (6): 771-783.

Ellis J.B. and Marsalek J. (1996). Overview of urban drainage: environmental impacts and concerns, means of mitigation and implementation policies. *Journal of Hydraulic Research.* **34** (6): 723-731.

Ermolin Y.A., Zats L.I. and Kajisa T. (2002). Hydraulic reliability index for sewage pumping stations. *Urban Water.* **4**: 301-306.

Ertl T. (2003). Kanalmanagement im Überblick. (in German). In: *Kanalmanagement - neues Schlagwort oder alte Herausforderung?* Wiener Mitteilungen. Band 182. Institut für Wasservorsorge, Gewässerökologie und Abfallwirtschaft, BOKU Wien, Wien: B1-B29.

European Environment Agency (1999). *Environmental Indicators: typology and overview.* Technical Report No 25. European Environment Agency, Copenhagen.

European Environment Agency (2001). *Late lessons from earlywarnings: the precautionary principle 1986-2000.* Environmetal Issues Series No 22. European Environment Agency, Copenhagen.

Fenner R.A. (2000). Approaches to sewer maintenance: a review. *Urban Water.* **2**: 343-356.

Fenner R.A. and Saward G. (2002). Towards assessing sewer performance and serviceability using knowledge based systems. In: *Proceedings of 9th International Conference on Urban Drainage.* Sept. 2002, Portland, Oregon, USA. CD-ROM edition.

Fenner R.A. and Sweeting L. (1998). A Bayesian statistical model of sewer system performance using historical event data. In: *Proceedings of 6th International Conference on Hydraulics in Civil Engineering and 3rd International Symposium on Stormwater Management. HydraStorm 98.* Sept. 2001, Adelaide, Australia: 149-154.

Fenner R.A. and Sweeting L. (1999). A decision support model for the rehabilitation of 'non-critical' sewers. *Water Science and Technology.* **39** (9): 193-200.

Fewtrell L. and Bartram J. (eds.) (2001). *Water Quality: Guidelines, standards and health.* Assessment of risk and risk management for water-related infectious disease. World Health Organisation Water Series. IWA Publishing, London

Fankhauser R. (1997). Measurement properties of tipping bucket rain gauges and their influence on urban runoff simulation. *Water Science and Technology.* **36** (8-9): 7-12.

Fraser A.G., Ashley R.M., Sutherland M.M. and Vollertsen J. (1998). Sewer solids management using invert traps. *Water Science and Technology.* **37** (1): 139-146.

Fuchs L. (1998). Hydrologic modelling of urban catchments. In: Maraslek J., Maksimovic C., Zeman E. and Price R. (eds.). *Hydroinformatics Tools for Planning, Design, Operation and Rehabilitation of Sewer Systems.* Kluwer Academic Publishers, Dordecht.

Funtowicz S.O. and Ravetz J.R. (1990). *Uncertainty and Quality in Science for Policy.* Kluwer, Dordrecht.

Galambos T.V. (1992). Design codes. In: Blockley D.I. (ed.). *Engineering Safety.* McGraw-Hill, London.

Geerse H. and Vrisou van Eck N. (2001). Analyse van de meterprijs van het vervangen van vrijverval riolering. (in Dutch). HKV Lijn in water, Lelystad.

Geerse J.M.U. and Lobbrecht A.H. (2002). Assessing the performance of urban drainage systems: 'general approach' applied to the city of Rotterdam. *Urban Water.* **4**: 199-209.

Genz A.C. and Malik A.A. (1980). Remarks on algorithm 006: An adaptive algorithm for numerical integration on n-dimensional rectangular region. *Journal of Computational and Applied Mathematics.* **6** (4): 295-302.

Gérard C. and Chocat B. (1999). Prediction of sediment build-up from analysis of physical network data. *Water Science and Technology.* **39** (9): 185-192.

Gilbert A.J. and Janssen R. (1998). Use of environmental functions to communicate the values of a mangrove ecosystem under different management regimes. *Ecological Economics.* **25**: 323-346.

Green C. (2003). *Handbook of Water Economics.* John Wiley & Sons, Chichester.

Gromaire-Mertz M.C., Chebbo G. and Saad M. (1998). Origins and characteristics of urban wet weather pollution in combined sewer systems: the experimental urban catchment "Le Marais" in Paris. . *Water Science and Technology.* **37** (1): 35-43.

Grum M. (1998). Incorporating concepts from physical theory into stochastic modelling of urban runoff pollution. *Water Science and Technology.* **37** (1): 179-185.

Grum M. and Aalderink R.H. (1999). Uncertainty in return period analysis of combined sewer overflow effects using embedded Monte Carlo simulations. *Water Science and Technology.* **39** (4): 233-240.

Gupta V.K. and Waymire E.C. (1979). A stochastic kinematic study of synoptic space-time rainfall. *Water Resources Research.* **15** (3): 637-644.

Haas C.N., Rose J.B., Gerba C. and Regli S. (1993). Risk assessment of virus in drinking water. *Risk Analysis.* **15** (5): 545-552.

Haase F.J.M. and Polder R.B. (1988). Sulfidevorming in persleidingen. (in Dutch). *H_2O.* **21** (18):523-526.

Hadjianghelou H., Hadjianghelou A. and Papachristou E. (1984). Über die Berechnung zu erwartenden Sulfidbildung in Abwasserdruckrohrleitungen. (in German). *Vom Wasser.* **62**: 267-278.

Hahn M.A., Palmer R.N., Merrill M.S. and Lukas A.B. (2002). Expert system for prioritizing the inspection of sewers: knowledge base formulation and evaluation. *Journal of Water Resources Planning and Management.* **128** (2): 121-129.

Hall P. (1980). *Great Planning Disasters.* Weidenfeld & Nicolson, London.

Hanley N., Shogren J.F. and White B. (1997). *Environmental Economics in Theory and Practice.* Macmillan, Basingstoke, U.K.

Harremoës P. (1994). Integrated and stochastic features of urban drainage systems. *Water Science and Technology.* **30** (1): 1-12.

Harremoës P. (2002). Integrated urban drainage, status and perspectives. *Water Science and Technology.* **45** (3): 1-10.

Harremoës P. (2003). Ethical aspects of scientific incertitude in environmental analysis and decision making. *Journal of Cleaner Production.* **11** (7): 705-712.

Harremoës P. and Madsen H. (1999). Fiction and reality in the modelling world - Balance between simplicity and complexity, calibration and identifiability, verification and falsification. *Water Science and Technology.* **39** (9): 47-54.

Hauger M.B., Rauch W., Linde J.J. and Mikkelsen P.S. (2002). Cost benefit risk - a concept for management of integrated urban water systems? *Water Science and Technology.* **45** (3): 185-193.

Haussmann R. (1997). Strategien für Kanalreinigung. (in German). In: *GWA.* **158**. Tagungsband 30. Essener Tagung.

Henckens G.J.R., Langeveld J.G. and Van Berkum P.P. (2003) Kalibratie van het hydrodynamische rioleringsmodel van Loenen. (in Dutch). *Rioleringswetenschap.* **3** (11): 45-60.

Herz R.K. (1996). Ageing processes and rehabilitation needs of drinking water rehabilitation networks. *Journal of Water Supply Research and Technology - Aqua.* **45** (5): 221-231.

Herz R.K. (1998). Exploring rehabilitation needs and strategies for water distribution networks. *Journal of Water Supply Research and Technology - Aqua.* **47** (6): 275-283.

HKV (1999). *Overschrijdingskansen van waterstanden in het Amsterdam-Rijnkanaal en de boezem en polders van HAGV.* (in Dutch). HKV lijn in water, Lelystad, the Netherlands.

Hoffman F.O. and Hammonds J.S. (1994). Propagation of uncertainty in risk assessments: The need to distinguish between uncertainty due to lack of knowledge and uncertainty due to variability. *Risk Analysis.* **14** (5): 707-712.

Hollander M. and Wolfe D.A. (1999). *Nonparametric Statistical Methods.* Second edition. John Wiley & Sons, New York.

Hora S.C. (1996). Aleatory and epistemic uncertainty in probability elicitation with an example from hazardous waste management. *Reliability and System Safety.* **54** (2-3): 217-223.

Horton R.E. (1940). An approach toward a physical interpretation of infiltration capacity. *Soil Science Society of America Journal.* **5**: 399-427.

Hosking J.R.M. (1990). L-moments. Analysis and estimation of distributions using linear combinations of order statistics. *Journal of the Royal Statistical Society. Series B.* **52**: 105-124.

Hosking J.R.M. and Wallis J.R. (1987). Parameter and quantile estimation for the generalized Pareto distribution. *Technometrics.* **23** (3): 339-349.

House M.A. (1996). Public perception and water quality management. *Water Science and Technology.* **34** (12): 25-32.

House M.A., Ellis J.B., Herricks E.E., Hvitved-Jacobsen T., Seager J., Lijklema L., Aalderink H. and Clifford I.T. (1993) Urban drainage - Impacts on receiving water quality. *Water Science and Technology.* **27** (12): 117-158.

Høybye J. and Rosbjerg D. (1999). Effect of input and parameter uncertainties in rainfall-runoff simulations. *Journal of Hydrologic Engineering.* **4** (3): 214-224.

Høybye J.A. (1998). Model error propagation and data collection design. An application in water quality modelling. *Water, Air and Soil Pollution.* **103** (1-4): 101-119.

Huber W.C. (1995). EPA Stormwater Managent Model - SWMM. In: Singh V.P. (ed.) *Computer Models of Watershed Hydrology.* Water Resources Publications. ISBN 0918334918.

Huber W.C. and Dickinson R.E. (1988). *Storm Water Management Model User's Manual. Version 4.* Environmental Protection Agency, Athens, Georgia.

Huisman J.L. (2001). *Transport and Transformation Processes in Combined Sewers.* Schriftehreihe des Instituts für Hydromechanik und Wasserwirtschaft der ETH Zürich. Band 10. ETH Zürich, Zürich.

ITWH (1995). *Mikrocomputer in der Stadtentwässerung - Mischwasserentlastungen.* Teil 1. KOSIM. Version 4.1. Institut für technish-wissenschaftliche Hydrologie, Hannover.

IWA (2004). *Solids in Sewers.* Scientific and Technical Reports Series No. 14. IWA Publishing, London.

Jeffreys H.J. (1961). *The Theory of Probability.* Third Edition. Clarendon Press, Oxford.

Jones G.M.A. (1984). The structural deterioration of sewers. In: *Procceding of International Conference on Planning, Construction,Maintenance and Operation of Sewerage Systems.* Sept. 1984, Reading, UK: 93-108.

Joosten R.P.F. (2002). Beschikbaarheid en bedrijfszekerheid van pompinstallaties in rioolgemalen. (In Dutch). *Rioleringswetenschap.* **2** (8). 37-49.

Karassik I.J. and McGuire T. (1998) *Centrifugal Pumps.* Second edition. Chapman & Hall, New York.

Karpf C. and Krebs P. (2003). Definition und Bilanzierung von Fremdwasser. (in German). *Umwelt Praxis: Abwasser, Abfall, Management.* **10**: 35-38.

Kass R.E. and Raftery A.E. (1995). Bayes factors. *Journal of the American Statistical Association.* **90** (430): 773-795.

Keeney R.L. and Raiffa H. (1993). *Decisions with Multiple Objectives. Preferences and value tradeoffs.* Cambridge University Press, New York.

KEMA (2001). *Vaststellen van de actuele status van het rioolnet met behulp van statistiek. Fase I Kritische factoren en modelvorming.* (in Dutch). Under the authority of Stichting RIONED. KEMA, Arnhem.

Kennedy M.C. and O'Hagan A. (2001). Bayesian calibration of computer models. *Journal of the Royal Statistical Society.* **63**: 425-464.

Kerkhof J.J. (1988). Rotterdam relateert rioolbeheer aan vullingsgraad rioolstreng. (in Dutch). *Land-Water-nu.* (7-8): 47-50.

KNMI (2002). *Klimaatatlas van Nederland.* (in Dutch). KNMI, De Bilt.

König A., Sægrov S. and Schilling W. (2002). Damage assessment for urban flooding. In: *Proceedings of 9th International Conference on Urban Drainage.* Sept. 2002, Portland, Oregon, USA. CD-ROM edition.

Korving H. (2003a). Impact of failures of sewage pumps on serviceability of sewer systems. In: *Proceedings of 17th Junior Scientist Workshop on Rehabilitation of Urban Infrastructure Networks.* Sept. 2003, Neunzehnhain, Germany.

Korving H. (2003b). *Analyse pompstoringen Gemeentewerken Rotterdam.* (in Dutch). Technische Universiteit Delft, Delft.

Korving H. and Clemens F. (2002). Bayesian decision analysis as a tool for defining monitoring needs in the field of effects of CSOs on receiving waters. *Water Science and Technology.* **45** (3): 175-184.

Korving H., Clemens F., Van Noortwijk J. and Van Gelder P. (2002a). Bayesian estimation of return periods of CSO volumes for decision-making in sewer system management. In: *Proceedings of 9th International Conference on Urban Drainage*. Sept. 2002, Portland, Oregon, USA. CD-ROM edition.

Korving H., Meijer M. and Ruijgh-Van der Ploeg T. (2001). Vandaag kiezen voor morgen; analyse van onzekerheid en robuuste keuzes bij verbetering van bestaande rioolstelsels. (in Dutch). *Rioleringswetenschap.* **1** (3): 9-36.

Korving H., Van Noortwijk J., Van Gelder P. and Clemens F. (2002b). Influence of model parameter uncertainties on decision-making for sewer system management. In: *Proceedings of 5th International Conference Hydroinformatics.* July 2002, Cardiff, UK: 1361-1366.

Korving H., Van Noortwijk J.M., Van Gelder P.H.A.J.M. and Parkhi R.S. (2003). Coping with uncertainty in sewer system rehabilitation. In: *Proceedings of European Safety and Reliability Conference 2003.* ESREL 2003. Safety and Reliability. June 2003, Maastricht, the Netherlands: 959-967.

Langeveld J.G. (2004). *Interactions within the Wastewater System.* PhD thesis. Technische Universiteit Delft, Delft.

Lawless J.F. and Nadeau C. (1995). Some simple robust methods for the analysis of recurrent events. *Technometrics.* **37** (2): 158-168.

Le Gat Y. and Eisenbeis P. (2000). Using maintenance records to forecast failures in water networks. *Urban Water.* **2** (3): 173-181

Le Gauffre P., Joannis C., Gibello C. and Breysse D. (2002). Performance indicators and decision support for rehabilitation of sewer networks. Contribution of the French R&D RERAU program. In: *Proceedings of International Conference on Sewer Operation and Maintenance. SOM 2002.* Nov. 2002, Bradford, UK. CD-ROM edition.

Lee L.T. and Essex T.L. (1983) Urban headwater flooding damage potential. *Journal of Hydraualic Engineering.* **109** (4): 519-535.

Lei J. and Sægrov S. (1998). Statistical approach for describing the lifetime of water mains - case Trondheim municipality. In: *Proceedings of 19th IAWQ Biennial International Conference on Water Quality.* June 1998, Vancouver, Canada: 206-213.

Lei J., Li J. and Schilling W. (1999) procedure of urban runoff design model and an alternative of Monte-Carlo simulation. In: *Proceedings of 8th International Conference on Urban Drainage.* Sept. 1999, Sydney, Australia: 973-981.

Lei J.H. and Schilling W. (1996). Preliminary uncertainty analysis - A prerequisite for assessing the predictive uncertainty of hydrological models. *Water Science and Technology.* **33** (2): 79-90.

Lewis P.A.W. (1967). Non-homogeneous branching Poisson processes. *Journal of the Royal Statistical Society. Series B.* **29** (2): 343-354.

Lewis P.A.W. (1972). Recent results in the statistical analysis of univariate point processes. In: Lewis P.A.W. (ed.). *Stochastic Point Processes: Statistical analysis, theory and applications.* Wiley-Interscience, New York: 1-54.

Ljung L. and Glad T. (1994). *Modelling of Dynamic Systems.* Prentice Hall, Englewood Cliffs.

Loke E., Warnaars E.A., Jacobsen P., Nelen F. and Almeida M. (1997). Artificial neural networks as a tool in urban storm drainage. *Water Science and Technology.* **36** (8-9): 101-109.

Lorenz C.M. (1999). *Indicators for Sustainable River Management.* PhD thesis. Vrije Universiteit, Amsterdam.

Lovejoy S and Mandelbrot B.B. (1985). Fractal properties of rain and a fractal model. *Tellus.* **37A** (3): 209-232.

Lovejoy S. and Schertzer D. (1995). Multifractals and rain. In: Kundzewicz Z.W. (ed.). *New Concepts in Hydrology and Water Resources.* Cambridge University Press, Cambridge: 61-103.

Luyckx G., Willems P. and Berlamont J. (1998). Influence of the spatial variability of rainfall on sewer system design. In: Wheather H. and C. Kirkby (eds.). *Hydrology in a Changing Environment.* Vol III: 339-349. John Wiley & Sons, Chichester.

Magne G., Phan L., Price R. and Wixcey J. (1996). Validation of HYDROWORKS-DM, a water quality model for urban drainage. In: *Proceedings of the 7th International Conference on Urban Storm Drainage.* Sept. 1996, Hannover, Germany: 1359-1364.

Maidment D.R. (1993). *Handbook of Hydrology.* McGraw-Hill, New York.

Maksimovic C. and Prodanovic D. (2001). Modelling of urban flooding - Breakthrough or recycling outdated concepts. In: *Urban Drainage Modeling. Proceedings of Specialty Symposium held in conjunction with World Water and Environmental Resources Congress.* May 2001, Orlando, Florida, USA: 1-9.

Matos R., Cardoso A., Ashley R., Duarte P. Molinari A, and Schultz A. (2003). *Performance Indicators for Wastewater Services.* IWA Publishing, London.

Mays L.W. (1989). *Reliability Analysis of Water Distribution Systems.* American Society of Civil Engineers, New York.

McBean E.A., Gorrie J., Fortin M., Ding J. and Moulton R. (1988). Flood depth-damage curves by interview survey. *Journal of Water Resources Planning and Management.* **114** (6): 613-634.

Meijer M.H. and Ruijgh-van der Ploeg M. (2001). Critical factors in strategic planning for infrastructure design. In: Weijnen M.P.C., Baueer J.M., Chamoux J.-P., Eherenfeld J.R. and Jones D.N. (eds.) *Walking a Thin Line in Infrastructures. Balancing short term goals and long term nature.* DUP Science, Delft.

Meirlaen J., Huyghebaert B., Sforzi F., Benedetti L. and Vanrolleghem P. (2001). Fast, simultaneous simulation of the integrated urban wastewater system using mechanistic surrogate models. *Water Science and Technology.* **43** (7): 301-309.

Ministerie van Financiën (1995). *Kabinetsstandpunt heroverweging disconteringsvoet.* The Hague, the Netherlands.

Ministerie van VROM (1989). *Eindrapportage en evaluatie van het onderzoek 1982-1989.* (in Dutch). Nationale Werkgroep Riolering en Waterkwaliteit. Staatsuitgeverij/DOP, 's Gravenhage.

Mood A.M., Graybill F.A. and Boes D.C. (1974). *Introduction to the Theory of Statistics.* Third edition. McGraw-Hill, Singapore.

Morgan M.G. and Henrion M. (1990). *Uncertainty: a guide to dealing with uncertainty in quantitative risk and policy analysis.* Cambridge University Press, Cambridge.

Müller K. and Dohmann M. (2002a). *Entwicklung eines allgemein anwendbaren Verfahrens zur selektiven Erstinspektion von Abwasserkanälen und Anschlussleitungen, Abschlussbericht Teil A: wissenschaftliche Untersuchungen.* (in German). Institut für Siedlungswasserwirtschaft der RWTH Aachen (ISA), Aachen.

Müller K. and Dohmann M. (2002b). *Entwicklung eines allgemein anwendbaren Verfahrens zur selektiven Erstinspektion von Abwasserkanälen und Anschlussleitungen Abschlussbericht Teil C: Handlungsanleitung.* (in German). Institut für Siedlungswasserwirtschaft der RWTH Aachen (ISA), Aachen.

Murray J.B. (1987). Infiltration rates for separated sewage collection. *Water Science and Technology.* **19** (3-4): 589-601.

NEN 3399. *Buitenriolering. Classificatiesysteem bij visuele inspectie van riolen.* (in Dutch). April 1992.

NEN-EN 752-2. *Drain and Sewer Systems Outside Building. Part 2: Performance requirements.* Sept. 1996.

NEN-EN 752-4. *Drain and Sewer Systems Outside Building. Part 4: Hydraulic design and environmental considerations.* March 1998.

NEN-EN 752-5. *Drain and Sewer Systems Outside Building. Part 5: Rehabilitation.* March 1998.

NEN-EN 752-6. *Drain and Sewer Systems Outside Building. Part 6: Pumping installations.* Sept. 1998.

NEN-EN 752-7. *Drain and Sewer Systems Outside Building. Part 7: Maintenance and operations.* Sept. 1998.

Nielsen P.H. and Hvitved-Jacobsen T. (1988). Effect of sulfate and organic matter on the hydrogen sulfide formation in biofilms of filled sanitary sewers. *Journal of the Water pollution Control Federation.* **60**: 627-634.

Nijkamp P. and Van den Bergh J.C.J.M. (1997) New advances in economic modelling and evaluation of environmental issues. *European Journal of Operational Research.* **99** (1): 180-196.

Nix S.J. (1994). *Urban Stormwater Modeling and Simulation.* Lewis Publishers, Boca Raton.

Novotny V. and Witte J.W. (1997). Ascertaining aquatic ecological risks of urban stormwater discharges. *Water Research.* **31** (10): 2573-2585.

Novotny, V., Clark, D., Griffin, R.J. & Booth, D. (2001). Risk based urban watershed management under conflicting objectives. *Water Science and Technology.* **43** (5): 69-78.

NPR 3220. *Buitenriolering. Beheer.* (in Dutch). February 1994.

NPR 3398. *Buitenriolering. Inspectie en toestandsbeoordeling van riolen.* (in Dutch). April 1992.

NWRW (1989a). *De vuiluitworp van gemengde rioolstelsels. Eindrapport.* Rapport 5.2. (In Dutch). April 1989. Ministerie van VROM, Den Haag.

NWRW (1989b). *Effecten van emissies op oppervlaktewater.* Hoofdrapport 9.1. (in Dutch). July 1989. Ministerie van VROM, Den Haag.

NWRW (1990). *Effecten van emissies op oppervlaktewater.* Lokatierapporten 9.1. (in Dutch). December 1990. Ministerie van VROM, Den Haag.

OFWAT (2001). *Development of Enhanced Serviceability Indicators for Sewerage Assets.* Final Report. Oct. 2001. OFWAT and Environment Agency, UK.

Oliveri E. and Santoro M. (2000). Estimation of urban structural flood damages: the case study of Palermo. *Urban Water.* **2** (3): 223-234.

Pandey M.D. (1998). Probabilistic models for condition assessment of oil and gas pipelines. *NDT&E International.* **31** (5): 349-358.

Pandey M.D. and Nathwani J.S. (2003). Canada wide standard for particulate matter and ozone: cost-benefit analysis using Life Quality Index. *Risk Analysis.* **23** (1): 55-67.

Pecher R. (1994). Bau- und Betriebskosten bestehender Anlagen zur Abwasserentsorgung in der Bundesrepublik Deutschland. (in German). *Korrespondenz Abwasser.* **41** (12): 2188-2194.

Pedersen E.R. and Perkins M.A. (1986). The use of benthic invertebrate data for evaluating impacts of urban runoff. *Hydrobiologia.* **139**: 13-22.

Penman H.L. (1948). Natural evaporation from open water, bare soil and grass. *Proceedings of the Royal Society of London. Series A.* **193**:120-145.

Penning-Rowsell E., Johnson C., Tunstall S., Tapsell S., Morris J., Chatterton J., Coker A. and Green C. (2003). *The Benefits of Flood and Coastal Defence: Techniques and Data for 2003.* Draft version. Flood Hazard Research Centre, Middlesex University, London.

Peters D.C. (1984). The social costs of sewer rehabilitation. In: *Procceding of International Conference on Planning, Construction,Maintenance and Operation of Sewerage Systems.* Sept. 1984, Reading, UK: 79-91.

Plenker T. (2002). Computer aided decision support on choosing the right technology for sewer rehabilitation. *Water Science and Technology.* **46** (6-7): 403-410.

Pohl R. (2002). Ausfallhäufigkeit von Verschlüssen in der Wasserversorgung und Abwassertechnik. (In German). In: *Dresdner Berichte Band 19. Wasserbauliche Mitteilungen Heft 21.* Technische Universität Dresden, Dresden: 209-226.

Poinard D., Le Gauffre P. and Haidar H. (2003). Markov model and climate factors for the rehabilitation planning of water networks. In: *Proceedings of 17th Junior Scientist Workshop on Rehabilitation of Urban Infrastructure Networks.* Sept. 2003, Neunzehnhain, Germany.

Pomeroy R.D. (1959). Generation and control of sulfide in filled pipes. *Sewage and Industrial Wastes.* **31**: 1082-1095

Pomeroy R.D. (1974). *The Problem of Hydrogen Sulphide in Sewers.* Clay Pipe Development Ass. Ltd.

Pomeroy R.D. and Parkhurst J.D. (1977). The forecasting of sulphide build-up rates in sewers. *Progress in Water Technology.* **9**: 621-628.

Portielje R., Hvitved-Jacobsen T. and Schaarup-Jensen K. (2000). Risk analysis using stochastic reliability methods applied to two cases of deterministic water quality models. *Water Research.* **34** (1): 153-170.

pr EN 13508-2. *Condition of Drain and Sewer Systems Outside Building. Part 2: Visual inspection coding systems.* Final draft. March 2001.

Pratt J.W., Raiffa H. and Schlaifer R. (1995). *Introduction to Statistical Decision Theory.* MIT Press, Cambridge.

Pratt J.W., Raiffa H. and Schlaifer R. (1995). *Introduction to Statistical Decision Theory.* MIT Press, Cambridge.

Price R.K. and Osborne M.P. (1986). Verification of sewer simulation models. In: *Proceedings of the International Symposium on Comparison of Urban Drainage Models with Real Catchment Data.* UDM'86. Dubrovnik, Yugoslavia: 99-106.

Price R.K. and Catterson G.J. (1997). Monitoring and modelling in urban drainage. *Water Science and Technology.* **36** (8-9): 283-287.

Rackwitz R. and Fiessler B. (1978). Structural reliability under combined random load sequences. *Computers and Structures.* **9** (5): 489-494.

Rauch W., Bertrand-Krajewski J.-L., Krebs P., Mark O., Schilling W., Schütze M. and Vanrolleghem P.A. (2002). Deterministic modelling of integrated urban drainage systems. *Water Science and Technology.* **45** (3): 81-94.

Rauch W., Thurner N. and Harremoës P. (1998). Required accuracy of rainfall data for integrated urban drainage modeling. *Water Science and Technology.* **37** (11): 81-89.

Reda A.L.L. and Beck M.B. (1997). Ranking strategies for stormwater management under uncertainty: sensitivity analysis. *Water Science and Technology.* **36** (5): 357-371.

Reichert P. (1997). On the necessity of using imprecise probabilities for modelling environmental systems. *Water Science and Technology.* **36** (5): 149-156.

Ribius F.J. (1951). Waterverontreiniging door regenoverstorten. (in Dutch). *Publieke Werken.* **19.**

Rigdon E.R. and Basu A.P. (2000). *Statistical Methods for the Reliability of Repairable Systems.* Wiley & Sons, New York.

Rogers M.D. (2001). Scientific and technological uncertainty, the precautionary principle, scnenarios and risk management. *Journal of Risk Research.* **4** (1): 1-15.

Rosenblatt M. (1952). Remarks on a multivariate transformation. *Annals of Mathematical Statistics.* **23** (3):470-472.

Rosenhead J. (1989). Robustness analysis: Keeping your options open. In: Rosenhead J. (ed). *Rational Analysis for a Problematic World..* John Wiley & Sons, Chicester.

Rostum J., Baur R., Sægrov S. and Schilling W. (1999). Predictive service-life models for urban water infrastructure management. In: *Proceedings of 8th International Conference on Urban Storm Drainage.* Sept. 1999, Sydney, Australia: 594-601.

Rousseau D., Verdonck F., Moerman O., Carrette R., Thoeye C., Meirlaen J. and Vanrolleghem P.A. (2001). Development of a risk assessment based technique for design/retrofitting of WWTPs. *Water Science and Technology.* **43** (7): 287-294.

Ruijgrok E.C.M. (1999). *Valuation of Nature in Coastal Zones.* PhD thesis. Vrije Universiteit, Amsterdam.

Sægrov S. and Schilling W. (2002). Computer aided rehabilitation of sewer and storm water networks. In: *Proceedings of 9th International Conference on Urban Drainage.* Sept. 2002, Portland, Oregon, USA. CD-ROM edition.

Sægrov S., Melo Baptista J.F., Conroy P., Herz R.K., Le Gauffre P., Moss G., Oddevald J.E., Rajani B. and Schiatti M. (1999). Rehabilitation of water networks survey of research needs and on-going efforts. *Urban Water.* **1** (1): 15-22.

Saul A.J. (2002). CSO: State of the art review. In: *Proceedings of 9th International Conference on Urban Drainage.* Sept. 2002, Portland, Oregon, USA. CD-ROM edition.

Schaum C.A. (2001). *Untersuchung der Prozessabläufe in der Kanalisation am Beispiel Apeldoorn.* (In German). MSc thesis. Technische Universiteit Delft, Delft.

Schilling W. (1984). Effect of Spatial Rainfall Distribution on Sewer Flows. *Water Science and Technology.* **16** (8-9): 177-188.

Schilling W. and Fuchs L. (1986). Errors in stormwater modelling - A quantitative assessment. *Journal of Hydraulic Engineering.* **112** (2): 111-123.

Schmitt T.G., Schilling W., Sægrov S. and Nieschultz K.-P. (2002). Flood risk management for urban drainage systems by simulation and optimisation. In: *Proceedings of 9th International Conference on Urban Drainage.* Sept. 2002, Portland, Oregon, USA. CD-ROM edition.

Schütze M.R., Butler D. and Beck M.B. (2002). *Modelling, Simulation and Control of Urban Wastewater Systems.* Springer Verlag, London.

Schwartz M.J.C. (1989). *De invloed van storingen op de overstortingsfrequentie van een rioolstelsel.* Een reële benadering van de overstoritngsprobbiematiek van het gemengde rioolstelsel van Loenen (Veluwe). MSc thesis. (In Dutch). Landbouwuniversiteit Wageningen, Wageningen.

Sevruk B. (1982). *Methods of Correction for Systematic Error in Point Precipitation Measurement for Operational Use.* Operational Hydrology Report No.21. WMO - No.589. World Meteorological Organization, Geneva.

Sevruk B. (1996). Adjustment of tipping-bucket orecipitation gauge measurements. *Atmospheric Research.* **42** (1-4): 237-246.

Shanahan P., Henze M., Koncsos L., Rauch W., Reichert P. Somlyódy L. and Vanrolleghem P. (1998) River water quality modelling: II. Problems of the art. *Water Science and Technology.* **38** (11): 245-252.

Shebab-Eldeen T. and Moselhi O. (2001). A decision support system for rehabilitation of sewer pipes. *Canadian Journal of Civil Engineering.* **28**: 394-401.

Slijkhuis K.A.H., Van Gelder P.H.A.J.M., Vrijling J.K. and Vrouwenvelder A.C.W.M. (1999). On the lack of information in hydraulic engineering models. In: Schüller G.I. and Kafka P. (eds.). *Safety and Reliability. Proceedings of Esrel '99 - 10th European Conference on Safety and reliability.* Munich-Garching, Germany: 713-718.

Snow J. (1854). *On the Mode of Communication of Cholera.* Second extended edition. John Churchill, New Burlington Street, London.

Sprent P. and Smeeton N.C. (2001). *Applied Nonparametric Statistical Methods.* Third edition. Chapman & Hall/CRC, Boca Raton.

Stein D. (2001). *Rehabilitation and Maintenance of Drains and Sewers.* Ernst & Sohn, Berlin.

Stichting RIONED (1994). *Leidraad Riolering. Module A1100.* Doelen, functionele eisen, maatstaven en meetmethoden. (in Dutch). July 1994. Kluwer, Alphen aan de Rijn, the Netherlands.

Stichting RIONED (1996). *Leidraad Riolering. Module B1200.* Verbetering van bestaande riolering. (in Dutch). March 1996. Kluwer, Alphen aan de Rijn, the Netherlands.

Stichting RIONED (1997a). *Leidraad Riolering. Module C2400.* Inspectie en beoordeling. (in Dutch). September 1997. Kluwer, Alphen aan de Rijn, the Netherlands.

Stichting RIONED (1997b). *Leidraad Riolering. Module D1100.* Kostenkengetallen. (in Dutch). May 1997. Kluwer, Alphen aan de Rijn, the Netherlands.

Stichting RIONED (1998). *Leidraad Riolering. Module C3000.* keuze en uitvoering van beheermaatregelen. (in Dutch). May 1998. Kluwer, Alphen aan de Rijn, the Netherlands.

Stichting RIONED (1999). *Leidraad Riolering. Module C2100.* Rioleringsberekeningen, hydraulisch functioneren. (in Dutch). July 1999. Kluwer, Alphen aan de Rijn, the Netherlands.

Stichting RIONED (2002). *Riool in cijfers 2002-3003.* (in Dutch). Stichting RIONED, Ede, the Netherlands.

Stichting RIONED, Stowa and WRW (1999). *Onderzoek naar de effecten van een verbeterd stelselontwerp op de vuilemissie en waterkwaliteit. Meetlocatie Dorp-Oost te Stolwijk, gemeente Vlist.* (in Dutch). Reportno. 632/ZF99/1728/07506.

Stok J. (2003). *Invloed avn influentfluctuaties op de werking van een afvalwaterzuivering.* (in Dutch). MSc thesis. Technische Universiteit Delft, Delft.

Streiner C. and Loomis J.B. (1995). Estimating the benefits of urban stream restoration using the hedonic price method. *Rivers – Studies in the Science, Environmental Policy, and Law of Instream Flow.* **5** (4): 267-278.

Tang W.H. (1980). Bayesian frequency analysis. *Journal of the Hydraulics Division.* **106** (HY7): 1203-1218.

Thauvin V. , E. Gaume and C. Roux (1998). A short time-step point rainfall stochastic model. *Water Science and Technology.* **37** (11): 37-45.

Thistlethwayte D.K.B. (ed.) (1972). *The Control of Sulphide in Sewerage Systems.* Butterworths, London.

Thyregod P., K. Arnbjerg-Nielsen, H. Madsen and J. Carstensen (1998). Modelling the embedded rainfall process using tipping bucket data. *Water Science and Technology.* **37** (11): 57-64.

Tung Y.-K., Wang P.-Y. and Yang U.-C. (1993). Water resources projects evaluation and ranking under economic uncertainties. *Water Resources mangement.* **7**: 311-333.

UKWIR (2002). *Capital Maintenance Planning: A common framework.* UKWIR Report No. 02/05/3. UKWIR/Tynemarch.

Vaes G. (1999). *The Infuence of Rainfall and Model Simplification on Combined Sewer System Design.* PhD thesis. Katholieke Universiteit Leuven, Leuven.

Vaes G., Clemens F., Willems P. and Berlamont J. (2002). Design rainfall for combined sewer system calculations. Comparison between Flanders and the Netherlands. In: *Proceedings of 9th International Conference on Urban Drainage.* Sept. 2002, Portland, Oregon, USA. CD-ROM edition.

Van Dantzig D. (1956). Economic decision problems for flood prevention. *Econometrica.* **24**: 276-287.

Van de Ven F.H.M. (1989). *Van neerslag tot rioolinloop in vlak gebied.* (in Dutch). PhD thesis. Van zee tot land No.57. Ministerie van Verkeer en Waterstaat, Rijkswaterstaat, Lelystad, the Netherlands.

Van den Akker J. (1952). *Rioleringen. Deel 1. Het ontwerpen en berekenen van een rioolnet.* (in Dutch). Sijthoffs Uitgeversmaatschappij, Leiden.

Van der Bolt F.J.E. and Kok M. (2000). *Hoogwaternormering Regionale Watersystemen. Schademodellering.* (in Dutch). HKV Lijn in water/Alterra, Lelystad.

Van der Sluijs J.P. (1997). *Anchoring amid uncertainty. On the management of uncertainties in risk assessment of anthropogenic climate change.* PhD thesis. Universiteit Utrecht, Utrecht.

Van Gelder P.H.A.J.M. (2000). *Statistical Methods for the Risk-Based Design of Civil Structures.* PhD thesis. Communications on Hydraulic and Geotechnical Engineering. Technische Universiteit Delft, Delft.

Van Gelder P.H.A.J.M., Van Noortwijk J.M. and Duits M.T. (1999). Selection of probability distributions with a case study on extreme Oder discharges. In: Schuëller G.I. and Kafka P. (eds.). *Proceedings of ESREL '99 10th European Safety and Reliability Conference 2003.* September 1999, Munich-Garching, Germany: 1475-1480.

Van Gelder P.H.A.J.M., Vrijling J.K. and Slijkhuis K.A.H (1997). Coping with uncertainty in the economical optimization of a dike design. In: *Water for a Changing Global Community.* ASCE, New York: 554-559.

Van Gestel P. (2002). Vastestellen actuele status riolering met behulp van statistiek. (in Dutch). In: Korving H. (ed.). *Rioolbeheer: de risico's in de hand.Voordrachtenbundel Symposium.* Sept. 2002, Delft, the Netherlands: 9-14.

Van Luijtelaar H. (1999). Design criteria, fooding of sewre systems in 'flat areas'. In: *Proceedings of 8th International Conference on Urban Drainage.* Sept. 1999, Sydney, Australia: 538-545.

Van Luijtelaar H. and Rebergen E.W. (1997). Guidelines for hydrodynamic calculations on urban drainage in the Netherlands: backgrounds and examples. *Water Science and Technology.* **36** (8-9): 253-258.

Van Mameren H. and Clemens F. (1997). Guidelines for hydrodynamic calculations on urban drainage in the Netherlands: overview and principles. *Water Science and Technology.* **36** (8-9): 247-252.

Van Nieuwenhuijzen A.F. (2002). *Scenario Studies into Advanced Particle Removal in the Physical-Chemical Pre-treatment of Wastewater.* PhD thesis. Technische Universiteit Delft, Delft.

Van Noortwijk J.M. (1996). *Optimal Maintenance Decisions for Hydraulic Structures under Isotropic Deterioration.* PhD thesis. Delft University of Technology, Delft.

Van Noortwijk J.M., Kalk H.J., Duits M.T. and Chbab E.H. (2001). The use of Bayes factors for model selection in structural reliability. In: *Proceedings of 8th International Conference on Structural Safety and Reliability (ICOSSAR).* June 2001, Newport Beach, California, USA.

Van Noortwijk J.M., Kalk H.J., Duits M.T. & Chbab E.H. (2004). *Bayesian Statistics for Flood Prevention.* Rijkswaterstaat RIZA & HKV Consultants, Lelystad.

Van Noortwijk J.M., Kok M. and Cooke R.M.(1997). Optimal decisions that reduce flood damage along the Meuse: an uncertainty analysis. In: French S. and Smith J.Q. (eds.). *The Practice of Bayesian Analysis.* Arnold, London: 151-172.

Van Zon H. (1986). *Een zeer onfrisse geschiedenis; studies over niet industriële verontreiniging in Nederland.* (in Dutch). Staatsuitgeverij, Den Haag.

Vanrolleghem P.A. and Keesman K.J. (1996). Identification of biodegredation models under model and data uncertainty. *Water Science and Technology.* **33** (2): 91-105.

Verdonck F.A.M., Jaworska J., Thas O. and Vanrolleghem P.A. (2001). Determining environmental standards using bootstrapping, Bayesian and maximum likelihood techniques: a comparative study. *Analytica Chimica Acta.* **446**: 429-438.

Vreugdenhil C.B. (1989). *Computational Hydraulics: an introduction.* Springer Verlag, Berlin.

Walker W.E., Rahman S.A. and Cave J. (2001). Adaptive policies, policy analysis, and policy-making. *European Journal of Operational Research.* **128** (2): 282-289.

Wallingford Software (2000). *HydroWorks Documentation.* On-line documentation. Version 6.0. Wallingford Software Ltd.

Water Research Centre (2001). *Sewer Rehabilitation Manual.* 4th edition, version 2. Water Research Centre, UK.

Waymire E. and Gupta V.K. (1981). The mathematical structure of rainfall representations 1. A review of the stochastic rainfall models. *Water Resources Research.* **17** (5): 1261-1282.

Waymire E., Gupta V.K. and Rodriguez-Iturbe I. (1984). A spectral theory of rainfall intensity at the meso-β scale. *Water Resources Research.* **20** (10): 1453-1465.

Willems P. (2000). *Probabilistic Immission Modelling of Receiving Surface Waters.* PhD thesis. Katholieke Universiteit Leuven, Leuven.

Willems P. (2001a). A spatial rainfall generator for small spatial scales. *Journal of Hydrology.* **252**: 126-144.

Willems P. (2001b). Stochastic description of the rainfall input errors in lumped hydrological models. *Stochastic Environmental Research and Risk Assessment.* **15** (2): 132-152.

Willems P. and Berlamont J. (1999). Probabilistic modelling of sewer system overflow emissions. *Water Science and Technology.* **39** (9): 47-54.

Willems P. and J. Berlamont (2002). Accounting for the spatial rainfall variability in urban modelling applications. *Water Science and Technology.* **45** (2): 105-112.

Williams K.J., Clarke B.A. and Ridgers D.F. (2002). An investigation into the deterioration of mortar sewer joints. In: *Proceedings of International Conference on Sewer Operation and Maintenance. SOM 2002.* Nov. 2002, Bradford, UK. CD-ROM edition.

Wilson C.B., J.B. Valdez and I. Rodriguez-Iturbe (1979). On the influence of the spatial distribution of rainfall on storm runoff. *Water Resources Research.* **15** (2): 321-328.

Wingo D.R. (1989). The left-truncated Weibull distribution: theory and computation. *Statistical Papers.* (Statistische Hefte). **30**: 39-48.

Wirahadikusumah R., Abraham D.M., Iseley T. and Prasanth R.K. (1998). Assessment technologies for sewer system rehabilitation. *Automation in Construction.* **7**: 259-270.

Wixcey J.R., Lewy M. and Price R.K. (1992). Computational modelling of highly looped networks. In: Blain W.R. and Cabrera E. *Hydraulic Engineering Software IV: Fluid Flow Modelling. Procedings of the 4th International Conference on Hydraulic Engineering Software: Hydrosoft '92.* July 1992, Valencia, Italy. Elsevier Applied Science, London.

WL Delft Hydraulics (1998). *Sobek Manual.* Sobek Urban. Version 2.04. May 1998. WL Delft Hydraulics, Delft.

Wynne B. (1992). Uncertainty and environmental learning. Reconceiving science and policy in the preventive paradigm. *Global Environmental Change.* **2** (2): 111-127.

Xanthopoulos C. and Hahn H. (1993). Anthropogenic pollutants wash-off from street surface. In: *Proceedings of 6th International Conference on Urban Storm Drainage.* Niagara Falls Canada: 417-422.

Xu C. and Goulter I.C. (1998). Probabilistic model for water distribution reliability. *Journal of Water Resources Planning and Management.* **124** (4): 218-228.

Xu K., Luxmoore R. and Davies T. (1998). Sewer pipe deformation assessment by image analysis of video surveys. *Pattern Recognition.* **31** (2): 169-180.

Zadeh L.A. (1965). Fuzzy sets. *Information Control.* **8**: 338-353.

Zawadski I.I. (1973) Statistical properties of precipitation patterns. *Journal of Applied Meteorology.* **12**: 459-472.

Zellner A. (1977). Maximal data information prior distributions. In: Aykaç A. and Brumat C. (eds.). *New Methods in the Applications of Bayesian Methods.* North-Holland Publishing Company, Amsterdam: 211-232.

Samenvatting

Doel van de studie is het ontwikkelen van een methodiek voor het beoordelen van de prestaties van een rioolstelsel, waarbij rekening gehouden wordt met de mogelijke invloed van onzekerheden en risico's. De prestaties van een rioolstelsel worden beoordeeld op basis van berekende overstortvolumes. Er is rekening gehouden met onzekerheden door technieken uit de onzekerheids- en risico-analyse toe te passen bij de beoordeling van het hydraulicsh functioneren en de technische toestand van een rioolstelsel.

Inleiding en kader

Hoofdstuk 1 beschrijft de rol die modellen spelen bij de beoordeling van het hydraulisch functioneren en de technische toestand van rioolstelsels. Verder wordt ingegaan op het beheer van de riolering in Nederland. Tenslotte volgt een uiteenzetting over de mogelijke invloed van onzekerheid op het functioneren en het beheer en onderhoud van de riolering.

Riolering is aangelegd als bescherming tegen besmetting door contact met fecaliën en tegen overstroming als gevolg van hevige neerslag. Het grootste gedeelte van de rioolstelsels in Nederland (64%) is gemengd, d.w.z. afvalwater en neerslag worden in één buis naar de zuivering getransporteerd. De overige stelsels bestaan uit gescheiden systemen, waarin afvalwater en neerslag afzonderlijk afgevoerd worden naar respectievelijk de afvalwaterzuiveringsinstallatie en het oppervlaktewater.

Voorschriften voor het beheer van rioolstelsels zijn in Nederland beschreven in een aantal richtlijnen. Beheer van de riolering betreft in essentie een afweging tussen gewenste bedrijfszekerheid en schaarse financiële middelen. Bedrijfzekerheid is gedefinieeerd als "De mogelijkheid van een goed om een specifieke dienst te leveren aan gebruikers". De diensten geleverd door een rioolstelsel bestaan uit de bescherming van de volksgezondheid en het voorkomen van overstromingen onder de voorwaarde dat de kwaliteit van het milieu gewaarborgd is. In Nederland wordt jaarlijks 1 miljard euro geïnvesteerd in het beheer van riolering.

De prestaties of bedrijfszekerheid van een rioolstelsel wordt gewoonlijk beoordeeld op basis modelresultaten, omdat metingen niet voorhanden zijn. De nauwkeurigheid van de gebruikte modellen hangt af van hun betrouwbaarheid en volledigheid. Gevolg is dat aan beslissingen over onderhouds- en verbeteringsmaatregelen aanzienlijke risico's verbonden kunnen zijn. Het hydraulisch functioneren wordt beoordeeld aan de hand van berekende overstortvolumes en water op straat situaties. Op basis hiervan wordt besloten of maatregelen nodig zijn om materiële en milieuschade te reduceren. Visuele inspecties en voorspellingen van de restlevensduur van rioolbuizen bepalen of reiniging, renovatie of vervanging noodzakelijk is.

Onzekerheden

In hoofdstuk 2 worden de onzekerheden met betrekking tot het beheer en onderhoud van de riolering geclassificeerd. Er bestaat echter in de literatuur geen overeenstemming over de classificering van onzekerheden, waardoor de gepresenteerde methoden om met die onzekerheden om te gaan sterk verschillen. In dit proefschrift worden twee types onzekerheid onderscheiden: inherente en epistemische onzekerheid. Het eerste type vertegenwoordigt de variatie die aanwezig is in natuurlijke processen. Het tweede type representeert gebrek aan kennis en gegevens over het bestudeerde systeem en omvat modelonzekerheid en statistische onzekerheid. Voordeel van de gebruikte classificering is dat hiermee verschillende typen onzekerheid los van elkaar gereduceerd kunnen worden. Epistemische onzekerheid bijvoorbeeld vermindert als meer gegevens beschikbaar komen.

De huidige beoordeling van de prestaties van een rioolstelsel is gebaseerd op voorspelde prestaties en waargenomen gebreken. Dit heeft echter tekortkomingen, omdat onzekerheden ten aanzien van de opbouw van het rioolstelsel, de afmetingen van rioolbuizen en de kennis over processen niet betrokken worden in de beoordeling. Daarnaast wordt de natuurlijke variatie in de neerslag niet beschouwd. Tenslotte wordt aangenomen dat de onderdelen van een rioolstelsel (bijv. rioolbuizen en pompen) niet kunnen falen, en dat gebreken aan die onderdelen visueel waargenomen en beoordeeld kunnen worden. Dit alles leidt tot een veel te optimistische inschatting van de bedrijfszekerheid van een rioolstelsel.

Het bepalen van de kosten verbonden aan het falen van een rioolstelsel is geen sinecure, omdat de economische waardering van overstortingen en water op straat erg subjectief is. Bovendien kunnen de eisen die gesteld worden aan de prestaties van een rioolstelsel in de loop van de tijd veranderen als gevolg van veranderingen in de publieke waardering van gezondheidsrisico's en milieuschade en de regelgeving.

Onzekerheids- en risico-analyse

Hoofdstuk 3 behandelt verschillende methoden voor onzekerheids- en risico-analyse, zoals risico-gebaseerde economische optimalisatie, statistische analyse van storingsgegevens en Bayesiaanse schattingsmethoden.

De optimale beheerstrategie voor een rioolstelsel kan bepaald worden met behulp van een risico-gebaseerde optimalisatie. Hiervoor dient niet alleen de kans op falen van een systeem ingeschat te worden, maar dient ook de schade als gevolg van falen economisch gewaardeerd te worden. De faalkans kan geschat worden op basis van ervaring of berekend worden met een probabilistisch model. In deze studie is voornamelijk Monte Carlo simulatie toegepast. De optimale ingreep in het rioolstelsel kan bepaald worden door minimalisatie van investeringskosten en schade. Verwachte schade is verdisconteerd over een oneindige tijdshorizon. Hoewel er verschillende methoden beschikbaar zijn om schade in geld te waarderen is dit niet eenvoudig, omdat hierin de telkens veranderende publieke waardering van schade uitgedrukt dient te worden.

Optimalisatie van het onderhoud van de onderdelen van een rioolstelsel vereist kennis over hun faaltempo. Afhankelijk van de veroudering van een onderdeel, de gevolgen van een storing en de aard van een reparatie kunnen verschillende modellen toegepast worden. Het zogenaamde homogene Poisson proces (HPP) is geldig onder de aanname dat tussentijden van storingen onafhankelijk en identiek verdeeld zijn. Bovendien zijn reparaties instantaan en maken het onderdeel 'zo goed als nieuw'. Dit model voldoet echter niet bij veroudering. Dan kan beter het niet-homogene Poisson proces toegepast worden. In dit model zijn storingen nog steeds onafhankelijk, maar verandert het faaltempo in de tijd.

Bayesiaanse statistiek is gebaseerd op de stelling van Bayes. Hierin kunnen zowel waarnemingen als persoonlijke meningen bijdragen aan de mate van onzekerheid in een parameter. De stelling van Bayes gaat over conditionele kansen, d.w.z. waarschijnlijkheden van uitspraken die afhankelijk zijn van de feiten die aan deze uitspraken ten grondslag liggen. Met de stelling van Bayes kunnen de waarschijnlijkheden worden aangepast op basis van nieuwe gegevens. Hoe meer nieuwe gegevens gebruikt worden, des te kleiner de onzekerheid. Een voorbeeld van het gebruik van de stelling van Bayes is het combineren van metingen van rivierafvoeren met aanvullende historische informatie (bijv. in de vorm van streepjes van maximale waterstanden op de kerkmuur). De subjectieve a priori informatie kan samengevat worden in een a priori kansverdeling. In deze studie is voornamelijk de zogenaamde Jeffreys verdeling toegepast. Dit is een niet-informatieve a priori verdeling die invariant is onder één-op-één-transformaties en altijd dimensieloos. Met behulp van Bayes gewichten kan geanalyseerd worden welke kansverdeling het best past bij een verzameling waarnemingen, bijvoorbeeld overstortvolumes of tussentijden van storingen. Voordeel van de Bayesiaanse aanpak is dat meerdere kansverdelingstypen tegelijk afgewogen kunnen worden.

Hydraulisch functioneren van de riolering

In hoofdstuk 4 wordt aan de hand van een tweetal casussen de invloed toegelicht van onzekerheid met betrekking tot systeemdimensies, neerslagvariatie en modelkalibratie. Het rioolstelsel van 'De Hoven' is een klein en relatief vlak systeem. Het stelsel van 'Loenen' daarentegen is veel hellender en heeft een relatief klein bergingsvolume en een grote droogweerafvoer.

De invloed van zowel onzekere systeemdimensies (berging, pompcapaciteit, verhard oppervlak en overlaatcoëfficiënt) als neerslagvariatie op de prestaties van een rioolstelsel is bepaald met behulp van Monte Carlo simulatie. Beide rioolstelsels zijn beschreven met een vereenvoudigd rioolmodel. Aangenomen is dat de onzekere systeemdimensies onafhankelijk en normaal verdeeld zijn. Hun variantie is gebaseerd op praktijkervaring. De natuurlijke variabiliteit in de neerslag is gemodelleerd met een ruimtelijke neerslaggenerator.

De onzekerheden hebben een aanzienlijke invloed op het functioneen van de riolering in termen van overstortvolumes per bui. De waargenomen variatie in

berekende overstortvolumes neemt toe bij grotere herhalingstijden. Onzekerheid in systeemdimensies resulteert in grotere gemiddelde jaarlijkse overstortvolumes dan neerslagvariatie. Daarentegen heeft variatie in de neerslag een grotere spreiding tot gevolg. Dit is mogelijk het gevolg van de beperkingen van de neerslaggenerator die het volume van vaak voorkomende buien met een langere duur onderschat.

Bayes gewichten laten zien dat berekende overstortvolumes het best beschreven kunnen worden met een zogenaamde Weibull verdeling. Hierbij wodt opgemerkt dat Bayes gewichten onzekerheid over het juiste kansverdelingstype slechts minimaliseren en niet elimineren. Recente resultaten laten echter zien dat beter zou zijn om overstortvolumes te beschrijven met een zogenaamde gegeneraliseerde Pareto verdeling.

Uitgebreide, hydrodynamische modellen van de rioolstelsels van 'De Hoven' en 'Loenen' zijn gekalibreerd op basis van een drietal buien. Kalibratie is het proces waarin een modelconcept en een set modelparameters gekozen worden die zodanig zijn dat met het model een gemeten situatie zo goed mogelijk nagebootst kan worden. De uitkomsten van een gekalibreerd model bevatten dus een zo klein mogelijke afwijking van een serie veldmetingen. De kalibraties zijn uitgevoerd voor losse buien en zijn deels iteratief. De kwaliteit van de kalibratieresultaten is beoordeeld op basis van de verdeling en gemiddelde gekwadrateerde fout van de afwijkingen en de (relatieve) bias in de modelresultaten.

In het algemeen verschilt per bui zowel het optimale aantal kalibratieparameters als de gekalibreerde waarde van die parameters. Gedurende bepaalde periodes is de relatieve bias onacceptabel hoog en zijn de kalibratieresultaten dus minder betrouwbaar. Dit treedt vooral op tijdens droogweerafvoer en gedurende het leegpompen van het systeem na afloop van een bui. De overdraagbaarheid van kalibratieparameters is relatief gering, omdat de neerslagafvoer, de infiltratiecapaciteit van de bodem en de (industriële) afvalwaterproductie variëren in de tijd. Hierdoor zijn de begincondities van elke kalibratie verschillend. De overdraagbaarheid neemt toe als het model gekalibreerd wordt met een buienreeks of een Bayesiaanse kalibratiemethodiek toegepast wordt.

Evenals bij het vereenvoudigde model is Monte Carlo simulatie toegepast om de invloed van onzekerheid in de kalibratieparameters te bepalen. Vanwege de correlatie tussen de gekalibreerde parameters zijn afhankelijke trekkingen toegepast. De spreiding in berekende overstortvolumes is het grootst als gevolg van de verschillen tussen de kalibraties onderling. De orde van grootte is vergelijkbaar met de spreiding als gevolg van onzekere systeemdimensies in het vereenvoudigde model. De spreiding van berekende overstortvolumes voor één enkele kalibratie is veel kleiner. Daarnaast blijkt dat bij gebruik van een vereenvoudigd model de overstorthoeveelheden voor hellende systemen sterk overschat worden. Een modellering in de vorm van een aantal in serie geschakelde reservoirs benadert de realiteit meer.

De economische waardering van schade als gevolg van overstortingen vormt een uiterst onzekere factor bij de beoordeling van het functioneren van een rioolstelsel. Om de invloed ervan te onderzoeken is een drietal kostenfuncties met onzekere parameters

geformuleerd: een stapfunctie, een S-curve gebaseerd op de Weibull verdeling en een lineaire functie. Deze functies zijn gebruikt om het bergingsvolume voor een casus te optimaliseren.

In het algemeen nemen de verwachting en variantie van het optimale bergingsvolume toe als gevolg van de onzekere kostenparameters. Bij een stapfunctie is echter de invloed van onzekerheden verwaarloosbaar. De Weibull en lineaire functie zijn vlakker rondom het optimum, wat duidt op een robuustere oplossing. De voorkeur gaat uit naar een lineaire functie om de schade te beschrijven, omdat deze analytisch opgelost kan worden en eenvoudiger vast te stellen is.

De economische waarde van schade als gevolg van overstortingen is geschat onder de aanname dat de huidige normering in Nederland leidt tot het economisch optimale bergingsvolume. Voor de casus houdt dit in dat de kosten per m^3 overstortwater gemiddeld 4,10 euro bedragen. In vergelijking met de kosten van het zuiveren van afvalwater is dit ongeveer 12 keer duurder.

Operationele en technische toestand van de riolering

Hoofdstuk 5 bestudeert de invloed van de operationele en technische toestand van de onderdelen van een rioolstelsel op het functioneren van het stelsel als geheel. Gewoonlijk wordt bij de beoordeling van het functioneren van een rioolstelsel verondersteld dat elk onderdeel perfect functioneert. Dit is echter vaak niet het geval, omdat pompen in storing kunnen zijn en rioolbuizen verstopt kunnen raken.

De uitgevoerde analyse van pompstoringen houdt rekening met de aard van de storingen, het beleid ten aanzien van gemaalonderhoud, de veroudering van pompen en mogelijke aanpassingen aan het rioolstelsel. Een pompstoring is gedefinieerd als het onvermogen van een pomp om de taak uit te voeren waarvoor hij oorspronkelijk ontworpen was, namelijk afvalwater transporteren tot maximaal zijn ontwerpcapaciteit. Chronologische storingsreeksen afkomstig uit Rotterdam en Amsterdam zijn geanalyseerd met betrekking tot trends in het faaltempo, tussentijd van storingen, duur van reparaties, beschikbaarheid van pompen onder rwa-omstandigheden en moment van storing tijdens buien.

Er is verschil tussen de storingskarakteristieken in Rotterdam en Amsterdam. Dit wordt grotendeels veroorzaakt door verschillen in de definitie van een pompstoring en het onderhoudsbeleid. Het gemiddelde aantal storingen per jaar bedraagt 13 in Rotterdam en 4 in Amsterdam. In vergelijking met pompen in drinkwaterdistibutienetten en poldergemalen treden storingen bij pompen in rioolgemalen relatief vaak op. Dit wordt onder meer veroorzaakt door de samenstelling van het afvalwater en het discontinue karakter van het pompproces. De gemiddelde duur van reparaties is respectievelijk 10 en 13,5 uur.

Storingen kunnen in clusters voorkomen, waardoor zij niet meer onafhankelijk zijn. De reden is dat een pomp die in storing staat niet volledig wordt gerepareerd, maar slechts opnieuw wordt opgestart. Verklarende informatie ontbreekt echter, omdat logboeken onvolledig zijn. Daarnaast zijn trendmatige veranderingen in het faaltempo

waarneembaar als gevolg van gebrekkige reparaties, veroudering, vervanging of opknapbeurten. Dit betekent dat een rioolpomp na afloop van een reparatie slechts zo goed is als juist voorafgaand aan de storing. Tenslotte bestaat er geen aanleiding om te veronderstellen dat pompen voor rwa (regenweerafvoer) in de regel aan het begin of aan het eind van een bui in storing vallen.

De invloed van pompstoringen op berekende overstortvolumes is gekwantificeerd met behulp van Monte Carlo simulatie. Hiertoe zijn reeksen pompstoringen gegenereerd die vervolgens ingevoegd zijn in het vereenvoudigde rioolmodel. De tussentijd en duur van de storingen is gebaseerd op de waarnemingen uit Rotterdam. Pompstoringen blijken een aanzienlijke invloed te hebben op het functioneren van een rioolstelsel. Zij verhogen de jaarlijkse overstorthoeveelheid voor de casus met meer dan 15%. Dit betekent dat de bedrijfszekerheid van een rioolstelsel verhoogd zou kunnen worden door een verbetering van het pomp- en gemaalonderhoud.

De beoordeling van de technische toestand van een rioolstelsel kan subjectief zijn, omdat een interpretatie door rioolinspecteurs vereist is. Om de betrouwbaarheid van die interpretatie te bepalen, is de visuele meetnauwkeurigheid van rioolinspecties gekwantificeerd. Hiervoor zijn toelatingsexamens van rioolinspecteurs in Nederland gebruikt. Betrouwbaarheid is beschreven in termen van entropie, kans op foute classificeringen en kans op foute beslissingen ten aanzien van beheer en onderhoud. De analyse is uitgevoerd voor de toestandsaspecten conform NEN 3399. De statistische onzekerheid van berekende kansen is bepaald met behulp van Bayesiaanse statistiek.

Voor 8 van de 18 toestandsaspecten is de visuele meetonnauwkeurigheid aanzienlijk. De meerderheid van deze aspecten is gerelateerd aan verstopping, lekkage en verzakking. De geconstateerde meetonnauwkeurigheid heeft tot gevolg dat voorspellingen van de restlevensduur en toekomstige bedrijfszekerheid minder betrouwbaar worden. Dit alles vermindert de effectiviteit van maatregelen ter verbetering van het functioneren.

Conclusie

Door een risico-gebaseerde optimalisatie van het rioleringsbeheer kan rekening gehouden worden met de invloed van onzekerheden op de beoordeling van een rioolstelsel. Deze aanpak vereist formulering van een kostenfunctie om schade ten gevolge van falen te beschrijven en schatting van de faalkans van het systeem. Bovendien is kennis vereist over de orde van grootte van de verschillende onzekere factoren, zoals dimensies van het systeem, spreiding van neerslag in ruimte en tijd, economische waardering van schade en betrouwbaarheid van onderdelen van het systeem. Conclusie is dat alleen nauwkeurig gekwantificeerde onzekerheid nuttig is bij het nemen van beslissingen over het beheer van de riolering.

Hans Korving, mei 2004

Curriculum vitae

Hans Korving werd op 9 maart 1972 geboren in Assen. Zijn VWO-opleiding volgde hij aan de Christelijke Scholengemeenschap Overvoorde te Den Haag, waar hij in 1990 zijn diploma behaalde. Een jaar later begon hij met een studie Civiele Techniek aan de Technische Universiteit Delft. In 1996 is hij cum laude afgestudeerd bij de Sectie Gezondheidstechniek op de modellering van het gedrag van een rioolstelsel met behulp van technieken uit de signaalverwerking. Tijdens zijn studie is hij enige jaren als studentassistent bij de sectie Vloeistofmechanica betrokken geweest bij de voorbereiding en begeleiding van practica. Uit interesse heeft hij van 1993 tot 1996 Niet-Westerse Sociologie gestudeerd aan de Rijksuniversiteit Leiden. Na zijn studie is hij korte tijd in dienst geweest bij Witteveen+Bos in Deventer als specialist waterkwaliteitsmodellen. Vervolgens werd hij in 1997 aangesteld als toegevoegd onderzoeker bij de Sectie Gezondheidstechniek van de Technische Universiteit Delft. Hier heeft hij zich beziggehouden met onderwijs en onderzoek. Het onderzoek had betrekking op het meten aan stedelijke watersystemen, in het bijzonder aan rioolstelsels. In 2001 is hij in dienst getreden bij HKV Lijn in water in Lelystad om verder onderzoek uit te voeren op het gebied van de kosteneffectiviteit van maatregelen in het rioleringsbeheer. Dit onderzoek werd uitgevoerd in samenwerking met de Stichting RIONED en de Technische Universiteit Delft. Het onderzoek richtte zich op onzekerheden in de beschikbare informatie en de invloed daarvan op de beslissingen ten aanzien van het rioleringsbeheer. De resultaten van het onderzoek vormen de basis voor dit proefschrift. Inmiddels is hij teruggekeerd bij Witteveen+Bos als adviseur riolering.

Dankwoord

Ten eerste wil ik mijn twee promotoren François Clemens en Jan van Noortwijk bedanken. Gezamenlijk hebben wij de afgelopen jaren afgetast of het mogelijk en wenselijk is om een probabilistische beoordelingsmethodiek voor rioolstelsels te introduceren. Inmiddels kunnen we beide vragen bevestigend beantwoorden, maar er moet nog heel wat werk verzet worden voordat we echt zover zijn.

François, we werken nu al een aantal jaren samen en lijken ook de komende tijd tot elkaar veroordeeld. Ik heb genoten van de afgelopen jaren en kijk uit naar de waanzinnige ideeën die we in de toekomst vast nog gaan krijgen. Ik bewonder jouw gedrevenheid om tot het gaatje te gaan en geen genoegen te nemen met alleen maar een idee.

Jan, jouw oog voor detail is heel bijzonder. Je bent de enige die van alle formules in dit proefschrift gecontroleerd hebt of ze kloppen. Jouw enorme kennis over Bayesiaanse statistiek is onmisbaar geweest voor het slagen van het onderzoek. Hopelijk kunnen we nog vaker samen onze tanden stuk bijten op ingewikkelde vraagstukken.

Het onderzoeksproject was een samenwerking tussen HKV Lijn in water, Stichting RIONED en de TU Delft. HKV en RIONED wil ik bedanken voor hun financiële en inhoudelijke bijdrage. Verder dank ik alle leden van de begeleidingsgroep voor hun kennis en inspiratie: Hans Geerse, Pieter van Gelder, Ton Beenen en Hans Hartong. Hans G., bedankt voor je betrokken en motiverende manier van leiding geven. Pieter, bedankt dat je telkens weer tijd vond om mijn vragen te beantwoorden.

Vertellen dat je onderzoek doet aan de riolering levert vaak verbaasde reacties op. "Dat je daar onderzoek aan kunt doen?" Mijn eerste stappen in het rioleringsonderzoek zette ik tijdens mijn afstuderen bij Jan Wiggers en enige tijd later als onderzoeker bij zijn sectie. Jan, bedankt voor de ruimte die je me gegeven hebt om me te ontwikkelen binnen de academische wereld. Jij leerde me dat een riool niet stinkt, maar geurt. Helaas moest je veel te vroeg afscheid nemen van de universiteit.

Vervolgens brak een hoogleraarloze periode aan. In deze roerige tijd is een aantal personen onmisbaar gebleken om het geheel op de rails te houden: Jan Kop, Jelte van der Heide, Ab Dirkzwager en Guus Stelling. Jan, bedankt voor je niet aflatende betrokkenheid bij het reilen en zeilen van je oude vakgroep. Jelte, bedankt voor je vriendschap en je luisterend oor. Ab, bedankt voor je wijze raad. Guus, bedankt dat ik even onder jouw vleugels mocht zitten.

Onderzoek doen binnen een samenwerkingsverband betekent dat je op meerdere plekken collega's hebt. Mijn jaren bij de sectie Gezondheidstechniek van de TU Delft waren mede door die collega's erg aangenaam, in het bijzonder de 'collega's van het eerste uur' Jaap de Koning, Arjen van Nieuwenhuijzen en Jasper Verberk. Mijn collega's bij HKV dank ik voor hun kritische blik. Blijf die vooral houden! Er zijn al meer dan genoeg meelopers in de waterwereld.

Veel dank ben ik verschuldigd aan mijn goede vriend en collega Jeroen Langeveld. Samen hebben we veel beleefd niet alleen op onderzoeksgebied, maar ook in onze passie voor koken en tijdens onze reis door Australië met ananassen op de hoedenplank. Ik bewaar heel goede herinneringen aan onze levendige discussies over het vak. Het was erg inspirerend om tegelijkertijd met jou mijn proefschrift af te ronden. Zo wil ik vaker met iemand samenwerken!

Het onderzoek heeft veel profijt gehad van kennis, ervaring en gegevens uit het werkveld. Sander Geenen (Gemeentewerken Rotterdam) en Egbert Baars (DWR Amsterdam) gaven toestemming om hun gegevens over pompstoringen te gebruiken voor deze studie. Verder dank ik Ron Cranen en Alex Retel voor het delen van hun ruime praktijkkennis over het al dan niet functioneren van gemalen. Stichting RIONED gaf toestemming om de examenresultaten van de cursus 'Visuele rioolinspecties' te analyseren. Tenslotte heeft Patick Willems (KU Leuven) de door hem ontwikkelde ruimtelijke neerslaggenerator beschikbaar gesteld voor het onderzoek.

I am also grateful to the members of the dissertation committee (Jean Berlamont - KU Leuven, Richard Ashley - University of Bradford, Tim Bedford - University of Strathclyde, Jean-Luc Bertrand-Krajewski - INSA de Lyon and Pieter van Gelder - TU Delft) for carefully reviewing the thesis and giving helpful comments.

Theo en Karin, bedankt voor jullie creatieve bijdragen aan dit proefschrift. Van je schoonfamilie moet je het maar hebben!

Lieve Plony, bedankt voor de geweldige manier waarop je me samen met opa en oma's grootgebracht hebt. Je hebt me geleerd met een sociale, bewogen blik naar de wereld om me heen te kijken en me telkens gestimuleerd om me verder te ontwikkelen.

Lieve Francien, jouw bijdrage is nauwelijks in woorden te vatten. Zonder jouw steun en liefde zou dit proefschrift nooit zo geworden zijn als het nu is.

Hans Korving
Delft, mei 2004

APPENDIX I Models for prediction of sewer corrosion

Models predicting sulphide formation in filled (or pressurised) sewers have been formulated by:

- **Pomeroy (1959 and 1974),**

$$\frac{d[S]}{dt} = 1 \cdot 10^{-3} \cdot [BOD_5] \cdot 1.07^{(T-20)} \cdot \frac{(1+0.37D)}{R} \tag{I.1}$$

where $d[S]/d[t]$ is sulphide build-up rate (mg/l/h), BOD_5 is standard 5-day, 20 °C biochemical oxygen demand (mg/l), T is sewage temperature (°C), R is hydraulic radius (m) and D is pipe diameter (m).

- **Boon and Lister (1975),**

$$\frac{d[S]}{dt} = 0.228 \cdot 10^{-3} \cdot [COD] \cdot 1.07^{(T-20)} \cdot \frac{(1+0.37D)}{R} \tag{I.2}$$

where $d[S]/d[t]$ is sulphide build-up rate (mg/l/h), COD is chemical oxygen demand (mg/l), T is sewage temperature (°C), R is hydraulic radius (m) and D is pipe diameter (m).

- **Hadjianghelou *et al.* (1984),**

$$\frac{d[S]}{dt} = \frac{0.975}{D}\,[\text{mg/l} \cdot \text{cm/min}] \cong \frac{0.15}{R}\,[\text{mg/l} \cdot \text{m/h}] \tag{I.3}$$

where $d[S]/d[t]$ is sulphide build-up rate (mg/l/h), D is pipe diameter (m) and R (= ¼ D, for filled pipes) is hydraulic radius (m).

Pomeroy's formula usually predicts higher values (up to 2 times) than Boon's and Lister's. The formula of Hadjianghelou *et al.* (1984) predicts values in between because it is based on the measurements of both Pomeroy (1959 and 1974) and Boon and Lister (1975). Nielsen and Hvitved-Jacobsen (1988) and Tanaka and Nielsen (2002) present an alternative description. Their model is based on biofilm activity in the sewer and predicts sulphate production downstream of a measuring location.

Pomeroy and Parkhurst (1977) also developed an equation for predicting sulphide build-up rates in partly filled sewers,

$$\frac{d[S]}{dt} = \frac{M \cdot [BOD_5] \cdot 1.07^{(T-20)}}{R} - \frac{N \cdot \left(\frac{s}{v}\right)^{3/8} \cdot [S]}{d} \tag{I.4}$$

where $d[S]/d[t]$ is sulphide build-up rate (mg/l/h), M is $0.32*10^{-3}$, N is 0.64 (conservative prediction) or 0.96 (median predictions), BOD_5 is standard 5-day, 20 °C biochemical oxygen demand (mg/l), T is sewage temperature (°C), R is hydraulic radius

(m), [*S*] is sulphide concentration (mg/l/h), *s* is pipe gradient (m/100m), *v* is flow velocity (m/s) and *d* is mean hydraulic depth which equals cross-sectional area divided by surface width (m). The first term of the equation represents the rate at which sulphide is added to the stream by the slime layer and the second term represents the losses due to transition of sulphide from the sewage to the air. According to this equation, the sulphide concentrations in partly filled sewers will reach an equilibrium, designated $[S]_{lim}$,

$$[S]_{\lim} = \frac{a \cdot [BOD_5] \cdot 1.07^{(T-20)}}{(s \cdot v)^{3/8}} \cdot \frac{P}{B} \tag{I.5}$$

where $[S]_{lim}$ is equilibrium sulphide concentration (mg/l/h), *a* is $0.5*10^{-3}$ (conservative prediction) or $0.33*10^{-3}$ (median prediction), BOD_5 is standard 5-day, 20 °C biochemical oxygen demand (mg/l), *T* is sewage temperature (°C), *s* is pipe gradient (m/100m), *v* is flow velocity (m/s) and *P/B* is ratio of wetted perimeter (m) and surface width of stream (m).

Using the formulae for sulphide build-up, the corrosion rate of cementitious material is calculated as described in **Pomeroy (1974)**. These formulae are also highly empirical. The approximate corrosion rate is as follows,

$$c = 11.5 \cdot k \cdot \varphi_{sw} \cdot \frac{1}{Alk} \tag{I.6}$$

where *c* is average rate of corrosion (mm/a), *k* is factor representing proportion of acid reacting (see Bielecki and Schremmer 1987), φ_{sw} is average flux of H_2S to pipe wall ($g/m^2/h$) and *Alk* is acid consuming capability (alkalinity) of pipe material. The average flux of H_2S to the pipe wall is proportional to the exposed proportion of the wall,

$$\varphi_{sw} = \sigma_2 \cdot 0.7 \cdot (s \cdot v)^{3/8} \cdot j \cdot [DS] \cdot \frac{B}{P'} \tag{I.7}$$

where φ_{sw} is average flux of H_2S to pipe wall ($g/m^2/h$), σ_1 is factor accounting for turbulence (introduced by Bielecki and Schremmer (1987)), *s* is pipe gradient (m/100m), *v* is flow velocity (m/s), *j* is pH dependent factor for proportion of un-ionised H_2S, [*DS*] is dissolved sulphide concentration. The flux of H_2S from the sewage into the air is,

$$\varphi_{sf} = \sigma_1 \cdot 0.7 \cdot (s \cdot v)^{3/8} \cdot j \cdot [DS] \tag{I.8}$$

where φ_{sf} is average flux of H_2S from sewage to air ($g/m^2/h$), σ_2 is factor accounting for aeration (introduced by Bielecki and Schremmer (1987)), *s* is pipe gradient (m/100m), *v* is flow velocity (m/s), *j* is pH dependent factor for proportion of un-ionised H_2S, [*DS*] is dissolved sulphide concentration. Many factors in these equations (*k*, σ_1 and σ_2) have to be selected on the basis of engineering judgement, thus introducing considerable, not quantified uncertainty.

APPENDIX II Economic valuation of nature

For economic valuation several methods are available (based on Hanley *et al.* 1997, Lorenz 1999, Ruigrok 1999, Pandey and Nathwani 2003, and Penning-Rowsell *et al.* 2003):

- **Travel costing** estimates travel costs individuals make to visit a recreational area. It is based on the assumption that people will spend more on travel to sites with high environmental values. Travel cost can be regarded as an indirectly revealed preference for nature. However, it is unclear whether the travel cost method actually measures preference for nature or for recreational trips. Bias results from individuals valuing nature who do not visit a specific recreational area.
- **Hedonic pricing** seeks to describe the value of a good or service as a bundle of valuable characteristics. For example, the value of a house may depend on the number of rooms, whether it has a garden, how close it is to shops or a nature area. The price of a house near nature is probably higher than next to a factory. The price difference is the 'willingness to pay' for living close to nature. Bias is related to problematic comparison of market goods (e.g. two houses will never be exactly the same and factors other than nature may influence the price difference) and possible government intervention in markets. In addition, the hedonic price technique has a large data requirement because both data on characteristics of the surroundings and market transactions need to be collected.
- **Contingent valuation method** is a survey method in which respondents are asked how much they are willing to pay for the use and conservation of natural goods. Respondents are presented with one or more hypothetical environmental scenarios and asked to state their 'willingness to pay', or less commonly their 'willingness to accept compensation', in terms of money for a change in environmental quality. Contingent valuation only provides valid estimates when respondents are familiar with the specific goods or services (e.g. improved water quality for swimming instead of increased biodiversity). In order to avoid bias, respondents should be reminded of the possibility of spending their income on goods other than nature. Contingent valuation is the only method that can describe non-use values, which are independent of peoples' current use of a resource (e.g. cultural heritage or social significance). The method is an example of a direct estimation method; all methods mentioned below are of the indirect type.
- **Conjoint analysis** is also a survey method, but differs from contingent valuation. Using this method, respondents are asked to make a series of decisions between different combinations and different levels of those aspects believed to be most important. The commodity of interest (e.g. increased opportunities for fishing) is included. For example, if the impact of quality of nearby surface waters on housing

prices is of interest, at first the critical aspects determining the amount of money individual households are prepared to pay for dwellings is determined. Secondly, the strength of the relationship between the commodity of interest and the price households are willing to pay for this good is estimated. Conjoint analysis is thus equivalent to hedonic pricing, but adds an expressed preference for the characteristics of the surroundings of a house.

- **Production factor method** assesses natural qualities by valuing their impacts on production cost. As many natural resources are used as production factors, the method allows for determining the value of the production capacity of nature. Therefore, a reduction of production costs for a sector making use of a natural resource may result from improvements of natural quality. In other words, the production factor method is meant to determine the value of changes in natural qualities on the economic production system. The results are biased due to averting behaviour of producers who shift to alternative production methods (e.g. using groundwater instead of surface water as source of drinking water production).
- **Averting behaviour** measures the expenditures made in order to avert or mitigate negative effects of environmental impacts. For example, ozone depletion increases the risk of skin cancer; consequently people buy sun creams and hats to protect themselves. This means that the 'willingness to pay' for a cleaner environment is deduced from individuals' purchases of goods and services to avert the negative effects of pollution. The validity of the method is questionable because it is assumed that people actually purchase certain goods for protection. In fact, they may be purchased for the sake of the product.
- **Life Quality Index** (LQI) is a social indicator comprising societal wealth and longevity which guides the selection of optimal strategies for risk management. It is equivalent to a utility function applied in decision analysis. The LQI maximises the net benefit of risk reduction in terms of quality of life in good health for all members of society and tests the effectiveness of allocation of scarce resources. It consists of two indicators: (1) the real gross domestic product per person as a measure of resources and (2) the quality of life and life expectancy as an indicator of social development, environmental quality and public health. Therefore, income required to support consumption and leisure time, are two determinants of life quality. Essentially, it is a work versus leisure trade-off. The LQI is derived using the principles of welfare economy accounting for uncertainty and expected utility theory. The result can be considered as an expression of the 'societal willingness to pay'. In other words, the LQI leads to a criterion determining the level beyond which it is no longer justifiable to spend resources in the name of safety.

APPENDIX III Maximum likelihood estimators of models with time-varying failure rate

The failure rate $v(t)$ of a system is defined as the expected number of failures per time interval,

$$v(t) = \frac{d}{dt} E\big(N(0,t]\big) \tag{III.1}$$

As a result, the expected number of failures in the interval (t_1,t_2) yields,

$$E\big(N(t_2) - N(t_1)\big) = \int_{t_1}^{t_2} v(t)dt \tag{III.2}$$

where $N(t_2)$ is number of failures at time t_2, $N(t_1)$ is number of failures at time t_1 and $v(t)$ is failure rate of the system.

The joint probability density of failures occurring at times T_1, T_2,...,T_n is,

$$\begin{aligned} &f(t_1,t_2,...,t_n) = f(t_1)f(t_2 \mid t_1)f(t_3 \mid t_1,t_2)...f(t_n \mid t_1,t_2,...,t_{n-1}) \\ &0 < t_1 < t_2 < ... < t_n \end{aligned} \tag{III.3}$$

where $f(t_2 \mid t_1)$ is the conditional probability density function of t_2 given $t_1=T_1$, $f(t_3 \mid t_1,t_2)$ is the conditional probability density function of t_3 given $t_1 = T_1$ and $t_2 = T_2$ and $f(t_n \mid t_1,t_2,\ldots,t_{n-1})$ is the conditional probability density function of t_n given $t_1 = T_1$, $t_2 = T_2$ and $t_{n-1} = T_{n-1}$. Then the probability density function of a system with time-dependent failure rate is defined as,

$$f(t_1) = v(t_1)\exp\left(-\int_0^{t_1} v(x)dx\right), \quad t_1 > 0 \tag{III.4}$$

$$\Pr(T_1 > t_1) = \exp\left(-\int_0^{t_1} v(x)dx\right), \quad t_1 > 0 \tag{III.5}$$

where $f(t_1)$ is the probability density function of failure at time T_1, $v(t_1)$ is the time-dependent failure rate and $\Pr(T_1 > t_1)$ is the probability that the time to the first failure is at least t_1. The likelihood function of failures at T_1, T_2,..., T_n, i.e. the joint probability density of the observations as a function of parameter vector v, can be derived from Eq. (III.3) and Eq. (III.4),

$$\begin{aligned}\ell(t_1,t_2,\ldots,t_n|n,\mathrm{t}) &= f(t_1)f(t_2|t_1)\cdots f(t_n|t_1,t_2,\ldots,t_{n-1}) \\ &= \left[\nu(t_1)\exp\left(-\int_0^{t_1}\nu(x)dx\right)\right]\left[\nu(t_2)\exp\left(-\int_{t_1}^{t_2}\nu(x)dx\right)\right]\cdots \\ &\times\left[\nu(t_n)\exp\left(-\int_{t_{n-1}}^{t_n}\nu(x)dx\right)\right] \\ &= \left(\prod_{i=1}^{n}\nu(t_i)\right)\exp\left(-\int_0^{t_n}\nu(x)dx\right)\end{aligned} \tag{III.6}$$

where $\ell(t_1,t_2,\ldots,t_n|\,n,t)$ is likelihood of failures at times T_1, T_2,..., T_n given the cumulative number of failures in time. If T_m is the end of the observation period and there is no failure between t_n and t_m, the likelihood becomes,

$$\begin{aligned}\ell(t_1,t_2,\ldots,t_n|n,\mathrm{t}) &= \left(\prod_{i=1}^{n}\nu(t_i)\right)\exp\left(-\int_0^{t_n}\nu(x)dx\right)\Pr(T_{n+1}>t_m) \\ &= \left(\prod_{i=1}^{n}\nu(t_i)\right)\exp\left(-\int_0^{t_n}\nu(x)dx\right)\exp\left(-\int_{t_n}^{t_m}\nu(x)dx\right)\end{aligned} \tag{III.7}$$

Maximum likelihood estimator of Crow's model

Crow's model describes the failure rate with a power law,

$$\nu(t)=\lambda\beta t^{\beta-1}\quad,\quad \lambda>0 \text{ and } \beta>0 \tag{III.8}$$

where $\nu(t)$ is the time-dependent failure rate, λ is scale parameter of Weibull function, β is growth parameter of Weibull function determining improvement or deterioration in time. The likelihood function of failures at T_1, T_2,..., T_n is,

$$\begin{aligned}\ell(\lambda,\beta|n,\mathrm{t}) &= \left(\prod_{i=1}^{n}\lambda\beta t_i^{\beta-1}\right)\exp\left(-\int_{t_0}^{t_m}\lambda\beta x^{\beta-1}dx\right) \\ &= \left(\prod_{i=1}^{n}\lambda\beta t_i^{\beta-1}\right)\exp\left(-\left(\lambda t_m^{\beta}-\lambda t_0^{\beta}\right)\right)\end{aligned} \tag{III.9}$$

where $\ell(\lambda,\beta|\,n,\mathrm{t})$ is likelihood of failures at T_1, T_2,..., T_n given number of failures n in time, t_i is time of i^{th} failure, t_0 is start of observation period and t_m is end of observation period. Hence, the log-likelihood is,

$$\log\ell(\lambda,\beta|n,\mathrm{t})=n\log\lambda+n\log\beta+(\beta-1)\sum_{i=1}^{n}\log(t_i)-\lambda\left(t_m^{\beta}-t_0^{\beta}\right) \tag{III.10}$$

Maximum likelihood (ML) estimators of the parameters λ and β in the Crow model are derived as,

$$\frac{\partial}{\partial\lambda}\log\ell(\lambda,\beta|n,\mathrm{t})=\frac{n}{\lambda}-\left(t_m^{\beta}-t_0^{\beta}\right)=0 \tag{III.11}$$

$$\frac{\partial}{\partial\beta}\log\ell(\lambda,\beta|n,t)=\frac{n}{\beta}+\sum_{i=1}^{n}\log(t_i)-\lambda\left(t_m{}^{\beta}\log(t_m)-t_0{}^{\beta}\log(t_0)\right)=0 \tag{III.12}$$

For $t_0\downarrow 0$, the ML estimator for β and λ yield after substitution of (III.11) in (III.12),

$$\hat{\beta}=\frac{n}{n\log(t_m)-\sum_{i=1}^{n}\log(t_i)} \tag{III.13}$$

$$\hat{\lambda}=\frac{n}{t_m{}^{\hat{\beta}}} \tag{III.14}$$

Maximum likelihood estimator of Cox and Lewis' model

Crow's model describes the failure rate with a log-linear function,

$$\nu(t)=\exp(\beta_0+\beta_1 t) \tag{III.15}$$

where $\nu(t)$ is time-dependent failure rate, β_0 is scale parameter of log-linear function, β_1 is growth parameter of log-linear function determining improvement or deterioration in time. The likelihood function of failures at T_1, T_2,..., T_n is,

$$\begin{aligned}\ell(\beta_0,\beta_1|n,t)&=\left(\prod_{i=1}^{n}\exp(\beta_0+\beta_1 t_i)\right)\exp\left(-\int_{t_0}^{t_m}\exp(\beta_0+\beta_1 x)dx\right)\\&=\left(\prod_{i=1}^{n}\exp(\beta_0)\exp(\beta_1 t_i)\right)\exp\left(-\exp(\beta_0)\left(\frac{1}{\beta_1}\left(\exp(\beta_1 t_m)-1\right)\right)\right)\end{aligned} \tag{III.16}$$

where $\ell(\beta_0,\beta_1\,|\,n,t)$ is likelihood of failures at T_1, T_2,..., T_n given number of failures n in time, t_i is time of i^{th} failure and t_m is end of observation period. Hence, the log-likelihood is,

$$\log\ell(\beta_0,\beta_1|n,t)=n\beta_0+\beta_1\sum_{i=1}^{n}t_i-\frac{\exp(\beta_0)\left(\left(\exp(\beta_1 t_m)-\exp(\beta_1 t_0)\right)\right)}{\beta_1} \tag{III.17}$$

Maximum likelihood (ML) estimators of the parameters β_0 and β_1 in the Cox-Lewis model are derived as,

$$\frac{\partial}{\partial\beta_0}\log\ell(\beta_0,\beta_1|n,t)=n-\frac{\exp(\beta_0)}{\beta_1}\left(\exp(\beta_1 t_m)-\exp(\beta_1 t_0)\right)=0 \tag{III.18}$$

$$\begin{aligned}\frac{\partial}{\partial\beta_1}\log\ell(\beta_0,\beta_1|n,t)&=\sum_{i=1}^{n}t_i-\frac{\exp(\beta_0)}{\beta_1}\ldots\\&\quad\times\left(\exp(\beta_1 t_m)\left(t_m-\frac{1}{\beta_1}\right)-\exp(\beta_1 t_0)\left(t_0-\frac{1}{\beta_1}\right)\right)\\&=0\end{aligned} \tag{III.19}$$

For $t_0 \downarrow 0$, the ML estimator for β_1 can be estimated by solving (after substitution of Eq. (III.18) in Eq. (III.19)),

$$\sum_{i=1}^{n} t_i - \frac{n}{\hat{\beta}_1} \frac{\left(t_m \exp\left(\hat{\beta}_1 t_m\right) - \hat{\beta}_1 \left(\exp\left(\hat{\beta}_1 t_m\right) - 1\right)\right)}{\left(\exp\left(\hat{\beta}_1 t_m\right) - 1\right)} = 0 \tag{III.20}$$

Then the ML estimator for β_0 is estimated with,

$$\hat{\beta}_0 = \log\left(\frac{n\hat{\beta}_1}{\exp\left(\hat{\beta}_1 t_m\right) - 1}\right) \tag{III.21}$$

APPENDIX IV Summary of distribution types, parameter estimators and prior distributions

This appendix presents several probability distribution functions and their corresponding estimation methods for parameters and prior distributions. Details on deriving log-likelihood estimators and prior distributions can be found in Van Noortwijk *et al.* (2003).

	EXPONENTIAL DISTRIBUTION
Probability density function	$\mathrm{Ex}(x\|\theta)=\frac{1}{\theta}\exp\left(-\frac{x}{\theta}\right)$, $\theta>0$, $x>0$
Survival function	$\overline{F}(x\|\theta)=\exp\left(-\frac{x}{\theta}\right)$
Mean and variance	$E(X)=\theta$ $\quad$ $\mathrm{Var}(X)=\theta^2$
Log-likelihood	$\log\ell(\mathrm{x}\|\theta)=-n\log(\theta)-\frac{1}{\theta}\sum_{i=1}^{n}x_i$
Maximum likelihood estimator	$\hat{\theta}=\frac{1}{n}\sum_{i=1}^{n}x_i$
Non-informative Jeffreys' prior	$\pi(\theta)\propto\frac{1}{\theta}$

	RAYLEIGH DISTRIBUTION
Probability density function	$\mathrm{Ra}(x\|\theta)=\frac{2x}{\theta}\exp\left(-\frac{x^2}{\theta}\right)$, $\theta>0$, $x>0$
Survival function	$\overline{F}(x\|\theta)=\exp\left(-\frac{x^2}{\theta}\right)$
Mean and variance	$E(X)=\frac{\sqrt{\pi}}{2}\theta$ $\quad$ $\mathrm{Var}(X)=\left(1-\frac{\pi}{4}\right)\theta$
Log-likelihood	$\log\ell(\mathrm{x}\|s,m)=-n\log(b)-\sum_{i=1}^{n}\frac{x_i-a}{b}-\sum_{i=1}^{n}\exp\left(-\frac{x_i-a}{b}\right)$
Maximum likelihood estimator	$\hat{\theta}=\frac{\mathbf{x}'\mathbf{x}}{n}$ $\mathbf{x}'\mathbf{x}$ is the sum of the squared data
Non-informative Jeffreys' prior	$\pi(\theta)\propto\frac{1}{\theta}$

NORMAL DISTRIBUTION	
Probability density function	$\mathrm{N}(x\|m,s)=\frac{1}{s\sqrt{2\pi}}\exp\left(-\frac{1}{2s^2}(x-m)^2\right)$, s>0
Survival function	$\overline{F}(x\|m,s)=1-\Phi\left(\frac{1}{s}(x-m)\right)$
	$\Phi(x)$ is the cumulative distribution of a standard normal distribution
Mean and variance	$E(X)=m \qquad \mathrm{Var}(X)=s^2$
Log-likelihood	$\log\ell(\mathrm{x}\|s,m)=-n\log(s)-\frac{n}{2}\log(2\pi)-\frac{1}{2s^2}\sum_{i=1}^{n}(x_i-m)^2$
Maximum likelihood estimators	$\hat{m}=\frac{1}{n}\sum_{i=1}^{n}x_i$
	$\hat{s}=\left(\frac{1}{n}\sum_{i=1}^{n}\left(x_i-\frac{1}{n}\sum_{i=1}^{n}x_i\right)^2\right)^{\frac{1}{2}}$
Non-informative Jeffreys' prior	$\pi(m,s)\propto\frac{\sqrt{2}}{s^2}$

LOGNORMAL DISTRIBUTION	
Probability density function	$\mathrm{LN}(x\|m,s)=\frac{1}{s\sqrt{2\pi}}\frac{1}{x}\exp\left(-\frac{1}{2s^2}(\log(x)-m)^2\right)$, s>0, x>0
Survival function	$\overline{F}(x\|m,s)=1-\Phi\left(\frac{1}{s}(\log(x)-m)\right)$
	$\Phi(x)$ is the cumulative distribution of a standard normal distribution
Mean and variance	$E(X)=\exp\left(m+\frac{s^2}{2}\right) \qquad \mathrm{Var}(X)=\exp(2m+2s^2)-\exp(2m+s^2)$
Log-likelihood	$\log\ell(\mathrm{x}\|s,m)=-n\log(s)-\frac{n}{2}\log(2\pi)-\sum_{i=1}^{n}\log(x_i)-\frac{1}{2s^2}\sum_{i=1}^{n}(\log(x_i)-m)^2$
Maximum likelihood estimator	$\hat{m}=\frac{1}{n}\sum_{i=1}^{n}\log(x_i)$
	$\hat{s}=\left(\frac{1}{n}\sum_{i=1}^{n}\left(\log(x_i)-\frac{1}{n}\sum_{i=1}^{n}\log(x_i)\right)^2\right)^{\frac{1}{2}}$
Non-informative Jeffreys' prior	$\pi(m,s)\propto\frac{\sqrt{2}}{s^2}$

GAMMA DISTRIBUTION

Probability density function

$$\mathrm{Ga}(x|a,b)=\frac{b^a}{\Gamma(a)}x^{a-1}\exp(-bx)\ ,\ a>0,\ b>0,\ x>0$$

$\Gamma(a)$ is the gamma function defined as $\Gamma(a)=\int_{t=0}^{\infty}t^{a-1}\exp(-t)dt$

Survival function

$$\overline{F}(x|a,b)=\frac{\Gamma(a,bx)}{\Gamma(a)}$$

$\Gamma(a,x)$ is the incomplete gamma function defined as

$$\Gamma(a,x)=\int_{t=x}^{\infty}t^{a-1}\exp(-t)dt$$

Mean and variance

$$E(X)=\frac{a}{b}\qquad \mathrm{Var}(X)=\frac{a}{b^2}$$

Log-likelihood

$$\log\ell(\mathrm{x}|s,m)=n\left(a\log(b)-\log(\Gamma(a))\right)+(a-1)\sum_{i=1}^{n}\log(x_i)-b\sum_{i=1}^{n}x_i$$

Maximum likelihood estimator

$$\hat{b}=\frac{n\hat{a}}{\sum_{i=1}^{n}x_i}$$

$\hat{a}$ is solved from: $\log(n\hat{a})-\log\left(\sum_{i=1}^{n}x_i\right)-\psi(\hat{a})+\frac{1}{n}\sum_{i=1}^{n}\log(x_i)=0$

$\psi(a)$ is the digamma function defined as $\psi(a)=\frac{d}{da}\log\Gamma(a)=\frac{\Gamma'(a)}{\Gamma(a)}$

Non-informative Jeffreys' prior

$$\pi(a,b)\propto\frac{\sqrt{a\ \psi'(a)-1}}{b}$$

WEIBULL DISTRIBUTION

Probability density function

$$\mathrm{We}(x|a,b)=\frac{a}{b}\left(\frac{x}{b}\right)^{a-1}\exp\left(-\left(\frac{x}{b}\right)^{a}\right)\ ,\ a>0,\ b>0,\ x>0$$

Survival function

$$\overline{F}(x|a,b)=\exp\left(-\left(\frac{x}{b}\right)^{a}\right)$$

Central moments

$$E(X)=b\Gamma\left(\frac{1}{a}+1\right)$$

$$\mathrm{Var}(X)=b^2\left(\Gamma\left(\frac{2}{a}+1\right)-\Gamma^2\left(\frac{1}{a}+1\right)\right)$$

Mean and variance

$\Gamma(a)$ is the gamma function defined as $\Gamma(a)=\int_{t=0}^{\infty}t^{a-1}\exp(-t)dt$

Log-likelihood	$\log \ell(\mathrm{x}\|s,m) = n(\log(a) - a\log(b)) + (a-1)\sum_{i=1}^{n}\log(x_i) - \sum_{i=1}^{n}\left(\frac{x_i}{b}\right)^a$
Maximum likelihood estimators	$\hat{b} = \left(\frac{1}{n}\sum_{i=1}^{n} x_i^{\hat{a}}\right)^{\frac{1}{\hat{a}}}$
	$\hat{a}$ is solved from: $\left(\frac{n}{\hat{a}} + \sum_{i=1}^{n}\log(x_i)\right)\left(\frac{1}{n}\sum_{i=1}^{n} x_i^{\hat{a}}\right) - \sum_{i=1}^{n} x_i^{\hat{a}}\log(x_i) = 0$
Non-informative Jeffreys' prior	$\pi(a,b) \propto \frac{1}{b}\frac{\pi}{\sqrt{6}}$

	GUMBEL DISTRIBUTION
Probability density function	$\mathrm{Gu}(x\|a,b) = \frac{1}{b}\exp\left(-\frac{x-a}{b}\right)\exp\left(-\exp\left(-\frac{x-a}{b}\right)\right)$, $b>0$
Survival function	$\overline{F}(x\|a,b) = 1 - \exp\left(-\exp\left(-\frac{x-a}{b}\right)\right)$
Mean and variance	$E(X) = a + b\gamma \qquad \mathrm{Var}(X) = \frac{\pi^2\beta^2}{6}$
	with Euler's constant $\gamma = 0.5772$
Log-likelihood	$\log \ell(\mathrm{x}\|a,b) = -n\log(b) - \sum_{i=1}^{n}\frac{x_i-a}{b} - \sum_{i=1}^{n}\exp\left(-\frac{x_i-a}{b}\right)$
Maximum likelihood estimators	$\hat{a} = -\hat{b}\log\left(\frac{1}{n}\sum_{i=1}^{n}\left(-\frac{x_i}{\hat{b}}\right)\right)$
	and $\hat{b}$ must be numerically solved from:
	$\frac{1}{n}\sum_{i=1}^{n}\frac{x_i-\hat{a}}{\hat{b}} - \frac{1}{n}\sum_{i=1}^{n}\frac{x_i-\hat{a}}{\hat{b}}\exp\left(-\frac{x_i-\hat{a}}{\hat{b}}\right) - 1 = 0$
Non-informative Jeffreys' prior	$\pi(\theta) \propto \frac{1}{b^2}\frac{\pi}{\sqrt{6}}$

APPENDIX V 'NWRW 4.3' runoff model

The runoff model commonly applied in The Netherlands comprises 4 processes, as shown in Figure V.1 (see Van Luijtelaar and Rebergen 1997 and Stichting RIONED 1999):

- initial losses: wetting of dry surface and storage in local surface depressions,
- infiltration,
- evaporation,
- flow routing.

The initial losses are introduced as an average constant value depending on the type of contributing surface, as shown in Table V.1.

The infiltration is calculated using the Horton infiltration model [Horton (1940)], given by,

1. Decrease of infiltration capacity

$$f(t) = f_c + (f_b - f_c)e^{-k_d t} \tag{V.1}$$

2. Recovery of infiltration capacity

$$f(t) = f_b + (f_b - f_c)e^{-k_r t} \tag{V.2}$$

where $f(t)$ is infiltration capacity at time t (mm/h), f_b is maximum infiltration capacity (t=0) (mm/h), f_c is minimum infiltration capacity (mm/h), k_d is recession factor of infiltration capacity (descending leg) (mm/h), k_r is recession factor of infiltration capacity (descending leg) (mm/h) and t is time (h). The default parameter values of the different types of surfaces are presented in Table V.1.

The evaporation is introduced as a monthly constant value in order to empty the surface storage in between storm events.

The overland flow towards the entry of the sewer system (e.g. gully pots) is introduced as,

$$q = c \cdot h \tag{V.3}$$

where q is flow (mm/min), c is routing constant (min^{-1}) and h is level of rainfall stored on surface (mm). The default parameter values of the different types of surfaces are presented in Table V.1.

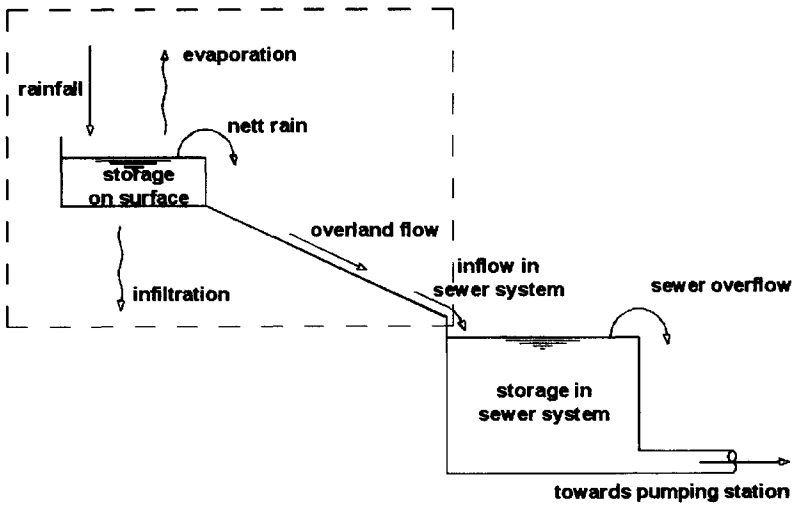

Figure V.1 Rainfall runoff model (Stichting RIONED 1999).

Table V.1 Default runoff parameters 'Leidraad Riolering' C2100 (Stichting RIONED 1999).

	type of surface		routing constant (min^{-1})	storage on surface (mm)	infiltration capacity (mm/h) max	infiltration capacity (mm/h) min	time factors (h^{-1}) decrease	time factors (h^{-1}) recovery
1	impervious	sloping	0.5	0.0				
2		flat	0.2	0.5				
3		flat, large area	0.1	1.0				
4	semi-	sloping	0.5	0.0	2.0	0.5	3.0	0.1
5	pervious	flat	0.2	0.5	2.0	0.5	3.0	0.1
6		flat, large area	0.1	1.0	2.0	0.5	3.0	0.1
7	roofs	sloping	0.5	0.0				
8		flat	0.2	2.0				
9		flat, large area	0.1	4.0				
10	pervious	sloping	0.5	2.0	5.0	1.0	3.0	0.1
11		flat	0.2	4.0	5.0	1.0	3.0	0.1
12		flat, large area	0.1	6.0	5.0	1.0	3.0	0.1

Appendix VI Bayes weights, Chi-square and Kolmogorov-Smirnov test for distribution selection

This appendix presents three different methods for choosing between candidate distribution types:

- Bayes weight assessment,
- Chi-square test,
- Kolmogorov-Smirnov test.

The methods have been applied to find the distribution type that fits best with a calculated series of CSO volumes of the sewer system of 'De Hoven'. These volumes have been calculated by means of Monte Carlo simulation (N = 500) accounting for either uncertain sewer system dimensions (Table VI.1 and Table VI.3) or natural variability in rainfall (Table VI.2 and Table VI.4). The choice between candidate distributions (exponential, Rayleigh, normal, lognormal, gamma, Weibull and Gumbel) is based on the average value of the Bayes weight or the rank (Chi-square and Kolmogorov-Smirnov) of a distribution type for 10 randomly selected runs.

The results of the different statistical tests show that a Weibull distribution (or eventually a gamma distribution) is most appropriate for describing calculated CSO volumes.

Bayes weight assessment is described in § 3.5.2.

The **Chi-square test** (see e.g. Hollander and Wolfe 1999) is based on a comparison of observed frequencies of events and frequencies estimated from a theoretical distribution function. The null hypothesis is written in terms of observed and sampled frequencies p,

$$H_0: \; p_1 = p_2 \tag{VI.1}$$

A measure of the discrepancy between observed frequencies O and estimated expected frequencies E under the null hypothesis is the Chi-squared statistic given by,

$$\chi^2 = \sum_{i=1}^{n} \frac{(O_i - E_i)^2}{E_i} \tag{VI.2}$$

If X_1, X_2,...,X_n represents a random sample from a standard normal distribution (N(0,1)) then for $n \geq 1$,

$$Y = \sum_{i=1}^{n} X_i^2 \tag{VI.3}$$

is said to have a Chi-squared distribution with index n ($\chi^2(n)$). The null hypothesis is rejected if $\chi^2 \geq \chi^2_{\alpha,n}$ where α is the upper percentile of the significance level and n is the number of degrees of freedom.

The **Kolmogorov-Smirnov test** (see e.g. Hollander and Wolfe 1999) compares an empirical distribution function $F_n(x)$ of samples $X_1, X_2,\ldots,X_n$ with a theoretical distribution function $G(y)$. The null hypothesis is that X and Y have the same probability distribution given that their common distribution is not specified. Formally stated this gives,

$$H_0: \left[F_n(t) = G(t) \text{ , for every } t\right] \tag{VI.4}$$

The test applies the following statistic,

$$T_{KS} = \sqrt{n} \max_x \left|F_n(x) - G(x)\right| \tag{VI.5}$$

where n is the total number of samples. This represents the distance between two cumulative distribution functions. The null hypothesis is rejected if $T_{KS} \geq T_\alpha$ where α is the upper percentile of the significance level.

Table VI.1 Bayes weights of 10 randomly selected runs from simulations accounting for uncertainty in sewer system dimensions of sewer system 'De Hoven'. The distribution type with the largest average Bayes weight fits best with the data, i.e. a Weibull distribution.

			Distribution type						
			Exp	Ray	Nor	Lgn	Gam	Wei	Gum
		Prior	0.1429	0.1429	0.1429	0.1429	0.1429	0.1429	0.1429
Run	1	Posterior	0.0088	0	0	0.0128	0.2308	0.7477	0
	2	Posterior	0.0047	0	0	0.0060	0.3223	0.6671	0
	3	Posterior	0	0	0	0	0.6770	0.3229	0
	4	Posterior	0.0112	0	0	0.0074	0.2489	0.7325	0
	5	Posterior	0.0321	0	0	0.0025	0.2934	0.672	0
	6	Posterior	0.0001	0	0	0	0.5093	0.4907	0
	7	Posterior	0.0053	0	0	0	0.3333	0.6614	0
	8	Posterior	0.0099	0	0	0	0.5769	0.4132	0
	9	Posterior	0.1017	0	0	0.6901	0.0658	0.1423	0
	10	Posterior	0.0006	0	0	0	0.386	0.6134	0
		Average	0.0174	0.0000	0.0000	0.0719	0.3644	0.5463	0.0000

Table VI.2 Bayes weights of 10 randomly selected runs from simulations accounting for natural variability in rainfall for sewer system 'De Hoven'. The distribution type with the largest average Bayes weight fits best with the data, i.e. either a Weibull or a gamma distribution.

			Distribution type						
			Exp	Ray	Nor	Lgn	Gam	Wei	Gum
		Prior	0.1429	0.1429	0.1429	0.1429	0.1429	0.1429	0.1429
Run	1	Posterior	0.5694	0	0	0.0041	0.2191	0.2074	0
	2	Posterior	0.0122	0	0	0	0.6241	0.3637	0
	3	Posterior	0.0316	0	0	0.0069	0.4078	0.5536	0
	4	Posterior	0.1243	0	0	0.0037	0.3355	0.5365	0
	5	Posterior	0	0	0	0.0048	0.3664	0.6289	0
	6	Posterior	0.2217	0	0	0.006	0.2858	0.4865	0
	7	Posterior	0.0747	0	0	0.0141	0.376	0.5352	0
	8	Posterior	0.0559	0	0	0.032	0.3722	0.5399	0
	9	Posterior	0.2852	0	0	0.0144	0.2255	0.4749	0
	10	Posterior	0	0	0	0.9869	0.0006	0.0125	0
		Average	0.1375	0.0000	0.0000	0.1073	0.3213	0.4339	0.0000

Table VI.3 Chi-square test and Kolmogorov-Smirnov test of 10 randomly selected runs from simulations accounting for uncertainty in sewer system dimensions of sewer system 'De Hoven'. The distribution type with the lowest rank fits best with the data. Based on the Kolmogorov-Smirnov test, the Weibull distribution type is chosen.

			Distribution type				
			Exp	Nor	Lgn	Gam	Wei
Run	1	Chi-square test	2.151	2389.395	0.179	0.314	0.361
		Rank	4	5	1	2	3
		K-S test	0.138	0.255	0.096	0.782	0.060
		Rank	3	4	2	5	1
	2	Chi-square test	1.892	414.421	0.173	0.310	0.336
		Rank	4	5	1	2	3
		K-S test	0.155	0.253	0.161	0.751	0.074
		Rank	2	4	3	5	1
	3	Chi-square test	1.417	155.457	0.361	0.308	0.249
		Rank	4	5	3	2	1
		K-S test	0.143	0.253	0.132	0.773	0.066
		Rank	3	4	2	5	1
	4	Chi-square test	1.653	517.060	0.172	0.299	0.316
		Rank	4	5	1	2	3
		K-S test	0.135	0.255	0.073	0.780	0.048
		Rank	3	4	2	5	1
	5	Chi-square test	1.822	1229.143	0.124	0.298	0.378
		Rank	4	5	1	2	3
		K-S test	0.138	0.250	0.133	0.719	0.074
		Rank	3	4	2	5	1
	6	Chi-square test	2.353	2312.852	0.178	0.319	0.280
		Rank	4	5	1	3	2
		K-S test	0.144	0.257	0.161	0.806	0.082
		Rank	2	4	3	5	1
	7	Chi-square test	1.676	485.708	0.231	0.308	0.317
		Rank	4	5	1	2	3
		K-S test	0.148	0.253	0.086	0.759	0.054
		Rank	3	4	2	5	1
	8	Chi-square test	1.234	80.720	0.303	0.286	0.334
		Rank	4	5	2	1	3
		K-S test	0.128	0.240	0.258	0.598	0.064
		Rank	2	3	4	5	1
	9	Chi-square test	1.049	98.035	0.133	0.257	0.428
		Rank	4	5	1	2	3
		K-S test	0.115	0.243	0.174	0.618	0.067
		Rank	2	4	3	5	1
	10	Chi-square test	0.834	813.642	0.221	0.270	0.153
		Rank	4	5	2	3	1
		K-S test	0.143	0.255	0.140	0.789	0.075
		Rank	3	4	2	5	1
Average		Rank: Chi-square	4	5	1.4	2.1	2.5
		Rank: K-S test	2.6	3.9	2.5	5	1

Table VI.4 Chi-square test and Kolmogorov-Smirnov test of 10 randomly selected runs from simulations accounting for natural variability in rainfall for sewer system 'De Hoven'. The distribution type with the lowest rank fits best with the data. Based on the Kolmogorov-Smirnov test, the Weibull distribution type is chosen.

			Distribution type				
			Exp	Nor	Lgn	Gam	Wei
Run	1	Chi-square test	0.469	1.674	0.394	0.301	0.458
		Rank	4	5	2	1	3
		K-S test	0.107	0.159	0.169	0.299	0.111
		Rank	1	3	4	5	2
	2	Chi-square test	0.458	16.209	0.261	0.221	0.192
		Rank	4	5	3	2	1
		K-S test	0.106	0.231	0.202	0.519	0.081
		Rank	2	4	3	5	1
	3	Chi-square test	0.718	3.753	0.167	0.267	0.335
		Rank	4	5	1	2	3
		K-S test	0.130	0.235	0.157	0.574	0.062
		Rank	2	4	3	5	1
	4	Chi-square test	0.429	36.115	0.109	0.221	0.176
		Rank	4	5	1	3	2
		K-S test	0.145	0.235	0.125	0.588	0.085
		Rank	3	4	2	5	1
	5	Chi-square test	11.866	1.13E+04	0.452	0.379	0.382
		Rank	4	5	3	1	2
		K-S test	0.246	0.293	0.127	0.694	0.065
		Rank	3	4	2	5	1
	6	Chi-square test	3.316	7.03E+04	0.162	0.283	0.526
		Rank	4	5	1	2	3
		K-S test	0.095	0.256	0.100	0.685	0.052
		Rank	2	4	3	5	1
	7	Chi-square test	0.510	2.666	0.145	0.229	0.269
		Rank	4	5	1	2	3
		K-S test	0.116	0.227	0.222	0.495	0.059
		Rank	2	4	3	5	1
	8	Chi-square test	0.537	12.224	0.151	0.241	0.186
		Rank	4	5	1	3	2
		K-S test	0.145	0.246	0.146	0.665	0.086
		Rank	2	4	3	5	1
	9	Chi-square test	19.983	5.12E+05	0.246	0.464	2.008
		Rank	4	5	1	2	3
		K-S test	0.094	0.284	0.137	0.927	0.086
		Rank	2	4	3	5	1
	10	Chi-square test	37.598	6.17E+03	0.269	0.543	0.804
		Rank	4	5	1	2	3
		K-S test	0.255	0.323	0.213	1.112	0.102
		Rank	3	4	2	5	1
Average		Rank: Chi-square	4	5	1.5	2	2.5
		Rank: K-S test	2.2	3.9	2.8	5	1.1

Appendix VII Calibration of hydro-dynamic model of 'De Hoven'

Storm event 25/08/98 (from Clemens 2001a)

Table VII.1 Values of calibrated parameters for storm event 25/08/98 'De Hoven' (reduced parameter set).

		Average	Std.	CV[1]
Storm 25/08/98	N1 (m^3/h)	26.160	0.070	0.268
	B* (mm)	0.491	0.009	1.784
	I* (mm/h)	0.229	0.002	0.655
	F* (s)	277.035	7.938	2.865
	CC* ($m^{0.5}$/s)	1.035	0.019	1.787

[1] CV = coefficient of variation = σ/μ*100%

Table VII.2 Correlation of calibrated parameters for storm event 25/08/98 'De Hoven' (reduced parameter set).

Storm 25/08/98	N*	B*	I*	F*	CC*
N1	1	0.46805	0.26417	-0.06969	-0.00472
B*	0.46805	1	-0.63208	-0.13283	0.02250
I*	0.26417	-0.63208	1	-0.23636	-0.01904
F*	-0.06969	-0.13283	-0.23636	1	-0.04690
CC*	-0.00472	0.02503	-0.01904	-0.04690	1

Table VII.3 Statistics of residuals for storm event 25/08/98 'De Hoven' (reduced parameter set).

		Gauge17.1	Gauge108.1	Gauge200.1	Total
MSE	(*10^{-4})	2.424	2.196	1.708	2.112
RMSE	(*10^{-2})	1.557	1.482	1.307	1.453
VAR	(*10^{-4})	2.303	2.195	1.700	2.102
STD	(*10^{-2})	1.518	1.482	1.304	1.449

Table VII.4 Statistics of residuals for storm event 25/08/98 'De Hoven' (full parameter set).

		Gauge17.1	Gauge108.1	Gauge200.1	Total
MSE	(*10^{-4})	2.528	2.624	1.664	2.253
RMSE	(*10^{-2})	1.590	1.623	1.290	1.513
VAR	(*10^{-4})	2.352	2.628	1.667	2.258
STD	(*10^{-2})	1.530	1.622	1.290	1.501

Storm event 07/10/98 (from Clemens 2001a)

Table VII.5 Values of calibrated parameters for storm event 07/10/98 'De Hoven' (full parameter set).

		Average	Std.	CV[1]
Storm 07/10/98	N1 (m^3/h)	65.480	2.730	4.169
	B2 (mm)	3.365	0.203	6.018
	I2 (mm/h)	0.138	0.021	15.455
	B7 (mm)	0.295	0.048	16.102
	I7 (mm/h)	0.105	0.018	16.667
	F* (s)	758.540	77.250	10.184

[1] CV = coefficient of variation = $\sigma/\mu*100\%$

Table VII.6 Correlation of calibrated parameters for storm event 07/10/98 'De Hoven' (full parameter set).

Storm 07/10/98	N*	B2	I2	B7	I7	F*
N1	1	0.026768	0.26234	-0.20913	0.11138	-0.51117
B2	0.0267	1	-0.49702	-0.5875	0.04193	-0.34412
I2	0.26234	-0.49702	1	-0.19013	-0.48033	0.23038
B7	-0.20913	-0.5875	-0.19013	1	-0.1748	-0.11643
I7	0.11138	0.04193	-0.48033	-0.1748	1	0.06183
F*	-0.51117	-0.34412	0.23038	-0.11643	0.06183	1

Storm event 24/10/98 (from Clemens 2001a)

Table VII.7 Values of calibrated parameters for storm event 24/10/98 'De Hoven' (reduced parameter set).

		Average	Std.	CV[1]
Storm 24/10/98	N1 (m^3/h)	51.970	0.675	1.299
	B* (mm)	0.448	0.015	3.408
	I* (mm/h)	0.183	0.003	1.827
	F* (s)	669.635	11.898	1.777
	CC* ($m^{0.5}/s$)	1.283	0.071	5.563

[1] CV = coefficient of variation = $\sigma/\mu*100\%$

Table VII.8 Correlation of calibrated parameters for storm event 24/10/98 'De Hoven' (reduced parameter set).

Storm 24/10/98	N*	B*	I*	F*	CC*
N1	1	-0.2467	0.66634	-0.71519	-0.082115
B*	-0.2467	1	-0.8252	-0.11643	0.001976
I*	0.66634	-0.8252	1	-0.36226	-0.087235
F*	-0.71519	-0.11643	-0.36226	1	0.15272
CC*	-0.082115	0.001976	-0.087235	0.15272	1

APPENDIX VIII Calibration of hydrodynamic model of 'Loenen'

Measured rainfall 'Loenen'

The hydrodynamic model of the sewer system of 'Loenen' has been calibrated on the basis of three storm events (see Figure VIII.1, Figure VIII.2 and Figure VIII.3)

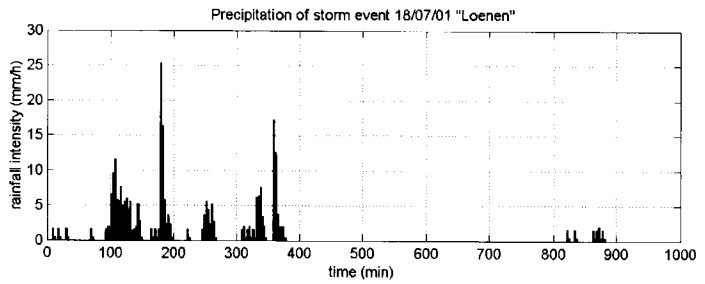

Figure VIII.1 Measured rainfall of storm event 18/07/01 'Loenen'.

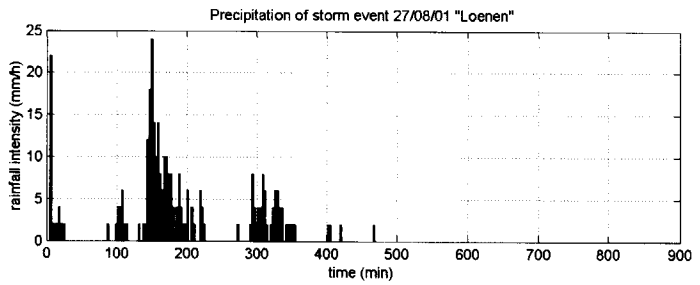

Figure VIII.2 Measured rainfall of storm event 27/08/01 'Loenen'.

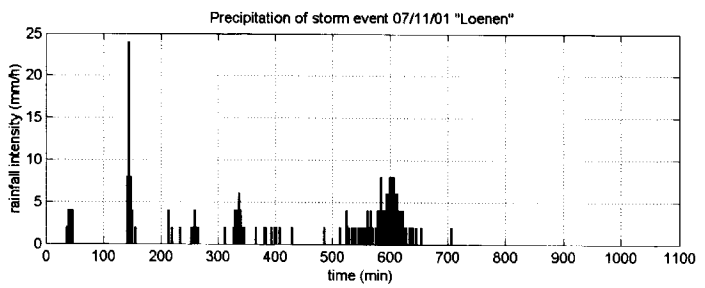

Figure VIII.3 Measured rainfall of storm event 07/11/01 'Loenen'.

Modelling inflow from 'Veldhuizen'

In the hydrodynamic model a constant inflow of $0.5*Q_{in,max}$ has been used. This value is slightly larger than the average plus the standard deviation of the measured inflow. The inflow is located at the pumping station.

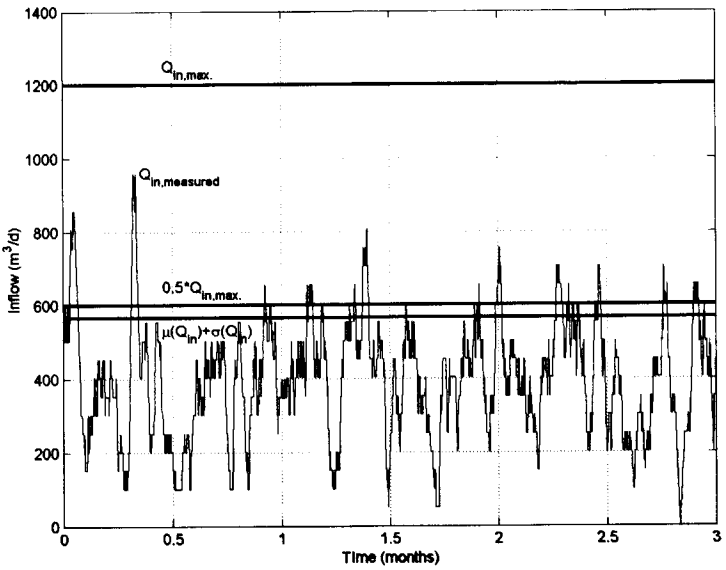

Figure VIII.4 Measured inflow from 'Veldhuizen'.

Storm event 18/07/01: reduced parameter set

Table VIII.1 Values of calibrated parameters for storm event 18/07/01 'Loenen' (reduced parameter set).

		Average	Std.	CV [1]
Storm 18/07/01	N1 (m^3/h)	104.3832	0.0551	0.0526
	B* (mm)	2.0955	0.0007	0.0322
	F* (s)	88.7164	0.1504	0.1695
	I* (mm/h)	0.4350	0.0056	1.2960
	CC ($m^{0.5}$/s)	0.8222	0.0103	1.2579

[1] CV = coefficient of variation = σ/μ*100%

Table VIII.2 **Correlation of calibrated parameters for storm event 18/07/01, 'Loenen' (reduced parameter set). Storage on streets shows relatively large correlation with routing coefficient and infiltration capacity.**

Storm 18/07/01	N1	B*	F*	I*	CC
N1	1	0.04482	-0.15304	0.03210	0.16979
B*	0.04482	1	-0.41863	-0.85181	0.05357
F*	-0.15304	-0.41863	1	0.05824	-0.02343
I*	0.03210	-0.85181	0.05824	1	-0.0575
CC	0.16979	0.05357	-0.02343	-0.0575	1

Table VIII.3 **Statistics of residuals for storm event 18/07/01 'Loenen' (reduced parameter set). The smaller the values, the higher the quality of the calibration.**

		S02	S03	S04	S07	S12	Total
REL.BIAS	($*10^{-2}$)	1.50	0.78	12.51	1.84	-	-
MSE	($*10^{-3}$)	4.04	2.12	0.68	2.39	3.47	2.57
RMSE	($*10^{-2}$)	6.36	4.61	2.61	4.89	5.89	5.07
VAR	($*10^{-3}$)	4.06	2.13	4.11	2.37	0.64	2.53
STD	($*10^{-2}$)	6.37	4.62	2.03	4.87	2.52	5.03

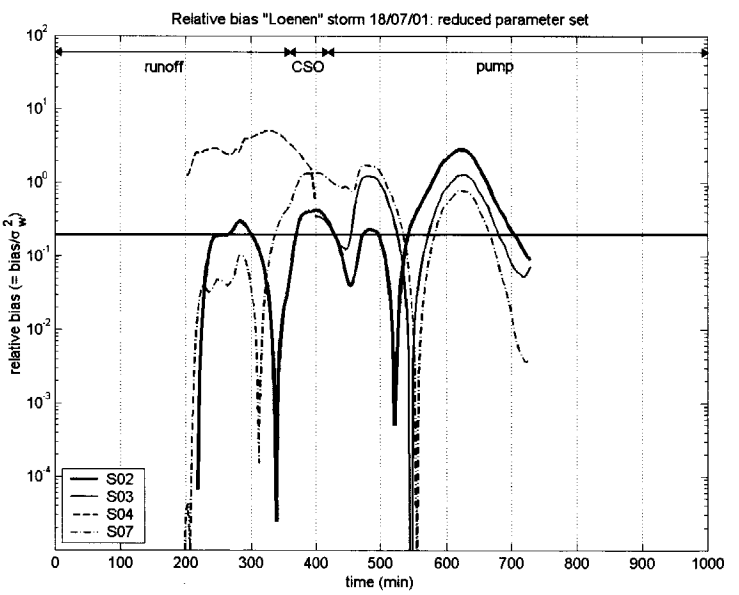

Figure VIII.5 **Relative bias 'Loenen' storm 18/07/01 (reduced parameter set). Except for S04, the relative bias is higher during the actual CSO and the emptying of the system. S04 is located in a small, relatively isolated part upstream in the system.**

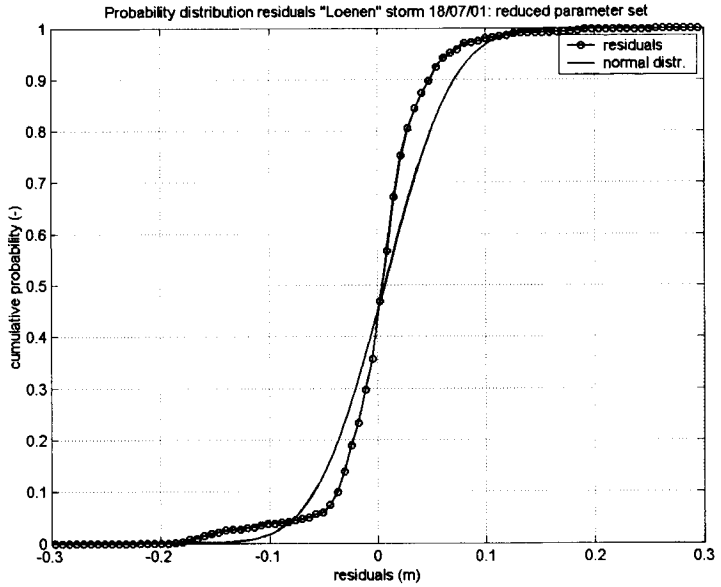

Figure VIII.6 Probability distribution residuals 'Loenen' storm 18/07/01 (reduced parameter set). The distribution of residuals differs from Gaussian, in particular for negative values. The average value of residuals is slightly larger than 0.

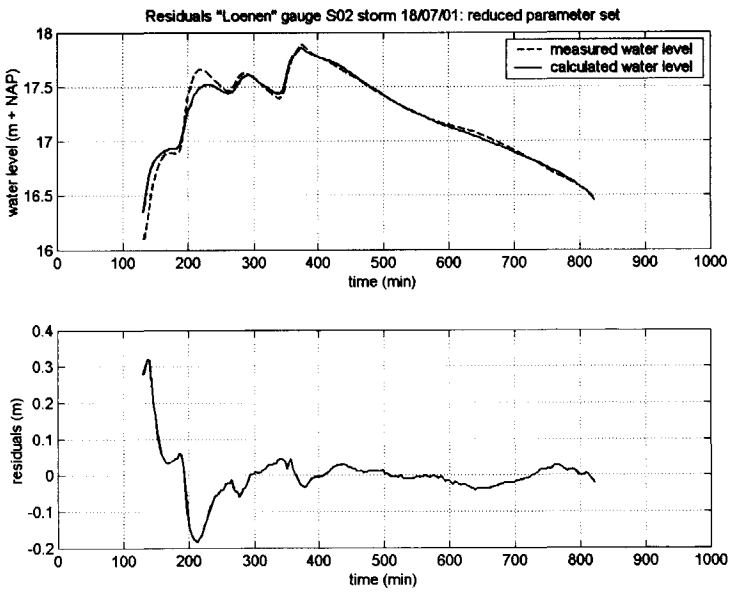

Figure VIII.7 Residuals 'Loenen' gauge S02 storm 18/07/01 (reduced parameter set). The largest difference occurs during the filling of the system.

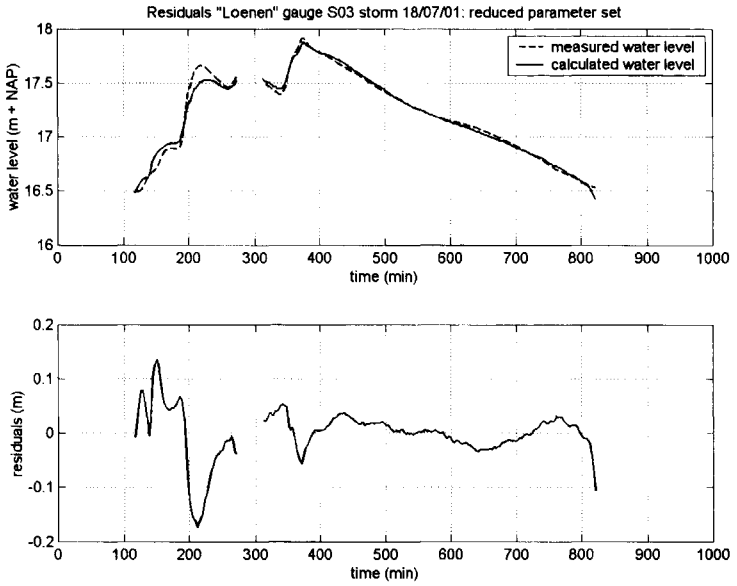

Figure VIII.8 Residuals 'Loenen' gauge S03 storm 18/07/01 (reduced parameter set). The largest difference occurs during the filling of the system.

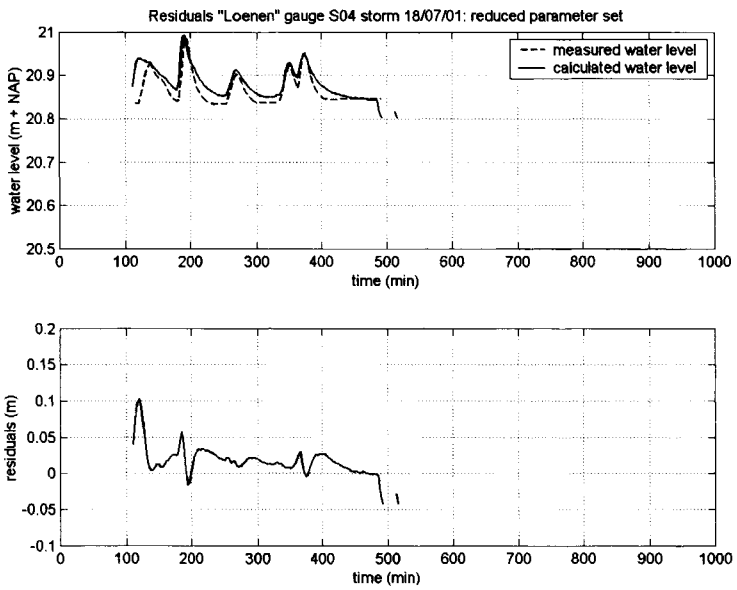

Figure VIII.9 Residuals 'Loenen' gauge S04 storm 18/07/01 (reduced parameter set). Calculated levels deviate considerably from measurements.

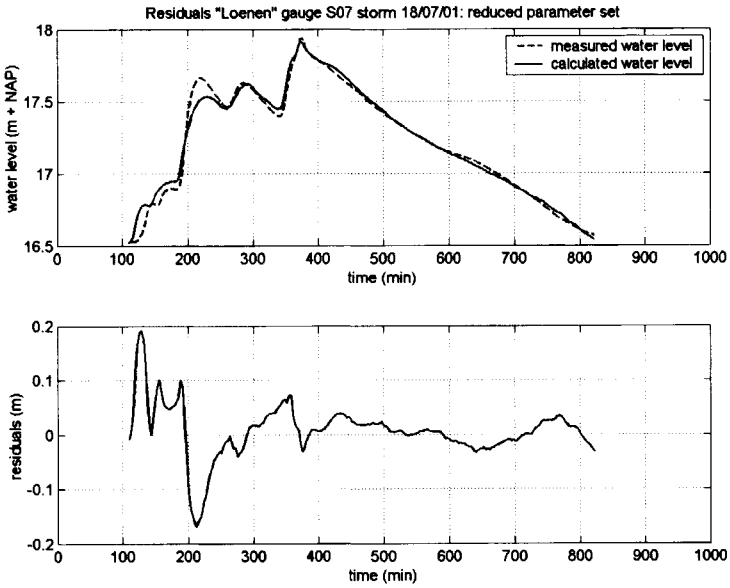

Figure VIII.10 Residuals 'Loenen' gauge S07 storm 18/07/01 (reduced parameter set). The largest difference occurs during the filling of the system.

Storm event 18/07/01: full parameter set

Table VIII.4 Values of calibrated parameters for storm event 18/07/01 'Loenen' (full parameter set).

	Parameter	Value
Storm event 18/07/01	N1	98.57
	B2	5.10
	F2	289.00
	B5	0.40
	F5	704.60
	I5	3.10
	B7	0.72
	F7	44.40
	B8	1.85
	F8	946.60
	CC	0.67

Table VIII.5 Statistics of residuals for storm event 18/07/01 'Loenen' (full parameter set). The smaller the values, the higher the quality of the calibration.

		S02	S03	S04	S07	S12	Total
REL.BIAS	($*10^{-2}$)	15.81	7.06	18.13	3.64	-	-
MSE	($*10^{-4}$)	6.22	5.27	4.17	4.98	23.66	6.45
RMSE	($*10^{-2}$)	2.49	2.30	2.04	2.23	4.86	2.54
VAR	($*10^{-4}$)	4.61	4.14	2.31	4.96	4.63	6.42
STD	($*10^{-2}$)	2.15	2.04	1.52	2.23	2.15	2.53

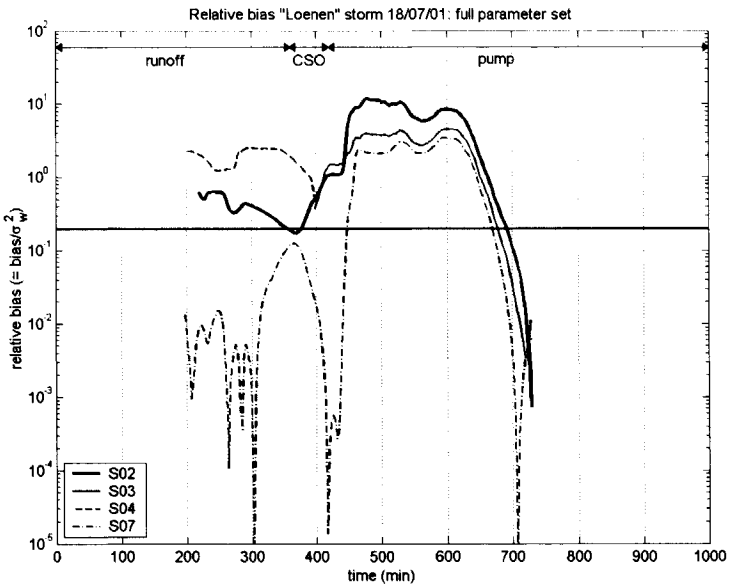

Figure VIII.11 Relative bias 'Loenen' storm 18/07/01 (full parameter set). In general, relative bias is more pronounced than for the reduced set. It is the highest during the emptying of the system.

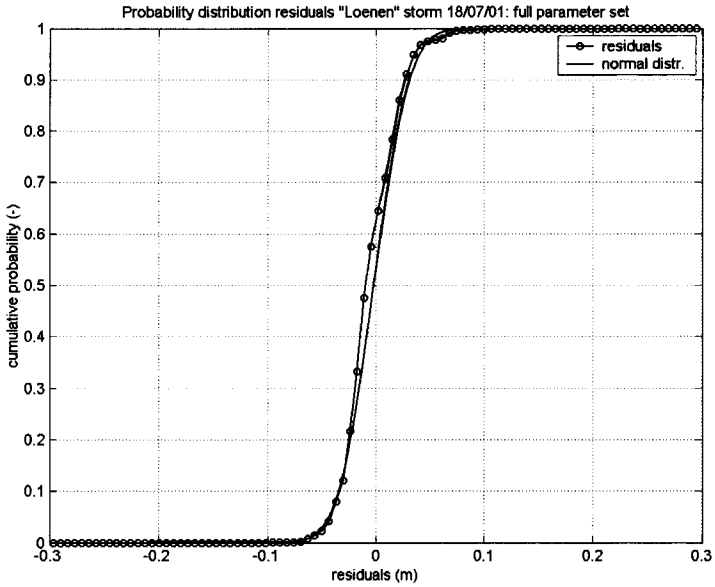

Figure VIII.12 Probability distribution residuals 'Loenen' storm 18/07/01 (full parameter set). There is a very good fit between the probability distribution of the residuals and a normal distribution.

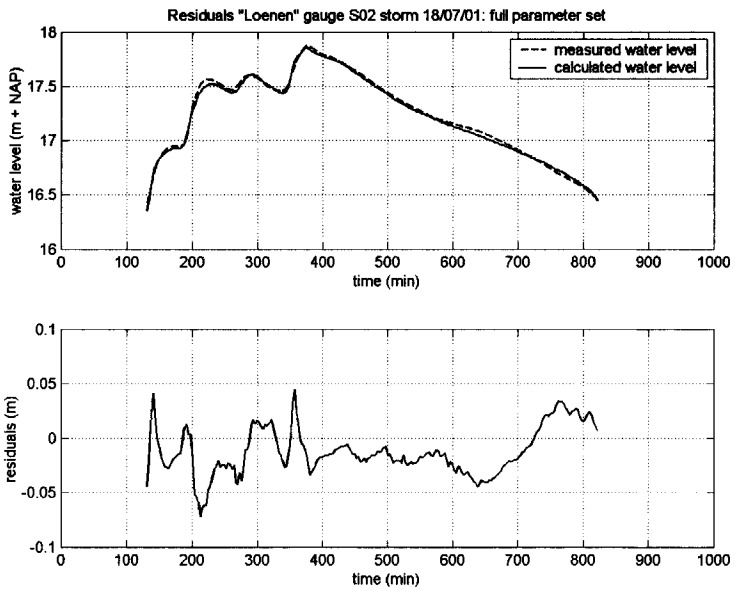

Figure VIII.13 Residuals 'Loenen' gauge S02 storm 18/07/01 (full parameter set). The residuals vary during the storm event with maxima during the actual CSO and at the beginning and end of the event.

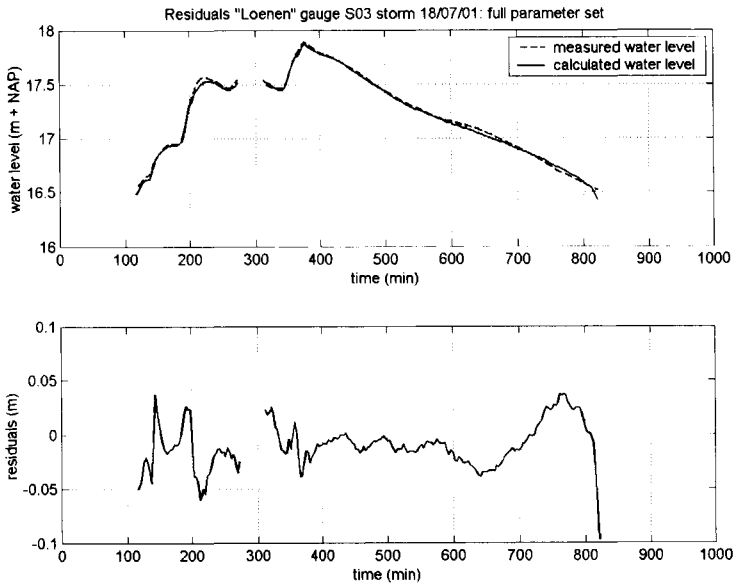

Figure VIII.14 Residuals 'Loenen' gauge S03 storm 18/07/01 (full parameter set). The residuals vary during the storm event with maxima during the actual CSO and at the beginning and end of the event.

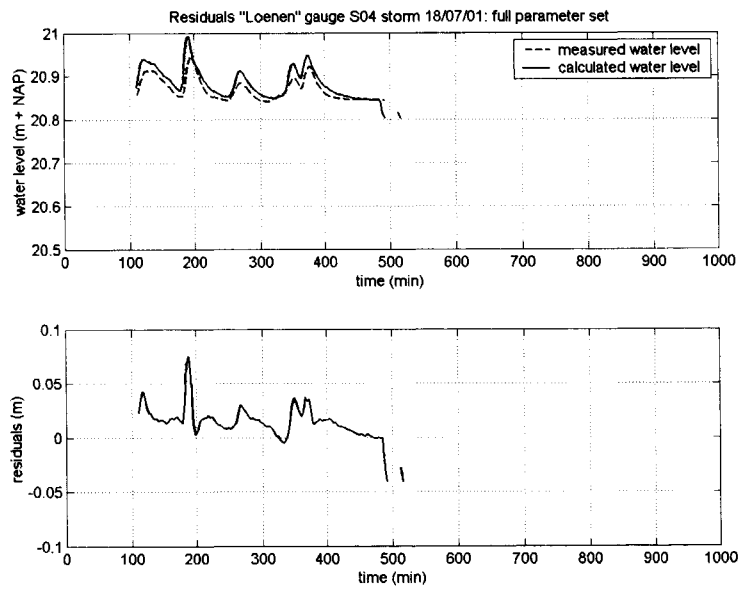

Figure VIII.15 Residuals 'Loenen' gauge S04 storm 18/07/01 (full parameter set). Calculated levels deviate considerably from measurements.

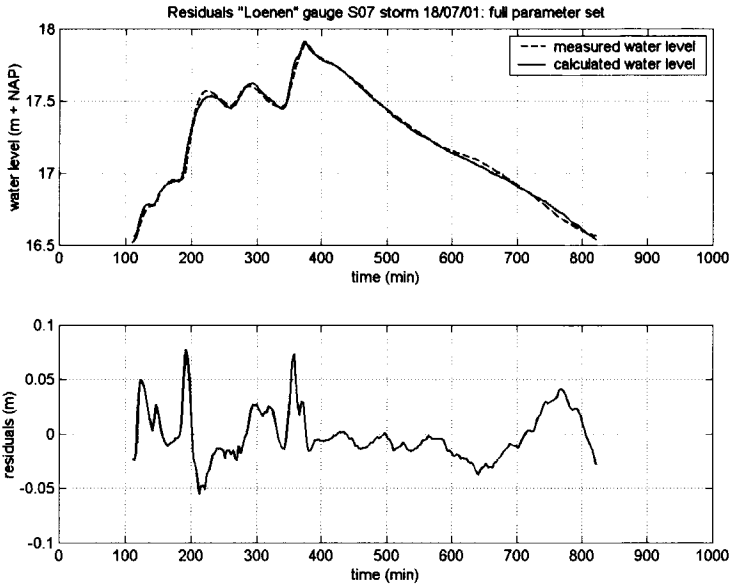

Figure VIII.16 Residuals 'Loenen' gauge S07 storm 18/07/01 (full parameter set). The residuals vary during the storm event with maxima during the actual CSO and at the beginning and end of the event.

Storm event 27/08/01: reduced parameter set

Table VIII.6 Values of calibrated parameters for storm event 27/08/01 'Loenen' (reduced parameter set).

		Average	Std.	CV[1]
Storm 2708/01(a)	N1 (m^3/h)	66.3801	0.0607	0.0914
	B* (mm)	1.9068	0.0020	0.1060
	F* (s)	540.4307	2.8755	0.5321
	I* (mm/h)	0.4595	0.0016	0.3462
	CC ($m^{0.5}/s$)	0.9929	0.0096	0.9657

[1] CV = coefficient of variation = σ/μ*100%

Table VIII.7 **Correlation of calibrated parameters for storm event 27/08/01, 'Loenen' (reduced parameter set). Storage on streets and dry weather flow show relatively large correlation with routing coefficient and infiltration capacity.**

Storm 27/08/01	N1	B*	F*	I*	CC
N1	1	-0.04799	-0.36070	0.30784	-0.00648
B*	-0.04799	1	-0.43397	-0.73850	0.13500
F*	-0.36070	-0.43397	1	-0.12948	0.12870
I*	0.30784	-0.73850	-0.12948	1	-0.25625
CC	-0.00648	0.13500	0.12870	-0.25625	1

Table VIII.8 **Statistics of residuals for storm event 27/08/01, 'Loenen' (reduced parameter set). The smaller the values, the higher the quality of the calibration.**

		S02	S03	S04	S07	S08	Total
REL.BIAS	($*10^{-2}$)	5.54	7.11	-	10.61	-	-
MSE	($*10^{-3}$)	1.62	0.96	0.81	1.94	11.68	1.57
RMSE	($*10^{-2}$)	4.03	3.10	2.85	4.41	10.81	3.96
VAR	($*10^{-3}$)	1.59	0.96	0.83	1.68	4.12	1.55
STD	($*10^{-2}$)	3.98	3.09	2.88	4.10	6.42	3.94

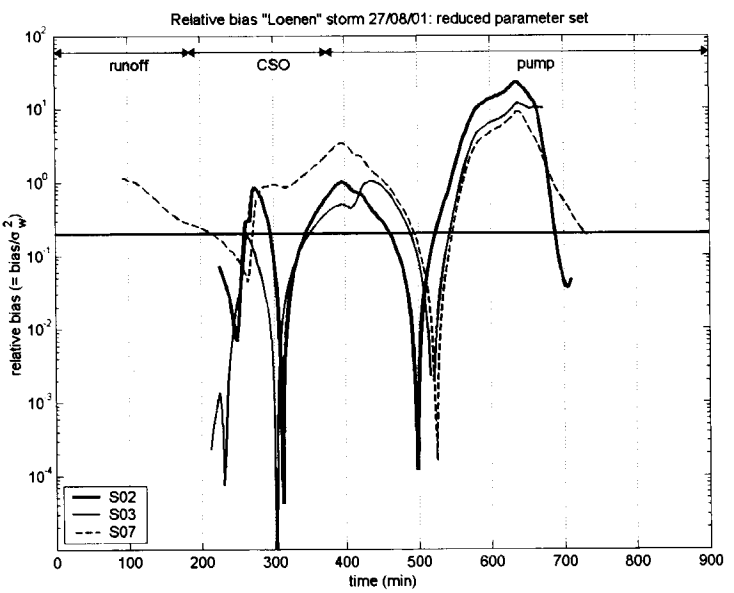

Figure VIII.17 **Relative bias 'Loenen' storm 27/08/01 (reduced parameter set). The relative bias is the highest during the emptying of the system. The transitions between the different phases are clearly recognisable.**

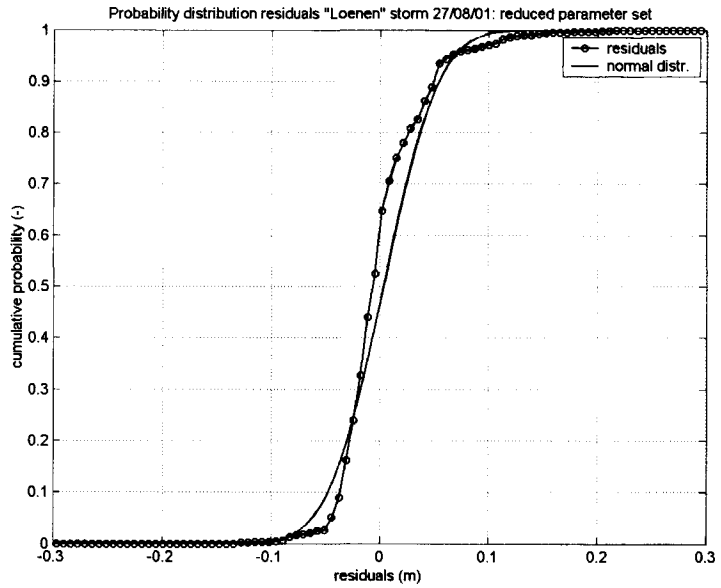

Figure VIII.18 Probability distribution residuals 'Loenen' storm 27/08/01 (reduced parameter set). The distribution of residuals is significantly different from Gaussian and the average is slightly smaller than 0.

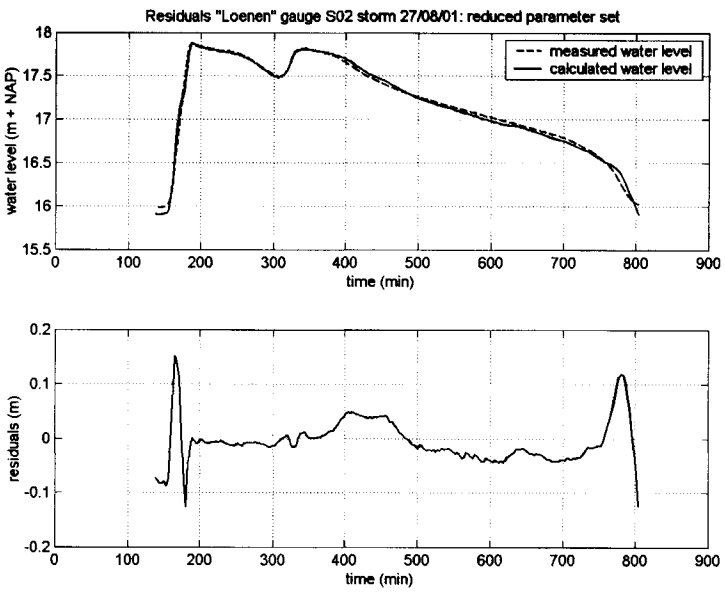

Figure VIII.19 Residuals 'Loenen' gauge S02 storm 27/08/01 (reduced parameter set). The residuals vary during the storm event with maxima at the beginning and end of the event.

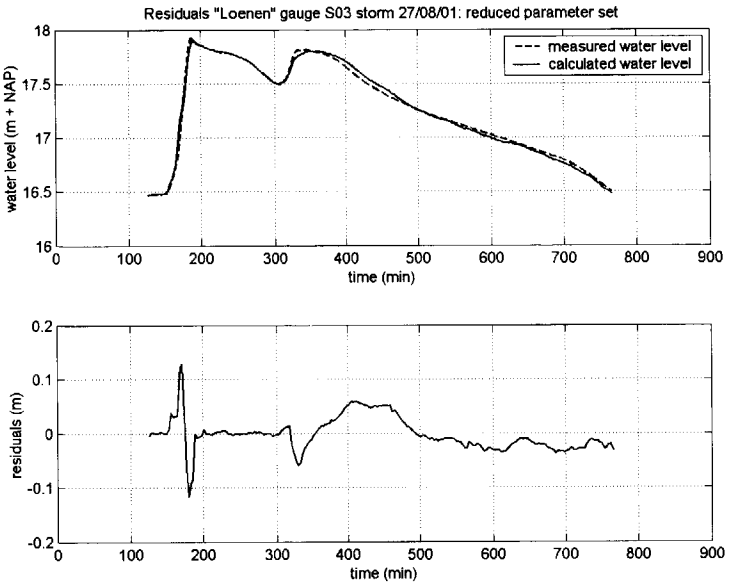

Figure VIII.20 Residuals 'Loenen' gauge S03 storm 27/08/01 (reduced parameter set). The residuals are relatively large during the filling of the system and the second part of the CSO event.

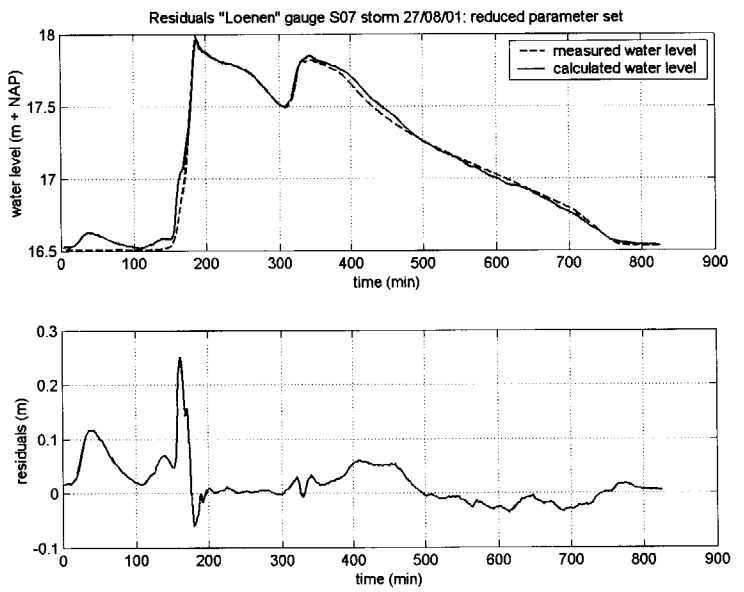

Figure VIII.21 Residuals 'Loenen' gauge S07 storm 27/08/01 (reduced parameter set). The residuals are relatively large vary during the filling of the system.

Storm event 27/08/01: reduced parameter set, database errors not removed

Table VIII.9 Values of calibrated parameters for storm event 27/08/01 'Loenen' (reduced parameter set, database errors not removed).

		Average	Std.	CV[1]
Storm 27/08/01	N1 (m^3/h)	59.9390	0.0959	0.1600
	B* (mm)	0.1857	0.0011	0.5723
	F* (s)	90.2239	1.0574	1.1720
	I* (mm/h)	2.303983	$4.6*10^{-14}$	$2.0*10^{-12}$
	CC ($m^{0.5}/s$)	9.552991	0.3576	3.7430

[1] CV = coefficient of variation = $\sigma/\mu*100\%$

Table VIII.10 Correlation of calibrated parameters for storm event 27/08/01, 'Loenen' (reduced parameter set, database errors not removed). Storage on streets is strongly correlated with infiltration capacity.

Storm 27/08/01	N1	B*	F*	I*	CC
N1	1	-0.0579	-0.09501	0.23639	-0.07353
B*	-0.0579	1	-0.28715	-0.95597	-0.03862
F*	-0.09501	-0.28715	1	0.14902	-0.04966
I*	0.23639	-0.95597	0.14902	1	-0.00697
CC	-0.07353	-0.03862	-0.04966	-0.00697	1

Table VIII.11 Statistics of residuals for storm event 27/08/01, 'Loenen' (reduced parameter set, database errors not removed). In general, the values are considerably larger than in case of removal of database errors. Consequently, the result of the calibration is worse.

		S02	S03	S04	S07	S08	Total
REL.BIAS	($*10^{-2}$)	6.03	7.34	-	10.75	-	-
MSE	($*10^{-3}$)	8.50	5.12	3.21	3.93	74.47	6.00
RMSE	($*10^{-2}$)	9.22	7.15	5.66	6.27	27.29	7.75
VAR	($*10^{-3}$)	7.10	4.89	0.31	3.63	7.94	5.74
STD	($*10^{-2}$)	8.43	6.99	1.77	6.02	8.91	7.57

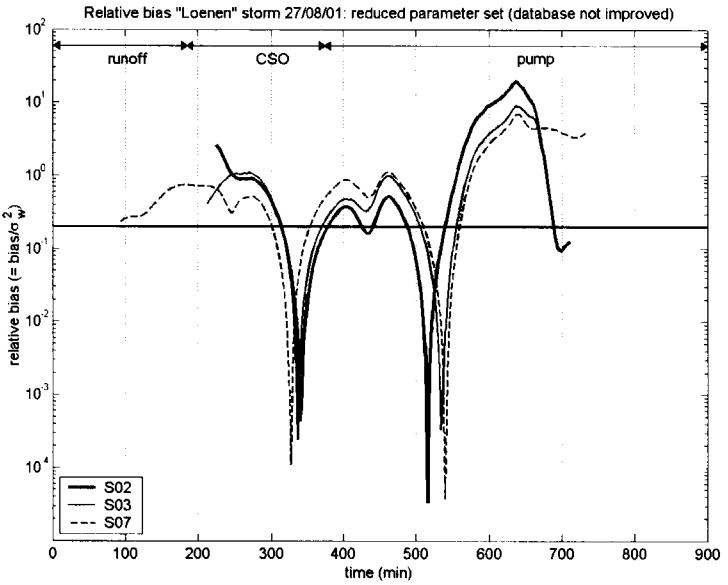

Figure VIII.22 Relative bias 'Loenen' storm 27/08/01 (reduced parameter set, database errors not removed). The relative bias is the highest during the emptying of the system.

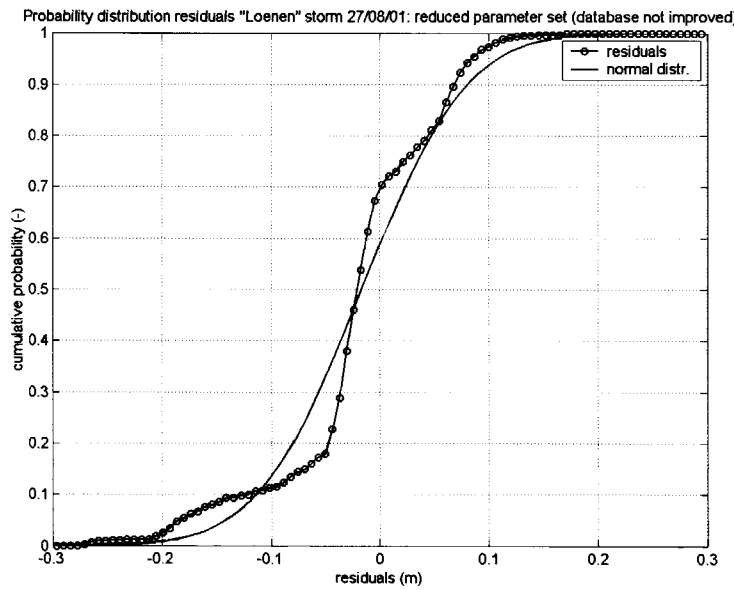

Figure VIII.23 Probability distribution residuals 'Loenen' storm 27/08/01 (reduced parameter set, database errors not removed). The distribution of residuals is different from Gaussian and is not smooth, indicating systematic errors in the database.

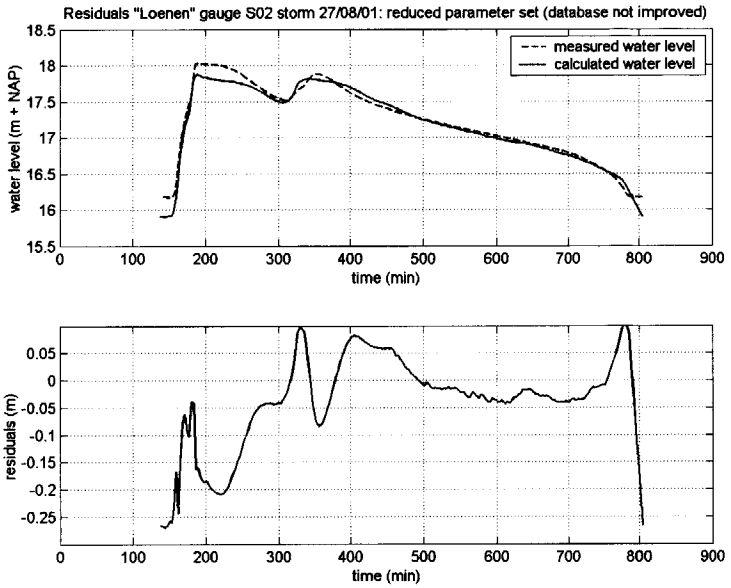

Figure VIII.24 Residuals 'Loenen' gauge S02 storm 27/08/01 (reduced parameter set, database errors not removed). The residuals are much larger than in case of removal of database errors, especially during the CSO event due to a too low weir level.

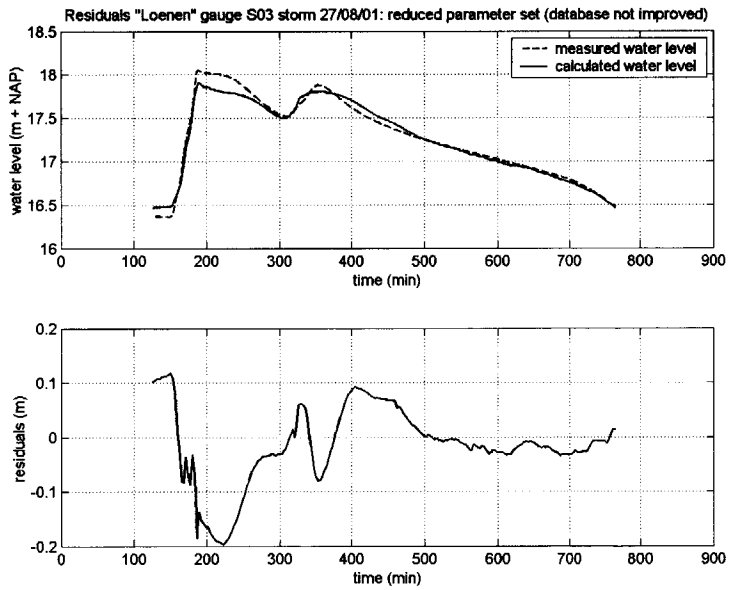

Figure VIII.25 Residuals 'Loenen' gauge S03 storm 27/08/01 (reduced parameter set, database errors not removed). The residuals are much larger than in case of removal of database errors.

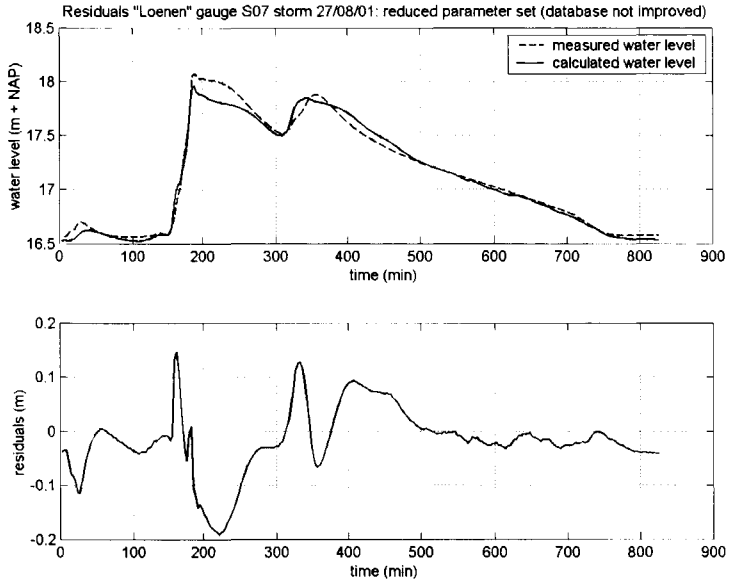

Figure VIII.26 Residuals 'Loenen' gauge S07 storm 27/08/01 (reduced parameter set, database errors not removed). The residuals are much larger than in case of removal of database errors.

Storm event 27/08/01: full parameter set

Table VIII.12 Values of calibrated parameters for storm event 27/08/01 'Loenen' (full parameter set).

	Parameter	Value
Storm event 18/07/01	N1	47.30
	B2	1.48
	F2	228.18
	B5	1.48
	F5	228.18
	I5	6.57
	B7	0.21
	F7	85.53
	B8	4.85
	F8	244.69
	CC	0.72

Table VIII.13 Statistics of residuals for storm event 27/08/01, 'Loenen' (full parameter set). The values are smaller than for the reduced parameter set, which is an indication of a better calibration.

		S02	S03	S04	S07	S08	Total
REL.BIAS	(*10^{-2})	7.10	13.08	-	9.72	-	-
MSE	(*10^{-3})	5.75	2.31	0.76	2.04	11.98	3.18
RMSE	(*10^{-2})	7.58	4.81	2.76	4.52	10.95	5.64
VAR	(*10^{-3})	5.04	1.86	0.55	2.02	3.98	2.98
STD	(*10^{-2})	7.10	4.31	2.34	4.50	6.31	5.46

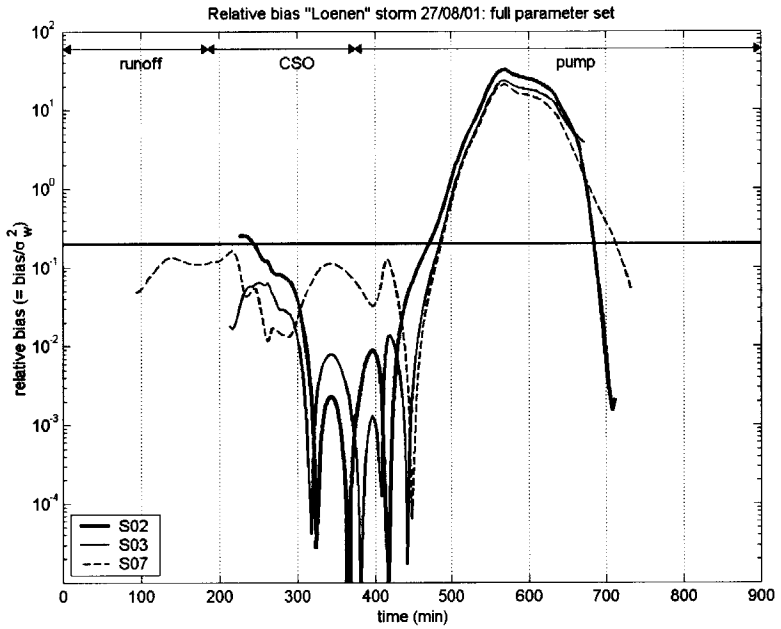

Figure VIII.27 Relative bias 'Loenen' storm 27/08/01 (full parameter set). The relative bias is the highest during the emptying of the system and lowest during the actual spilling. The transitions between the different phases are clearly recognisable.

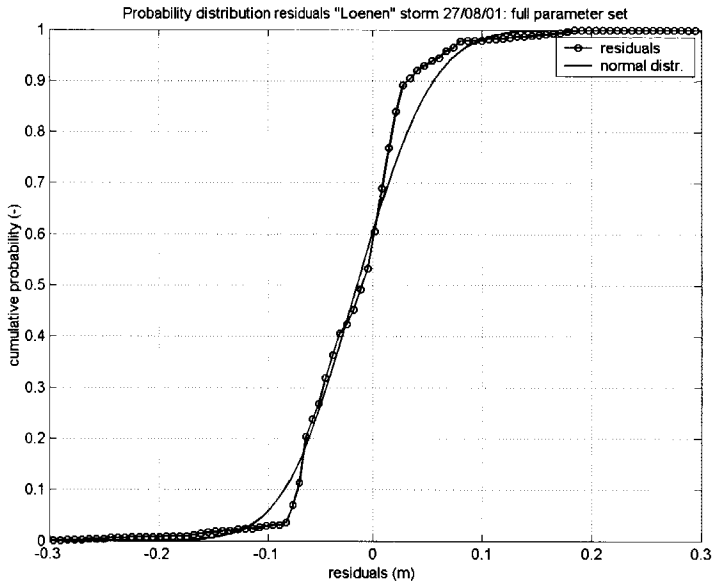

Figure VIII.28 Probability distribution residuals 'Loenen' storm 27/08/01 (full parameter set). The distribution of residuals is different from Gaussian. The contribution of relatively large residuals is smaller.

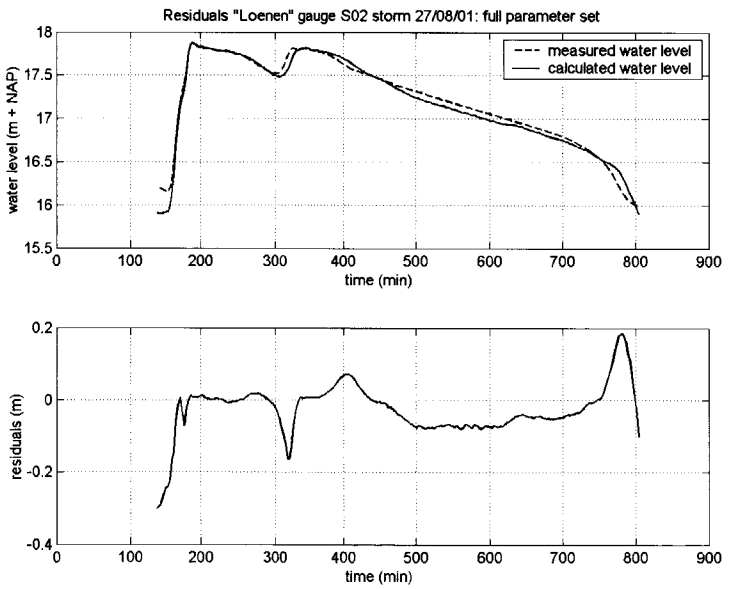

Figure VIII.29 Residuals 'Loenen' gauge S02 storm 27/08/01 (full parameter set). The residuals are relatively large at the beginning and end of the storm event and during the second part of the CSO event.

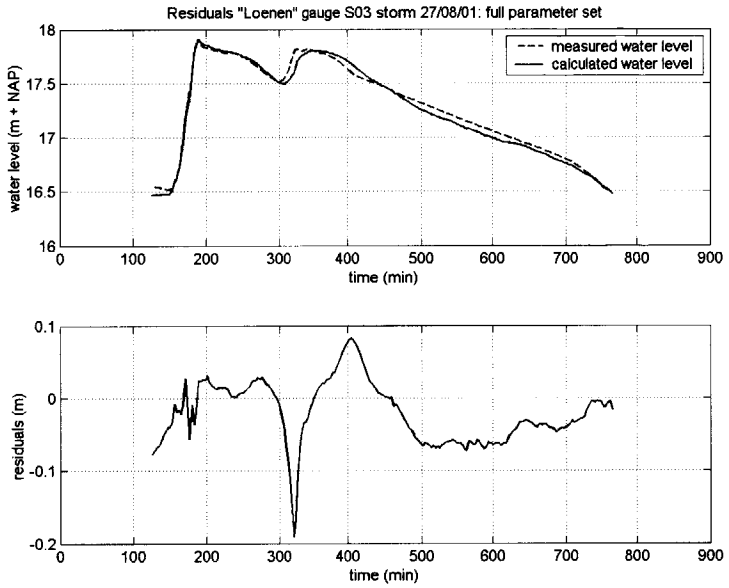

Figure VIII.30 Residuals 'Loenen' gauge S03 storm 27/08/01 (full parameter set). The residuals are during the second part of the CSO event.

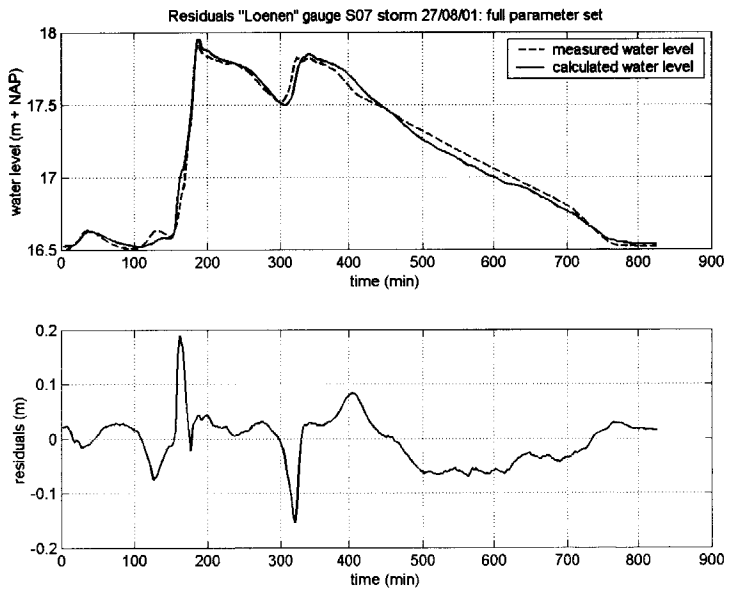

Figure VIII.31 Residuals 'Loenen' gauge S07 storm 27/08/01 (full parameter set). The residuals are relatively large during the rise of the water level of the CSO event.

Storm event 07/11/01: reduced parameter set

Table VIII.14 Values of calibrated parameters for storm event 07/11/01 'Loenen' (reduced parameter set).

		Average	Std.	CV[1]
Storm 07/11/01	N1 (m^3/h)	79.5218	0.0874	0.1099
	B* (mm)	0.8516	0.0016	0.1903
	F* (s)	303.0296	1.0736	0.3543
	I* (mm/h)	0.3483	$7.0*10^{-15}$	$2.0*10^{-12}$
	CC ($m^{0.5}$/s)	0.7858	0.0030	0.3811

[1] CV = coefficient of variation = σ/μ*100%

Table VIII.15 Correlation of calibrated parameters for storm event 07/11/01, 'Loenen'. Dry weather flow shows relatively large correlation with infiltration capacity and overflow coefficient. Storage on streets is also correlated with infiltration capacity.

Storm 07/11/01	N1	B*	F*	I*	CC
N1	1	0.07557	-0.12514	0.79353	-0.82573
B*	0.07557	1	-0.15115	-0.49980	-0.07298
F*	-0.12514	-0.15115	1	-0.11049	0.01573
I*	0.79353	-0.49980	-0.11049	1	-0.63900
CC	-0.82573	-0.07298	0.01573	-0.63900	1

Table VIII.16 Statistics of residuals for storm event 07/11/01, 'Loenen' (reduced parameter set). The smaller the values, the higher the quality of the calibration.

		S02	S03	S04	S06	S07	S11	Total
REL.BIAS	($*10^{-1}$)	0.19	1.16	-	-	2.58	6.33	-
MSE	($*10^{-3}$)	5.53	1.82	0.54	1.40	1.47	3.13	2.68
RMSE	($*10^{-2}$)	7.44	4.27	2.33	3.74	3.83	5.60	5.17
VAR	($*10^{-3}$)	5.38	1.75	0.24	0.55	1.02	0.64	2.51
STD	($*10^{-2}$)	7.34	4.19	1.57	2.36	3.19	2.54	5.01

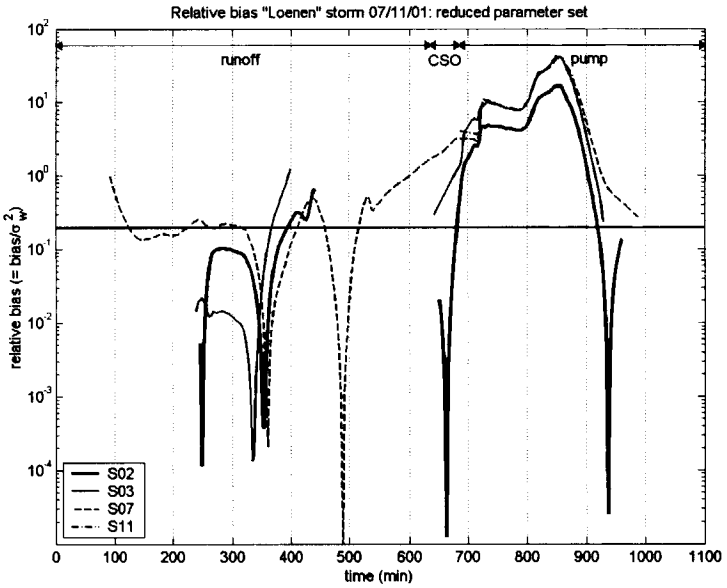

Figure VIII.32 Relative bias 'Loenen' storm 07/11/01 (reduced parameter set). The relative bias is the highest during the emptying of the system.

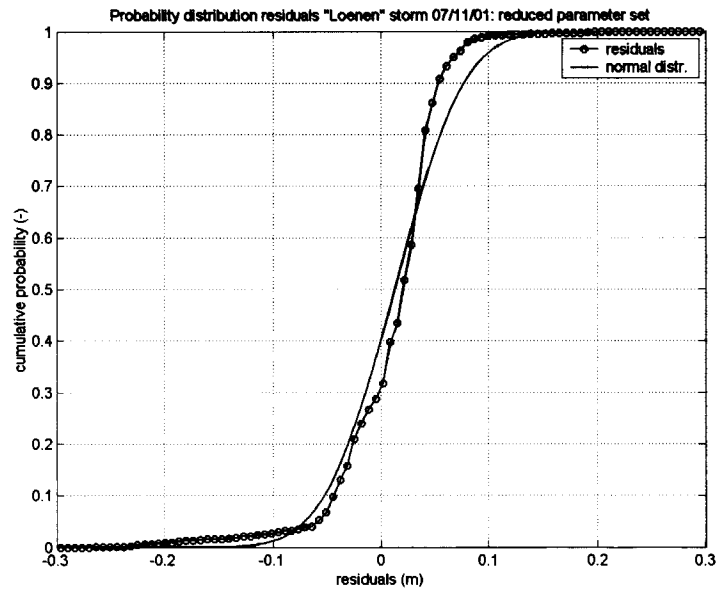

Figure VIII.33 Probability distribution residuals 'Loenen' storm 07/11/01 (reduced parameter set). The distribution of residuals is different from a normal distribution.

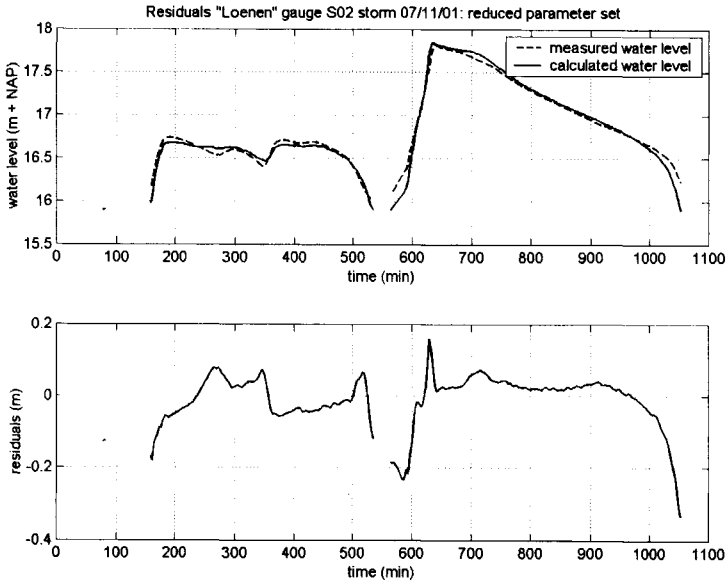

Figure VIII.34 Residuals 'Loenen' gauge S02 storm 07/11/01 (reduced parameter set). The residuals are relatively high during the rise of the water level and the emptying of the system.

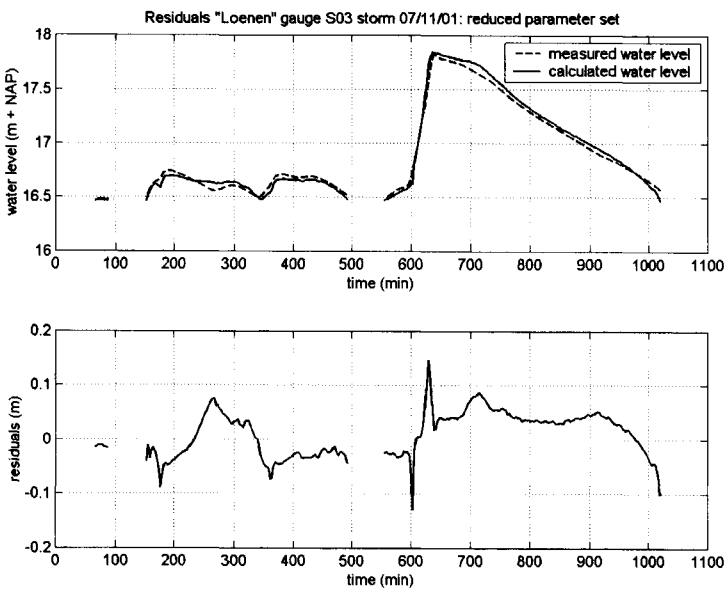

Figure VIII.35 Residuals 'Loenen' gauge S03 storm 07/11/01 (reduced parameter set). The residuals are relatively high during the rise of the water level and the emptying of the system.

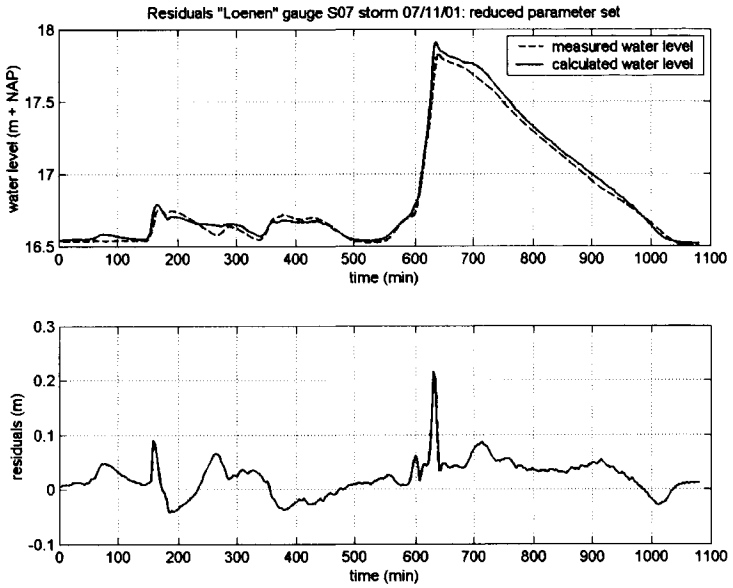

Figure VIII.36 Residuals 'Loenen' gauge S07 storm 07/11/01 (reduced parameter set). The residuals are relatively high during the rise of the water level and the emptying of the system.

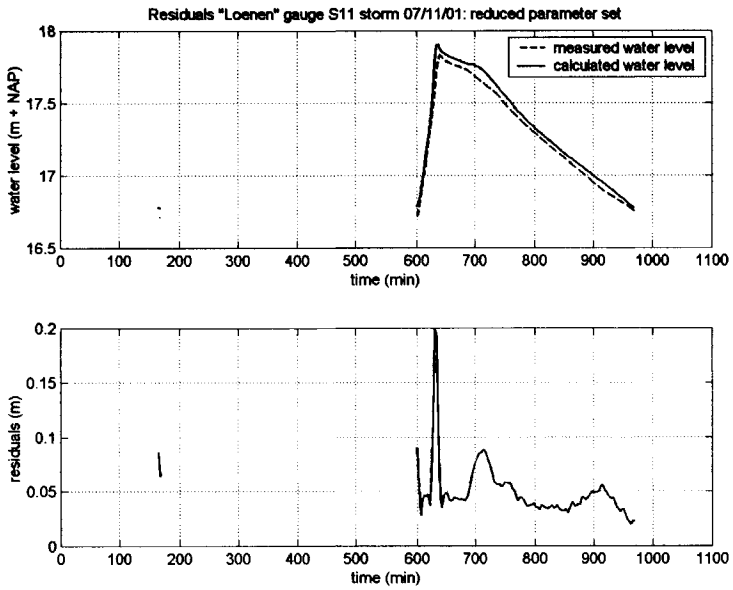

Figure VIII.37 Residuals 'Loenen' gauge S11 storm 07/11/01 (reduced parameter set). The residuals are relatively high during the rise of the water level.

Storm event 07/11/01: full parameter set

Table VIII.17 Values of calibrated parameters for storm event 07/11/01 'Loenen' (full parameter set).

	Parameter	Value
Storm event 18/07/01	N1	82.62
	B2	1.77
	F2	846.03
	B5	3.54
	F5	440.00
	I5	0.43
	B7	0.29
	F7	836.02
	B8	3.50
	F8	447.82
	CC	0.76

Table VIII.18 Statistics of residuals for storm event 07/11/01, 'Loenen' (full parameter set). The values are larger than for the reduced parameter set indicating a poorer quality of the calibration.

		S02	S03	S04	S06	S07	S11	Total
REL.BIAS	($*10^{-1}$)	0.61	1.05	-	-	2.67	5.05	-
MSE	($*10^{-3}$)	11.56	5.99	0.72	1.68	3.74	5.42	6.00
RMSE	($*10^{-2}$)	10.75	7.74	2.68	4.10	6.11	7.36	7.75
VAR	($*10^{-3}$)	11.03	5.33	0.33	0.67	2.95	1.32	5.09
STD	($*10^{-2}$)	10.50	7.30	1.83	2.59	5.43	3.63	7.14

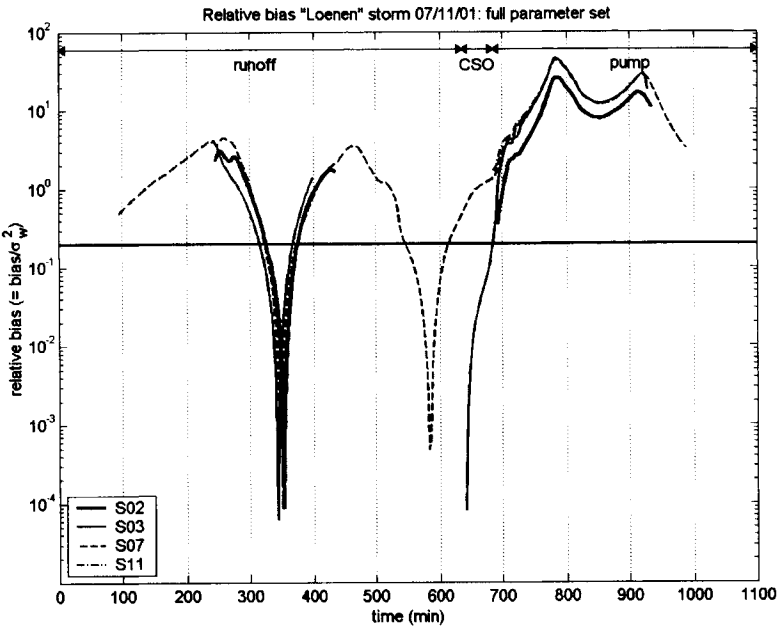

Figure VIII.38 Relative bias 'Loenen' storm 07/11/01 (full parameter set). The relative bias is larger than 0.2, which indicates a less reliable calibration. The maximum is reached during the emptying phase.

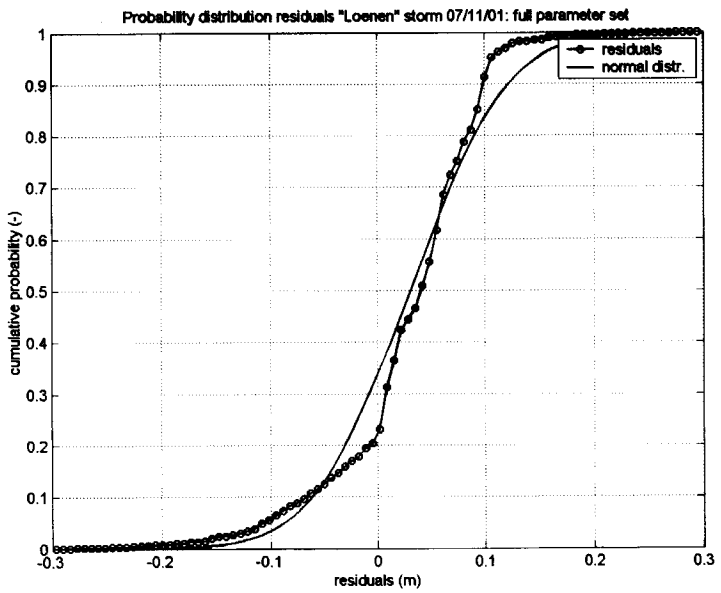

Figure VIII.39 Residuals 'Loenen' storm 07/11/01 (full parameter set). Fit is worse than for the reduced parameter set.

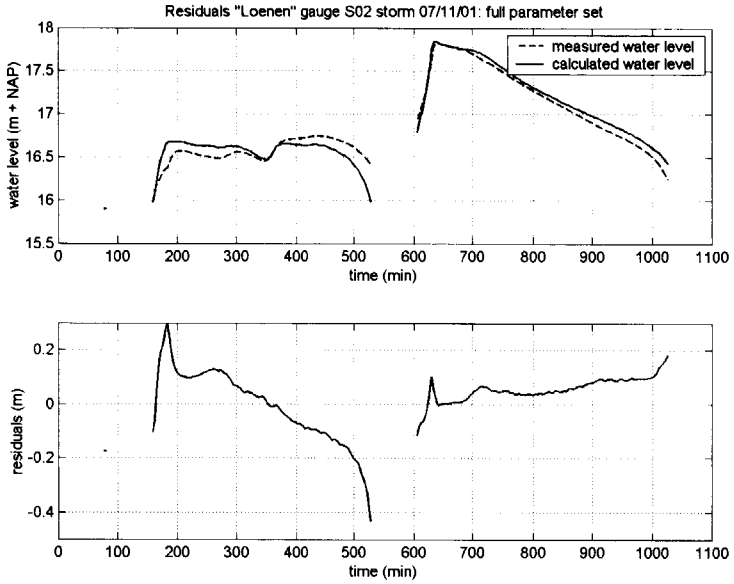

Figure VIII.40 Residuals 'Loenen' gauge S02 storm 07/11/01 (full parameter set). Large differences between model and measurements during first half of storm event.

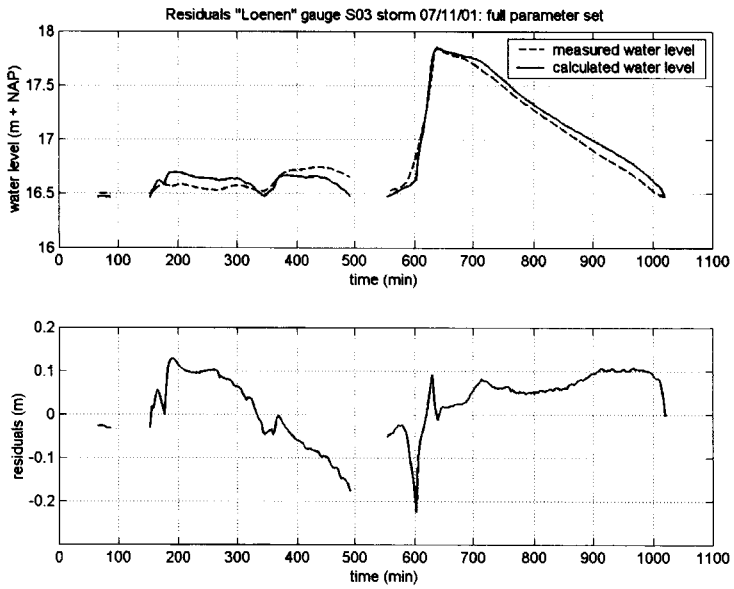

Figure VIII.41 Residuals 'Loenen' gauge S03 storm 07/11/01 (full parameter set). Large differences between model and measurements during first half of storm event and emptying of system.

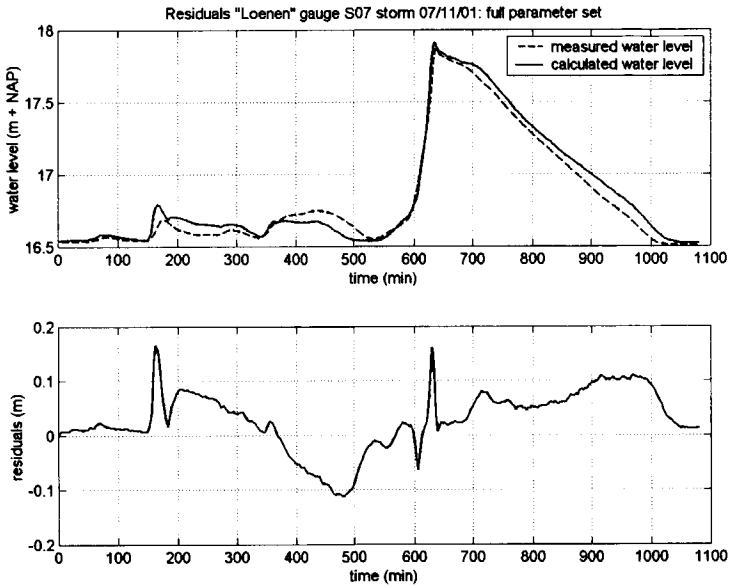

Figure VIII.42 Residuals 'Loenen' gauge S07 storm 07/11/01 (full parameter set). Large differences between model and measurements during first half of storm event and emptying of system.

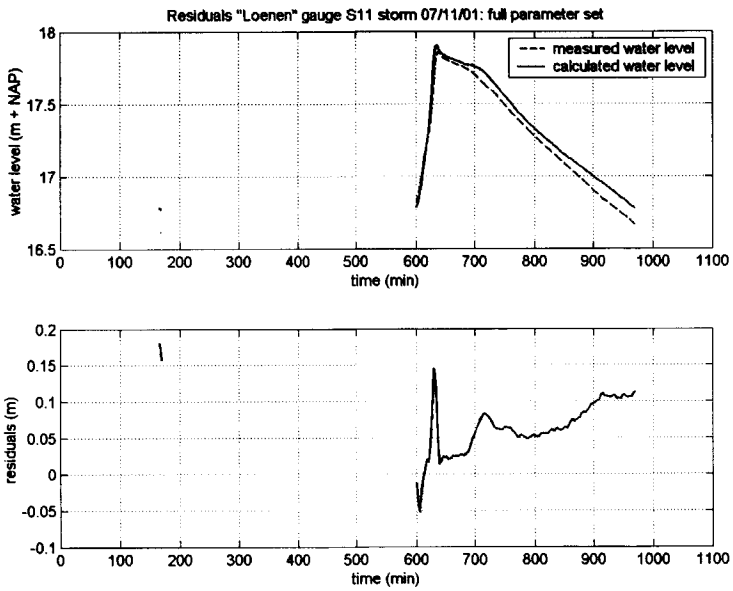

Figure VIII.43 Residuals 'Loenen' gauge S11 storm 07/11/01 (full parameter set). Large differences between model and measurements during rise of water level and emptying of system.

Appendix IX Dependent sampling by means of Cholesky decomposition

Correlation of calibrated model parameters can be incorporated in a Monte Carlo simulation by means of Cholesky decomposition (see e.g. Carlin and Lewis 2000). Using the covariance matrix of the model parameters, it enables random drawing of parameters from distribution functions accounting for interdependencies. Covariances are calculated from the correlations of two parameters,

$$\operatorname{cov}(p_i, p_j) = E\left[\left(p_i - \mu(p_i)\right)\left(p_j - \mu(p_j)\right)\right] = \rho(p_i, p_j)\sigma(p_i)\sigma(p_j) \tag{IX.1}$$

where $\operatorname{cov}(p_i,p_j)$ is the covariance between model parameters p_i and p_j, $\mu(p_i)$ and $\mu(p_j)$ are expectation of parameter p_i and p_j, respectively, $\rho(p_i,p_j)$ is the correlation coefficient between model parameters p_i and p_j, and $\sigma(p_i)$ or $\sigma(p_j)$ is the standard deviation of model parameters $p_1, p_2, \ldots, p_n$. Then the covariance matrix becomes,

$$\begin{aligned} V &= \begin{bmatrix} \operatorname{var}(p_1) & \operatorname{cov}(p_1,p_2) & \cdots & \operatorname{cov}(p_1,p_n) \\ \operatorname{cov}(p_2,p_1) & \operatorname{var}(p_2) & \cdots & \operatorname{cov}(p_2,p_n) \\ \vdots & \vdots & \ddots & \vdots \\ \operatorname{cov}(p_n,p_1) & \operatorname{cov}(p_n,p_2) & \cdots & \operatorname{var}(p_n) \end{bmatrix} \\ &= \begin{bmatrix} \sigma(p_1)\sigma(p_1) & \rho_{12}\sigma(p_1)\sigma(p_2) & \cdots & \rho_{1n}\sigma(p_1)\sigma(p_n) \\ \rho_{21}\sigma(p_2)\sigma(p_1) & \sigma(p_2)\sigma(p_2) & \cdots & \rho_{2n}\sigma(p_2)\sigma(p_n) \\ \vdots & \vdots & \ddots & \vdots \\ \rho_{n1}\sigma(p_n)\sigma(p_1) & \rho_{n2}\sigma(p_n)\sigma(p_2) & \cdots & \sigma(p_n)\sigma(p_n) \end{bmatrix} \end{aligned} \tag{IX.2}$$

where V is the covariance matrix of parameters $p_1, p_2, \ldots, p_n$, $\operatorname{var}(p_i)$ is the variance of model parameter p_i, $\operatorname{cov}(p_i,p_j)$ is the covariance between model parameters p_i and p_j

By applying Cholesky decomposition, the covariance matrix can be rewritten as the product of an under triangular matrix and its transpose,

$$V = LL^T$$

$$\begin{bmatrix} v_{11} & v_{12} & \cdots & v_{1n} \\ v_{21} & v_{22} & \cdots & v_{2n} \\ \vdots & \vdots & \ddots & \vdots \\ v_{n1} & v_{n2} & \cdots & v_{nn} \end{bmatrix} = \begin{bmatrix} l_{11} & 0 & \cdots & 0 \\ l_{21} & l_{22} & \cdots & 0 \\ \vdots & \vdots & \ddots & \vdots \\ l_{n1} & l_{n2} & \cdots & l_{nn} \end{bmatrix} \begin{bmatrix} l_{11} & l_{21} & \cdots & l_{n1} \\ 0 & l_{22} & \cdots & l_{n2} \\ \vdots & \vdots & \ddots & \vdots \\ 0 & 0 & \cdots & l_{nn} \end{bmatrix} \tag{IX.3}$$

Thus, the Cholesky decomposition of V is defined as,

$$\operatorname{chol}(V) = \operatorname{chol}\begin{bmatrix} v_{11} & v_{12} & \cdots & v_{1n} \\ v_{21} & v_{22} & \cdots & v_{2n} \\ \vdots & \vdots & \ddots & \vdots \\ v_{n1} & v_{n2} & \cdots & v_{nn} \end{bmatrix} = \begin{bmatrix} l_{11} & 0 & \cdots & 0 \\ l_{21} & l_{22} & \cdots & 0 \\ \vdots & \vdots & \ddots & \vdots \\ l_{n1} & l_{n2} & \cdots & l_{nn} \end{bmatrix} \tag{IX.4}$$

Therefore, drawing one parameter combination (p_1, p_2,…,p_k) from a k-variate normal distribution with mean μ and covariance matrix V is simulated as follows,

$$P = \mu + \left(\text{chol}(V)\right)^T * \text{randn}(k)$$

$$\begin{bmatrix} p_1 \\ p_2 \\ \vdots \\ p_k \end{bmatrix} = \begin{bmatrix} \mu_1 \\ \mu_2 \\ \vdots \\ \mu_k \end{bmatrix} + \left(\text{chol}\left\{ \begin{bmatrix} \text{cov}(p_1,p_1) & \text{cov}(p_1,p_2) & \cdots & \text{cov}(p_1,p_k) \\ \text{cov}(p_2,p_1) & \text{cov}(p_2,p_2) & \cdots & \text{cov}(p_2,p_k) \\ \vdots & \vdots & \ddots & \vdots \\ \text{cov}(p_k,p_1) & \text{cov}(p_k,p_2) & \cdots & \text{cov}(p_k,p_k) \end{bmatrix} \right\} \right)^T \cdots \times \begin{bmatrix} \text{randn}_1 \\ \text{randn}_2 \\ \vdots \\ \text{randn}_k \end{bmatrix} \quad \text{(IX.5)}$$

where $p_1, p_2, \ldots, p_k$ are random values of model parameters drawn from their distributions accounting for parameter correlation, $\mu_1, \mu_2, \ldots, \mu_k$ is mean value of model parameters, $\text{cov}(p_i, p_j)$ is covariance of parameters p_i and p_j and randn_i is a random value drawn from a standard normal distribution.

Appendix X Derivation of cost functions describing environmental damage

Three types of cost functions are considered to model environmental damage due to overflows: one discrete and two continuous cost functions The continuous functions are proportional with the CSO volume and either Weibull-shaped or linear.

The **discrete cost function** is a step function, i.e. it is assumed that the loss (D_0) due to CSO discharges is constant. As a result, each overflow event has an immediate effect independent of its volume,

$$D_1(\tilde{v}, v) = \begin{cases} D_0 , & \text{for } v \geq \tilde{v} \\ 0 , & \text{for } v < \tilde{v} \end{cases} \tag{X.1}$$

where v is an actual overflow volume, which is a random quantity, and $\tilde{v}$ is the storage volume to be built. The expected damage is equal to,

$$E\{D_1(\tilde{v}, V)\} = \int_{v=\tilde{v}}^{\infty} D_0 f(v) dv = D_0 \Pr\{v > \tilde{v}\} = D_0 \exp\left(-\left(\frac{\tilde{v}}{b}\right)^a\right) \tag{X.2}$$

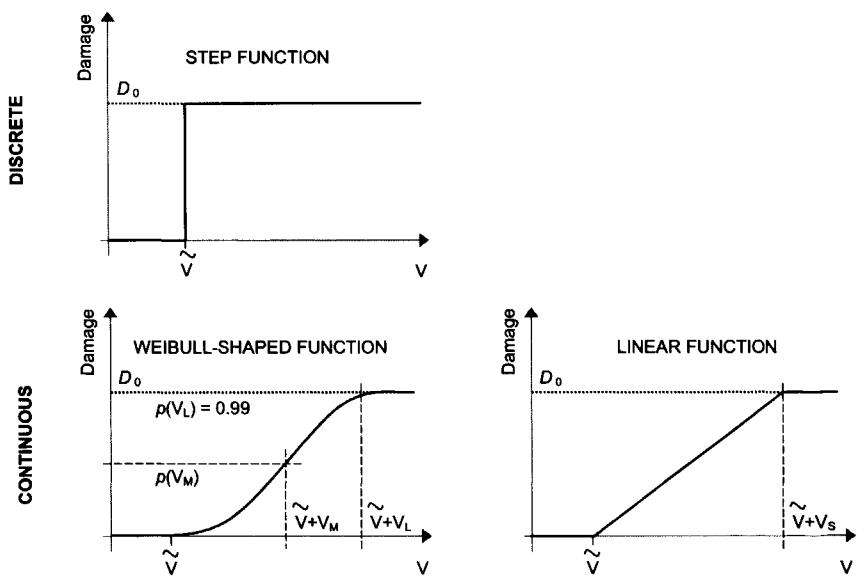

Figure X.1 Cost functions describing environmental damage due to CSOs, where v is an actual overflow volume, which is a random quantity, and $\tilde{v}$ is the storage volume to be built.

Intuitively, a continuous cost function probably fits better with the proportional character of the environmental effects of CSOs. If damage is described with a **Weibull-shaped cost function** depending on the actual CSO volume, the cost function reads,

$$D_2(\tilde{v},v)=\begin{cases} D_0\left[1-\exp\left\{-\left(\dfrac{v-\tilde{v}}{b_1}\right)^{a_1}\right\}\right] & \text{for } v\geq\tilde{v} \\ 0 & \text{for } v<\tilde{v} \end{cases} \tag{X.3}$$

where v is an actual overflow volume, which is a random quantity, $\tilde{v}$ is the storage volume to be built, a_1 and b_1 are parameters on which the shifted Weibull-shaped cost function depends. They differ from the parameters a and b of the Weibull distribution describing the inherent uncertainty of overflow volumes per storm event,

$$f(v)=\frac{a}{b}\left(\frac{v}{b}\right)^{a-1}\exp\left\{-\left(\frac{v}{b}\right)^{a}\right\} \tag{X.4}$$

Since the overflow volume v is a random quantity, the expectation of Eq. (X.3) is required,

$$\begin{aligned} E\{D_2(\tilde{v},V)\} &= \int_{v=\tilde{v}}^{\infty} D_0\left[1-\exp\left\{-\left(\frac{v-\tilde{v}}{b_1}\right)^{a_1}\right\}\right] f(v)dv \\ &= \int_{v=\tilde{v}}^{\infty} D_0\left[1-\exp\left\{-\left(\frac{v-\tilde{v}}{b_1}\right)^{a_1}\right\}\right]\frac{a}{b}\left(\frac{v}{b}\right)^{a-1}\exp\left\{-\left(\frac{v}{b}\right)^{a}\right\}dv \end{aligned} \tag{X.5}$$

Since $v\geq\tilde{v}$ for all $\tilde{v}$, the right tail of the Weibull distribution is considered which is called the left-truncated Weibull distribution (see Wingo 1989). This probability distribution can be obtained from the Weibull distribution by conditioning on values larger than $\tilde{v}$,

$$\begin{aligned} \Pr\{V>v|V>\tilde{v}\} &= \frac{\Pr\{V>v\cap V>\tilde{v}\}}{\Pr\{V>\tilde{v}\}}=\frac{\Pr\{V>v\}}{\Pr\{V>\tilde{v}\}} \\ &= \exp\left\{-\left(\frac{v}{b}\right)^{a}+\left(\frac{\tilde{v}}{b}\right)^{a}\right\} \end{aligned} \tag{X.6}$$

The probability density function of the left-truncated Weibull distribution is given by,

$$f(v)=\frac{a}{b}\left(\frac{v}{b}\right)^{a-1}\exp\left\{-\left(\frac{v}{b}\right)^{a}+\left(\frac{\tilde{v}}{b}\right)^{a}\right\} \tag{X.7}$$

Using the left-truncated Weibull distribution, the expected damage (Eq. (X.5)) is reformulated as,

$$E\{D_2(\tilde{v},V)\} = \int_{v=\tilde{v}}^{\infty} D_0\left[1-\exp\left\{-\left(\frac{v-\tilde{v}}{b_1}\right)^{a_1}\right\}\right]\cdots$$
$$\times\frac{a}{b}\left(\frac{v}{b}\right)^{a-1}\exp\left\{-\left(\frac{v}{b}\right)^{a}+\left(\frac{\tilde{v}}{b}\right)^{a}\right\}\exp\left\{-\left(\frac{\tilde{v}}{b}\right)^{a}\right\}dv \qquad \text{(X.8)}$$
$$= D_0 P_f(\tilde{v})\int_{v=\tilde{v}}^{\infty}\left[1-\exp\left\{-\left(\frac{v-\tilde{v}}{b_1}\right)^{a_1}\right\}\right]\frac{a}{b}\left(\frac{v}{b}\right)^{a-1}\exp\left\{-\left(\frac{v}{b}\right)^{a}+\left(\frac{\tilde{v}}{b}\right)^{a}\right\}dv$$

The integral has to be numerically solved. Because this integral can be reformulated in terms of an expectation of a cost function depending on a random quantity having a left-truncated Weibull distribution, Monte Carlo integration can be used (i.e. sampling from the left-truncated Weibull distribution). This can be considered as a kind of importance sampling. Therefore, the expectation of the damage cost is given by,

$$E\{D_2(\tilde{v},V)\} \approx D_o P_f(\tilde{v})\frac{\sum_{i=1}^{n}\left[1-\exp\left\{-\left(\frac{v_i-\tilde{v}}{b_1}\right)^{a_1}\right\}\right]}{n} \qquad \text{(X.9)}$$

where n is the number of samples of the Monte Carlo integration and v_i is the i^{th} sample from the left-truncated Weibull distribution ($i = 1,\ldots, n$).

The parameters a_1 and b_1 are estimated as follows. Let v_L be the CSO volume at which the damage cost becomes almost constant, i.e. the damage cost is almost D_0, say, $0.99*D_0$. Let v_M be a specific part of this volume, i.e. $v_M = v_L/\gamma$ (with $\gamma>1$). Further, assume that the cost at v_M is equal to $0.5*D_0$. The values of v_M and γ determine the steepness and shape of the cost function (Eq. (X.8)). The Weibull-shaped cost function is uniquely described with the two percentiles (v_M and $p(v_M)$, v_L and $p(v_L)$). Then the values of a_1 and b_1 can be calculated by choosing v_M and γ and, subsequently, solving the equations,

$$p(v_M) = 1-\exp\left(-\left(\frac{v_M}{b_1}\right)^{a_1}\right) = 0.5$$

$$p(v_L) = 1-\exp\left(-\left(\frac{v_L}{b_1}\right)^{a_1}\right) = 0.99$$

$$v_M = \frac{v_L}{\gamma}$$

where $p(v)$ is defined as,

$$p(v) = 1-\exp\left\{-\left(\frac{v-\tilde{v}}{b_1}\right)^{a_1}\right\} = \frac{D_2(v)}{D_0}\text{, for } v \geq \tilde{v} \qquad \text{(X.10)}$$

Thus, parameters a_1 and b_1 yield,

$$a_1 = \frac{1}{\log(\gamma)} \log\left(\frac{\log(1-p(v_L))}{\log(1-p(v_M))}\right)$$

$$b_1 = \frac{v_M}{\left(-\log(1-p(v_M))\right)^{1/a_1}}$$

In the case of a **linear cost function** with a maximum value at v_S, the environmental damage is defined as,

$$D_3(\tilde{v}, v) = \begin{cases} D_0 & , \text{ for } v > v_S \\ \dfrac{D_0}{v_S} & , \text{ for } \tilde{v} \le v \le v_S \\ 0 & , \text{ for } v < \tilde{v} \end{cases} \tag{X.11}$$

where v is an actual overflow volume, which is a random quantity, $\tilde{v}$ is the storage volume to be built and v_S is the CSO volume at which the environmental damage reaches its maximum (D_0).

Again the overflow volume v is a random quantity and the expectation of Eq. (X.11) is required,

$$\begin{aligned} E\{D_3(\tilde{v}, V)\} &= \int_{v=\tilde{v}}^{\infty} D_3(v) f(v) dv \\ &= \int_{v=\tilde{v}}^{\infty} \frac{D_0}{v_S}(v-\tilde{v}) \frac{a}{b}\left(\frac{v}{b}\right)^{a-1} \exp\left(-\left(\frac{v}{b}\right)^a\right) dv \\ &\quad - \int_{v=\tilde{v}+v_S}^{\infty} \frac{D_0}{v_S}(v-(v_S+\tilde{v})) \frac{a}{b}\left(\frac{v}{b}\right)^{a-1} \exp\left(-\left(\frac{v}{b}\right)^a\right) dv \end{aligned} \tag{X.12}$$

By applying the left-truncated Weibull distribution (Eq. (X.7)) and the transformation $t = (v/b)^a$ the expected cost can be rewritten in terms of the incomplete gamma function as follows,

$$\begin{aligned} E\{D_3(\tilde{v}, V)\} &= \frac{D_0}{v_S} P_f(\tilde{v}) \left(b \exp\left(\left(\frac{\tilde{v}}{b}\right)^a\right) \Gamma\left(\frac{1}{a}+1, \left(\frac{\tilde{v}}{b}\right)^a\right) - \tilde{v} \right) \\ &\quad - \frac{D_0}{v_S} P_f(\tilde{v}+v_S) \left(b \exp\left(\left(\frac{\tilde{v}+v_S}{b}\right)^a\right) \Gamma\left(\frac{1}{a}+1, \left(\frac{\tilde{v}+v_S}{b}\right)^a\right) - (\tilde{v}+v_S) \right) \end{aligned} \tag{X.13}$$

where $\Gamma(a,x)$ is the incomplete gamma function for $x \ge 0$ and $a > 0$ which is defined as,

$$\Gamma(a,x) = \int_{t=x}^{\infty} t^{a-1} \exp(-t) dt \tag{X.14}$$

Appendix XI Results of analysis of pump failures Rotterdam

Table XI.1 Characteristics of all pumps.

Pumping station	Pump No.	Purpose	Pumping capacity (m^3/h)	Power (kW)	Repair priority
Rm1	1	dwf	240	11	2
	2	wwf	630	55	2
	3	wwf	630	55	2
Rm2	1	wwf/dwf	720	22	1
	2	wwf	720	22	1
	3	wwf	720	22	1
	4	dwf/wwf	510	18.5	2
Rm3	1	dwf&wwf	198	7.5	1/2
	2	dwf&wwf	198	7.5	1/2
Rm4	1	dwf	584	18.5	2
	2	wwf	872	75	1
	3	wwf	872	75	1
Rm5	1	dwf	150	15	2
	2	wwf	300	30	1
Rm6	1	dwf	360	-	2
	2	wwf	2500	-	2
	3	wwf	2500	-	2
Rm7	1	dwf	300	30	2
	2	wwf	1330	90	1
	3	PO	1330	90	2
Rm8	1	dwf	1938	85	2
	2	dwf&wwf	1938	85	2
	3	wwf	4320	85	1
	4	wwf	4320	85	1
Rm9	1	dwf&wwf	96	7.8	1/2
	2	PO	210	18.5	1/2
Rm10	1	dwf	600	14	2
	2	wwf	1200	55	2
	3	PO	1800	93	1/2
Rm11	1	dwf	200	-	2
	2	wwf	-	-	1
	3	wwf	-	-	1
Rm12	1	dwf	39	2.2	3
	2	wwf	125	7.5	3
Rm13	1	dwf&wwf	26	2.2	3
	2	wwf	15	2.2	3
Rm14	1	dwf&wwf	30	2.2	3
	2	wwf	59	7.5	3
Rm15	1	dwf&wwf	23	1.5	3
	2	wwf	52	3	3
Rm16	1	dwf	85	4	3
	2	wwf	157	30	3

Rm17	1	dwf	72	3	3
	2	wwf	267	15	3
Rm18	1	dwf/wwf	43	0.9	3
	2	dwf/wwf	43	0.9	3

Table XI.2 Results of Laplace trend test (see Ansell and Phillips 1994).

Station	Pump Number	of failures	U_L (H_0: HPP)	U_{LR} (H_0: RP)	$Z_{\alpha/2}$ (α=0.025)	Trend H_0=HPP	Trend H_0=RP
Rm1	2	18	1.189	0.698	1.960	-	-
	3	11	-0.562	-0.243	1.960	-	-
Rm2	1	158	-0.552	-0.404	1.960	-	-
	2	201	-0.978	-0.622	1.960	-	-
	3	292	-1.402	-0.875	1.960	-	-
	4	47	9.420	4.662	1.960	<<	<<
Rm3	1	7	-2.284	-2.285	1.960	-	-
Rm4	1	117	-3.665	-1.765	1.960	>>	-
	2	117	-0.329	-0.183	1.960	-	-
	3	110	-2.612	-1.402	1.960	>>	-
Rm5	1	42	1.162	0.828	1.960	-	-
	2	7	-1.780	-1.985	1.960	-	-
Rm6	1	364	-4.928	-1.628	1.960	>>	-
	2	13	-2.161	-1.615	1.960	-	-
	3	11	-1.576	-1.584	1.960	-	-
Rm7	1	96	-8.874	-3.046	1.960	>>	>>
	2	13	-2.798	-2.551	1.960	-	-
	3	18	-2.508	-2.460	1.960	>>	>>
Rm8	1	128	-3.690	-2.477	1.960	>>	>>
	2	175	-2.110	-0.889	1.960	>>	-
	3	46	2.719	2.291	1.960	<<	<<
	4	183	4.326	2.409	1.960	<<	<<
Rm9	1	23	0.369	0.337	1.960	-	-
	2	29	-6.528	-2.611	1.960	>>	>>
Rm10	1	52	-4.456	-3.571	1.960	>>	>>
	2	13	-3.304	-2.209	1.960	-	-
	3	29	1.976	1.680	1.960	-	-
Rm11	1	13	0.395	0.307	1.960	-	-
	2	12	2.324	2.619	1.960	-	-
	3	19	1.567	1.397	1.960	-	-
Rm12	1	75	-5.857	-2.668	1.960	>>	>>
	2	36	-1.989	-0.967	1.960	-	
Rm13	1	38	3.354	1.443	1.960	<<	-
	2	17	-1.116	-0.965	1.960	-	-
Rm14	1	1	0.611	0.812	1.960	-	-
Rm16	1	71	1.948	1.567	1.960	-	-
Rm17	1	10	-0.281	-0.281	1.960	-	-
	2	17	2.038	0.647	1.960	-	-
Rm18	1	92	1.138	0.856	1.960	-	-
	2	107	0.562	0.402	1.960	-	-

- = no trend << = deteriorating >> = improving

Table XI.3 Number of TME failures of all pumps.

Station	Purpose	Pump	1998	1999	2000	2001	2002	Total
Rm1	dwf	1		2	1			3
	wwf	2	1	1	11	1	4	18
	wwf	3	1		10			11
Rm2	wwf/dwf	1	31	44	55	28		158
	wwf	2	44	55	68	34		201
	wwf	3	75	68	99	50		292
	dwf/wwf	4	1	17	2	21	6	47
Rm3	dwf&wwf	1	4	1	1	1		7
	dwf&wwf	2	2		1	1		4
Rm4	dwf	1	28	35	26	22	6	117
	wwf	2	13	30	34	32	4	113
	wwf	3	24	35	22	19	10	110
Rm5	dwf	1	2	15	7	11	7	42
	wwf	2	2	1	3		1	7
Rm6	dwf	1	109	60	108	52	35	364
	wwf	2	3	5	3		2	13
	wwf	3	2	4	3		2	11
Rm7	dwf	1	45	44	2	4	1	96
	wwf	2	6	3	2	2		13
	PO	3	7	4	2	5		18
Rm8	dwf	1	31	44	21	24	8	128
	dwf&wwf	2	34	29	68	34	10	175
	wwf	3	6	7	12	6	15	46
	wwf	4	32	30	26	45	50	183
Rm9	dwf&wwf	1	4	6	4	2	7	23
	PO	2	26		2	1		29
Rm10	dwf	1	18	15	12	3	4	52
	wwf	2	8	1	1	3		13
	PO	3	3	5	3	10	8	29
Rm11	dwf	1		4	3	3	3	13
	wwf	2	2	1	2	5	2	12
	wwf	3	3	5	2	7	2	19
Rm12	dwf	1	33	28	1	4	9	75
	wwf	2	14	9		3	10	36
Rm13	dwf&wwf	1	9	9	1	4	15	38
	wwf	2	4	4	2	5	2	17
Rm14	dwf&wwf	1	1	2	1	5	1	10
	wwf	2			1			1
Rm15	dwf&wwf	1						
	wwf	2	4	4	7	6	1	22
Rm16	dwf	1	8	18	14	18	13	71
	wwf	2			1		1	2
Rm17	dwf	1	1	1	3	3	2	10
	wwf	2				15	2	17
Rm18	dwf/wwf	1	12	28	28	12	12	92
	dwf/wwf	2	12	26	31	16	22	107

Table XI.4 Total duration of TME failures of all pumps (in hours).

Station	Purpose	Pump	1998	1999	2000	2001	2002	Total
Rm1	dwf	1		2.96	3.15			6.09
	wwf	2	4.60	0.88	54.01	0.97	20.60	81.00
	wwf	3	4.28		29.80			34.10
Rm2	wwf/dwf	1	94.55	367.84	288.75	194.60		946.42
	wwf	2	384.12	574.75	529.72	151.30		1640.16
	wwf	3	691.50	927.52	735.57	292.50		2648.44
	dwf/wwf	4	5.93	203.32	430.20	266.07	56.64	962.09
Rm3	dwf&wwf	1	62.88	0.02	0.03	0.63		63.56
	dwf&wwf	2	0.24		0.07	0.43		0.72
Rm4	dwf	1	308.00	47.25	241.80	481.58	58.26	1137.24
	wwf	2	50.44	277.50	379.78	134.72	0.48	842.98
	wwf	3	672.96	583.80	156.86	148.39	338.40	1900.80
Rm5	dwf	1	38.40	218.70	129.78	77.33	95.13	559.44
	wwf	2	21.70	7.13	0.42		6.68	35.91
Rm6	dwf	1	1900.96	810.00	2406.24	632.84	716.10	6464.64
	wwf	2	34.41	1.45	0.24		4.18	40.30
	wwf	3	26.22	1.32	0.21		4.72	32.45
Rm7	dwf	1	473.40	548.68	12.90	0.12	15.83	1051.20
	wwf	2	27.36	9.36	19.34	1.14		57.20
	PO	3	28.91	11.72	9.54	11.35		61.56
Rm8	dwf	1	157.79	362.56	248.22	178.32	7.28	953.60
	dwf&wwf	2	401.20	266.80	886.72	519.86	121.40	2196.25
	wwf	3	82.74	31.22	58.44	66.06	54.75	293.02
	wwf	4	226.56	228.90	199.16	220.95	222.00	1098.00
Rm9	dwf&wwf	1	6.40	14.76	9.04	8.98	26.32	65.55
	PO	2	41.60	0.00	18.62	0.02	0.00	60.03
Rm10	dwf	1	2.70	47.85	63.24	1.41	88.32	203.32
	wwf	2	32.08	0.10	0.07	0.90		33.15
	PO	3	10.38	19.80	3.60	66.30	16.16	116.29
Rm11	dwf	1	0.00	3.28	0.33	6.99	2.61	13.13
	wwf	2	23.92	2.92	0.32	6.70	2.64	36.48
	wwf	3	32.76	167.80	0.44	70.35	2.76	274.17
Rm12	dwf	1	205.26	494.20	0.37	80.76	89.91	870.75
	wwf	2	188.30	42.39		17.16	96.90	344.88
Rm13	dwf&wwf	1	152.91	117.90	15.83	9.24	238.65	534.28
	wwf	2	42.56	25.32	7.18	138.85	38.32	252.28
Rm14	dwf&wwf	1	1.13	27.92	0.25	18.70	1.35	49.30
	wwf	2			0.03			0.03
Rm15	dwf&wwf	1						
	wwf	2	7.28	18.24	25.69	28.08	19.80	99.22
Rm16	dwf	1	26.88	202.86	306.60	281.34	155.22	972.70
	wwf	2			0.85		2.95	3.80
Rm17	dwf	1	0.13	10.82	75.48	23.01	0.48	109.90
	wwf	2				188.40	0.72	189.21
Rm18	dwf/wwf	1	104.64	218.12	281.12	152.28	51.48	807.76
	dwf/wwf	2	67.92	267.80	343.79	387.68	330.00	1396.35

Table XI.5 Number of safety fuses failures of all pumps. Safety fuses failures represent planned long-term maintenance.

Station	Purpose	Pump	1998	1999	2000	2001	2002	Total
Rm1	dwf	1		1		1	1	3
	wwf	2	1			1		2
	wwf	3	1					1
Rm2	wwf/dwf	1	5	2		3		10
	wwf	2	7		1	1		9
	wwf	3	8	2		1		11
	dwf/wwf	4						
Rm3	dwf&wwf	1					1	1
	dwf&wwf	2		1			1	2
Rm4	dwf	1	11	3	1	2		17
	wwf	2	9	2		2		13
	wwf	3	11	4	1	1		17
Rm5	dwf	1	3				1	4
	wwf	2	1				1	2
Rm6	dwf	1	4	2	1	3	2	12
	wwf	2	2	3		1	1	7
	wwf	3	2	2				4
Rm7	dwf	1	9	1		1		11
	wwf	2	2	1		4		7
	PO	3	1	1		1	2	5
Rm8	dwf	1	3	3	6	2	1	15
	dwf&wwf	2	7	1	3	1	1	13
	wwf	3	1				1	2
	wwf	4	2	1				3
Rm9	dwf&wwf	1		1			1	2
	PO	2		2			1	3
Rm10	dwf	1	15	8	4	2	3	32
	wwf	2	9	4				13
	PO	3	7	5			1	13
Rm11	dwf	1	1	2		1	1	5
	wwf	2		2	1			3
	wwf	3		2	1	2		5
Rm12	dwf	1	6					6
	wwf	2	2		1	1		4
Rm13	dwf&wwf	1						
	wwf	2						
Rm14	dwf&wwf	1						
	wwf	2						
Rm15	dwf&wwf	1						
	wwf	2						
Rm16	dwf	1	4	4				8
	wwf	2	3	2				5
Rm17	dwf	1	1	1		1		3
	wwf	2	1	1				2
Rm18	dwf/wwf	1						
	dwf/wwf	2						

Table XI.6 Total duration of safety fuses failures of all pumps (in hours). Safety fuses failures represent planned long-term maintenance.

Station	Purpose	Pump	1998	1999	2000	2001	2002	Total
Rm1	dwf	1		0.83		4.53	218.07	223.44
	wwf	2	193.18			4.03		197.22
	wwf	3	2.90					2.90
Rm2	wwf/dwf	1	229.70	19.28	0.00	972.24		1221.20
	wwf	2	92.26		771.00	7.73		871.02
	wwf	3	35.68	31.16		9.00		75.90
	dwf/wwf	4						
Rm3	dwf&wwf	1		0.00		0.00	0.98	0.98
	dwf&wwf	2		4.17			0.80	4.96
Rm4	dwf	1	1982.75	17.01	192.58	95.80		2288.03
	wwf	2	1630.26	24.90		2.96		1658.15
	wwf	3	2484.02	33.20	0.83	2.38		2520.42
Rm5	dwf	1	507.96				195.97	703.92
	wwf	2	3.90				0.70	4.60
Rm6	dwf	1	89.76	6.82	7.48	555.12	1417.82	2076.96
	wwf	2	23.68	9.48		858.90	355.93	1248.03
	wwf	3	18.24	6.76				25.00
Rm7	dwf	1	45.00	0.77		1.17		46.97
	wwf	2	2.84	0.75		752.32		755.93
	PO	3	27.57	0.98		2.90	700.24	731.70
Rm8	dwf	1	18.96	24.27	913.98	5.54	0.73	963.45
	dwf&wwf	2	180.67	2.38	26.97	367.30	5.83	583.18
	wwf	3	3.68				279.28	282.96
	wwf	4	4.44	31.33			0.00	35.76
Rm9	dwf&wwf	1	0.00	4.73			287.75	292.48
	PO	2	0.00	174.90			0.65	175.56
Rm10	dwf	1	257.55	48.96	109.04	75.06	22.74	513.28
	wwf	2	42.21	29.92			0.00	72.15
	PO	3	38.92	397.50			1.77	438.10
Rm11	dwf	1	195.12	6.10		576.30	218.17	995.70
	wwf	2		6.14	836.57	0.00	0.00	842.70
	wwf	3		115.16	770.13	17.60	0.00	902.90
Rm12	dwf	1	240.24	0.00	0.00	0.00	0.00	240.24
	wwf	2	2.40	0.00	2.17	380.80	0.00	385.36
Rm13	dwf&wwf	1						
	wwf	2						
Rm14	dwf&wwf	1						
	wwf	2						
Rm15	dwf&wwf	1						
	wwf	2						
Rm16	dwf	1	245.84	1735.08				1980.96
	wwf	2	9.75	172.14				181.90
Rm17	dwf	1	5.15	4.02		1560.02		1569.18
	wwf	2	1.33	4.05				5.38
Rm18	dwf/wwf	1						
	dwf/wwf	2						

Table XI.7 Number of switch-ons of all pumps.

Station	Purpose	Pump	1998	1999	2000	2001	2002	Total
Rm1	dwf	1	880	806	868	844	786	4184
	wwf	2	78	114	104	276	161	733
	wwf	3	319	236	244	172	180	1151
Rm2	wwf/dwf	1	880	514	656	1081	978	4109
	wwf	2	3772	2304	705	720	55	7556
	wwf	3	1322	1827	436	2083	60	5728
	dwf/wwf	4	6002	6210	4146	2353	48	18759
Rm3	dwf&wwf	1	5481	9976	9047	5009	9310	38823
	dwf&wwf	2	8944	3339	3047	5326	9578	30234
Rm4	dwf	1	1739	11364	4596	9736	26628	54063
	wwf	2	828	4920	3029	5252	8170	22199
	wwf	3	1532	3927	2881	5060	4922	18322
Rm5	dwf	1	3039	3149	3121	3197	2236	14742
	wwf	2	241	184	270	179	1684	2558
Rm6	dwf	1	3755	3786	2683	2744	1289	14257
	wwf	2	2737	1990	2237	517	989	8470
	wwf	3	7869	3665	2747	1207	923	16411
Rm7	dwf	1	1321	2040	2217	2187	1716	9481
	wwf	2	1323	655	383	579	611	3551
	PO	3	90	21	17	84	7	219
Rm8	dwf	1	1836	1981	1544	1881	1197	8439
	dwf&wwf	2	571	386	475	797	1067	3296
	wwf	3	1081	846	931	772	644	4274
	wwf	4	312	262	396	479	277	1726
Rm9	dwf&wwf	1	3879	3626	3750	3406	2439	17100
	PO	2	91	33	36	114	158	432
Rm10	dwf	1	996	1280	1981	1789	2458	8504
	wwf	2	434	456	355	234	221	1700
	PO	3	336	76	11	28	22	473
Rm11	dwf	1	20615	20857	18728	16432	12193	88825
	wwf	2	763	351	199	871	535	2719
	wwf	3	640	70	161	2002	294	3167
Rm12	dwf	1	10645	43768	45105	27381	38170	165069
	wwf	2	1101	1965	690	1031	6798	11585
Rm13	dwf&wwf	1	16902	9189	20297	18972	18645	84005
	wwf	2	4493	11240	4080	4296	5794	29903
Rm14	dwf&wwf	1	1349	1338	1293	1347	954	6281
	wwf	2	103	139	146	129	106	623
Rm15	dwf&wwf	1	30287	29873	31620	31972	21370	145122
	wwf	2	1237	978	1452	1568	2199	7434
Rm16	dwf	1	6419	21857	31991	32404	29830	122501
	wwf	2	189	436	158	155	135	1073
Rm17	dwf	1	8051	6744	7290	5701	6561	34347
	wwf	2	146	133	166	475	175	1095
Rm18	dwf/wwf	1	5818	13394	9293	901	9619	39025
	dwf/wwf	2	18497	12349	8380	831	14048	54105

Table XI.8 Total hours run of all pumps (in days).

Station	Purpose	Pump	1998	1999	2000	2001	2002	Total
Rm1	dwf	1	230	228	230	249	203	1139
	wwf	2	9	13	13	25	16	76
	wwf	3	34	26	28	19	15	122
Rm2	wwf/dwf	1	27	25	30	118	247	447
	wwf	2	75	66	31	58	18	249
	wwf	3	29	34	24	39	18	144
	dwf/wwf	4	208	188	192	114	15	717
Rm3	dwf&wwf	1	115	131	152	122	204	724
	dwf&wwf	2	150	85	83	114	210	642
Rm4	dwf	1	114	164	180	189	392	1039
	wwf	2	76	76	90	85	58	386
	wwf	3	33	71	104	85	33	326
Rm5	dwf	1	123	127	120	125	73	568
	wwf	2	23	12	12	15	21	81
Rm6	dwf	1	174	206	166	206	105	856
	wwf	2	27	18	32	16	30	122
	wwf	3	60	33	39	43	28	202
Rm7	dwf	1	206	201	235	232	185	1059
	wwf	2	83	42	39	40	36	240
	PO	3	10	2	2	13	1	27
Rm8	dwf	1	300	280	289	328	300	1498
	dwf&wwf	2	145	178	188	133	127	771
	wwf	3	43	32	35	40	35	185
	wwf	4	24	16	22	30	26	118
Rm9	dwf&wwf	1	232	229	224	248	203	1136
	PO	2	4	2	1	4	8	18
Rm10	dwf	1	221	220	222	249	186	1098
	wwf	2	96	65	67	63	41	332
	PO	3	9	2	1	6	4	23
Rm11	dwf	1	167	199	200	186	206	957
	wwf	2	19	28	39	43	19	147
	wwf	3	48	8	25	40	17	138
Rm12	dwf	1	174	234	239	247	225	1120
	wwf	2	65	31	28	39	35	198
Rm13	dwf&wwf	1	157	252	151	151	116	827
	wwf	2	31	54	24	25	25	158
Rm14	dwf&wwf	1	83	82	83	77	86	411
	wwf	2	10	11	10	11	10	52
Rm15	dwf&wwf	1	142	142	169	132	132	717
	wwf	2	12	15	10	10	8	56
Rm16	dwf	1	174	142	149	153	153	771
	wwf	2	23	26	16	20	18	103
Rm17	dwf	1	104	116	138	120	151	628
	wwf	2	16	13	12	24	17	82
Rm18	dwf/wwf	1	38	59	61	49	48	256
	dwf/wwf	2	98	61	58	63	43	323

Table XI.9 Unavailability of all pumps (= 1/P(Failure|Demand for pump)).

Station	Purpose	Pump	1998	1999	2000	2001	2002	Total
Rm1	dwf	1		404	869			1395
	wwf	2	79	115	10	277	41	41
	wwf	3	320		25			105
Rm2	wwf/dwf	1	29	12	12	39		27
	wwf	2	86	42	11	22		38
	wwf	3	18	27	5	42		20
	dwf/wwf	4	6003	366	2074	113	9	400
Rm3	dwf&wwf	1	1371	9977	9048	5010		5547
	dwf&wwf	2	4473		3048	5327		7559
Rm4	dwf	1	63	325	177	443	4439	463
	wwf	2	64	165	90	165	2043	197
	wwf	3	64	113	131	267	493	167
Rm5	dwf	1	1520	210	446	291	320	352
	wwf	2	121	185	91		1685	366
Rm6	dwf	1	35	64	25	53	37	40
	wwf	2	913	399	746		495	652
	wwf	3	3935	917	916		462	1492
Rm7	dwf	1	30	47	1109	547	1717	99
	wwf	2	221	219	192	290		274
	PO	3	13	6	9	17		13
Rm8	dwf	1	60	46	74	79	150	66
	dwf&wwf	2	17	14	7	24	107	19
	wwf	3	181	121	78	129	43	93
	wwf	4	10	9	16	11	6	10
Rm9	dwf&wwf	1	970	605	938	1704	349	744
	PO	2	4		19	115		15
Rm10	dwf	1	56	86	166	597	615	164
	wwf	2	55	457	356	79		131
	PO	3	113	16	4	3	3	17
Rm11	dwf	1		5215	6243	5478	4065	6833
	wwf	2	382	352	100	175	268	227
	wwf	3	214	15	81	287	148	167
Rm12	dwf	1	323	1564	45106	6846	4242	2201
	wwf	2	79	219		344	680	322
Rm13	dwf&wwf	1	1879	1022	20298	4744	1244	2211
	wwf	2	1124	2811	2041	860	2898	1760
Rm14	dwf&wwf	1	1350	670	1294	270	955	629
	wwf	2			147			624
Rm15	dwf&wwf	1						
	wwf	2	310	245	208	262	2200	338
Rm16	dwf	1	803	1215	2286	1801	2295	1726
	wwf	2			159		136	537
Rm17	dwf	1	8052	6745	2431	1901	3281	3435
	wwf	2				32	88	65
Rm18	dwf/wwf	1	485	479	332	76	802	425
	dwf/wwf	2	1542	475	271	52	639	506

Table XI.10 Bayes weights of duration of pump failures (based on Laplace approximation).

		Exp	Ray	Nor	Lgn	Gam	Wei	Gum
Location parameter		0	0	0	0	0	0	0
Prior weights		0.1429	0.1429	0.1429	0.1429	0.1429	0.1429	0.1429
Station	**Pump**	**Exp**	**Ray**	**Nor**	**Lgn**	**Gam**	**Wei**	**Gum**
Rm1	2	0.2461	0	0		0.1685	0.1853	0.0006
Rm2	1	0	0	0		0	0.0728	0
	2	0	0	0	0.0385	0.0163		0
	3	0	0	0	0	0.0359		0
	4	0	0	0		0	0.0151	0
Rm4	2	0	0	0		0	0.1328	0
	3	0	0	0	0.0659	0.0192		0
Rm5	1	0	0	0	0.2312	0.2166		0
Rm6	1	0	0	0	0		0.3170	0
	2	0	0	0		0.0836	0.2457	0
Rm7	1	0	0	0	0.1822	0.1534		0
	2	0.0003	0	0		0.1616	0.2856	0
	3	0.0009	0	0	0.3608	0.2282	0.4100	0
Rm8	1	0	0	0	0.0010	0.1869		0
	2	0	0	0	0		0.1105	0
	3	0	0	0	0.3917	0.0897		0
	4	0	0	0		0	0.0017	0
Rm9	1	0.2265	0	0	0.0272		0.3270	0.0002
	2	0	0	0		0.0008	0.0198	0
Rm10	1	0	0	0		0	0.0029	0
	3	0	0	0		0.0051	0.0542	0
Rm11	3	0.0002	0	0		0.2086		0
Rm12	1	0	0	0	0.0144			0
	2	0	0	0		0.0137	0.2270	0
Rm13	1		0	0	0.0437	0.2154	0.2181	0.0002
	2	0.2370	0	0	0.1172			0.0007
Rm16	1	0.0614	0.1001					
Rm18	1	0.0016	0	0		0.0696	0.2129	0
	2	0	0	0		0	0.0005	0

Table XI.11 Bayes weights of interarrival time of pump failures (based on Laplace approximation).

		Exp	Ray	Nor	Lgn	Gam	Wei	Gum
Location parameter		0	0	0	0	0	0	0
Prior weights		0.1429	0.1429	0.1429	0.1429	0.1429	0.1429	0.1429
Station	**Pump**	**Exp**	**Ray**	**Nor**	**Lgn**	**Gam**	**Wei**	**Gum**
Rm1	2	0	0	0		0.0609	0.1625	0
Rm2	1	0	0	0	0.1521	0.1134		0
	2	0	0	0		0.0009	0.1209	0
	3	0	0	0		0	0.0148	0
	4	0	0	0		0.0407	0.4031	0
Rm4	2	0	0	0		0.0129	0.4404	0
	3	0	0	0		0.0001	0.0266	0
Rm5	1	0	0	0	0.0285		0.4056	0
Rm6	1	0	0	0		0	0	0
	2	0.0736	0	0	0.0479			0.0003
Rm7	1	0	0	0		0	0.0009	0
	2	0.1850	0	0.0003	0.0079		0.3030	0.0088
	3		0.0001	0.0001				0.0249
Rm8	1	0	0	0	0.0012	0.2724		0
	2	0	0	0	1.0000	0	0	0
	3	0	0	0	0.0016		0.1882	0
	4	0	0	0		0.0007	0.3336	0
Rm9	1	0	0	0	0.0113		0.1796	0
	2	0	0	0		0.0135	0.1381	0
Rm10	1	0.0011	0	0	0.0010		0.3434	0
	3	0.0005	0	0	0.0015		0.1803	0
Rm11	3	0.0758	0	0	0.0223		0.3627	0.0001
Rm12	1	0	0	0		0.0011	0.1050	0
	2	0	0	0	0.1215	0.3549		0
Rm13	1	0	0	0		0.0007	0.0392	0
	2		0	0	0.1153			0.0010
Rm16	1	0.0080	0	0	0.0007			0
Rm18	1	0.0343	0	0	0.0011	0.3332		0
	2	0.0007	0	0	0.0142	0.2506		0

Table XI.12 Parameters of Crow's model and Cox-Lewis' model. The majority of pumps shows improvement (β >1 and β_1 >0).

Station	Pump	Number of failures	U_L	Trend	Crow's model		Cox-Lewis' model	
					β	λ	β_0	β_1
Rm1	2	18	1.1891	N	1.5121	$1.86*10^{-08}$	-8.1459	$1.81*10^{-05}$
Rm1	3	11	-0.56242	N	1.055	0.00014726	-8.5803	$1.56*10^{-05}$
Rm2	1	158	-0.55199	N	1.0204	0.0036382	-5.7382	$1.82*10^{-05}$
Rm2	2	201	-0.9777	N	1.0744	0.0026314	-5.4933	$1.80*10^{-05}$
Rm2	3	292	-1.4023	N	0.98473	0.009771	-5.1172	$1.78*10^{-06}$
Rm2	4	47	9.42	Y	2.0503	$1.01*10^{-08}$	-7.8226	$2.16*10^{-05}$
Rm3	1	7	-2.2842	Y	0.8197	0.001145	-8.9522	$1.21*10^{-05}$
Rm3	2	4	-2.0782	Y	0.76043	0.0012289	-9.5269	$1.28*10^{-05}$
Rm4	1	117	-3.6648	Y	0.83912	0.015566	-6.167	$1.35*10^{-05}$
Rm4	2	113	-0.32945	N	1.1574	0.0005092	-6.2475	$1.55*10^{-05}$
Rm4	3	110	-2.6124	Y	0.83951	0.014575	-6.2427	$1.41*10^{-05}$
Rm5	1	42	1.1622	N	1.3302	$3.01*10^{-05}$	-7.2731	$1.70*10^{-05}$
Rm5	2	7	-1.78	N	1.0348	0.00011616	-9.0015	$1.43*10^{-05}$
Rm6	1	364	-4.9277	Y	0.82825	0.054361	-5.0414	$1.39*10^{-05}$
Rm6	2	13	-2.1605	N	0.85545	0.0014538	-8.3605	$1.33*10^{-05}$
Rm6	3	11	-1.5755	N	1.0532	0.00015014	-8.5538	$1.45*10^{-05}$
Rm7	1	96	-8.8739	Y	0.63411	0.11304	-6.2687	$9.19*10^{-06}$
Rm7	2	13	-2.7982	Y	0.69057	0.0083967	-8.3193	$1.15*10^{-05}$
Rm7	3	18	-2.508	Y	0.74315	0.006646	-8.0202	$1.26*10^{-05}$
Rm8	1	128	-3.6895	Y	0.85684	0.014105	-6.0787	$1.35*10^{-05}$
Rm8	2	175	-2.1101	Y	0.87822	0.015361	-5.79	$1.46*10^{-05}$
Rm8	3	46	2.7194	Y	1.5039	$5.20*10^{-08}$	-7.2101	$1.82*10^{-05}$
Rm8	4	183	4.3264	Y	1.3063	0.00016918	-5.8115	$1.75*10^{-05}$
Rm9	1	23	0.3694	N	1.1077	0.0001758	-7.8709	$1.68*10^{-06}$
Rm9	2	29	-6.528	Y	0.47374	0.18798	-7.4162	$6.93*10^{-06}$
Rm10	1	52	-4.456	Y	0.64538	0.054311	-6.9386	$1.17*10^{-05}$
Rm10	2	13	-3.3042	Y	0.51417	0.054815	-8.3004	$1.06*10^{-06}$
Rm10	3	29	1.9763	N	1.7614	$2.12*10^{-07}$	-7.6724	$1.83*10^{-05}$
Rm11	1	13	0.39489	N	1.6186	$4.34*10^{-07}$	-8.4605	$1.76*10^{-05}$
Rm11	2	12	2.3239	Y	2.7779	1.77*10-12	-8.6157	$2.08*10^{-05}$
Rm11	3	19	1.5666	N	1.7854	$1.08*10^{-07}$	-8.1041	$1.86*10^{-05}$
Rm12	1	75	-5.8568	Y	0.61618	0.10686	-6.5592	$1.11*10^{-05}$
Rm12	2	36	-1.989	N	0.79446	0.0077013	-7.3565	$1.39*10^{-05}$
Rm13	1	38	3.3543	Y	1.7791	$2.30*10^{-07}$	-7.4217	$1.91*10^{-05}$
Rm13	2	17	-1.1163	N	0.73471	0.006866	-8.1324	$1.51*10^{-05}$
Rm14	1	10	0.61079	N	1.6699	$1.94*10^{-07}$	-8.7419	$1.85*10^{-06}$
Rm15	2	22	-0.64222	N	1.1134	0.00015832	-7.8845	$1.55*10^{-05}$
Rm16	1	71	1.9482	N	1.425	$1.86*10^{-05}$	-6.7508	$1.71*10^{-05}$
Rm17	1	10	-0.2811	N	1.3056	$9.32*10^{-06}$	-8.7018	$1.67*10^{-05}$
Rm17	2	17	2.0383	Y	2.7089	5.22*10-12	-8.2294	$1.92*10^{-05}$
Rm18	1	92	1.138	N	1.3806	$3.86*10^{-05}$	-6.4753	$1.64*10^{-05}$
Rm18	2	107	0.56161	N	1.1628	0.00045548	-6.3142	$1.60*10^{-05}$
Average		62.28			1.1846	0.0155	-7.4968	$1.54*10^{-05}$
Std.		78.99			0.5261	0.0371	1.2871	$3.14*10^{-06}$

Appendix XII Results of analysis of pump failures Amsterdam

Table XII.1 Number of thermal failures of all pumps.

Pumping station	Pump No.	Purpose	Pumping capacity (m^3/h)	Power (kW)
Am1	1	wwf	630	75
	2	dwf	270	37
	3	dwf	270	37
Am2	1	dwf/wwf	108	7.5
	2	dwf/wwf	108	7.5
Am3	1	dwf/wwf	1008	45
	2	dwf/wwf	1008	45
	3	dwf/wwf	1008	45
Am4	1	dwf/wwf	29	1.1
	2	dwf/wwf	29	1.1
Am5	1	wwf	165	18.5
	2	dwf/wwf	165	18.5
	3	dwf/wwf	270	11
Am6	1	dwf/wwf	2600	250
	2	wwf	2600	355
	3	dwf/wwf	2600	250
	4	wwf	2600	355
	5	dwf/wwf	2600	250
Am7	1	dwf/wwf	162	22
	2	dwf/wwf	162	22

Table XII.2 Results of Laplace trend test (see Ansell and Phillips 1994).

Station	Pump	Number of failures	U_L (H_0: HPP)	U_{LR} (H_0: RP)	$Z_{\alpha/2}$ (α=0.025)	Trend H_0=HPP	Trend H_0=RP
Am3	1	4	1.035	0.697	1.960	-	-
	2	5	1.036	0.899	1.960	-	-
	3	5	1.036	0.899	1.960	-	-
Am5	1	9	-0.519	-0.479	1.960	-	-
	2	19	0.268	0.202	1.960	-	-
	3	15	-0.119	-0.097	1.960	-	-
Am6	1	33	-1.709	-1.193	1.960	-	-
	2	6	-1.625	-2.117	1.960	-	>>
	3	43	-1.187	-0.940	1.960	-	-
	4	7	1.421	0.541	1.960	-	-
	5	31	-1.244	-1.092	1.960	-	-
Am7	1	22	1.191	0.976	1.960	-	-
	2	16	1.080	0.933	1.960	-	-

- = no trend << = deteriorating >> = improving

Table XII.3 Number of thermal failures of all pumps.

Station	Purpose	Pump	1998	1999	2000	2001	2002	Total
Am3	dwf/wwf	1				1	3	4
	dwf/wwf	2			1	1	3	5
	dwf/wwf	3			1	1	3	5
Am4	dwf/wwf	1		1		1	1	3
	dwf/wwf	2		2			1	3
Am5	wwf	1			4	4	1	9
	dwf/wwf	2		1	4	13	1	19
	dwf/wwf	3		2	2	10	1	15
Am6	dwf/wwf	1		7	18	3	5	33
	wwf	2		3	1	1	1	6
	dwf/wwf	3		5	18	14	6	43
	wwf	4		0	0	0	7	7
	dwf/wwf	5		3	16	6	6	31
Am7	dwf/wwf	1		4	1	7	10	22
	dwf/wwf	2		2	1	7	6	16

Table XII.4 Total duration of thermal failures of all pumps (in hours).

Station	Purpose	Pump	1998	1999	2000	2001	2002	Total
Am3	dwf/wwf	1				0.01	3.54	3.55
	dwf/wwf	2			0.03	0.01	3.54	3.58
	dwf/wwf	3			0.03	0.01	3.54	3.58
Am4	dwf/wwf	1		0.03		3.75	22.45	26.23
	dwf/wwf	2		44.46			3.13	47.59
Am5	wwf	1			44.90	2.61	16.99	64.51
	dwf/wwf	2		0.22	24.69	93.63	0.11	118.65
	dwf/wwf	3		0.36	8.66	179.05	0.10	188.17
Am6	dwf/wwf	1		6.70	1413.30	1.77	1070.90	2492.67
	wwf	2		0.04	0.03	0.14	0.03	0.23
	dwf/wwf	3		5.80	465.19	624.85	294.16	1390.00
	wwf	4					1.33	1.33
	dwf/wwf	5		1.01	371.69	403.12	48.46	824.28
Am7	dwf/wwf	1		11.16	1.87	144.70	91.23	248.96
	dwf/wwf	2		9.25	0.02	23.82	26.48	59.57

Table XII.5 Number of installation failures of all pumping stations.

Station	1998	1999	2000	2001	2002	Total
Am1				25	7	32
Am2		9	3	2	4	18
Am3	10	1	2	7	3	23
Am4		147	1	73	176	397
Am5	11	10	3	97	3	124
Am6		14	72	43	65	194
Am7		10	62	34	12	118

Table XII.6 Duration of installation failures of all pumping stations.

Station	1998	1999	2000	2001	2002	Total
Am1				39.27	16.56	55.84
Am2		20.22	19.37	0.02	1.51	41.11
Am3	10.53	0.98	0.03	3.96	8.48	23.97
Am4		4.43	0.12	4.41	5.69	14.65
Am5	1.99	38.34	6.51	39.60	1.80	88.24
Am6		146.93	1281.70	1060.50	405.94	2895.07
Am7		10.71	68.12	26.14	8.04	113.00

Table XII.7 Number of switch-ons of all pumps.

Station	Purpose	Pump	1998	1999	2000	2001	2002	Total
Am2	dwf/wwf	1		1406	1277	1271	1140	5094
	dwf/wwf	2		1394	1270	1268	1131	5063
Am3	dwf/wwf	1		1226	1736	1668	2471	7097
	dwf/wwf	2		1562	1743	1660	2324	7284
	dwf/wwf	3		1225	1723	1657	2334	6934
Am4	dwf/wwf	1					16497	16497
	dwf/wwf	2					16420	16420
Am5	wwf	1	11	14	33	20	11	89
	dwf/wwf	2	14	495	2121	2187	247	5064
	dwf/wwf	3	12	505	2111	2293	255	5176
Am6	dwf/wwf	1		1456	1535	2379	395	5765
	wwf	2		73	104	114	113	404
	dwf/wwf	3		259	2973	2149	699	6080
	wwf	4		66	74	107	103	350
	dwf/wwf	5		555	6048	1614	516	8733
Am7	dwf/wwf	1		3390	900	614	614	5518
	dwf/wwf	2		3390	916	571	617	5494

Table XII.8 Total hours run of all pumps (in days)

Station	Purpose	Pump	1998	1999	2000	2001	2002	Total
Am2	dwf/wwf	1		34.36	38.93	37.42	32.38	143.09
	dwf/wwf	2		35.34	39.64	38.28	29.82	143.08
Am3	dwf/wwf	1		76.29	74.48	70.46	69.34	290.57
	dwf/wwf	2		52.21	58.54	58.92	57.22	226.89
	dwf/wwf	3		45.15	67.09	67.17	73.13	252.55
Am4	dwf/wwf	1					30.19	30.19
	dwf/wwf	2					28.79	28.79
Am5	wwf	1	0.31	1.01	1.40	0.97	1.04	4.74
	dwf/wwf	2	0.79	28.19	27.70	35.96	26.19	118.83
	dwf/wwf	3	1.17	28.58	29.82	25.89	16.95	102.40
Am6	dwf/wwf	1		14.99	217.48	221.80	231.83	686.10
	wwf	2		2.61	8.41	10.92	11.77	33.71
	dwf/wwf	3		81.06	234.20	124.00	250.02	689.27
	wwf	4		3.41	7.61	9.95	8.08	29.05
	dwf/wwf	5		84.30	110.18	247.62	115.33	557.43
Am7	dwf/wwf	1		22.22	33.22	22.70	40.00	118.14
	dwf/wwf	2		22.61	21.65	20.80	15.22	80.28

Table XII.9 Moment of failure related to occurrence of storm events.

Station	Purpose	Pump	No storm event	At start of storm event	At end of storm event	Total
Am3	dwf/wwf	1	4			4
	dwf/wwf	2	4		1	5
	dwf/wwf	3	4		1	5
Am4	dwf/wwf	1	3			3
	dwf/wwf	2	3			3
Am5	wwf	1	7	2	0	9
	dwf/wwf	2	14	4	1	19
	dwf/wwf	3	14	1	0	15
Am6	dwf/wwf	1	33	1	2	36
	wwf	2	0	3	3	6
	dwf/wwf	3	40	1	2	43
	wwf	4	4	3	0	7
	dwf/wwf	5	27	2	2	31
Am7	dwf/wwf	1	21	0	1	22
	dwf/wwf	2	16	1	0	17

Table XII.10 Statistics of duration of thermal failures of all pumps.

Station	Purpose	Pump	Number of failures (1/a)	Average duration of failures (h)	Total duration of failures (h/a)
Am3	dwf/wwf	1	0.80	0.89	0.71
	dwf/wwf	2	1.00	0.72	0.72
	dwf/wwf	3	1.00	0.72	0.72
Am4	dwf/wwf	1	0.60	8.74	5.25
	dwf/wwf	2	0.60	15.86	9.52
Am5	wwf	1	1.80	7.17	12.90
	dwf/wwf	2	3.80	6.24	23.73
	dwf/wwf	3	3.00	12.54	37.63
Am6	dwf/wwf	1	6.60	75.54	498.53
	wwf	2	1.20	0.04	0.05
	dwf/wwf	3	8.60	32.33	278.00
	wwf	4	1.40	0.19	0.27
	dwf/wwf	5	6.20	26.59	164.86
Am7	dwf/wwf	1	4.40	11.32	49.79
	dwf/wwf	2	3.20	3.72	11.91
Average			2.95	13.51	72.97
Std.			2.52	19.71	140.92

Table XII.11 Unavailability of all pumps (= 1/P(Failure|Demand for pump)).

Station	Purpose	Pump	1998	1999	2000	2001	2002	Total
Am3	dwf/wwf	1				1668	824	1774
	dwf/wwf	2			1743	1660	775	1457
	dwf/wwf	3			1723	1657	778	1387
Am4	dwf/wwf	1					16497	16497
	dwf/wwf	2					16420	16420
Am5	wwf	1			8	5	11	10
	dwf/wwf	2		495	530	168	247	267
	dwf/wwf	3		253	1056	229	255	345
Am6	dwf/wwf	1		208	85	793	79	175
	wwf	2		24	104	114	113	67
	dwf/wwf	3		52	165	154	117	141
	wwf	4					15	50
	dwf/wwf	5		185	378	269	86	282
Am7	dwf/wwf	1		848	900	88	61	251
	dwf/wwf	2		1695	916	82	103	343
Average				470	692	574	2425	1168
Std.				562	631	685	5705	1841

Table XII.12 Bayes weights of duration of pump failures (based on Laplace approximation).

		Exp	Ray	Nor	Lgn	Gam	Wei	Gum
Location parameter		0	0	0	0	0	0	0
Prior weights		0.1429	0.1429	0.1429	0.1429	0.1429	0.1429	0.1429
Station	**Pump**	**Exp**	**Ray**	**Nor**	**Lgn**	**Gam**	**Wei**	**Gum**
Am5	1	0.1116	0	0.0002				0.0023
	2	0	0	0		0.1333	0.3824	0
	3	0	0	0		0.163	0.3141	0
Am6	1	0.0682	0	0	0.0962			0
	3	0	0	0		0	0.0068	0
	5	0.2303	0	0	0.0736			0
Am7	1	0	0	0	0.0213		0.2550	0
	2	0	0	0		0.1557	0.2608	0

Table XII.13 Bayes weights of interarrival time of pump failures (based on Laplace approximation).

		Exp	Ray	Nor	Lgn	Gam	Wei	Gum
Location parameter		0	0	0	0	0	0	0
Prior weights		0.1429	0.1429	0.1429	0.1429	0.1429	0.1429	0.1429
Station	**Pump**	**Exp**	**Ray**	**Nor**	**Lgn**	**Gam**	**Wei**	**Gum**
Am5	1	0.1806	0	0.0029	0.0920			0.0093
	2	0.0004	0	0	0.0529		0.3206	0
	3		0	0		0.1842		0.0008
Am6	1	0	0	0	0.1197			0
	3	0	0	0	0.0036		0.2624	0
	5	0	0	0		0	0.0041	0
Am7	1	0.0120	0	0	0.0043		0.2905	0
	2	0.0001	0	0	0.0259		0.2393	0

Table XII.14 Parameters of Crow's model and Cox-Lewis' model. The majority of pumps shows improvement ($\beta > 1$ and $\beta_1 > 0$).

Station	Pump	Number of failures	U_L	Trend	Crow's model		Cox-Lewis' model	
					β	λ	β_0	β_1
Am3	1	4	1.035	N	8.494	$1.493*10^{-39}$	-9.805	$2.133*10^{-05}$
	2	5	1.036	N	4.852	$1.503*10^{-22}$	-9.558	$2.039*10^{-05}$
	3	5	1.036	N	4.852	$1.503*10^{-22}$	-9.558	$2.039*10^{-05}$
Am5	1	9	-0.519	N	1.515	$1.177*10^{-06}$	-8.633	$1.972*10^{-05}$
	2	19	0.268	N	1.526	$2.209*10^{-06}$	-7.888	$1.981*10^{-05}$
	3	15	-0.119	N	1.353	$1.062*10^{-05}$	-8.120	$1.959*10^{-05}$
Am6	1	33	-1.709	N	0.978	$1.287*10^{-03}$	-7.194	$1.697*10^{-05}$
	2	6	-1.625	N	1.068	$8.444*10^{-05}$	-8.989	$1.717*10^{-05}$
	3	43	-1.187	N	1.146	$2.656*10^{-04}$	-7.028	$1.761*10^{-05}$
	4	7	1.421	N	3.726	$8.152*10^{-17}$	-8.974	$2.426*10^{-05}$
	5	31	-1.244	N	1.118	$2.581*10^{-04}$	-7.354	$1.752*10^{-05}$
Am7	1	22	1.191	N	1.650	$6.960*10^{-07}$	-7.766	$2.110*10^{-05}$
	2	16	1.080	N	1.860	$6.000*10^{-08}$	-8.034	$2.160*10^{-05}$
Average		16.5			2.626	$1.469*10^{-04}$	-8.377	$1.980*10^{-05}$
Std.		12.6			2.250	$3.560*10^{-04}$	0.944	$2.097*10^{-06}$

Appendix XIII Results of analysis of coding of sewer inspection data

Table XIII.1 Summary of number of candidates and norms per exam slide and per aspect.

		Norms per observation type								
Slide No.	Number of candidates	A1	A2	A3	A4	A5	A6	A7	B1	B2
21	325	2							5	
22	314					5				2-3
25	325							2		2
27	325		2			5				2-3
111	325					1-5				
112	11	2								
117	314	1-2						5	5	
129	314							1-4		3-4
144	314	2						1-3		
149	325	1-2								
182	11	4						4		
184	11				5	5				
241	325	2								2
420	11	2							1	
% of exams incl. specific aspect		50.3	10.0		0.3	30.0		39.3	20.0	49.3

		Norms per observation type								
Slide No.	Number of candidates	B3	B4	C1	C2	C3	C4	C5	C6	C7
21	325	1-2		3				4		
22	314									1-2
25	325						1-2	3-4		2
27	325	5								2
111	325						2-3			2
112	11					1-2				3
117	314							4		2
129	314							1-3		2-3
144	314								4	
149	325				3-4					2
182	11									4
184	11								4	
241	325							1-2	3	
420	11		1-2		3-4		1-2			2
% of exams incl. specific aspect		20.0	0.3	10.0	10.3	0.3	20.3	49.3	20.0	70.0

The following figures present the probability of individual classifications for all observation types. In addition, the statistical uncertainty is shown as the 5th and 95th percentile. Both have been determined with Bayesian estimation from the examination results of the RIONED Foundation.

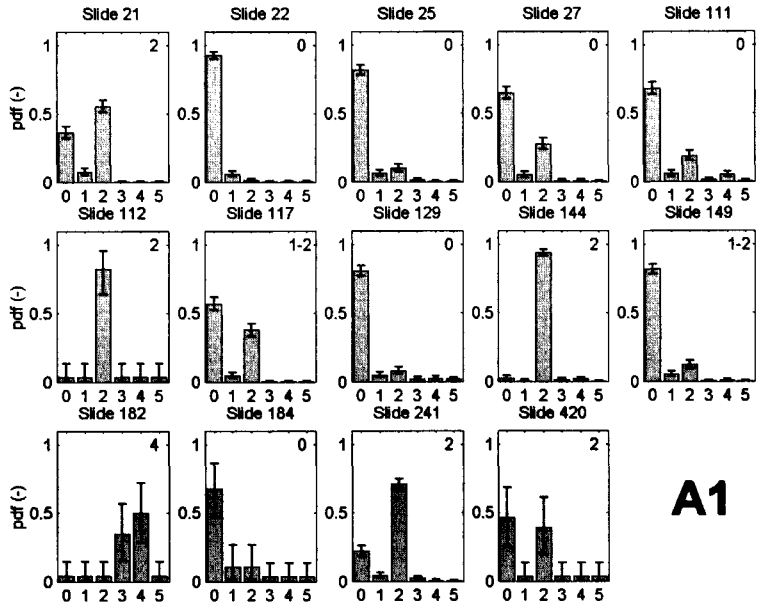

Figure XIII.1 Coding of aspect A1 for all slides.

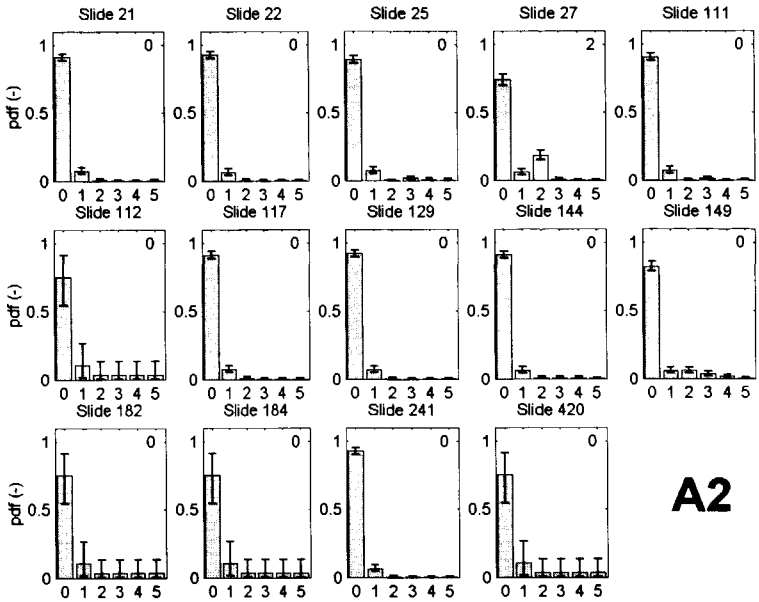

Figure XIII.2 Coding of aspect A2 for all slides.

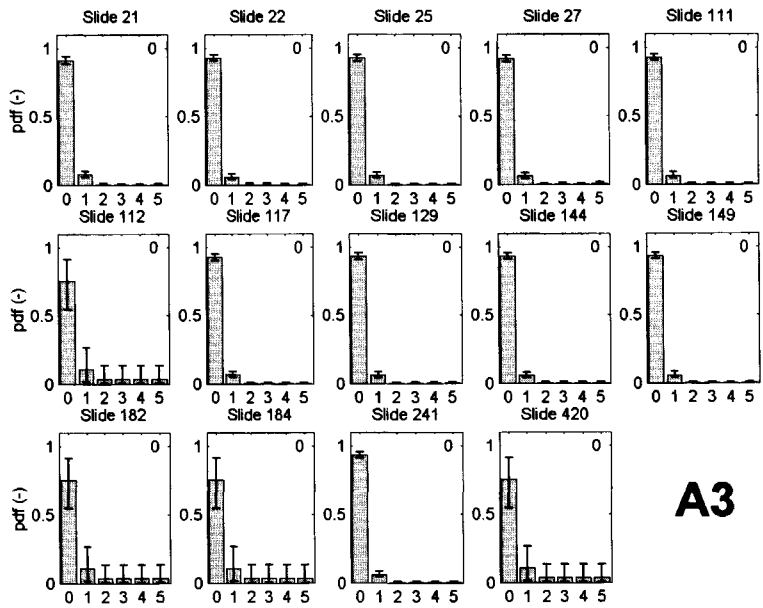

Figure XIII.3 Coding of aspect A3 for all slides.

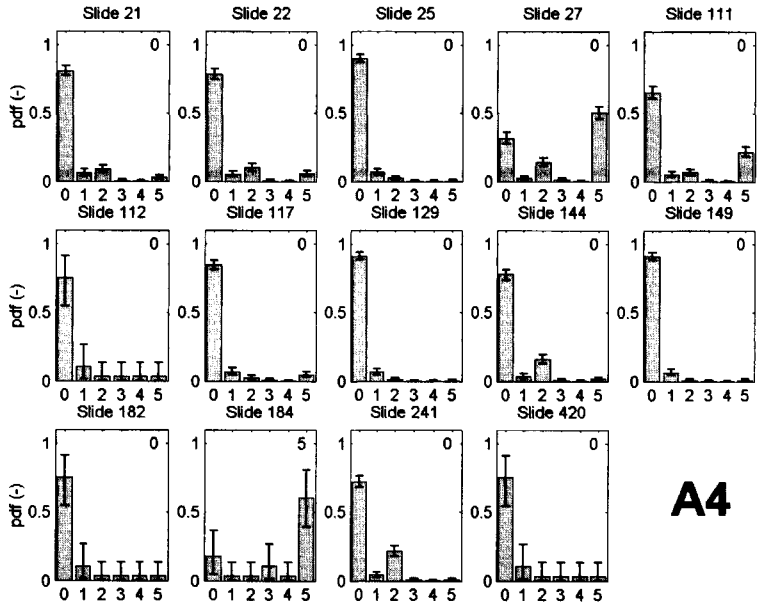

Figure XIII.4 Coding of aspect A4 for all slides.

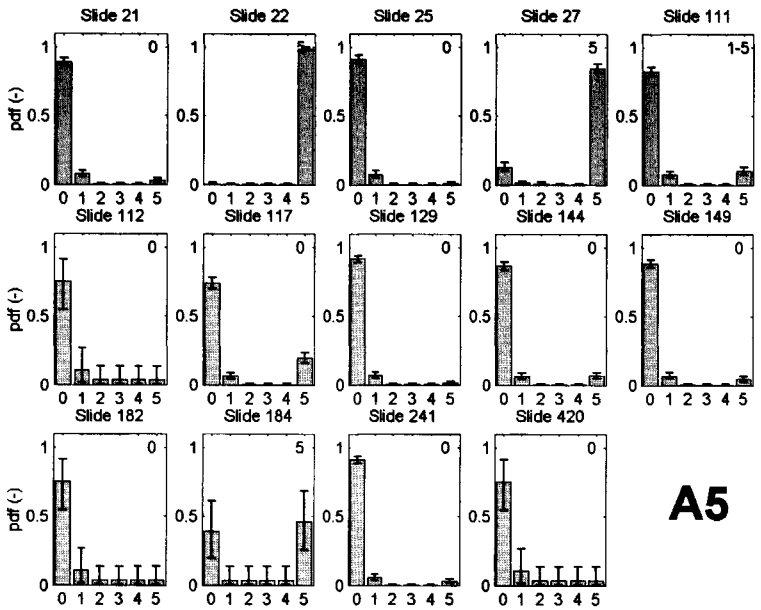

Figure XIII.5 Coding of aspect A5 for all slides.

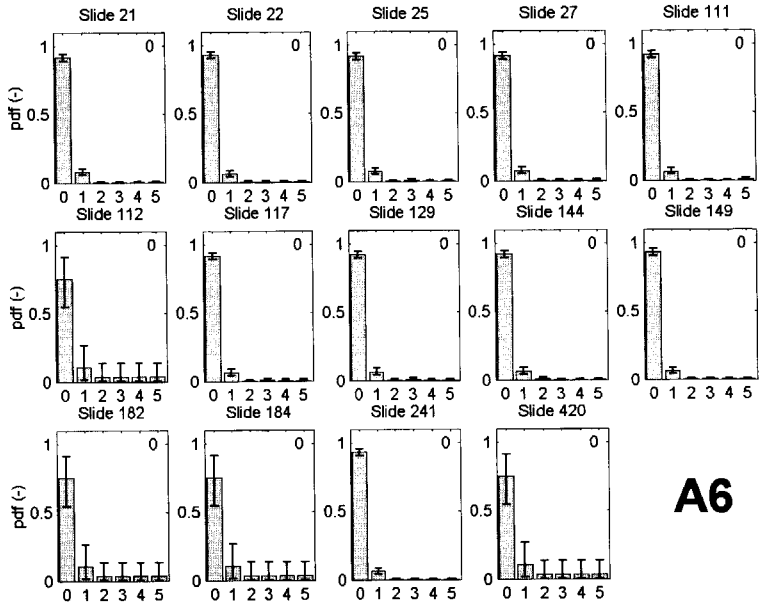

Figure XIII.6 Coding of aspect A6 for all slides.

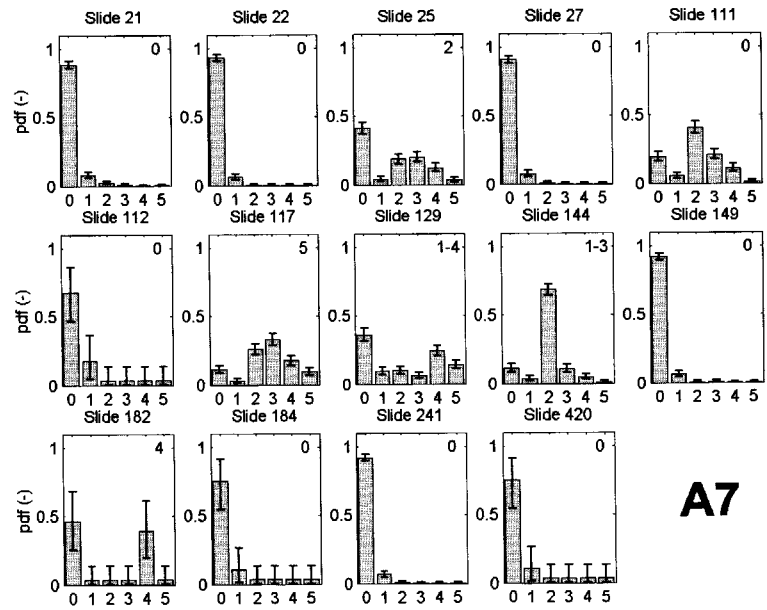

Figure XIII.7 Coding of aspect A7 for all slides.

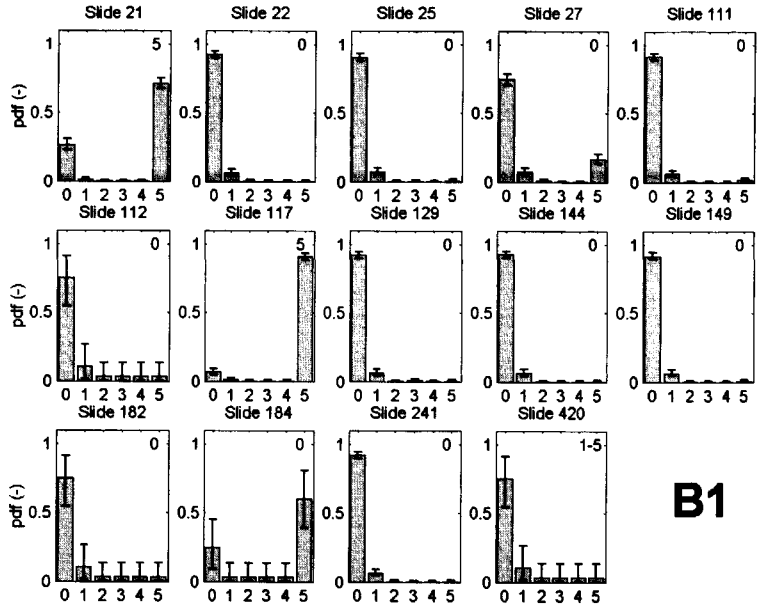

Figure XIII.8 Coding of aspect B1 for all slides.

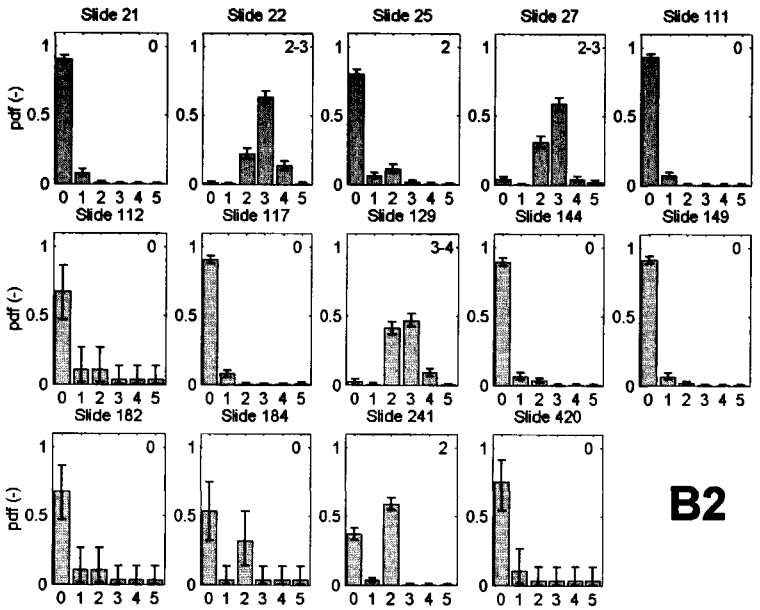

Figure XIII.9 Coding of aspect B2 for all slides.

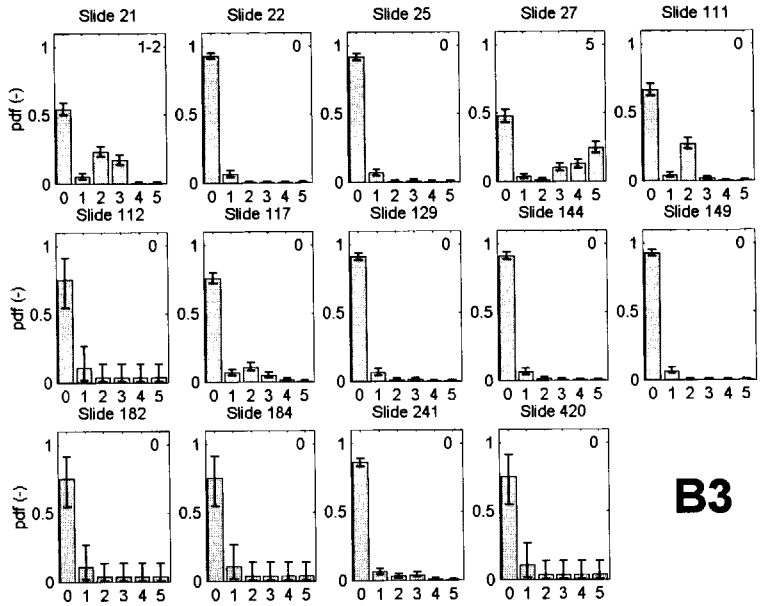

Figure XIII.10 Coding of aspect B3 for all slides.

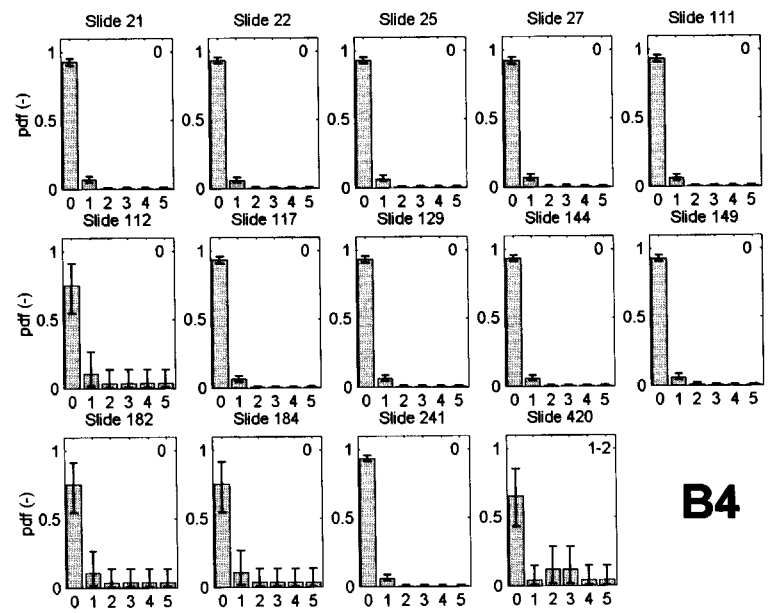

Figure XIII.11 Coding of aspect B4 for all slides.

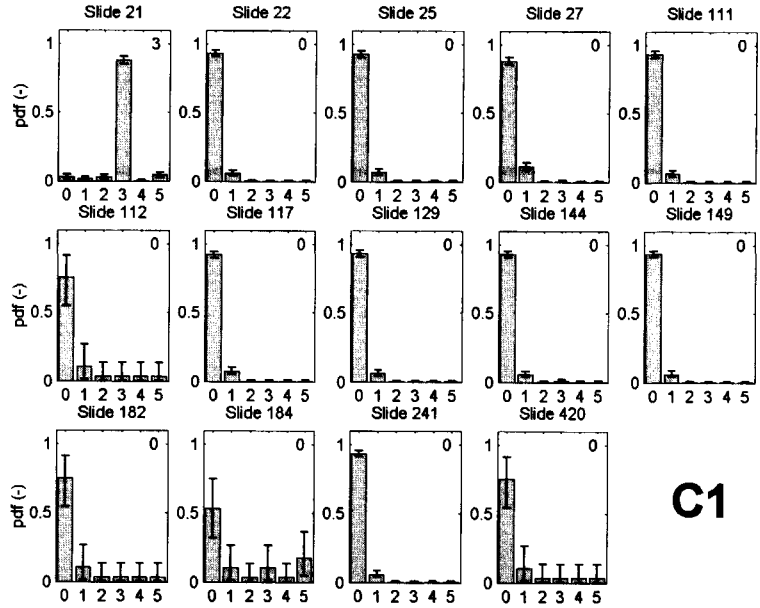

Figure XIII.12 Coding of aspect C1 for all slides.

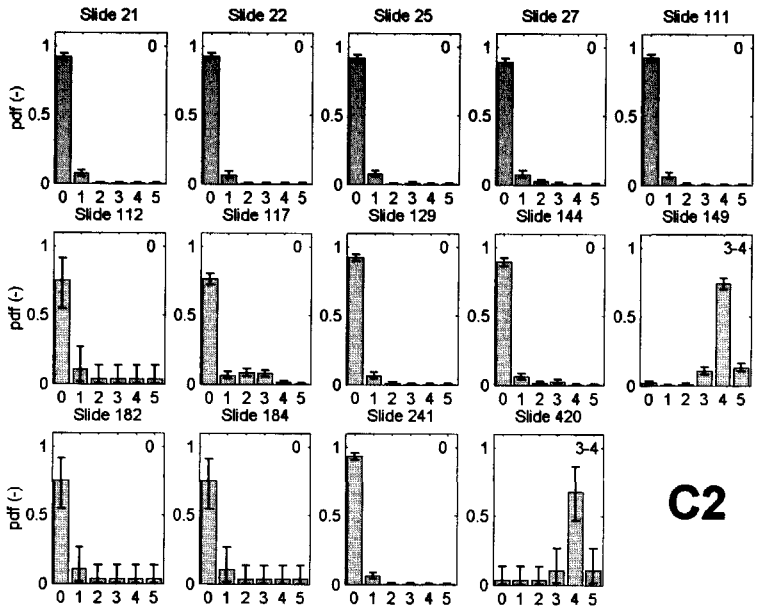

Figure XIII.13 Coding of aspect C2 for all slides.

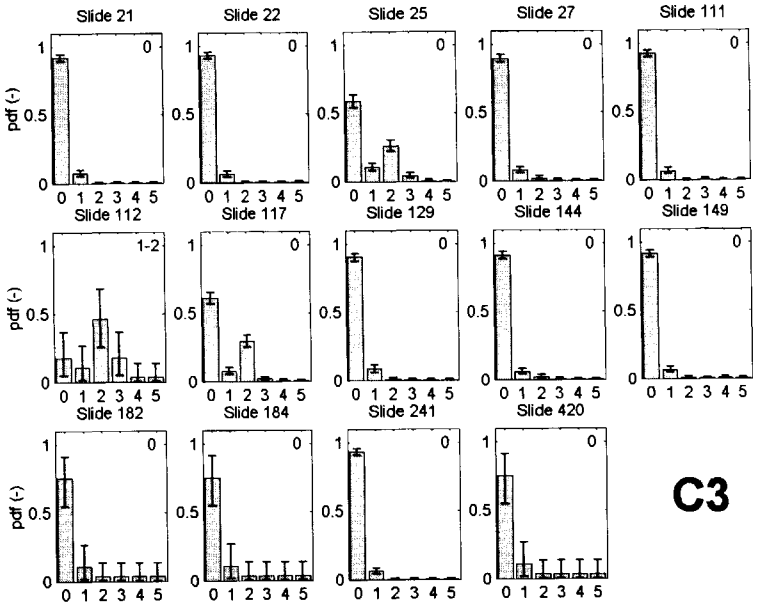

Figure XIII.14 Coding of aspect C3 for all slides.

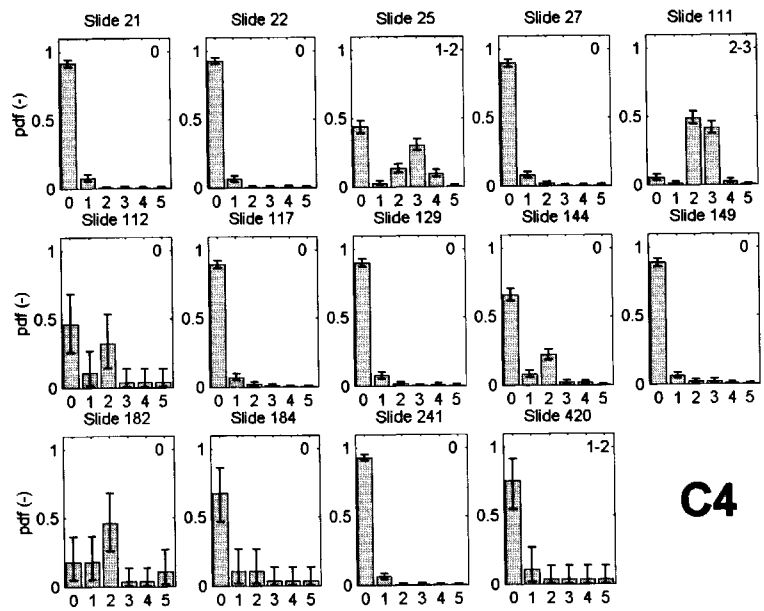

Figure XIII.15 Coding of aspect C4 for all slides.

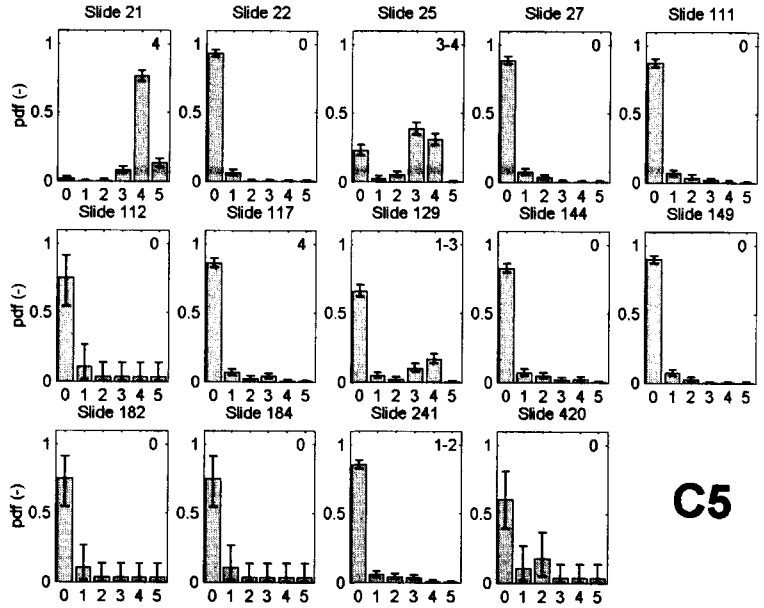

Figure XIII.16 Coding of aspect C5 for all slides.

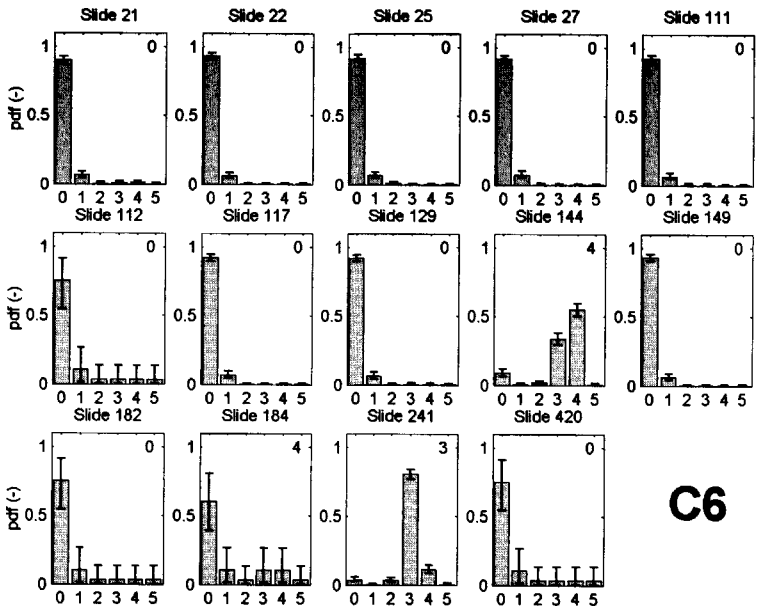

Figure XIII.17 Coding of aspect C6 for all slides.

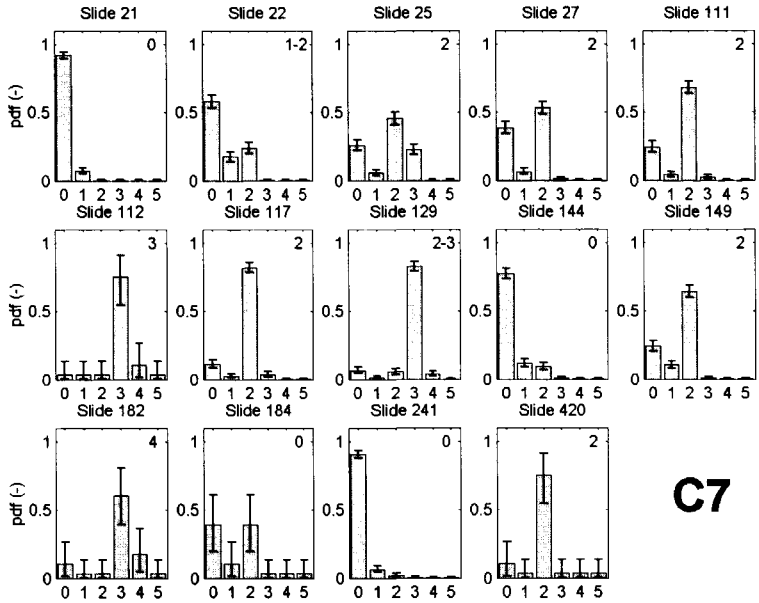

Figure XIII.18 Coding of aspect C7 for all slides.

Entropy provides a measure of the variation of the coding of visual inspections. Figure XIII.19 presents the entropy of each observation type given the specific slide. The larger the triangle, the larger the entropy and the corresponding variation. The entropy of aspects (bottom of figure) and slides (right of figure) has been calculated as a weighted average in vertical and horizontal direction, respectively. The weights have been based on the number of candidates for a specific aspect or slide.

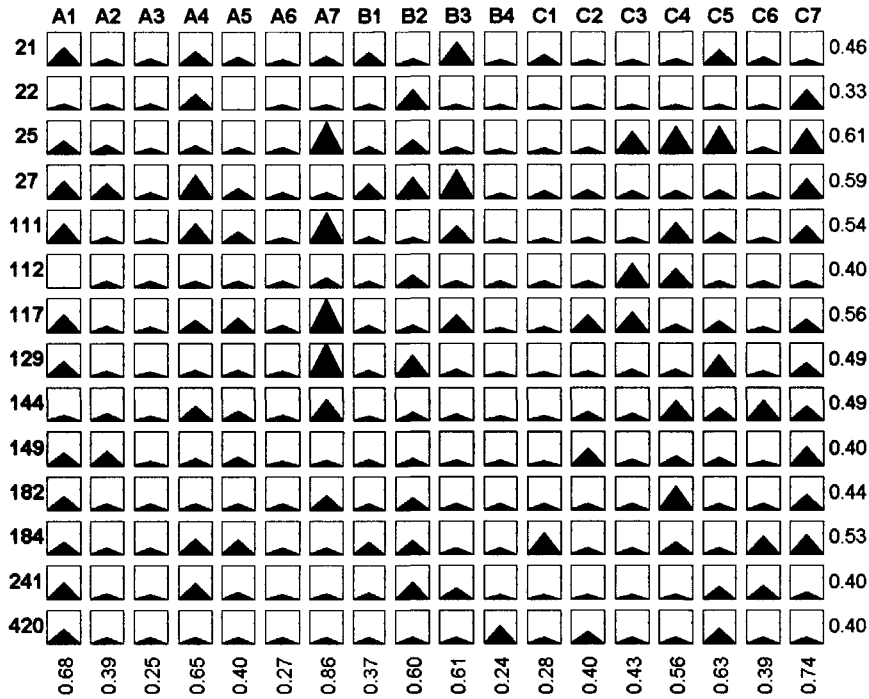

Figure XIII.19 Entropy for all slides and aspects.

Probability of incorrect coding determines the quality of predicted serviceability of a sewer system. Figure XIII.20 presents the probability of incorrect coding of each observation type given the specific slide. The larger the triangle, the more probable the misinterpretation of an observation type. The probability of misinterpretation of aspects (bottom of figure) and slides (right of figure) has been calculated as a weighted average in vertical and horizontal direction, respectively. The weights have been based on the number of candidates for a specific aspect or slide.

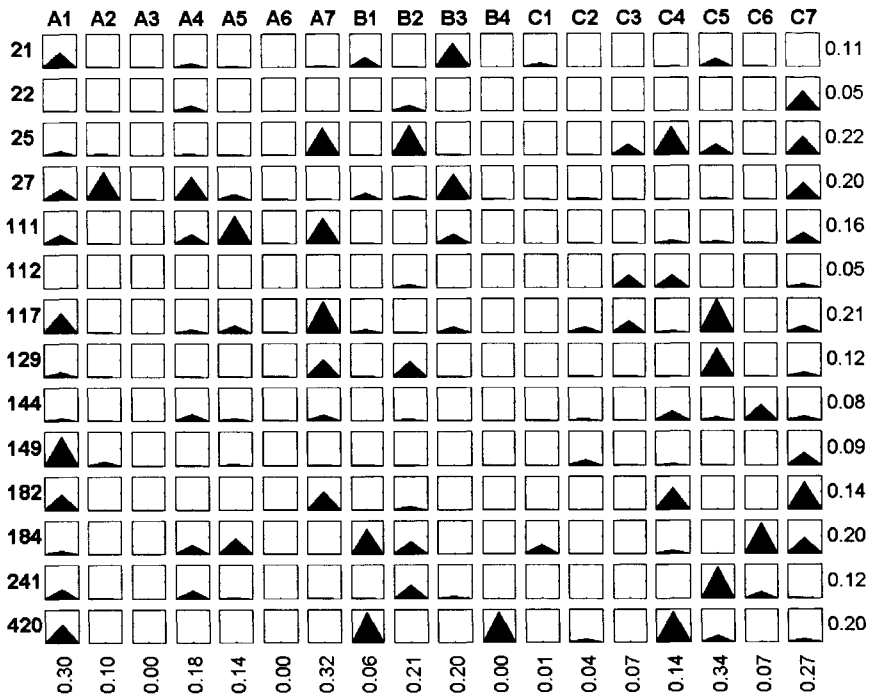

Figure XIII.20 Probability of misinterpretation for all slides and aspects.

Probability of incorrect decision-making on further research or rehabilitation partially determines the efficiency of planned interventions. Figure XIII.21 presents the probability of incorrect decisions regarding further research of each observation type given the specific slide. Figure XIII.22 presents the probability of incorrect decisions regarding maintenance and rehabilitation of each observation type given the specific slide. The larger the triangle, the more probable incorrect decision-making becomes. The probability of incorrect decisions of aspects (bottom of figure) and slides (right of figure) has been calculated as a weighted average in vertical and horizontal direction, respectively. The weights have been based on the number of candidates for a specific aspect or slide.

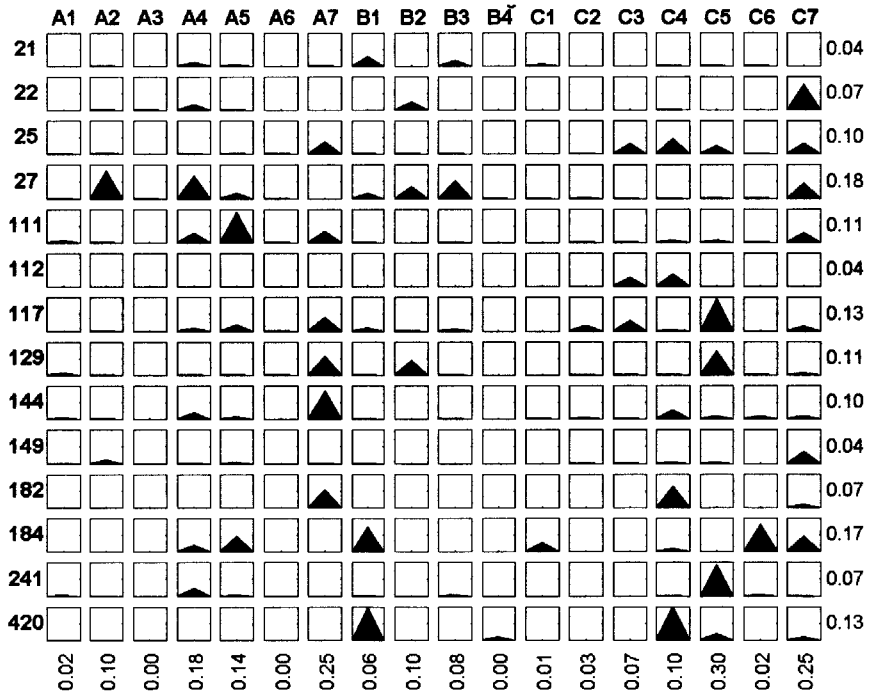

Figure XIII.21 Probability of wrong decisions regarding further research ('warning criterion').

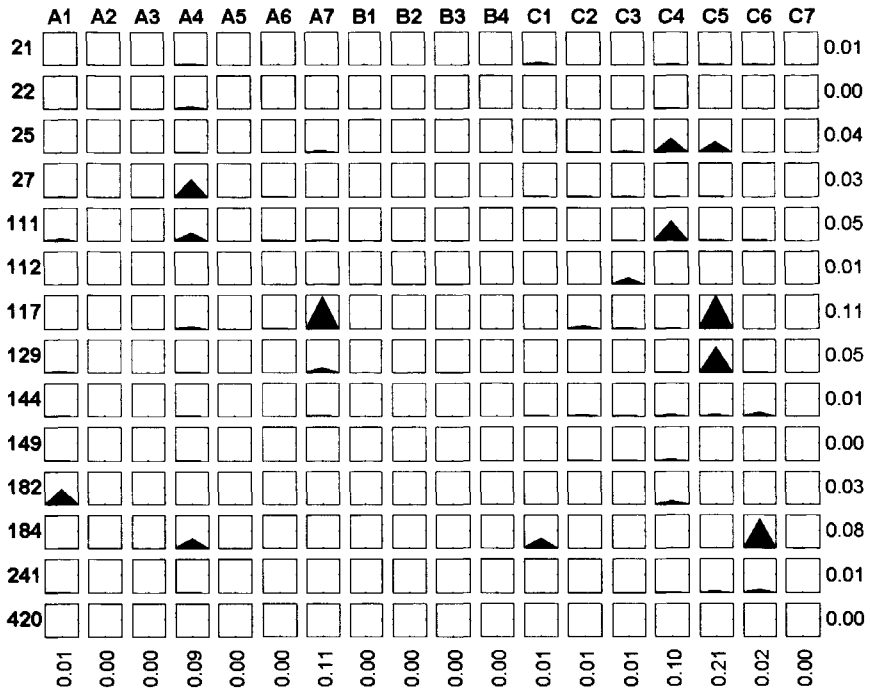

Figure XIII.22 Probability of wrong decisions regarding cleaning or replacement ('intervention criterion').

Appendix XIV Abbreviations

BOD	biochemical oxygen demand
CCTV	closed circuit television
cdf	cumulative density function
COD	chemical oxygen demand (mg O_2/l)
CSO	combined sewer overflow
CV	coefficient of variation
DO	dissolved oxygen
dwf	dry weather flow
EMC	event mean concentration
Exp	exponential
Gam	gamma
Gum	Gumbel
IDF	intensity-duration-frequency
inh	inhabitant
Lgn	lognormal
ML	maximum likelihood
MSE	mean squared error
NH_3	ammonia
NH_4	ammonium
$NH_{Kjeldahl}$	total ammonium nitrogen and organic bound nitrogen
Nor	normal
NWRW	Nationale Werkgroep Riolering en Waterkwaliteit (national working group on sewerage and water quality)
pc	pumping capacity
pdf	probability density function
p.e.	population equivalent: the oxygen equivalent to the amount of oxygen demand related to one inhabitant. A p.e. corresponds with 136 g TOD per day or with 54 g BOD per day
PLC	programmable logic controller
PO	pumped overflow
P_{total}	total of phosphorous in wastewater
Q	flow
Ray	Rayleigh
RMSE	root mean squared error

SS	suspended solids
Std.	standard deviation
TME	thermal, mechanical and electrical failures
TSS	total suspended solids
Var.	variation
Wei	Weibull
WVO	Wet Verontreiniging Oppervlaktewater (Pollution of Surface Waters Act)
wwf	wet weather flow
wwtp	wastewater treatment plant

STELLINGEN

Behorende bij het proefschrift 'Probabilistic assessment of the performance of combined sewer sewer systems' door Hans Korving, Delft 18 mei 2004

I Verbeteren van de storingsafhandeling van rioolgemalen levert meer op voor de vermindering van de vuiluitworp dan bouwen van extra berging.

II Zonder goed gedefinieerde beheerinspanning valt het welslagen van de 'Basisinspanning' niet te meten.

III Zolang de veiligheid van de huidige ontwerpnorm voor rioolstelsels onbekend is, heeft het invoeren van extra veiligheidsfactoren om klimaatveranderingen op te vangen geen enkele zin.

IV Zekere onzekerheid maakt besluitvorming ten aanzien van rioleringsbeheer beter.

V Verwachting is een afspiegeling van het beste dat we hopen en het ergste dat we vrezen (vrij naar: Jacob Bernoulli, 1654-1705).

VI Al wordt een computer nog zo snel, berekeningen blijven even lang duren.

VII Een universitair geldverdelingsmodel op basis van publicaties stimuleert het vergaren van meer kennis, op basis van citaties het opzoeken van meer kennissen.

VIII De kloof tussen politiek en burger is veel te klein. Politici zijn te gevoelig voor de waan van de dag en de peiling van morgen.

IX In tegenstelling tot wetenschappers zijn schrijvers zich ervan bewust dat zij de werkelijkheid omliegen tot waarheid.

X Vrijheid staat vandaag de dag voor ruim baan maken voor assertieve individuen om de top te bereiken en hun zakken te vullen.

Deze stellingen worden verdedigbaar geacht en zijn als zodanig goedgekeurd door de promotoren prof.dr.ir. F.H.L.R. Clemens en prof.dr.ir J.M. van Noortwijk.